Report SAM-TR-73-25

DETECTION AND PREVENTION OF G-INDUCED REGIONAL ATELECTASIS, EDEMA, AND HYPOPERFUSION

Division of Pulmonary Diseases,
Mount Sinai Medical Center,
Miami Beach, Florida 33140

December 1973

Final Report for Period October 1972–October 1973

[redacted]

[redacted]

WORK UNIT

This final report was submitted by the Division of Pulmonary Diseases of Mount Sinai Medical Center, Miami Beach, Florida, under contract F41608-72-C-0004, job order 7718-0344, with the USAF School of Aerospace Medicine, Aerospace Medical Division (AFSC), Brooks Air Force Base, Texas. Major Edward D. Michaelson, USAF Biodynamics Branch (VNB), who was initially the Laboratory project Scientist-in-Charge, was replaced by Dr. Sidney D. Lewitt, Jr., during the final six months of the contract period.

(6)
(10)

When U.S. Government drawings, specifications, or other data are used for any purpose other than a definitely related Government procurement operation, the Government thereby incurs no responsibility nor any obligation whatsoever; and the fact that the Government may have formulated, furnished, or in any way supplied the said drawings, specifications, or other data is not to be regarded by implication or otherwise, as in any manner licensing the holder or any other person or conveying any rights or permission to manufacture, use, or sell any patented invention that may in any way be related thereto.

The animals involved in this study were procured, maintained, and used in accordance with the Animal Welfare Act of 1970 and the "Guide for the Care and Use of Laboratory Animals" prepared by the Institute of Laboratory Animal Resources - National Academy of Sciences.

Human subjects gave informed consent, as monitored by the Institutional Review Committee, and were protected in accordance with the guidelines published by the Department of Health, Education and Welfare.

This report has been reviewed by the Information Office (OI) and is releasable to the National Technical Information Service (NTIS). At NTIS, it will be available to the general public, including foreign nations.

This technical report has been reviewed and is approved for publication.

[redacted]

UNCLASSIFIED

SECURITY CLASSIFICATION OF THIS PAGE (When Data Entered)

REPORT DOCUMENTATION PAGE	READ INSTRUCTIONS BEFORE COMPLETING FORM
SAM-TR-75-25	2 GOVT ACCESSION NO. / 3 RECIPIENT'S CATALOG NUMBER
4 TITLE (and Subtitle): DETECTION AND PREVENTION OF G-INDUCED REGIONAL ATELECTASIS, EDEMA, AND HYPO-PERFUSION.	5 TYPE OF REPORT & PERIOD COVERED: Final Rpt. Oct 71 — Oct 73 / 6 PERFORMING ORG. REPORT NUMBER
7 AUTHOR(s): Marvin A. Sackner, M.D., and Adam Wanner, M.D.	8 CONTRACT OR GRANT NUMBER(s): F41609-72-C-0004
9 PERFORMING ORGANIZATION NAME AND ADDRESS: Division of Pulmonary Diseases of Mt. Sinai Medical Center, Miami Beach, Florida 33140	10 PROGRAM ELEMENT, PROJECT, TASK AREA & WORK UNIT NUMBERS: 62202F / AE-7930 [illegible] / 713093
11 CONTROLLING OFFICE NAME AND ADDRESS: USAF School of Aerospace Medicine (VNB) Aerospace Medical Division (AFSC) Brooks Air Force Base, Texas 78235	12 REPORT DATE: Dec [illegible]75 / 13 NUMBER OF PAGES: 274
14 MONITORING AGENCY NAME & ADDRESS(if different from Controlling Office)	15 SECURITY CLASS. (of this report): UNCLASSIFIED / 15a DECLASSIFICATION DOWNGRADING SCHEDULE

16 DISTRIBUTION STATEMENT (of this Report)

Approved for public release; distribution unlimited.

17 DISTRIBUTION STATEMENT (of the abstract entered in Block 20, if different from Report)

18 SUPPLEMENTARY NOTES

19 KEY WORDS (Continue on reverse side if necessary and identify by block number)

Atelectasis, G-induced	Phrenic nerve stimulation
Cardiac output	Pulmonary capillary blood flow
Edema, G-induced	Pulmonary function
Hypoperfusion, G-induced	Whole body plethysmograph

20 ABSTRACT (Continue on reverse side if necessary and identify by block number)

These investigations were concerned with the evaluation of pulmonary circulation and the distribution of ventilation in response to maneuvering acceleration. In order to study the responses of $+G_z$ protection by the anti-G suit, respiratory maneuvers, and pharmacologic agents, it was necessary to improve existing methods and to develop new ones--both in anesthetized dogs and in human volunteers. To standardize noninvasive tests of the pulmonary circulation and distribution of ventilation, invasive studies were necessarily performed on

DD FORM 1 JAN 73 1473 EDITION OF 1 NOV 65 IS OBSOLETE

UNCLASSIFIED

SECURITY CLASSIFICATION OF THIS PAGE (When Data Entered)

AD 737 [illegible]

20. ABSTRACT (Continued)

anesthetized animals for comparison. Several programs for a small digital computer were developed to process the resulting voluminous data. One of the studies which dealt with the action of anti-G suits led to the hypothesis that anti-G suits would be more efficient if they inflated from below, upward (rather than from the abdominal bladder, downward, as in the standard USAF anti-G suit). A prototype of this suit was tested with the subject in the seated +1 G_z position and data were consistent with the notion that both cardiac output and diffusing capacity were increased in contrast to standard USAF anti-G suit which had no effect on cardiac output under these circumstances.

PREFACE

The authors gratefully acknowledge: the unstinting and devoted assistance, meticulous attention to details, and suggestions of Mr. Richard Dougherty, Chief Research Technician; and the contributions of Mr. Neal Atkins, System Analyst, for the many computer programs used in these studies.

EDITOR'S NOTE: The present address for Drs. Marvin Sackner and Adam Wanner is--Mount Sinai Medical Center, 4300 Alton Road, Miami Beach, Florida 33140.

Information on related research by the same authors will be available in a forthcoming (USAFSAM) technical report concerning the Modification of G-Induced Effects on Pulmonary Circulation.

CONTENTS

Figures and Tables

Figures and Tables

Figures and Tables

Figures and Tables

Figures and Tables

Figures and Tables

Figures and Tables

Figures and Tables

CONTENTS, Cont'd.

Figures and Tables

Figures and Tables

DETECTION AND PREVENTION OF G-INDUCED REGIONAL ATELECTASIS, EDEMA, AND HYPOPERFUSION

I. PURPOSE AND DESCRIPTION OF EACH RESEARCH STUDY (II - XII)

In the past, blackout and unconsciousness were considered as the factors which limited man's exposure to positive acceleration ($+G_z$). Such phenomena occurred at acceleration levels well below the point at which an intolerable reduction in pulmonary function became an additional consideration. In recent years, it has been found that anti-G suits can prevent unconsciousness at acceleration levels where alterations in pulmonary function might jeopardize man's performance. Aviators, while flying modern high-performance operational aircraft, may be subjected to prolonged exposure (30 to 60 sec) of acceleration forces as high as 7 to 10 $+G_z$. Increasing $+G_z$ will produce an increased hydrostatic gradient down the lung, such that pulmonary blood flow will be more preferentially distributed to the bases. Eventually the increase in basilar capillary pressures will lead to transudation of fluid into the alveoli (i.e., regional pulmonary edema). In addition, since pleural pressures become more positive at the bases with increases of $+G_z$, there will be a tendency to closure of more airways at the bases. The anti-G suit which helps in alleviating the circulatory stress of $+G_z$ under these circumstances may be deleterious to pulmonary function; for the anti-G suit produces elevation of the diaphragms, such that the subject breathes at a lung volume where airways are closed. Together with oxygen breathing, frank atelectasis may develop as the pulmonary blood flow through the dependent alveoli absorbs the oxygen trapped behind the closed airways. Both pulmonary edema and atelectasis lead to right-to-left intrapulmonary shunting, with attendant arterial hypoxemia.

In order to investigate the response of the pulmonary circulation not only to alterations in acceleration but also to $+G_z$ protection by the anti-G suit, respiratory maneuvers, and pharmacologic agents, it was necessary to improve existing methods and to develop new ones. For example, in G-stressed anesthetized animals, spontaneous breathing would be preferable over mechanical ventilation to avoid altering hemodynamic status by the

EDITOR'S NOTE: The principal abbreviations, acronyms, and symbols used throughout this report are listed and briefly defined on the concluding pages (pp. 271 - 274).

Illustrations and tables have been grouped, when feasible, at the close of each report section (II - XII).

positive pressure breathing (PPB) itself. Unfortunately, anesthetic agents cause depression of the respiratory center, and adequate alveolar hypoventilation may be left to chance. To circumvent this problem, a method using transvenous phrenic nerve stimulation for respiratory assistance had to be developed (1). To assess the pulmonary circulation by noninvasive means, the methods for measuring pulmonary capillary blood flow ($\dot{Q}_C$) by the nitrous oxide plethysmographic method (2, 3) and for rebreathing with acetylene (4) had to be improved and refined. Further, the problem of processing these large volumes of data required the writing of computer programs. The effects of pulmonary interdependence on pulmonary arterial blood volume required refinements and standardization of the ether plethysmographic and pneumotachographic methods.

Anesthetized dogs were used to test the noninvasive techniques (which we planned to use in humans) against standard invasive procedures. For example, the N_2O plethysmographic and C_2H_2 rebreathing methods were tested against the simultaneously determined dye dilution estimation of pulmonary blood flow. When a reproducible reliable technique was achieved in the animal laboratory, the technique was applied to human investigations. For example, the effects of tilting, exercise, and anti-G suit inflation were studied in humans through the N_2O plethysmographic method (5). The performance of a newly designed anti-G suit was evaluated by the rebreathing C_2H_2 method. The effects of catecholamines and hypoxia on the pulmonary and systemic circulation were assessed by the N_2O plethysmographic method in conjunction with analysis of the phonocardiogram, systolic time intervals, and blood flows of the extremities.

The displacement of the diaphragm upwards by the inflated anti-G suit is well recognized. In patients with obstructive lung disease, diaphragmatic breathing exercises have long been employed to facilitate gas distribution or improve efficiency of respiratory work. Because the physiologic effects of diaphragmatic breathing had not received attention, we investigated: distribution of ventilation, as measured by nitrogen washout; and topographic distribution, as determined by radioisotopic scanning after inspiring radioactive xenon. Since uneven distribution of inspired air may occur during acceleration, we developed methods to analyze the nitrogen washout curves at different respiratory frequencies in order noninvasively to estimate frequency dependence of lung compliance.

Section II of this report is devoted to the technique of transvenous stimulation of the phrenic nerve in the anesthetized dog. Such a method had to be developed: (a) to prevent obscuring the effects of changes in $+G_z$ by PPB, since ventilatory support is necessary for long-term studies; (b) to control respiratory maneuvers during the N_2O plethysmographic and C_2H_2 rebreathing techniques for estimation of pulmonary $\dot{Q}_C$; and (c) to provide

a means for ventilatory support to anesthetized animals riding a centrifuge during the assessment of the pulmonary and systemic circulations.

Section III deals with the standardization and data processing of the pulmonary $\dot{Q}_C$ pulses obtained by the N_2O plethysmographic method. Computer programs for data processing of both the N_2O plethysmographic and dye dilution methods are described.

In section IV, we measured in normal volunteers the effects on pulmonary $\dot{Q}_C$ of tilting up to 90° head-up to provide a gravitational stress. We assessed the protection of the standard USAF anti-G suit on the fall in cardiac output induced by the upright position, measured the effects of isometric exercise in the 90° head-up tilted position, and studied the effects of the standard USAF anti-G suit on cardiac output in the seated position. To our knowledge, these are the first data obtained under such circumstances--although the anti-G suit is always applied in the seated position in aviators. On the basis of our investigations, we modified the standard USAF anti-G suit in an effort to promote more anti-G protection. (Preliminary data on cardiac output determinations using this new anti-G suit are included in section VIII.)

Reuben (6) has shown that a curvilinear relationship exists between pulmonary arterial conduction time and mean pulmonary arterial pressure. The shorter the conduction time, the higher the mean pulmonary arterial pressure, and vice-versa. The pulmonary arterial conduction time can be determined noninvasively by measuring the interval from the third vibration of the first heart sound, which corresponds to opening of the pulmonic valve, to the upstroke of the pulmonary $\dot{Q}_C$ pulse. The validity of this parameter (as described in section V) was tested in 10 normal volunteers breathing hypoxic mixtures; and analysis of these data indicated that the method, as presently used, may be insensitive to small changes in pulmonary arterial pressure.

Increase of cardiac output during accelerative maneuvering ought to afford increased $+G_z$ protection. By means of the nitrous oxide technique, the effect of adrenergic agents on cardiac output was determined in 10 normal volunteers. These data (reported in section VI) indicate that relatively small doses of these agents may cause large increases in cardiac output. Moreover, indirect information indicates that pulmonary vasodilation may occur.

In section VII, the rebreathing technique for estimation of cardiac output and diffusing capacity of the lung is described, along with the computer program for data processing. This noninvasive method gives mean rather then instantaneous pulmonary $\dot{Q}_C$ as the N_2O plethysmographic

method. However, the noninvasive method has the advantage that a body plethysmograph is not required, and therefore exercise studies are readily accomplished. Finally, studies were carried out using a battery of physical analyzers. However, the pulmonary tissue volume--one of the parameters of interest in evaluating the effects of accelerative maneuvering on the lungs--could not be obtained. The pulmonary tissue volume gives a noninvasive estimate of the presence of pulmonary edema. Research results eventually indicated that mass spectrometer analysis of the test gases might be a feasible way to obtain pulmonary tissue volume in addition to pulmonary $\dot{Q}_C$ and diffusing capacity measurements.

In section VIII, the rebreathing method was used to study the effects of an anti-G suit, which inflated from the calves upwards to the abdomen, on cardiac output and diffusing capacity. The data indicate that cardiac output is increased by inflation of the anti-G suit in this manner, and suggest that such a suit might afford more $+G_z$ protection.

Section IX is concerned with the standardization and data processing of the pulmonary arterial circulation time as determined by ether plethysmographic methods. This technique was developed because, in future studies requiring anesthetized dogs, the use of a body plethysmograph during centrifugation might not be feasible. This ether plethysmographic method, which is an invasive one and requires a pulmonary arterial catheter, cannot be readily employed in human volunteers. The information obtained is useful in describing pulmonary hemodynamics during acceleration and includes pulmonary $\dot{Q}_C$, lung density, pulmonary tissue volume, and pulmonary arterial compliance. Furthermore, regional changes might possibly be measured by using the pneumotachograph as the sensing device connected to catheters placed within the lungs of anesthetized animals. (At the close of section IX are instructions on how to order supplementary information on the computer method for the processing of these data.)

In section X, the ether plethysmographic method was used to measure the pulmonary arterial compliance and the effects of interdependence in anesthetized dogs. The latter are the first reported measurements, in intact animals, on the influence of the two factors: the change in transpulmonary pressure; and the change in transmural pulmonary arterial pressure on pulmonary arterial blood volume.

Section XI deals with the effects of diaphragmatic breathing on topographic distribution of ventilation. The aim was to ascertain whether conscious diaphragmatic breathing maneuvers in the sitting position could alter preferentially direct ventilation toward the lower zones of the lungs. This question is important, because one of the well-known effects of $+G_z$

acceleration is the preferential distribution of ventilation to the upper zones and perfusion to the lower zones (7). The conclusion was that normal subjects who inspired from the residual volume position, a level analogous to $+G_z$ acceleration with the anti-G suit inflated, could preferentially direct ventilation to the lower zones--thus promoting a favorable ventilation-perfusion relationship. Whether the work of breathing in this way might be too excessive was not measured, and further study is needed before trials are set up during centrifugation.

Section XII deals with a study on the frequency dependence of distribution of ventilation. One of the purposes of this investigation was to develop a noninvasive method to assess the frequency dependence of lung compliance. The latter test is the standard means by which small airway obstruction can be detected. It requires, however, that a subject swallow an esophageal balloon and that the equipment for its analysis be rigorously calibrated and maintained. Since small airway closure might occur during accelerative maneuver, this test might provide useful physiologic information. We found that results of the noninvasive test correlate closely with those obtained by the analysis of frequency dependence of lung compliance.

REFERENCES

1. Wanner, A., and M. A. Sackner. Transvenous phrenic nerve stimulation in anesthetized dogs. J Appl Physiol 34:489-494 (1973).

2. Dougherty, R. L., et al. A new body plethysmograph for cardiopulmonary studies in man. Analyzer 3:18-27 (1972).

3. Sackner, M. A., et al. Techniques of pulmonary capillary blood flow determination. Bull Physiopathol Respir 9:1189-1209 (1973).

4. Lewis, B. M., et al. The measurement of pulmonary diffusing capacity for carbon monoxide by a rebreathing method. J Clin Invest 38: 2073-2086 (1959).

5. Segel, N., R. Dougherty, and M. A. Sackner. Effects of tilting, anti-G suit inflation and exercise on pulmonary capillary blood flow. J Appl Physiol 35:244-249 (1973).

6. Reuben, S. R. Wave transmission in the pulmonary arterial system in disease in man. Circ Res 28:523-529 (1970).

7. Glaister, D. H. Regional ventilation and perfusion of the lung during gravitational stress measured with radioactive xenon. FPRC Report No. 1236. Flying Personnel Research Committee, M.O.D. (Air Force Dept.), London, England, 1965.

II. TRANSVENOUS PHRENIC NERVE STIMULATION IN ANESTHETIZED DOGS

ABSTRACT

In this investigation we found that transvenous phrenic nerve stimulation (PNS), which maintains adequate ventilation over a prolonged period in anesthetized dogs, is useful in producing breathing maneuvers for physiologic measurements of the respiratory system. A bipolar electrode was positioned in the superior vena cava and/or the left innominate vein for right, left, and bilateral PNS by applying trains of square waves (40 - 60/sec) of 5-9 V. Normal arterial blood gases were maintained over a 6-hr period. Nitrogen washout from the lungs with oxygen revealed a single exponential curve over a range of 10 - 37.5 respirations/min during both bilateral and unilateral PNS. Static lung compliance was 0.086 liter/cm H_2O, SD 0.026; and dynamic lung compliance at 20 respirations/min was 0.078 liter/cm H_2O, SD 0.024 (P = NS). Thoracic gas volume and airway resistance were determined by a body plethysmographic technique during rapid PNS (panting). Functional residual capacity (FRC) was 45.8 ml/kg, SD 8.1; and specific lower airway conductance (from the trachea upstream) at FRC was 0.93 liter/sec per cm H_2O/liter, SD 0.31. Inspiratory airway resistance-volume curves were obtained by changing lung volume through expiratory resistances and chest strapping.

INTRODUCTION

During general anesthesia in dogs, spontaneous breathing and also intermittent PPB may lead to arterial hypoxemia due to development of shunts through atelectatic regions of the lungs (12, 18). Periodic hyperinflation of the lungs often is insufficient to completely reverse this condition. Although PNS with attendant diaphragmatic muscular contraction produces intrapleural pressure swings similar to those in spontaneous breathing, its utility in respiratory assistance has not been sufficiently explored until recently because of technical difficulties (23, 24). In 1966, Daggett et al. (7) described a convenient transvenous approach for unilateral pacing of the right diaphragm in dogs. We have extended their technique to permit either unilateral pacing of each diaphragm, or bilateral pacing of both leaves of the diaphragm. This study concerns two aspects of transvenous phrenic nerve pacing in anesthetized dogs: (a) its effectiveness in maintaining adequate ventilation as estimated from serial determinations of arterial blood gases; and (b) its usefulness in obtaining physiologic parameters not heretofore obtainable--or obtainable only by applying positive pressure on the airway. In (b), the physiologic parameters include nitrogen-washout curves, determination of thoracic gas volume, airway resistance, airway conductance-volume plots, static lung

compliance, and dynamic lung compliance at different respiratory frequencies.

RESEARCH PROCEDURES

Animals

Adult mongrel dogs were anesthetized with sodium pentobarbital, 15 - 25 mg/kg, followed by single doses of 50 - 100 mg every few hours to suppress spontaneous breathing. The animals were studied in the lateral decubitus, supine, and prone suspended positions. Altogether, electrophrenic pacing was carried out in 150 animals, including the 80 animals used in a study of tracheal mucus velocity (20). In the latter, studies were done without endotracheal intubation.

Electrophrenic Pulse Generator

A battery-powered pulse generator (Cordis, Inc., Miami, Fla.) was used for PNS (14). This device provides adjustable pulse rates and pulse durations and six different pulse amplitude modulation envelopes (monophasic or biphasic ramp, triangle, and square). It permits a range of respiratory frequency from 6.7 to 60/min. The duration of the pulse trains can be varied from 10% to 60% of the respiratory cycle. The voltage output ranges from 0 to 9 V. For square pulse train envelopes, a standard pulse generator (Grass model S 48 B, Grass Instrumentation Co., Quincy, Mass.) can also be used and has the advantage of providing a wider variety of respiratory frequencies.

For bilateral PNS with varying phase angles between the contraction of the two leaves of the diaphragm, a continuous pulse generator (American Electronic Laboratories, model 104A) was used in conjunction with the Cordis stimulator. The output signal of the Cordis stimulator to one phrenic nerve triggered an adjustable delay and pulse train duration circuit. This circuit was placed in series with the electrical output of the continuous pulse train generator whose output stimulated the contralateral phrenic nerve.

Catheter Placement for Transvenous Electrophrenic Stimulation

Catheters were introduced under fluoroscopic guidance for certain experiments, and blindly for others. The right, left, or both jugular vein(s) were exposed; and the catheter, with or without a plastic introducer, was inserted into the vein. Of the two types of 3F 125-cm-long bipolar catheters (Electrocath Corp., Rahway, N.J.) employed, one had

both platinum electrodes at the distal tip separated by a distance of 1 cm. This catheter was used without a straight end and was best suited for unilateral PNS. The electrode tip was positioned in the right or left innominate vein for ipsilateral PNS. Improper catheter position too close to the neck was indicated by simultaneous stimulation of the ipsilateral brachial plexus. Right PNS was also accomplished by positioning this catheter in the superior vena cava, as described by Daggett et al. (7). The other type of electrode catheter had one platinum electrode at the distal tip, and one which was 9.5 cm proximal from the tip; a distal loop ensured fixation of the catheter in large vessels. This type of electrode catheter was useful for achieving bilateral PNS when inserted through the left jugular vein. The catheter was so positioned that the distal pole lay in the superior vena cava, and the proximal pole in the left innominate vein close to its origin.

Electrode catheters were also introduced blindly by initiating electrical signals from the phrenic nerve stimulator immediately after inserting the catheter, and advancing it until stimulation of the brachial plexus occurred with attendant contraction of the upper limb. The catheter was then advanced a little further until the limb ceased to move and the diaphragm contracted. This method, which had the advantage of rapidity and simplicity, could not be used for bilateral stimulation. It also carried a minimal risk of producing ventricular fibrillation if the right ventricle was entered by error.

Three types of PNS were employed: (a) unilateral, resulting in contraction of one diaphragmatic leaf only; (b) bilateral synchronous, resulting in synchronous contraction of both diaphragmatic leaves; and (c) bilateral asynchronous, leading to contraction of the two diaphragmatic leaves out of phase. The time delay (phase angle) between the beginning of contraction of the two diaphragmatic leaves was determined from an electrical signal produced by the phrenic nerve stimulator--or, if possible, from the mouth-flow tracing--and expressed as an angle, taking one respiratory cycle as 360°.

Blood Gases

In 35 dogs who received bilateral or unilateral PNS in the lateral decubitus position, arterial blood was obtained every hour for 6 hr; and P_{O_2}, P_{CO_2}, and pH were determined at 37°C with an Instrumentation Laboratory blood gas analyzer (model 113). Intrapulmonary right-to-left shunt was estimated in 5 dogs after 15 min of 100% oxygen breathing at hourly intervals during 4 hr of electrophrenic stimulation (4). The oxygen saturation of the hemoglobin was measured with a Co-oxymeter (Instrumentation Laboratory model 182, Boston, Mass.).

-II-

Distribution of Ventilation

In 10 intubated dogs suspended in the prone position, nitrogen washout from the lung by 100% O_2 breathing was carried out at respiratory rates of 10, 20, and 37.5/min using bilateral synchronous, and unilateral PNS. Breath-by-breath signals of expired N_2 concentration (Nitralyzer model 505, Med. Science, St. Louis, Mo.) and tidal volume from a bag-in-box system were played through an oscilloscope recorder (Electronics for Medicine DR 12) onto analog tape. This tape was input into a small digital computer (LINC 8, Digital Equipment Co., Maynard, Mass.) for data processing by a computer program, "WASH," which plots end tidal N_2 or mixed expired N_2 log concentration against breath number, time, or accumulated volume (19). Both end-tidal and mixed-expired nitrogen concentrations were analyzed and found to be similar except during bilateral asynchronous PNS, where frequently two distinct alveolar nitrogen plateaus could be demonstrated. For this type of breathing, mixed-expired nitrogen plots will be reported, whereas end-tidal plots will be considered for all other breathing types. We found that the latter type of analysis tended to better bring out a fast compartment which occasionally could not be detected by determining the mixed-expired nitrogen concentration. Methods of analysis were based upon the equations of Fowler et al. (13), Becklake (3), and Edelman et al. (11). Corrections for tissue elimination of N_2 were made according to the equations of Simmons and Hemingway (25).

Lung Compliance

Static lung compliance was obtained with the dogs in the suspended prone position after the lungs were fully inflated with air from an AMBU-bag. Volume was measured from the bag-in-box system and transpulmonary pressure with a differential gage (DP-9, $\pm$ 2.5 psi Validyne) in which one side was connected to an esophageal balloon and the other to a catheter at the distal end of the endotracheal tube. The phrenic nerve was stimulated for 4 - 5 sec at stepwise changes of voltage in order to obtain points for a pressure-volume curve. Dynamic compliance was estimated by dividing the peak-to-peak tidal volume by the transpulmonary pressure measured at points of zero flow as delineated by a No. 0 Fleisch pneumotachograph.

Thoracic Gas Volume and Airway Resistance

These measurements were carried out upon intubated dogs who were placed in the lateral decubitus or prone position within a 170-liter Plexiglas body plethysmograph (2). For the determination of thoracic gas volume (29 dogs), rapid electrophrenic stimulation (60 breaths/min) was carried out while the animal breathed against a closed solenoid valve (9). For airway resistance measurements (12 dogs), the slope of inspiratory air

flow against plethysmograph pressure was obtained by rapid electrophrenic stimulation as the animal breathed through a No. 2 Fleisch pneumotachograph (10). Airway resistance was measured from zero to a peak inspiratory flow rate of 0.5 liter/sec. The resistance of the breathing apparatus, including an 8.5-mm endotracheal tube, was 1.38 cm/liter sec^{-1} at a flow rate of 0.5 liter/sec. The resistance was subtracted from the measured value in order to obtain lower airway resistance from the trachea upstream.

Resistance-volume and conductance-volume plots were obtained as follows: A one-way breathing valve (Rudolph Valve, Warren Collins, Braintree, Mass.) was attached to the pneumotachograph which was, in turn, connected to the endotracheal tube through a solenoid valve system. The expiratory side of the Rudolph valve was obstructed with fixed resistances which varied in magnitude. As the diaphragm was stimulated at high frequencies (60/min), air trapping occurred and the thoracic gas volume increased, thus enabling us to measure inspiratory airway resistance at lung volumes greater than the resting FRC. Volumes below FRC were obtained by strapping the animal's chest with elastic tape.

RESULTS

Feasibility of Transvenous Electrophrenic Stimulation

In preliminary experiments, we attempted to carry out phrenic nerve pacing by direct surgical exposure of the phrenic nerve in the neck. We found that, in using this technique, the passage of electrode catheters was much easier and more rapid to perform; even placement of two catheters generally required less than 30 min. The movements of animals into different body positions occasionally caused catheter dislodgement which was generally easy to correct by blindly repositioning the catheter. However, ventricular fibrillation occurred in 5 dogs (3%) in whom catheters were moved without fluoroscopic guidance.

Tidal volume ranged from 50 to 750 ml and the magnitude depended on: whether one or both leaves of the diaphragm were stimulated; the size of the animal; and the output voltage of the phrenic nerve stimulator. The square pulse amplitude envelope produced the largest tidal volume for a given output voltage, whereas the triangle and ramp elicited a smoother diaphragmatic motion. The square envelope was used for all experiments. The pulse duration, 0.4 - 0.8 msec, was delivered at a rate between 40 and 60 pulses/sec. The dc voltage ranged between 5 V and 9 V. In dogs stimulated over a 6- to 8-hr period, no signs of phrenic nerve fatigue were observed.

Table 1 shows arterial oxygen tension (P_{O_2}), carbon dioxide tension (P_{CO_2}), pH, and base excess (BE) in 45 dogs at hourly intervals without

sighing from 1 to 6 hr after initiation of PNS with a respiratory frequency of 10/min. A paired Student's t-test analysis was used, and no significant changes of these parameters with time were observed. The regression equations were: P_{O_2}: 92.43 - 0.69 mm Hg/hr (r = 0.27); P_{CO_2}: 28.25 + 0.29 mm Hg/hr (r = 0.56); pH: 7.50 - 0.01 units/hr (r = 0.78); and BE: - 1.05 - 0.28 mm/liter/hr (r = -0.48). [In these equations, r = regression ratio.] In 5 of the 45 dogs, mean intrapulmonary shunt flow was: 13% after 1 hr; 9.7% after 2 hr; 11.4% after 3 hr; and 8.5% after 4 hr (Fig. 1).

Distribution of Ventilation

The nitrogen-washout curves were analyzed to yield values for pulmonary nitrogen clearance delay, alveolar ventilation/lung volume ratios, mixing ratio, and lung clearance index. Washouts were performed at 10, 20, and 37.5 breaths/min (Table 2). In a group of 5 dogs, bilateral synchronous PNS was compared to unilateral stimulation. In another group of 5 dogs, bilateral synchronous stimulation was compared to bilateral asynchronous stimulation with a mean phase angle of 58° (range 13° - 90°). Tidal volume ranged from 117 to 387 ml at the different respiratory frequencies. Under all the preceding conditions, the lung behaved as a uniformly ventilated compartment. No significant alterations were noted in the mixing ratio and lung clearance index between the control and unilateral or bilateral out-of-phase stimulation for the same respiratory frequency (P = NS). The tidal volumes during the different maneuvers were not significantly different at the same respiratory frequency except during bilateral out-of-phase stimulation at a respiratory frequency of 37.5/min.

Lung Compliance

Static and dynamic lung compliance was determined during bilateral synchronous PNS in 22 dogs in the suspended prone position. The mean value for static lung compliance was 0.086 liter/cm H_2O, SD 0.026; and, for dynamic lung compliance at 20 breaths/min, 0.078 liter cm H_2O, SD 0.024 (P = NS). Attempts were made to measure dynamic lung compliance during unilateral or asynchronous bilateral diaphragmatic pacing. However, because of differences in transmission of true intrapleural pressure to the esophagus during such maneuvers, sufficient artifacts were introduced into the esophageal balloon pressure tracing to render it useless for dynamic compliance measurements. Occasionally, falsely low transpulmonary pressures were recorded--possibly secondary to PNS-induced contraction of the esophagus which, in dogs, contains striated muscle throughout its length (1). In most instances, this artifact could be corrected by repositioning the pacing catheter.

Thoracic Gas Volume

The mean FRC during electrophrenic stimulation in 29 dogs was 45.8 ml/kg, SD 8.1. In 12 of these dogs, placed in the lateral decubitus position, the mean FRC was 47.2 ml/kg, SD 7.5; and, in the remaining 17, in the prone suspended position, 44.8 ml/kg, SD 8.5 (P = NS).

Airway Resistance

Airway resistance was measured in 12 dogs (mean weight: 15.2; range: 9.1 - 21.4 kg) at FRC and at higher lung volumes by using a mechanical resistance during expiration; and, at lower lung volumes, by chest strapping. In all instances the panting maneuver, which is used in human determinations, was reproduced by electrophrenic stimulation at 60 breaths/min. Figure 2 shows lower airway resistance-volume plots after subtraction of the resistance of the endotracheal tube; and Figure 3, the respective lower airway conductance-volume plots. Each point represents the mean of three measurements of airway resistance and thoracic gas volume for an expiratory resistance or chest strapping. A group of smaller dogs (A) with smaller FRC can be distinguished from a group of larger dogs (B) with larger FRC on the resistance-volume and conductance-volume plots. A hyperbolic-like relation is evident between lower airway resistance and thoracic gas volume. There is also an alinear relation between lower airway conductance and thoracic gas volume.

DISCUSSION

During prolonged experiments, arterial hypoxemia and metabolic acidosis frequently occur in dogs which are moderately or deeply anesthetized, spontaneously breathing or mechanically ventilated. PNS, as evidenced by serial measurements of arterial blood gases and intrapulmonary right-to-left shunts, appears to be more advantageous in this respect. This advantage might be related to the forceful descent of the diaphragm, which occurred with phrenic nerve pacing, and to the use of sufficiently large tidal volumes to induce moderate arterial hypocapnia. Further, there was no need to induce sighing to prevent the development of atelectasis. In this respect, our findings extend the observations of Daggett et al. (8). These authors reported a marked difference in arterial oxygen tension in deeply anesthetized dogs ventilated with 100% O_2 by mechanical positive-negative pressure respirator (310 mm Hg, SD 100) and unilateral right phrenic nerve stimulator (490 mm Hg, SD 70), indicating that less intrapulmonary right-to-left shunt was present during electrophrenic stimulation. Recently, Ledsome et al. (16) found that arterial oxygenation and acid-base balance were well maintained in lightly anesthetized spontaneously

breathing dogs with chloralose or pentobarbital over an 8-hr observation period. Their regression equations for P_{O_2}, P_{CO_2}, pH, and base excess during pentobarbital anesthesia were similar to ours during PNS. However, the depth of their anesthesia might not be sufficient for invasive types of experiments.

During bilateral electrophrenic stimulation, a change in body position occasionally resulted in dislodgement of the catheter tip, with subsequent asynchronous pacing of the diaphragmatic leaves or complete loss of capture of one diaphragm. For this reason, distribution of ventilation was measured during bilateral synchronous, bilateral asynchronous, and unilateral pacing. Up to respiratory frequencies of 37.5/min, no unevenness of distribution of ventilation was detectable. The nitrogen-washout curve behaved as a single exponential. We were unable to stimulate at more rapid respiratory rates to determine whether two exponentials would become apparent because of air trapping and a marked decrease in tidal volume below the apparatus dead space volume. Trapping was related to the passive expiration during phrenic nerve pacing with insufficient time for elastic recoil to passively return lung volume to the initial resting position at rapid breathing rates.

During unilateral phrenic nerve pacing, less tidal volume was distributed to the contralateral lung; but no unevenness of distribution of ventilation could be detected by analysis of the nitrogen washout curve. Fluoroscopy revealed passive displacement of the mediastinum toward the stimulated hemidiaphragm, and a passive downward displacement of the contralateral hemidiaphragm. The result was a longer washout time than with bilateral stimulation. In man, unilateral electrophrenic stimulation produces a similar passive displacement of the mediastinum, but elevation rather than a downward movement of the contralateral diaphragm (22). This species difference might be due to the differences in integrity of the mediastinal pleura. In man, the mediastinal pleura does not permit free transmission of intrapleural pressures from one side to the other.

Asynchronous bilateral electrophrenic stimulation failed to produce an abnormal nitrogen washout curve. Since significant Pendelluft (i.e., ventilation of one lobe of a lung from another lobe without first moving the air into the bronchus) occurred during this maneuver (Fig. 4), washout time was prolonged. However, it has been shown in model lungs that Pendelluft occurring in two compartments with a common dead space tends to equalize the nitrogen concentration in each compartment (21), even when the time constants of the two compartments differ markedly. Since the time constants of the two lungs in our experiment can be presumed to be equal, it is not surprising that we were unable to demonstrate uneven distribution of ventilation.

Electrophrenic pacing permits ready determination of static lung compliance and dynamic lung compliance at different respiratory frequencies. As might be expected from the data of Brown et al. (6) no frequency dependence of lung compliance exists in normal dogs. The ability to simulate shallow panting by PNS facilitates measurements of thoracic gas volume and airway resistance by body plethysmographic techniques. It is of interest that the FRC in electrophrenically paced anesthetized dogs is significantly higher than in spontaneously breathing or paralyzed dogs (2) (48.8 ml/kg, SD 8.1, vs, 37 ml/kg, SD 9.4) ($P < .01$). Perhaps this difference is related to the lesser tendency toward atelectasis during electrophrenic stimulation. Finally, for the first time, electrophrenic pacing has made it possible to obtain airway conductance-volume plots in dogs analogous to those obtained by Briscoe and DuBois using human subjects (5). Our data show a lower airway conductance for a given thoracic gas volume in large dogs with larger FRC than in smaller dogs with smaller FRC. Our findings are in contrast to those of Briscoe and DuBois (5), who demonstrated that the values for airway conductance grouped around one regression line for children and adults. Comparison is difficult, however; for we measured lower airway resistance from the trachea upstream, whereas the values of Briscoe and DuBois for airway resistance included the glottis. The relative contribution of the glottis to the total airway resistance at different thoracic gas volumes is not clear. The difference may also be due to the fact that children have growing lungs, whereas we used adult dogs of different body weights. Further investigations will be needed to clarify why the lower airway conductance at the same absolute thoracic gas volume is higher in a dog with a small FRC than in a dog with a large FRC. Our lower airway conductance volume curves compare favorably with the lower pulmonary conductance volume curves in humans reported by Vincent et al. (26) who demonstrated a similar nonlinear relationship. Unfortunately, our method did not enable us to measure airway resistance at higher thoracic gas volumes, because it was not possible to stimulate the passively depressed diaphragm.

In the present investigations, 80 dogs were used for the study of tracheal mucus velocity. In these experiments, serial measurements had to be obtained over several hours without intubation and mechanical ventilation, while still maintaining normal blood gases in order not to affect the respective parameters. Such a study would have been impossible to accomplish without the support of electrophrenic stimulation. We have been able to demonstrate the utility of PNS in performing respiratory maneuvers in dogs where, previously, PPB had been necessary: during inspiration of a large volume of nitrous oxide in oxygen mixture for determination of pulmonary $\dot{Q}_c$ (15); and in rapid rebreathing estimation of

diffusing capacity of the lung (17). Finally, the Muller maneuver can be accomplished by stimulating the phrenic nerve against a closed airway, a prerequisite to determine pulmonary arterial compliance.

REFERENCES

1. Agostoni, E. Mechanics of the pleural space. Physiol Rev 52:57-128 (1972).

2. Avery, W. G., and M. A. Sackner. A rapid measurement of functional residual capacity in paralyzed dogs. J Appl Physiol 33:515-518 (1972).

3. Becklake, M. R. A new index of the intrapulmonary mixture of inspired air. Thorax 7:111-116 (1952).

4. Berggren, S. M. The oxygen deficit of arterial blood caused by non-ventilating parts of the lung. Acta Physiol Scand [Suppl] 2 (1942).

5. Briscoe, W. A., and A. B. Dubois. The relationship between airway resistance, airway conductance and lung volume in subjects of different age and body size. J Clin Invest 37:1279-1285 (1958).

6. Brown, R., et al. Physiological effects of experimental airway obstruction with beads. J Appl Physiol 27:328-335 (1969).

7. Daggett, W. M., J. C. Piccinini, and W. G. Austen. Intracaval electrophrenic stimulation. Part I. J Thorac Cardiovasc Surg 51: 676-684 (1966).

8. Daggett, W. M., et al. Intracaval electrophrenic stimulation. Part II. J Thorac Cardiovasc Surg 60:98-107 (1970).

9. Dubois, A. B., et al. A rapid plethysmographic method for measuring thoracic gas volume: a comparison with a nitrogen washout method for measuring functional residual capacity in normal subject. J Clin Invest 31:40-50 (1952).

10. DuBois, A. B., S. Y. Botelho, and J. H. Comroe, Jr. A new method for measuring airway resistance in man using a body plethysmograph: Values in normal subjects and in patients with respiratory disease. J Clin Invest 35:327-335 (1956).

11. Edelman, N. H., et al. Effects of respiratory pattern on age differences in ventilation uniformity. J Appl Physiol 24:49-53 (1968).

12. Finley, T. N., et al. Venous admixture in the pulmonary circulation of anesthetized dogs. J Appl Physiol 15:418 (1960).

13. Fowler, W. S., E. R. Cornish, Jr., and S. S. Kety. Lung function studies VIII. Analysis of alveolar ventilation by pulmonary N_2 clearance curves. J Clin Invest 31:40-50 (1952).

14. Furman, S., et al. Transvenous stimulation of the phrenic nerves. J Thorac Cardiovasc Surg 62:743-751 (1971).

15. Greenberg, J. J., et al. Preoperative and postoperative cardiac output determinations using an instantaneous pulmonary capillary blood flow method. Ann Thorac Surg 12:639-649 (1971).

16. Ledsome, J. R., R. J. Linden, and J. Norman. The effect of light chloralose and pentobarbitone anesthesia on the acid-base state and oxygenation of arterial blood in dogs. J Physiol (London) 212: 611-627 (1971).

17. Lewis, R. M., et al. The measurement of pulmonary diffusing capacity for carbon monoxide by a rebreathing method. J Clin Invest 38: 2073-2086 (1959).

18. Mead, J., and C. Collier. Relation of volume history of lungs to respiratory mechanics in anesthetized dogs. J Appl Physiol 14: 669-678 (1959).

19. Sackner, M. A., and N. D. Atkins. Pulpac: an on-line data processing system for pulmonary function testing. Am Rev Respir Dis 105:1013-1014 (1972).

20. Sackner, M. A., et al. Tracheal mucus velocity in dogs. (Abstract) Fed Proc 31:823 (1972).

21. Safonoff, I., and G. E. Emmanuel. The effect of Pendelluft and dead space on nitrogen clearance: Mathematical and experimental models and their application to the study of the distribution of ventilation. J Clin Invest 46:1683-1693 (1967).

22. Sarnoff, S. J., E. A. Gaensler, and J. V. Maloney, Jr. Electrophrenic respiration. IV. J Thorac Surg 19:929-937 (1950).

23. Sarnoff, S. J., E. Hardenbergh, and J. L. Whittenberger. Electrophrenic respiration. Am J Physiol 155:1-9 (1948).

24. Sarnoff, S. J., L. C. Sarnoff, and J. L. Whittenberger. Electrophrenic respiration. VII. The motor point of the phrenic nerve in relation to external stimulation. Surg Gynecol Obstet 93:109-196 (1951).

25. Simmons, D. H., and A. Hemingway. Functional residual capacity and respiratory nitrogen excretion of dogs. J Appl Physiol 8:95-101 (1955).

26. Vincent, N. J., et al. Factors influencing pulmonary resistance. J Appl Physiol 29:236-243 (1970).

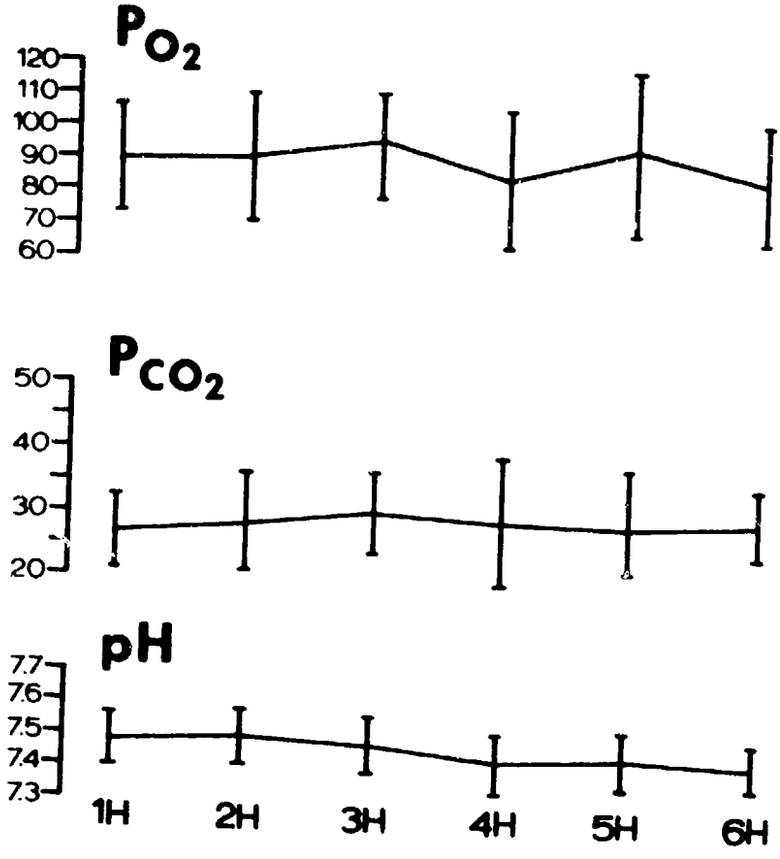

Figure 1. Mean arterial P_{O_2} (mm Hg), P_{CO_2} (mm Hg), and pH (units) in 45 dogs at hourly (H) intervals after initiation of phrenic nerve stimulation (PNS). [The vertical bars represent 1 SD.]

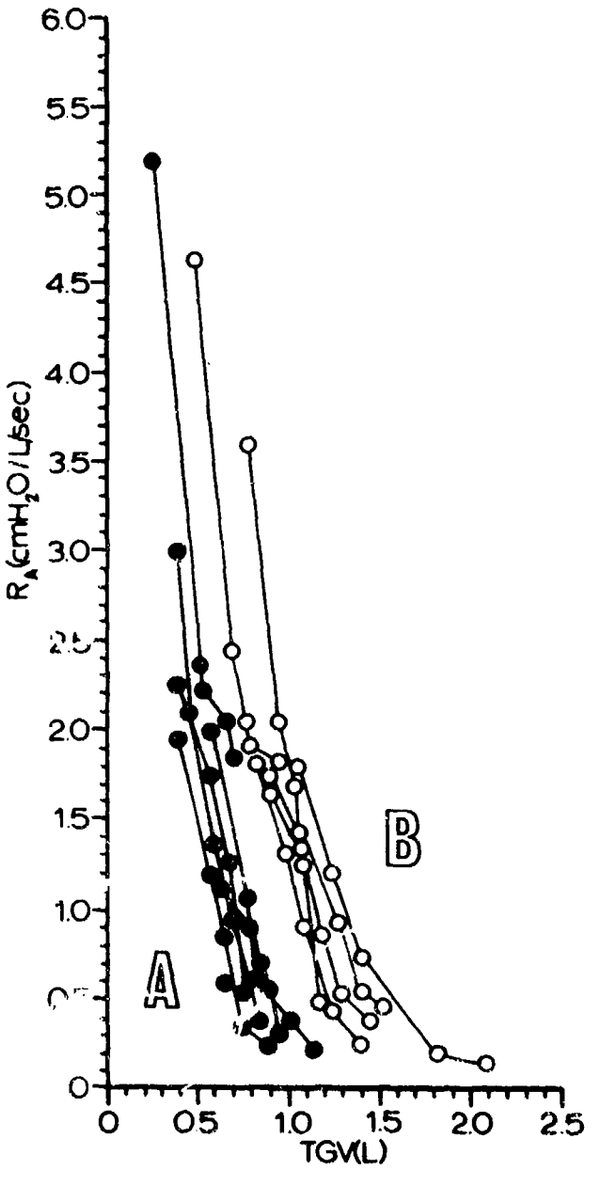

Figure 2. Lower airway resistance-volume curves of 12 dogs. [Solid symbols represent a group (A) of smaller dogs (mean weight: 11.6 kg; range: 9.1 - 13.2 kg) with a mean FRC of 0.525 liter (range: 0.400 - 0.700 liter). The open symbols represent a group (B) of large dogs (mean weight: 18.9 kg; range: 15.9 - 21.4 kg) with a mean FRC of 0.925 liter (range: 0.600 - 1.100 liter). TGV = total gas volume; R_A = alveolar resistance.]

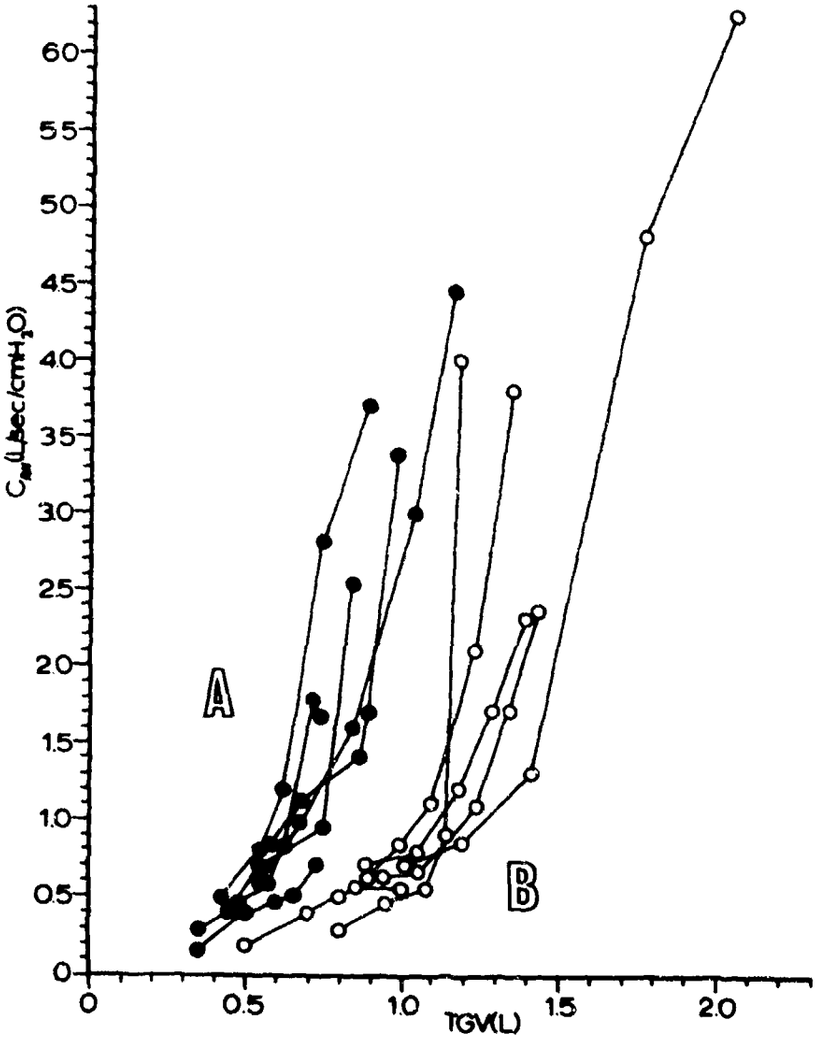

Figure 3. Lower airway conductance-volume curves of 12 dogs. (For key to symbols, consult legend for Fig. 2. C_{AW} = compliance airways.)

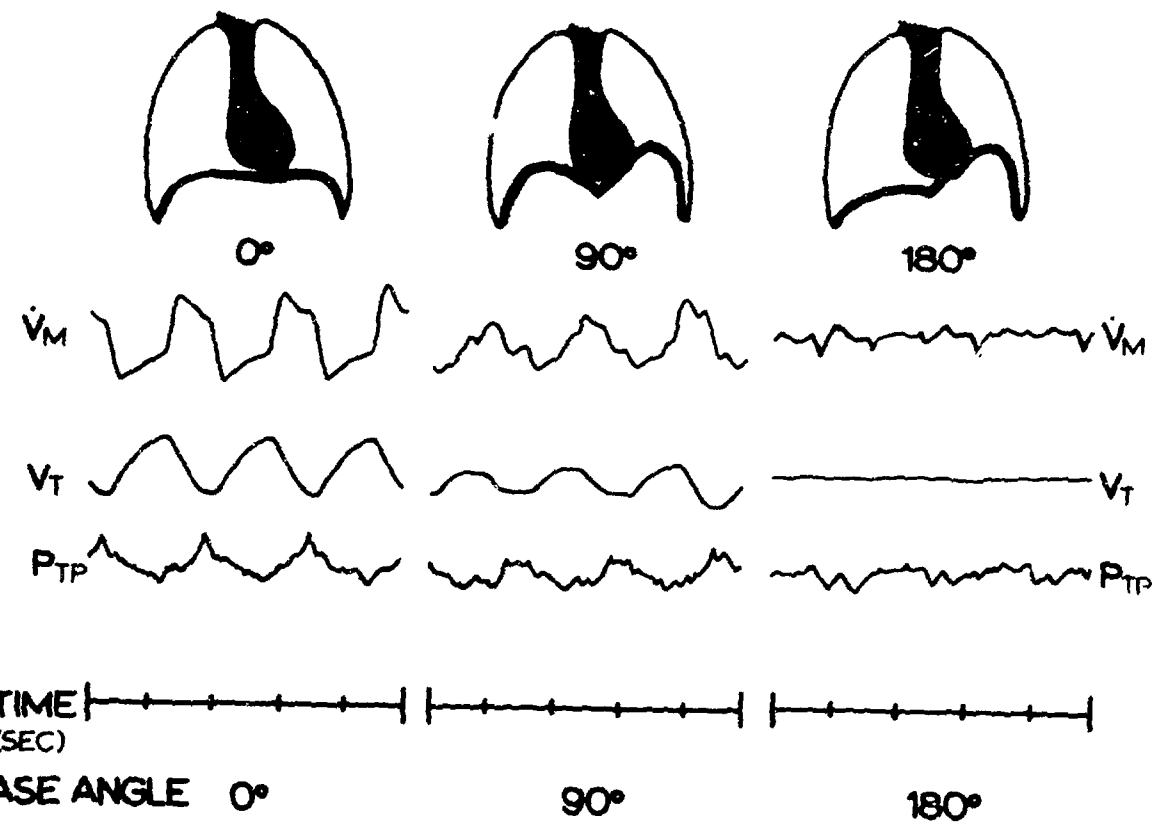

Figure 4. Indirect evidence of Pendelluft during bilateral asynchronous PNS at 0°, 90°, and 180° phase angle between the stimulation of the left and right phrenic nerve. [$\dot{V}_M$ = mouth flow; V_T = tidal volume; P_{TP} = transpulmonary pressure (measured with esophageal balloon catheter). The corresponding fluoroscopic appearance of the positions of the right and left hemidiaphragm at mid-inspiration is schematically shown at top of figure.]

TABLE 1. EFFECTS OF PNS ON ARTERIAL BLOOD GASES AND ACID BASE STATE OVER A 6-HR PERIOD. (VALUES ARE MEANS OF 45 DOGS WITH 1 SD.)

Time (hr)	1	2	3	4	5	6
P_{O_2} (mm Hg)	89.5 (± 17.1)	90.3 (± 20.0)	96 (± 16.2)	85.4 (± 21.7)	94.8 (± 24.8)	84.1 (± 18.9)
P_{CO_2} (mm Hg)	27.9 (± 6.5)	28.7 (± 9.3)	30.7 (± 7.1)	29.1 (± 10.4)	29.3 (± 8.8)	29.9 (± 6.6)
pH (units)	7.47 (± 0.08)	7.50 (± 0.09)	7.48 (± 0.08)	7.44 (± 0.09)	7.45 (± 0.09)	7.44 (± 0.07)
BE (mEqu /L)	-1.8 (± 0.5)	0 (± 0.7)	-2.8 (± 0.4)	-3 (± 0.5)	-2.0 (± 0.3)	-2.5 (± 0.4)

BE = base excess.

TABLE 2. COMPARISON OF NITROGEN WASHOUT DURING BILATERAL SYNCHRONOUS AND UNILATERAL PNS (5 DOGS), AND BILATERAL SYNCHRONOUS AND BILATERAL ASYNCHRONOUS (5 DOGS) PNS AT 3 DIFFERENT RESPIRATORY FREQUENCIES. (MEAN VALUES WITH 1 SD IN PARENTHESES.)

	Nitrogen Washout During PNS									
RF	V_T	$V_{A/L}$	N_2-CD	MR	LCI	V_T	$V_{A/L}$	N_2-CD	MR	LCI
	(Bilateral synchronous PNS)					(Unilateral PNS)				
10	0.223 (0.080)	2.10 (0.69)	0	1.61 (0.55)	7.83 (2.80)	0.225 (0.074)	3.08 (0.67)	0	1.49 (0.42)	7.26 (2.14)
20	0.224 (0.055)	3.01 (0.87)	0	1.97 (0.62)	9.52 (3.04)	0.186 (0.076)	3.40 (0.72)	0	1.51 (0.37)	7.53 (1.94)
37.5	0.176 (0.040)	5.05 (0.95)	0	2.34 (1.10)	11.40 (5.44)	0.143 (0.038)	3.69 (1.50)	0	1.81 (0.73)	9.70 (4.56)
	(Bilateral synchronous PNS)					(Bilateral asynchronous PNS)				
10	0.387 (0.060)	2.17 (0.47)	0	2.39 (0.67)	11.37 (3.16)	0.366 (0.052)	1.78 (0.56)	0	2.50 (0.57)	12.00 (2.54)
20	0.344 (0.098)	2.39 (0.41)	0	2.51 (0.45)	11.87 (1.97)	0.219 (0.063)	1.64 (0.82)	0	2.92 (0.85)	13.71 (3.87)
37.5	0.174 (0.013)	2.03 (0.58)	0	3.58 (0.96)	16.78 (4.37)	0.117* (0.013)	1.33 (0.45)	0	2.91 (0.71)	14.64 (3.61)

RF = respiratory frequency (breaths/min); V_T = tidal volume (L); $V_{A/L}$ = alveolar ventilation per lung volume ratio; N_2-CD = nitrogen clearance delay (%); MR = mixing ratio; and LCI = lung clearance index.

* $p < .02$.

III (Parts 1, 2, and 3). DESIGN OF BODY PLETHYSMOGRAPH AND TECHNIQUES OF DETERMINATION OF INSTANTANEOUS PULMONARY $\dot{Q}_c$

PART 1: DESIGN OF BODY PLETHYSMOGRAPH

ABSTRACT

Technical details of a body plethysmographic system are described which permits ease of operation of standard tests (e.g., airway resistance) as well as research examinations (e.g., a noninvasive nitrous oxide technique to measure cardiac output). The chamber is designed to operate between horizontal and vertical angles such that changes in pulmonary and hemodynamic parameters can be studied with the subject in different body positions. In addition to noninvasive techniques, studies which require placement of a pulmonary arterial catheter (e.g., estimation of pulmonary arterial blood volume and tissue volume) have been carried out with this system for the first time in man.

INTRODUCTION

The technical specifications of the body plethysmograph used for human studies are described in Part 1 of this report section. Part 2 deals with the actual techniques used, and their standardization. (In Part 3, instructions are given concerning how to order supplementary information on the operation of the computer program, "LAUGH," for data processing of instantaneous pulmonary capillary blood flow pulses.)

MATERIALS AND METHODS

Plethysmograph, Supporting Cradle, and Drive Mechanism

The shell of the plethysmograph and its supporting frame were manufactured by contractors(1) according to our specifications, but both components required extensive in-house modification during the installation in our laboratory. The shell of the chamber (Fig. 1) consisted of 1-in.-thick Plexiglas, molded into a half-cylindrical shape (Fig. 1, point a). Its radius of curvature was 31 in.; and its length, 89 in. The chamber volume was approximately 650 liters. Initially, the edge of the half-cylinder was cemented as a butt joint to a flat sheet of Plexiglas, 1-in.-thick, which

EDITOR'S NOTE: Sources of specific equipment and materials are keyed, by parenthesized numerals in the text, to corresponding list at the close of Part 1 (pp. 40-42).

formed the base of the chamber (Fig. 1, point b). This union proved faulty and cracked upon pressure testing at 50 cm H_2O. It was necessary to redo the flat sheet of Plexiglas so that the edge of the half-cylinder dome could be cemented into a "rooted out" 1-in. track, forming a tongue-in-groove joint. Such a joint has remained airtight to the limit we have tested (i.e., 100 cm H_2O pressure).

Angle-iron brackets (2" x 2" x $\frac{1}{2}$") form the framework which supports the chamber (Fig. 1, point c). The framework is joined to the cradle by two self-aligning roller bearings located at the midpoint of the chamber (Fig. 1, point d). The cradle is constructed from welded sections ($2\frac{1}{2}$" x $2\frac{1}{2}$" x $\frac{1}{4}$") of steel tubing (Fig.1, point e). Hard rubber casters (5 in. diam.) are attached to the base of the cradle, thus allowing the entire assembly (weighing about 3,000 lb) to be moved with minimal efforts (Fig. 1, point f).

The drive mechanism allows the plethysmograph to be tilted to any point between its horizontal and vertical positions. It consists of a 3/4-hp electric motor (2) attached to a speed reducer (3) which drives a 1-in.-thick worm gear. The time required to tilt from the horizontal to an extreme vertical position is 1 min 32 sec. The speed reducer has been modified for dual inputs, allowing a pneumatic motor (4)--in case of electrical power failure in the tilted position--to return the chamber to the horizontal position. This modification is accomplished through an interlocking quick-connect motor-drive coupling.

Patient Table and Door

A table, upon which the patient is placed, rides on 8 roller bearings in aluminum tracks attached to the inner walls of the Plexiglas shell (Fig. 1 point g). The table is a standard fluoroscopic item (5) strengthened by a stainless-steel channel bordering its edge. In the horizontal, or patient entry position, the table can be partially or completely removed from the chamber by supporting its weight with one or two steel stands, each having a vertical height adjustment. The stands have casters which permit rapid transfer of the patient to and from the cardiac catheterization room for fluoroscopic studies, if these are required. A footrest (Fig. 1, point h), guided by stainless-steel tracks at the base of the table, is adjusted by two 3/4-in. aluminum rods with locking wheel type bolts. The footrest is used to keep the patient properly positioned when the plethysmograph is tilted into a vertical position. A blower (6), placed at the edge of the footrest, is used to circulate the air within the chamber between tests.

The door of the chamber, shaped from 1-in.-thick anodized aluminum plate (Fig. 1, point i), can be readily removed from the head end of the table by loosening two bolts on a bracket and can be sterilized (if desired) by exposure to ethylene oxide gas. The door has a number of penetrations for 1/8-in. and 1-in. Swagelok bulkhead connectors (7) (Fig. 1, point j). Hermetically sealed bulkhead unions permit electrical penetrations (8).

Six pneumatic lamps (9) are used to seal the door against the flange of the chamber which is covered with a $\frac{1}{2}$-in.-thick closed cell neoprene gasket (Fig. 1, point k). The pneumatic clamps operate on a line pressure of 110 psig and are activated through a 4-way electrical solenoid valve (10). The opening and closing speed of each clamp is controlled by two flow-governors per clamp (11).

Breathing Apparatus

This apparatus consists of a manifold controlled by electrical solenoid valves from switches located outside the chamber (Fig. 1, point l). A 24-VDC power supply (12), located on a shelf on the cradle, supplies the necessary current to the valves. All electrical penetrations into the chamber are of DC voltage, 12 to 24 VDC, so as not to create a safety hazard. In the manifold of 5 electrical solenoid valves (13), the following four breathing maneuvers are possible: (a) flow directly through a pneumotachograph for measurement of airway resistance; (b) flow of air from the chamber on a directional basis; (c) inspiration of a test gas contained in a bag within the chamber, and expiration into the chamber; and (d) breathing of air or test gas on a directional basis from outside the chamber. The breathing manifold may be positioned through rotation of a shaft in a ball pressure joint mounted on the door bracket (14), thus allowing the subject to be studied in the prone, supine, decubitus, and vertical positions. The breathing manifold has penetrations for sampling gas and measuring pressure at the subject's mouth. Fleisch pneumotachographs (15) are used to measure rapid or slow respiratory flow rates. The pressure difference across the pneumotachographic resistance is sensed by a variable reluctance transducer (16) connected to a carrier demodulator (17). The output from the carrier demodulator is fed into an oscilloscopic recorder, and is also input into a center reading dc microampere meter with a variable 100 K ohms shunt. The meter is placed outside the chamber at eye level, so that the subject can monitor his own expiratory flow rates should the test require this control (Fig. 1, point m).

-III-
(Part 1)

Electropneumatic Servo Unit

Changes in chamber pressure occur with time, owing to an increase in temperature and humidity from the breathing subject and in heat transferred from the chamber to the room. Consequently, it is necessary to vent the chamber to the room before performing such tests as pulmonary $\dot{Q}_C$. Upon closing of the vent, however, unpredictable baseline drifts of chamber pressure may occur due to room air of different temperature and humidity (from that in the chamber) entering the plethysmograph (Fig. 2). Because variable baseline drift affects the accuracy of pulmonary $\dot{Q}_C$ measurements, we modified an electropneumatic servo system to function as a compensating device between tests to eliminate venting of the chamber. The block diagram of the servo system is depicted in Figure 3. One side of a variable reluctance differential pressure gage (18) is connected to the plethysmograph (Fig. 3, point a), while the other side is referenced to the chamber through a short length of insulated high-pressure nylon tubing immediately preceding activation of a servo loop. The reference side of the gage is closed via a solenoid valve (Fig. 3, point b). We have modified an electropneumatic transducer relay (19) such that its output is zero flow through a linear resistor (20) at atmospheric pressure. An increase in chamber pressure causes air to be withdrawn from the chamber; a decrease causes air to be added to it. A detailed drawing of the electropneumatic servo relay modification constitutes Figure 4. An augmenting differentiator circuit is necessary to linearize the flow output of this device (Fig. 5). The function of the servo system is to maintain the chamber at atmospheric pressure by a negative feedback loop. Although this device has been used as a differentiator to obtain a record of instantaneous flow of gas into the lungs--a parameter necessary for pulmonary $\dot{Q}_C$ measurements--at Mount Sinai Hospital the device has tended not to be as stable as electrical differentiation of the pressure signal (Fig. 6). A schematic of the circuit of the differentiating network is shown in Fig. 7. The servo device is useful in conjunction with the differentiating network because it maintains baseline pressure when the electrical differentiator circuit is switched in as the detecting device during expiration or breathholding maneuvers. In actual test procedure, the electropneumatic servo system is used to keep the chamber at atmospheric pressure during tidal breathing as well as during inspiration of air or N_2O, a procedure necessary for pulmonary $\dot{Q}_C$ measurements. As the subject slowly expires, or breathholds, the servo system is turned off by a solenoid valve; changes in chamber pressure are detected by the sensitive variable reluctance differential transducer, and then electrically differentiated. The signal, before output, is passed through a low-pass filter (21) with a cutoff frequency of 9.5 Hz to eliminate any high-frequency artifacts. Under these conditions, the run always starts from the same absolute chamber pressure.

-III-
(Part 1)

Pneumatic Accessories

Two variable volume piston pumps (22) are on the underside of the chamber. The larger pump has a capacity from 50 to 500 ml/stroke, and a 2-speed drive from 10 cpm to 30 Hz. The small pump has a capacity from 1 to 60 ml/stroke, and a speed from 1 to 36 Hz. The large pump is used for research studies; the small pump is used for calibration of the chamber, the electropneumatic servo unit, and the differentiator network. On the cradle of the plethysmograph are two other pumps. A syringe pump (23) with a constant stroke of 30 ml and a 0 to 50 cpm speed is used to calibrate the plethysmograph for measurements of airway resistance and FRC. A combination vacuum-pressure pump (24) is used to apply constant pressure or vacuum to the chamber. Regulation of the latter is achieved by means of a photohelic switch (25).

Data Collection System

Information from the body plethysmograph is input into a DR-12 oscillographic recorder equipped with a Universal Matching Amplifier system (26). This amplifier system insures a signal output onto analog tape, or into a computer, of $\pm$ 1 volt. Data are either read out directly from the oscillographic recorder (as in studies of airway resistance or FRC), or are input into the LINC digital computer or a 7-channel analog tape recorder (27) for off-line processing by the LINC 8 digital computer (28) (as in N_2O capillary blood flow or ether circulation time studies). For the latter, data are played from the tape first into an IR-4 recorder (29) with dc amplifiers, so that signals can be monitored on the oscilloscope of the recorder before their input into the analog-to-digital convertors of the LINC 8 computer through a Universal Matching Amplifier System.

Safety Factors

Safety factors have been designed into the plethysmographic system according to the following schema: electrical failure, pneumatic failure, and general factors. If electrical failure occurs while the subject is enclosed within the plethysmograph, the pneumatic clamps will open automatically. If the plethysmograph is in the tilted position, the pneumatic motor can be connected to the drive shaft and the chamber brought from the fully vertical to horizontal position within 1 min 58 sec. In case of pneumatic failure, the clamps can be opened manually. If both electrical and pneumatic failure occur, a standby "G" cylinder of compressed air is in readiness for the pneumatic motor and clamps. General safety factors include flow-governors on each door clamp, to limit closing and opening speed. The Plexiglas shell allows visual communication in and out of the

chamber, and a telephone system (30) affords "hands free" audio communication. The penetration for the electrocardiographic cable is made through the Plexiglas shell and is isolated from other electrical cables. Direct current of low voltage is used for power within the plethysmograph; no alternating current device is enclosed within the chamber. The door of the chamber can be sterilized if a joint cardiac catheterization study is contemplated.

SOURCES OF EQUIPMENT AND MATERIALS

1. Plexiglas shell manufactured by "K" Plastics, San Francisco, Calif.; cradle constructed by Research Machine Shop, U. of California, Medical Center, San Francisco, Calif.

2. Century Electric Co., St. Louis, Mo.; electric motor model #CSX-68-FKK3-Fa, 3/4 hp, 1750 rpm.

3. Winsmith, Division of UMC Industries Inc., Springville, Erie Co., N. Y., N. Y.; speed reducer model #3SF, ratio 18:1.

4. Dotco, Inc., P.O. Box 182, Hicksville, Ohio; pneumatic motor model #22V7340, 0.9 hp, 3,200 rpm.

5. Picker X-Ray Corp., Watte Mfg. Division, Cleveland, Ohio; standard Fluoroscopic table.

6. Dayton Electric Mfg. Co., Chicago, Ill.; wheel blower model #2C646, 12 VDC, 1380 rpm.

7. Crawford Fitting Co., 29500 Solon Road, Solon, Ohio; Swagelok 1/8-in. bulkhead union part #200-61-316, Swagelok 1-in. bulkhead union part #1610-61-316.

8. Deutsch, Electronics Components Division, Municipal Airport, Banning, Calif.; electrical bulkhead union part #DM5621-7pp.

9. De-Sta-Co Division, Dover Corp., 350 Midland Ave., Detroit, Mich.; pneumatic clamp model #CH-1012.

10. Automatic Switch Co., Florham Park, N.J.; 4-way solenoid valve cat. #834472, 24 VDC.

11. Scovill Mfg. Co., Fluid Power Division, Wake Forest, N.C.; Schrader speed control valve part #3250 MA.

12. Kepco Inc., 131-38 Sanford Ave., Flushing, N.Y.: power supply, #PRM 24-5, 24 VDC, 5 amp.

13. Automatic Switch Co., Florham Park, N.J.: the manifold consists of three normally open solenoid valves cat. #82 15 33, 3/4 in. pipe, and two normally closed valves cat. #82 100 95, 3/4 in. pipe. All are 24 VDC.

14. Wilton Mfg. Co., Schiller Park, Ill.: Powerram Jr. ball pressure joint.

15. Instrumentation Assoc., 17 West 60th St., N.Y., N.Y.: for rapid flow rates, Fleisch pneumotachograph #7320 (#2); and for slow flow rates, Fleisch pneumotachograph #7318 (#0).

16. Pace Engineering Co., North Hollywood, Calif.: variable reluctance transducer model #P7D 0.2 PSID.

17. Validyne Corp., Northridge, Calif.: carrier demodulator transducer indicator model #CD 12.

18. Validyne Corp., Northridge, Calif.: differential pressure gage, model #DP 45, 1" H_2O.

19. Worthington Controls Co., Division Worthington Corp., Norwood, Mass.: Masoneilan Transducer Model 8006-3-15-PS, Relay #60942-4-999.

20. Nupro Company, 15635 Sarnac Road, Cleveland, Ohio 44110: Inline Filter catalog #4F, 7 micron Element $\frac{1}{2}$ Swagelok.

21. Burr Brown, International Airport Industrial Park, Tucson, Ariz.: Active Filter, #5706-LP7B-9R50.

22. Small Parts Inc., 6901 N.E. Third Ave., Miami, Fla.: special acknowledgement to Edward Favre for the design and manufacture of both the large and small piston pumps.

23. Harvard Apparatus Co., Dover, Mass.: syringe pump and speed control model #607.

24. Gast Mfg. Corp., Benton Harbor, Mich.: combination vacuum-pressure pump model #0440-P107A.

25. Dwyer Instruments Inc., Michigan City, Ind.: photohelic switch cat. 2050C.

26. Electronics for Medicine, White Plains, N.Y.: oscillographic recorder model #DR 12 and compatible Universal Matching Amplifier.

27. N.V. Philips, Gloeilampenfabrieken, Endhoven: seven-channel analog tape recorder model #EL 1020/02/04/07.

28. Digital Equipment Co., Maynard, Mass.: LINC 8 computer.

29. Electronics for Medicine, White Plains, N.Y.: oscillographic recorder model #IR 4 and compatible Universal Matching Amplifier.

30. Southern Bell Telephone and Telegraph Co., 330 Biscayne Blvd., Miami, Fla.: hands free conference phone audio communication system.

FIGURES 1 - 7

for

Section III: Part 1

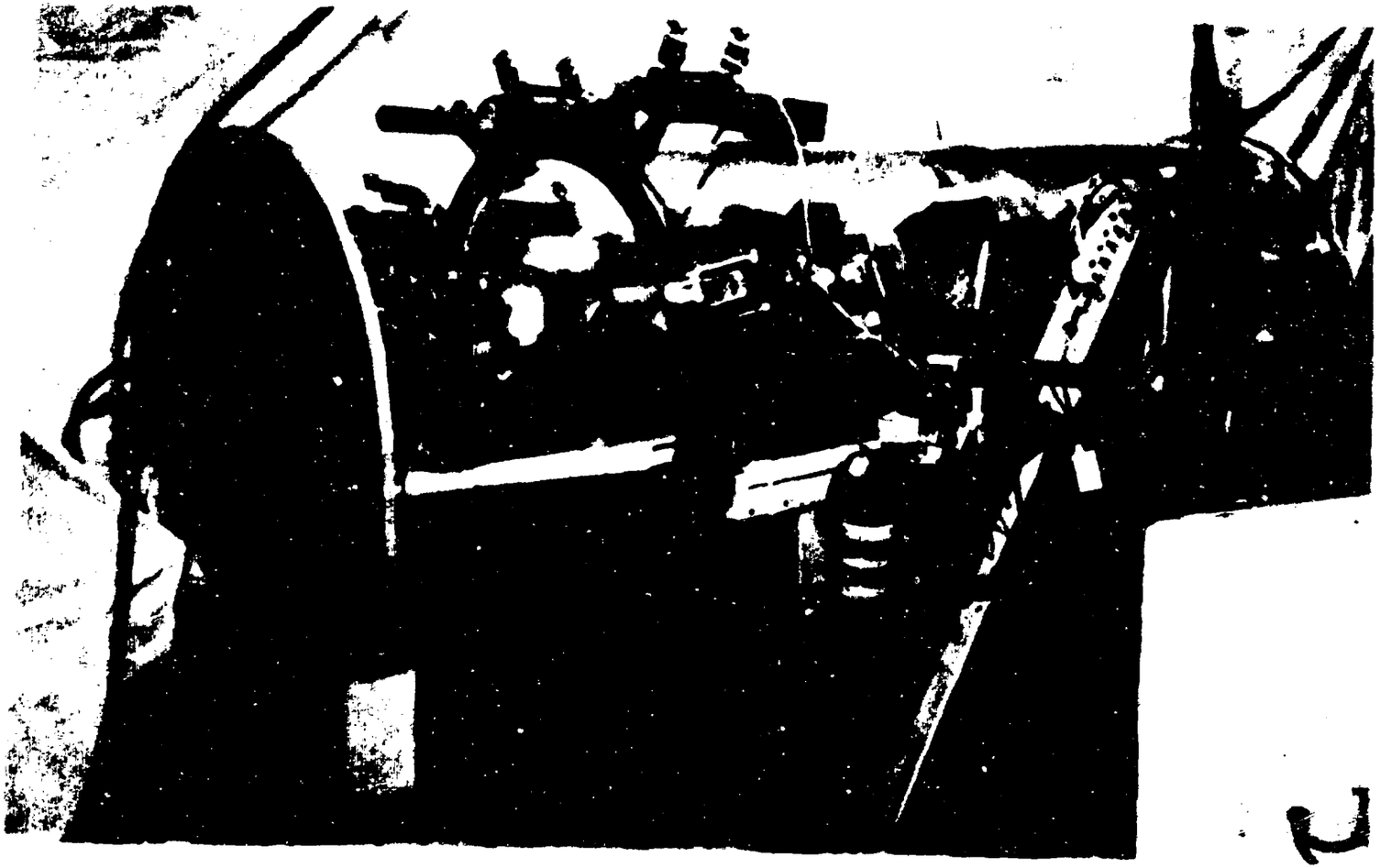

Figure 1: View A. Body plethysmograph in a horizontal, or patient entry, position.
[Continued in View B, on facing page (below)]

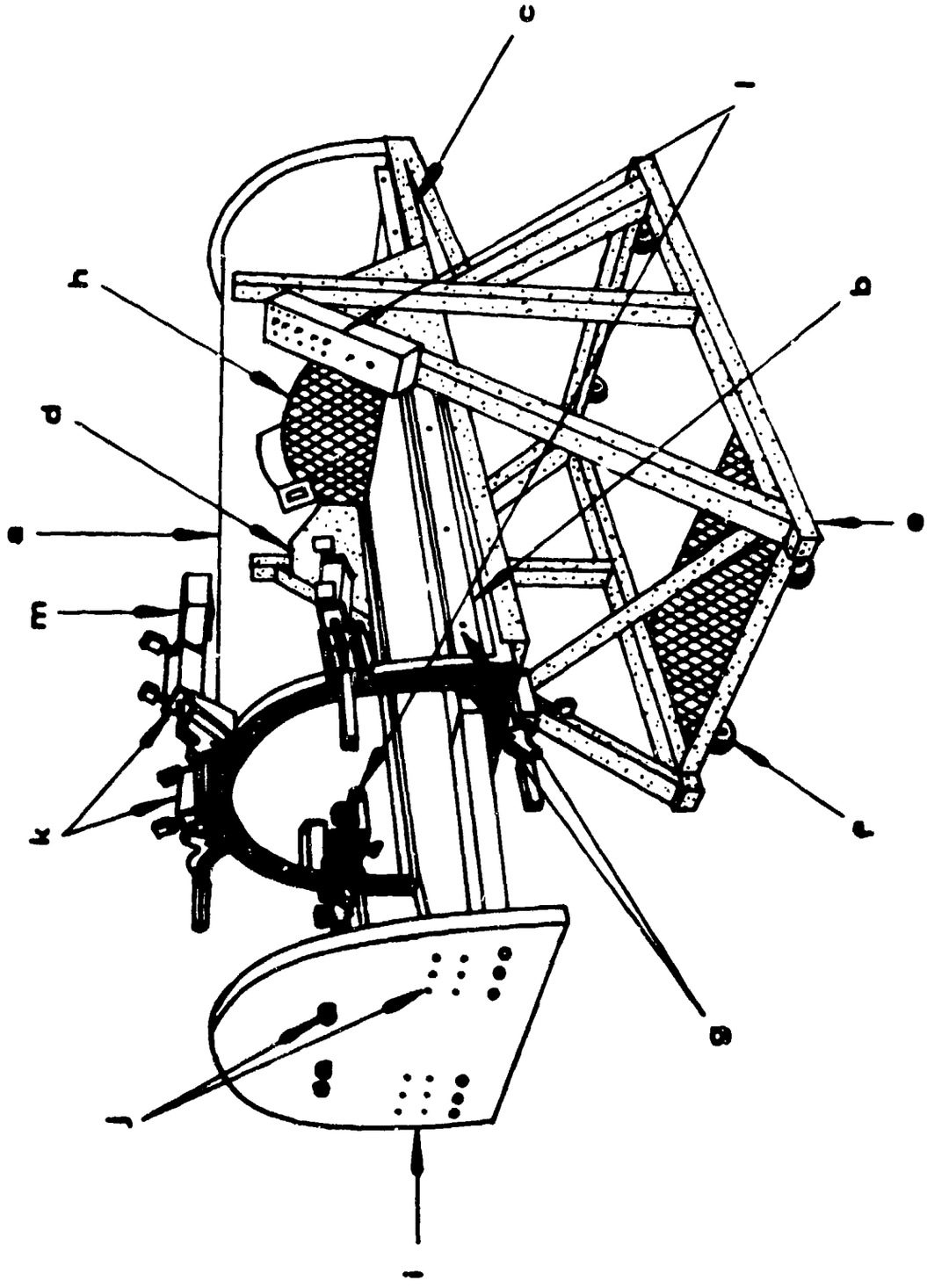

Figure 1 [continued from facing page (above)]: View B. Schematic diagram of body plethysmograph. (Points a - m are identified in text.)

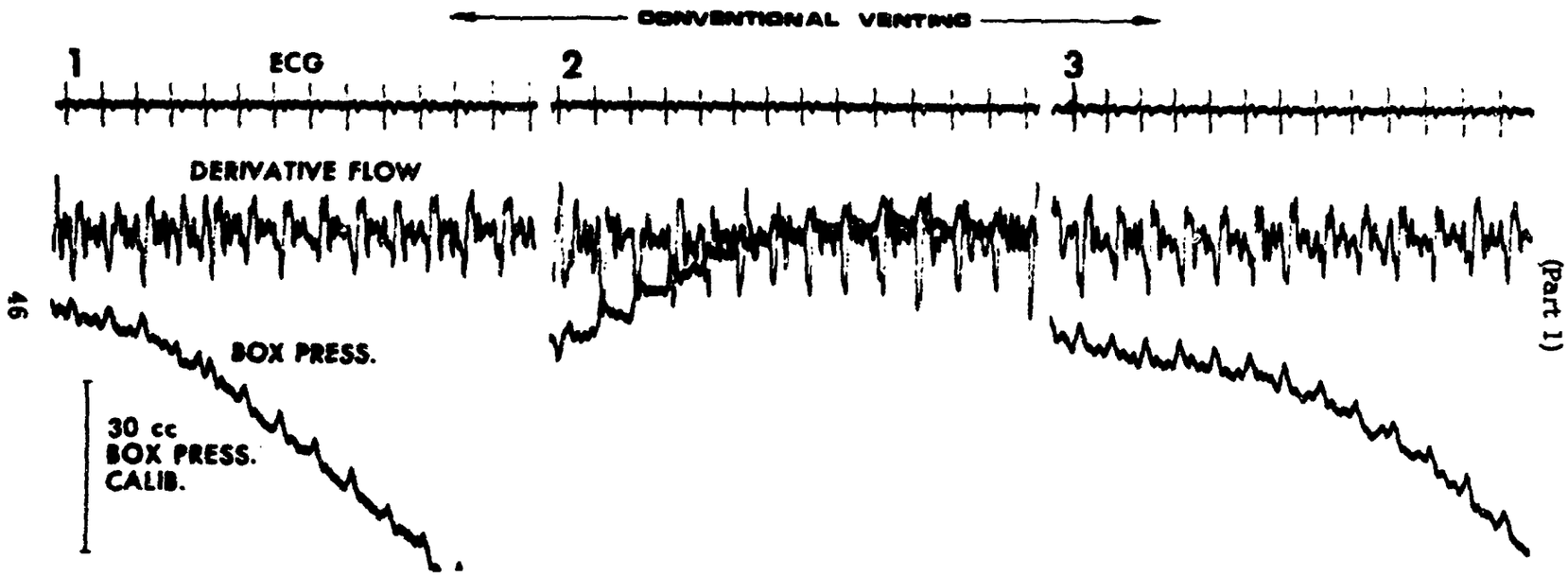

Figure 2. Comparison of conventional chamber venting (View A, above), revealing random box pressure baseline drifts, to the electropneumatic servo system (View B, below) which appears more stable.

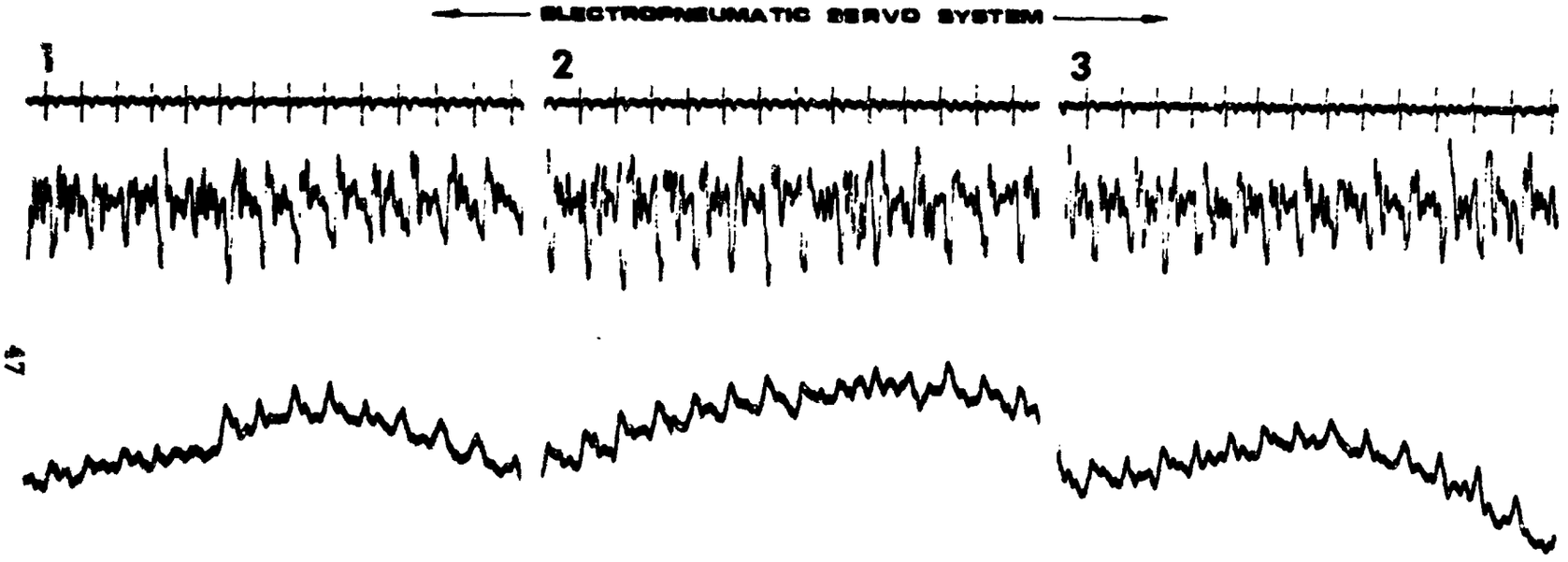

Figure 2 (continued from facing page, above): View B.

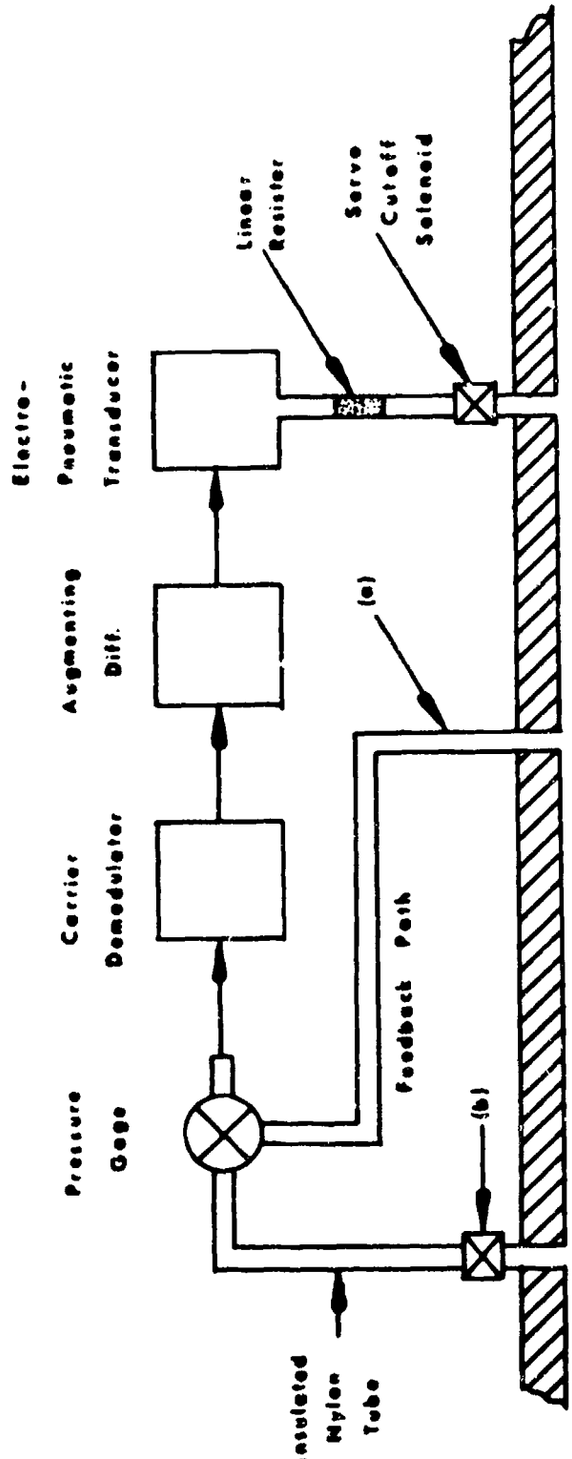

Figure 3. Electropneumatic servo system with unity feedback control. (Block diagram)

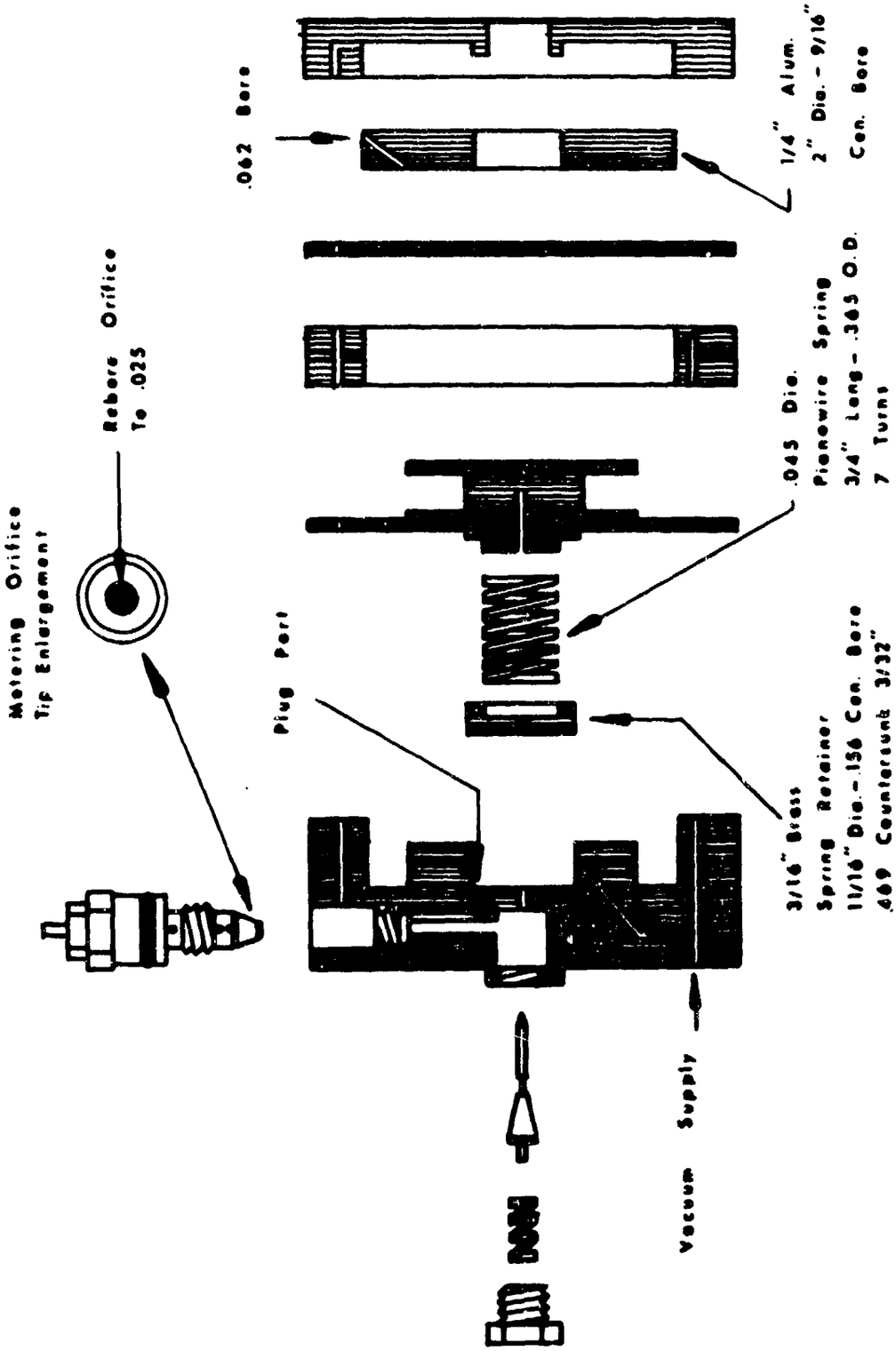

Figure 4. Modification of the Masonellan electropneumatic servo relay for positive and negative pressure output.

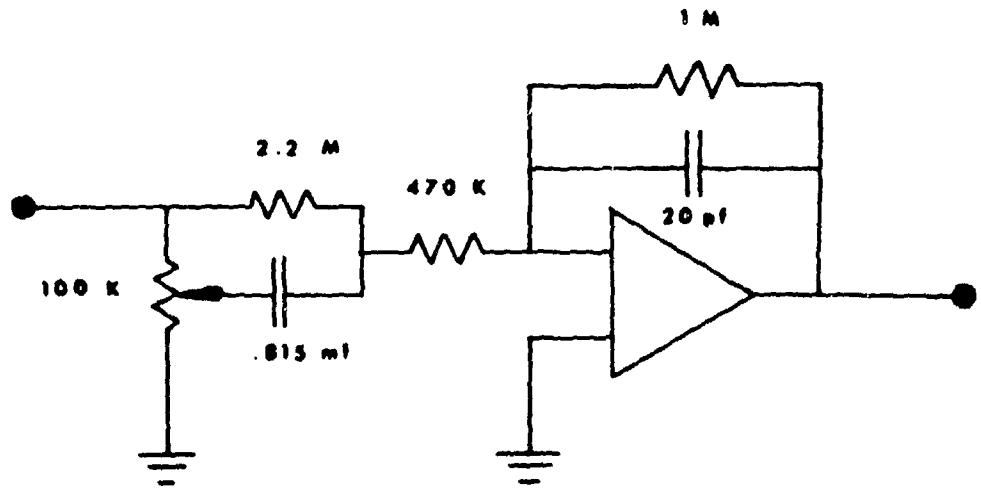

Figure 5. The augmenting differentiator. (Schematic diagram)

AIR RUN

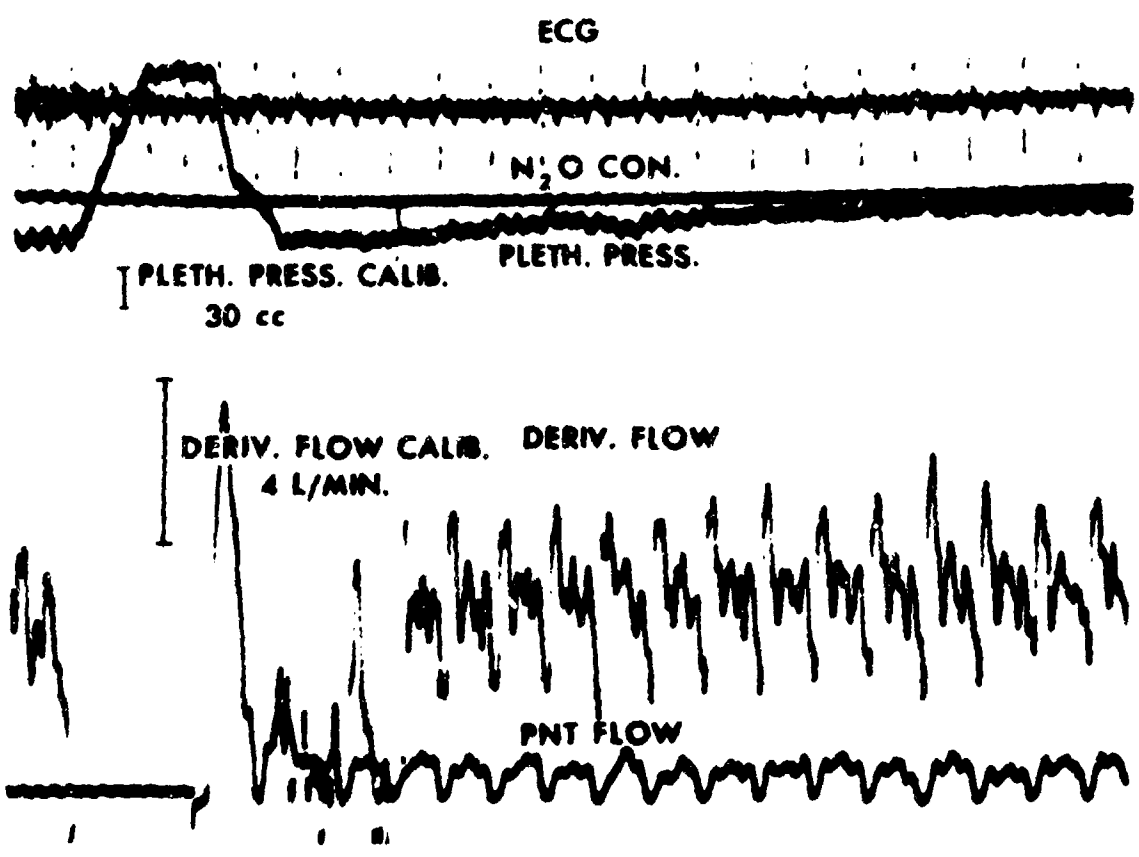

Figure 6: View A. Air and N_2O runs using the differentiating network for measurement of pulmonary $\dot{Q}_c$. [See facing page for View B.]

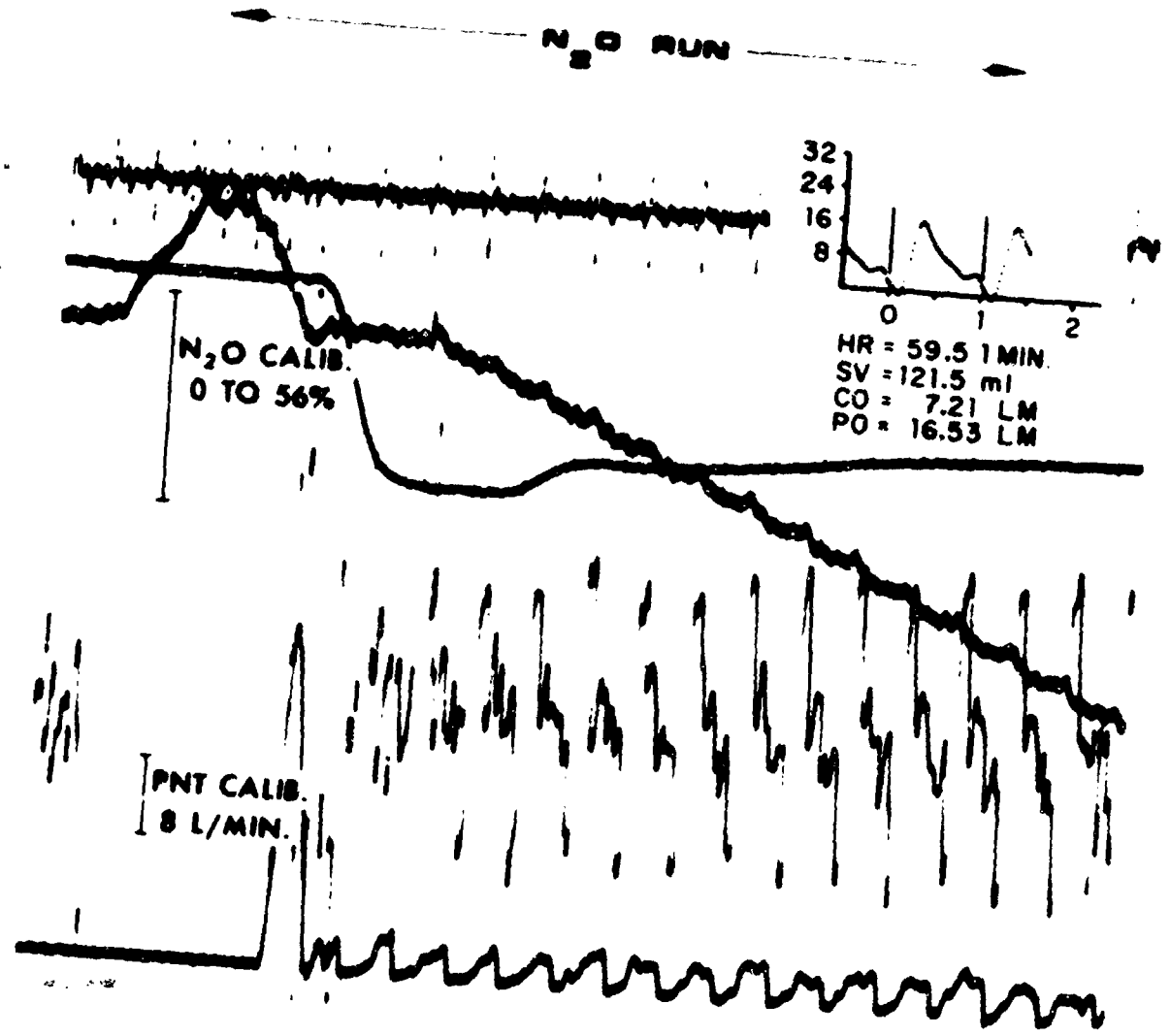

Figure 6 (cont'd.): View B. Air and N_2O runs using the differentiating network for measurement of pulmonary $\dot{Q}_C$. [Key (inserted upper right) shows computer display of final processed data:

HR = heart rate
SV = stroke volume
CO = cardiac output
PO = peak output.

See facing page for View A.]

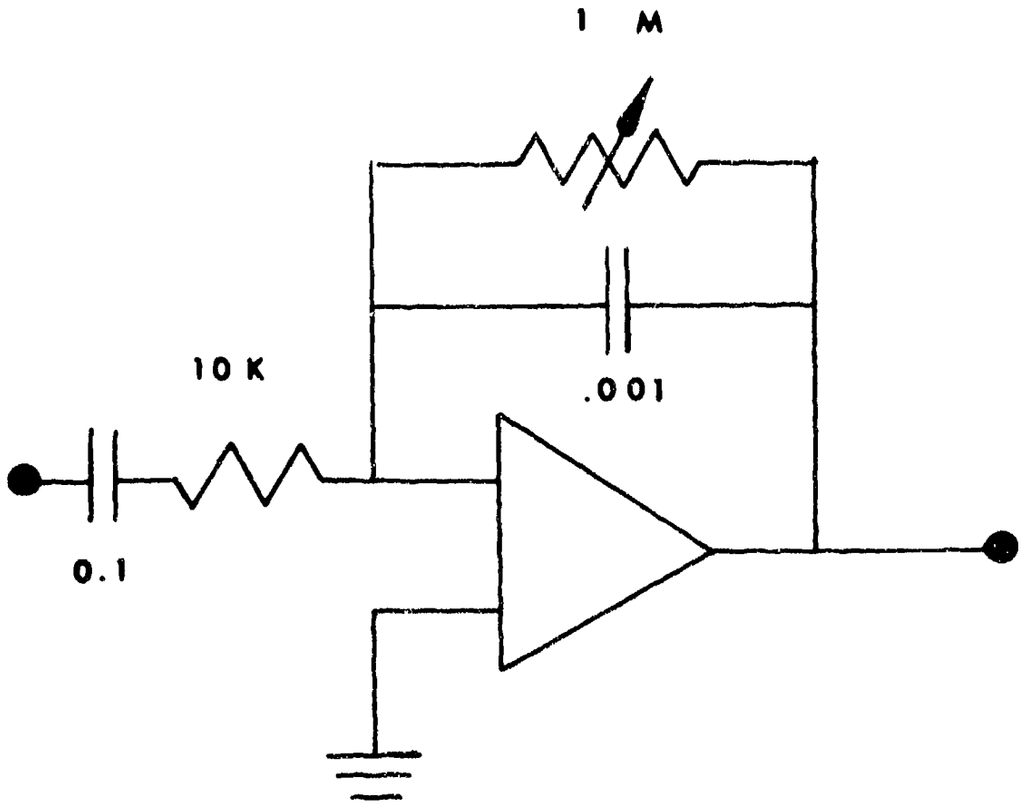

Figure 7. The differentiating circuit. (Schematic diagram) (The operational amplifier is a Philbrick-Nexus P85 AU. All capacitors are in microfarads.)

-III-
(Part 2)

PART 2: TECHNIQUES OF PULMONARY CAPILLARY BLOOD FLOW ($\dot{Q}_c$) DETERMINATIONS

ABSTRACT

Instantaneous pulmonary capillary blood flow ($\dot{Q}_C$) can be measured by: a plethysmographic method in conscious humans; a pneumotachographic method in anesthetized humans; and a plethysmographic or pneumotachographic method in anesthetized dogs. We have written a program for a small digital computer which permits on- or off-line processing of these data. The values of pulmonary $\dot{Q}_C$ plus right-to-left intrapulmonary shunt flow in dogs compare favorably to simultaneously determined values of cardiac output by dye dilution; but variations among three consecutive estimations of capillary blood flow in dogs are significantly greater than by dye dilution. Nevertheless, over a 25-min period the repeatability of the plethysmographic method in seated or supine conscious humans is excellent, possibly because the method is more precise at higher cardiac outputs. The noninvasive nature of the plethysmographic method, together with rapid data processing by the computer, appears to offer a practical approach to serial measurements of cardiac output and pulmonary hemodynamics in man.

METHODS

Theory

During breathholding or slow expiration, oscillations of flow in the body plethysmograph and at the mouth occur as a result of the heartbeat. These mechanical oscillations during breathholding with air are also present during breathholding with nitrous oxide, and therefore must be subtracted from the oscillatory signal after inspiration of nitrous oxide to derive the instantaneous uptake of this gas by the pulmonary capillaries. Each N_2O pulse is synchronous with the heartbeat; but, since the heart rate is not usually exactly regular, air pulses must be subtracted from N_2O pulses on a beat-by-beat basis. It is assumed that the onset of these pulses bears a constant time relationship to the QRS complex of the electrocardiogram (EKG). Therefore, the subtraction process is begun from the R wave of the EKG and terminated with the R wave accompanying the next N_2O pulse. If the air pulse has a longer time interval than the N_2O pulse, the subtraction terminates at the end of the N_2O pulse, and the remaining data of the air pulse are discarded. If the air pulse is shorter than the N_2O pulse, an average level from the end of the air pulse is subtracted from the N_2O pulse. Consequently, there is some uncertainty for the flow at the end of the R-R interval which is a function of the

disparity in time between the air and N_2O pulses. Under usual circumstances, the result is less than a 4% error in total pulmonary $\dot{Q}_C$ because the flow at the end of the R-R interval is falling toward a minimum. After the investigator selects the pulses of interest, the program averages the N_2O and the air pulses, and subtracts the latter from the former. The computer displays the pulmonary $\dot{Q}_C$ pulse (Fig. 1) by dividing the uptake of N_2O by the product of the alveolar fraction of N_2O by the alveolar fraction of N_2O and its solubility coefficient (3).

Data Processing

The program for processing pulmonary $\dot{Q}_C$ pulses is written in machine language for a small digital computer with 4K of core: the LINC 8 (Digital Computer Equipment Co., Maynard, Mass.), and also will run (with modifications) an updated version of this computer: the PDP 12. The system is designed to accept analog signals from the several devices which have been used to measure pulmonary $\dot{Q}_C$ (Fig. 2). Its operation is fully described in the supplementary information for this report section. A program to process dye dilution curves is also described.

Plethysmographic Techniques In Humans

Measurements of pulmonary $\dot{Q}_C$ were made in horizontal and vertical plethysmographs by electrically differentiating the plethysmographic pressure signal. Changes in chamber pressure occurred with time, owing to an increase in temperature and humidity from the breathing subject, and with transfer of heat between the chamber and room air. Consequently, the chamber had to be vented to the room before estimating changes in plethysmographic pressure during breathholding on air or N_2O. Upon closing the vent, however, there were often unpredictable baseline drifts of chamber pressure due to room air of a different temperature and humidity from that in the chamber entering the plethysmograph. We used an electropneumatic servo device to maintain the chamber at atmospheric pressure during tidal breathing as well as during inspiration of air or N_2O (4, 6). Immediately before slow expiration or breathholding, the servo system was inactivated; and changes in chamber pressure were detected by a sensitive variable reluctance differential transducer (DP 45 $\pm$ 1 in water, Validyne Corp., Northridge, Calif.), and were then electrically differentiated. Before the signal was output to the recorder, it was conditioned by a low-pass filter with a cutoff frequency of 9.5 Hz to eliminate high-frequency artifacts. The servo system ensured that each run started from the same absolute pressure level.

Calibration of the derivative of box pressure was carried out by withdrawing a constant amount of air from the chamber through a calibrated rotameter. The volume of the chamber was first reduced by adding Plexiglas cylinders, calibrated in liters to a volume equivalent to the value of body weight in kilograms. A breathing manifold of 24-vdc solenoid valves within the chamber permitted the outside operator to control the selection of inspired gases (4). A small Fleisch pneumotachograph on an expiratory line sensed flow, and the output from the amplifier for this device was fed into a center reading dc microampere meter with a variable 100-ohm shunt. The meter was placed at eye level so that the subject could monitor his expiratory flow rate. A penetration at the mouthpiece of the manifold carried a sampling line to an infrared N_2O gas analyzer, and its return was delivered back to the plethysmograph.

The subject expired to residual volume, inspired air from the chamber to just below total lung capacity (TLC), rapidly expired 1 - 2 liters of air, and then expired at a constant rate of 2 - 3 liters/min for 15 sec while the differentiated signal of plethysmographic pressure and the EKG were recorded. He repeated this maneuver within 15 - 30 sec with an 80% N_2O, 20% O_2 mixture, while a continuous record of expired alveolar N_2O concentration was recorded at the mouth. After correcting for delay in the gas analyzer, the concentration of N_2O was calculated from the mean of the sum of the values of each pulse during the run. Paired runs of breath-holding on air and N_2O could be repeated approximately every 3 min, at which time alveolar N_2O concentrations had fallen to less than 1%.

Serial measurements of pulmonary $\dot{Q}_C$ in 6 male volunteers, ages 23 - 40 yr, were made every 5 min up to a 35-min period. Fourier analysis of the pulmonary $\dot{Q}_C$ pulses was performed on these data as well as on those obtained in the supine and tilted position and during exercise in other studies in our laboratory.

Plethysmographic and Pneumotachographic Techniques In Anesthetized Dogs

The plethysmographic and pneumotachographic methods used in this study in dogs and humans are modifications of those techniques previously reported (5). In one series of experiments, the animals (anesthetized by pentobarbital sodium, 25 mg/kg body weight) were mechanically ventilated. In a second series, ventilation was assisted by transvenous PNS (10), and the animals were hyperventilated on an arterial P_{CO_2} of 25 - 30 mm Hg so that apnea for 15 sec would occur after cessation of PNS. For the experiments involving those dogs supported by mechanical ventilation: two

breaths of 500 - 600 ml air were given in rapid succession from the respirator, and the animal's lungs were allowed to deflate passively. Simultaneous records of flow at the airway through a #00 Fleisch Pneumotachograph together with electrically differentiated plethysmographic pressure were obtained over a 15-sec period. Mechanical ventilation was resumed for about 5 breaths, and then 2 breaths of 500 - 600 ml of an 80% N_2O, 20% O_2 mixture were administered. The animal's lungs were allowed to deflate passively and the initial alveolar N_2O concentration was measured with a rapid responding N_2O infrared analyzer. Pneumotachographic flow and electrically differentiated plethysmographic pressure were recorded for 15 sec, and then a chest plate was depressed by a remote switch outside the plethysmograph (1) so that a final alveolar N_2O concentration could be obtained. Initial and final alveolar N_2O concentrations were plotted on semilogarithmic paper, and the mean concentration was estimated, after correcting for the time delay between the sampling site and the infrared analyzer. In those dogs ventilated by means of transvenous PNS, the procedure was similar except that air and the N_2O mixture were delivered by adjusting the phrenic nerve stimulator to produce large tidal volumes.

Eighteen mongrel dogs, each weighing 13.5 - 29.5 kg, were anesthetized by administration of pentobarbital sodium 25 mg/kg body weight. They were intubated with a cuffed endotracheal tube, and catheters were placed within the pulmonary and carotid arteries and a peripheral vein. The dog was placed within the body plethysmograph, and systemic heparinization was carried out with administration of 50 mg heparin. Blood from the carotid artery was drawn through a penetration in the door of the plethysmograph to a densitometer (Gilford Instrument Labs., Oberlin, Ohio) and returned by means of a recirculating pump (Holter Co., Mt. Laurel Tnp., N.J.) to a peripheral vein. This system prevented a change in plethysmographic pressure due to withdrawal of blood for analysis by the densitometer. The pulmonary artery catheter was led to the outside of the chamber to serve as an injection site of Cardiogreen for estimation of cardiac output by dye dilution. During breathholding with N_2O, simultaneous measurement of cardiac output was made by the dye-dilution technique. Three estimations of pulmonary $\dot{Q}_C$ and dye-dilution cardiac outputs were done, and then intrapulmonary right-to-left shunt determined. The shunt was estimated, using the standard shunt equation (3), after 15 min of 100% oxygen breathing.

Over a 2- to 3-hr period, 3 sets of 3 runs of capillary blood flow measurements were performed in each of 18 dogs--except for 2 dogs in whom only 2 sets were obtained. In 5 dogs whose respirations were

supported by mechanical ventilation, pulmonary $\dot{Q}_C$ was estimated by the plethysmographic method, with the airway occluded by a valve and with the airway patent; these conditions were alternated for a total of 6 runs.

Differences among the various techniques for measuring cardiac output were assessed by means of a Student's t-test. The three runs of cardiac output measured by the dye dilution, N_2O plethysmographic, and N_2O pneumotachographic methods (animal studies) were compared by an analysis of co-variance.

RESULTS

Computer Processing

Waveforms from signal generators were fed into the computer to permit exact comparison between computer analysis and hand calculation. These forms included sine, square, and ramp functions. Complex sine waves were obtained by mixing sine waves from two signal generators. In all cases, good agreement was obtained between the computer and the hand-calculated results.

Human Studies

Reproducibility of nitrous oxide plethysmographic pulmonary $\dot{Q}_C$ studies, in 4 normal supine subjects and in 6 normal seated subjects, is depicted in Figure 3. There were no systematic differences in heart rate, cardiac index (pulmonary $\dot{Q}_C$ index), stroke volume index, and peak pulmonary $\dot{Q}_C$ during the 25- to 35-min period in which these parameters were measured. Sequential paired measurements of individual subjects were analyzed for average deviation from the mean. For the supine position, the average of these deviations from the mean of two determinations of pulmonary $\dot{Q}_C$ was 3%; for the seated position, 9%. There were no significant differences in harmonic content of the pulmonary $\dot{Q}_C$ pulse among the various body positions at rest and during exercise (Table 1). Beyond the sixth harmonic, the Fourier analysis was not too accurate because of the high noise-to-signal ratios in this range. Thus, harmonic content was found at frequencies much higher than the cutoff frequency of the 9.5 Hz low-pass filter, and therefore represented noise. Between 85% and 90% of the harmonic content of the pulse wave could be represented by the first five harmonics.

TABLE 1. FOURIER ANALYSIS OF PULMONARY $\dot{Q}_C$

Position	No. of Subjects	Heart Rate*	Harmonics* 1	2	3	4	5	6
Supine	11	66 ± 7	41 ± 8	28 ± 6	13 ± 5	4 ± 2	4 ± 3	3 ± 2
Sitting	9	71 ± 8	42 ± 7	23 ± 6	10 ± 5	6 ± 3	4 ± 2	3 ± 1
Vertical (90° Tilt)	8	83 ± 17	45 ± 10	24 ± 7	7 ± 4	5 ± 3	6 ± 4	2 ± 1
Supine - exercise	8	98 ± 10	39 ± 8	24 ± 6	12 ± 3	7 ± 3	8 ± 3	2 ± 1
Vertical - exercise	6	121 ± 26	42 ± 16	20 ± 4	11 ± 3	6 ± 4	7 ± 3	3 ± 3

*Mean ± SD as %.

-III-
(Part 2)

Animal Studies

Because no significant difference existed among the methods for estimation of cardiac output for the 14 anesthetized dogs ventilated by PPB and the 6 supported by transvenous PNS, the data were lumped together. The mean pulmonary $\dot{Q}_C$ by the plethysmographic derivative method was 1.64 L/min, SD 0.71; and $\dot{Q}_C$ by the pneumotachographic method, 1.76 L/min, SD 0.70 (P = NS). However, the mean right-to-left shunt blood flow ($\dot{Q}_S$) during oxygen breathing was 0.31 L/min, SD 0.22--which was added to $\dot{Q}_C$ in order to provide a comparison with the pulmonary blood flow ($\dot{Q}_p$) measured by the dye-dilution method. Mean $\dot{Q}_p$ was 1.97 L/min, SD 0.65; $\dot{Q}_S + \dot{Q}_C$ derivative, 1.96 L/min, SD 0.84; and $\dot{Q}_S + \dot{Q}_C$ pneumotachograph, 2.09 L/min, SD 0.84 (P = NS). Although the means of the three methods were similar, there was considerably more scatter of $\dot{Q}_S + \dot{Q}_C$ pneumotachograph compared to $\dot{Q}_p$ than $\dot{Q}_S + \dot{Q}_C$ derivative (Fig. 4). In the 20 dogs, $\dot{Q}_S + \dot{Q}_C$ derivative in 4 animals differed by more than 20% from $\dot{Q}_p$--but, in 3 of these animals, cardiac output was at a low level; for the $\dot{Q}_S + \dot{Q}_C$ pneumotachograph methods, 11 of the 20 values differed by more than 20% from $\dot{Q}_p$.

The capillary blood flow pulse, although pulsatile by pneumotachograph method, was distorted when compared to the pulse obtained by the derivative method. In a comparison of peak flows between the two N_2O methods, the data points did not fall on a line of identity. Even though mean values for $\dot{Q}_S + \dot{Q}_C$ derivative compared well to dye-dilution estimates of $\dot{Q}_p$, variance among the 3 runs making up a set was 4 times greater in the derivative method ($P < .001$). The standard deviation within a set for the derivative method was 0.54 L/min; and, for the dye-dilution method, 0.27 L/min.

No significant difference was found in estimation of $\dot{Q}_C$ derivative between measurements made when the air control and N_2O test runs were both done with the airway patent or with the airway occluded.

Peak pulmonary $\dot{Q}_C$ showed a high degree of correlation to stroke volume ($r = 0.95$) (Fig. 5). Peak flow = 0.03 + 0.26 stroke volume, SD 0.40. Peak flow also showed a high degree of correlation to $\dot{Q}_C$ ($r = 0.97$), peak flow = 0.22 + 1.58 $\dot{Q}_C$, SD = 0.36.

DISCUSSION

Human Studies

Pulmonary $\dot{Q}_C$ determinations in normal subjects were quite reproducible over a ½-hr period. The good agreement between this method and the

-III-
(Part 2)

Fick determination of cardiac output has been reported by others (2). In our laboratory, comparative measurements of cardiac output in three subjects by the N_2O plethysmographic method and dye dilution revealed agreement within 10% of the mean of the two methods. Fourier analysis of the pulmonary $\dot{Q}_C$ pulse showed marked similarity of the harmonic content, despite large differences in mean pulmonary $\dot{Q}_C$ among different body positions during resting and exercising states. Further, it was found between 85% and 90% of the harmonic content could be represented by the first five harmonics--which meant that, during moderate exercise with heart rate of 120, the differentiated pressure should have a flat frequency response to 10 Hz in order accurately to display the waveform. Our device was flat to 9.5 Hz, and thereafter rolled off at 42 dB/octave, thus satisfying this requirement.

Animal Studies

The present investigation confirms the results of Cheney et al. (3). These authors have compared the plethysmographic and pneumotachographic methods for pulmonary $\dot{Q}_C$ to dye-dilution estimations of cardiac output; and they find good agreement, provided that the intrapulmonary right-to-left shunt has been added to the pulmonary $\dot{Q}_C$. If the shunt flow is not added, the pulmonary $\dot{Q}_C$ tends to underestimate the cardiac output, although most values fall within 20% of a line of identity unless the shunt flow is pathologically increased. The close agreement between the N_2O method and dye-dilution or Fick estimates of cardiac output, in anesthetized dogs, has been observed by other authors (2, 8).

The pneumotachographic method in dogs gave much more scatter of values for mean pulmonary $\dot{Q}_C$ than the plethysmographic methods. This result is most likely due to the inherent inaccuracies in subtracting the large pulsations on the air-flow curve from the large pulsations present during N_2O breathholding to yield a relatively small signal of N_2O uptake. The values for cardiac output in our study were not as close in agreement to dye-dilution estimates as those of Cheney et al. (3); but these authors measured dogs who might have been healthier and had much higher cardiac outputs than our animals. Many of the mongrel dogs we used had dog heartworms, and large right-to-left shunts. Further, although this method revealed pulsatility of pulmonary $\dot{Q}_C$, distortion of the pulse waveform was considerable as revealed by marked deviation of the peak flow values of the pneumotachographic and plethysmographic methods from the line of identity. In contrast to our animal studies, comparisons (in a previous study) of the pneumotachographic method with dye dilution in anesthetized humans (5) gave much less scatter--possibly because the values for

cardiac output, and hence N_2O uptake, were greater and could be estimated with more accuracy.

Wasserman and Naimark (11) reported alterations in plethysmographic pressure during glottal closure, and suggested that N_2O capillary blood flow could best be determined with the glottis opened. They did not monitor intratracheal pressure, however, and the effects they observed might have been due to straining. We found that pulmonary $\dot{Q}_C$ in apneic dogs was the same whether the glottis was opened or closed, provided that both the air and N_2O runs were carried out with the same maneuver.

The computer program allowed us to analyze the average pulmonary $\dot{Q}_C$ in dogs. Peak flow vs. stroke volume estimations in dogs were highly correlated, an empirical relationship previously documented by Segel and McIlroy (9) in humans. The regression equation for the animal data intercepted the origin and fell within 1 SD of the extrapolation of the regression equation obtained in humans studied in our laboratory. A similar relationship was obtained for peak flow vs. pulmonary blood flow.

BIBLIOGRAPHY

1. Avery, W. G., and M. A. Sackner. A rapid measurement of functional residual capacity in the paralyzed dog. J Appl Physiol 33:515-518 (1972).

2. Bosman, A. R., et al. A method for measuring instantaneous pulmonary capillary blood flow and right ventricular stroke volume in man. Clin Sci 26:248-260 (1964).

3. Cheney, F. W., S. Takahashi, and J. Butler. Comparison of two methods of measuring pulmonary capillary blood flow in dogs. J Appl Physiol 27:127-131 (1969).

4. Dougherty, R. L., et al. Body plethysmograph; a new body plethysmograph for cardiopulmonary studies in man. Analyzer 3:18-27 (1972).

5. Greenberg, J. J., et al. Preoperative and postoperative cardiac output determinations using an instantaneous pulmonary capillary blood flow method. Ann Thorac Surg 12:639-648 (1971).

6. Karatzas, N. B., G. J. De Lee, and F. D. Stott. A new electropneumatic flowmeter for the plethysmograph. J Appl Physiol 23: 276-278 (1967).

7. Lee, G. J. De, and A. B. DuBois. Pulmonary capillary blood flow in man. J Clin Invest 34:1380-1390 (1955).

8. Morkin, E., O. R. Levin, and A. P. Fishman. Pulmonary capillary flow pulse and the site of pulmonary vasoconstriction in the dog. Circ Res 15:146-160 (1964).

9. Segel, N., and M. B. McIlroy. Influence of respiration, stroke volume, and heart rate on pulmonary capillary pulsatility. J Appl Physiol 26: 771-779 (1969).

10. Wanner, A., and M. D. Sackner. Transvenous phrenic nerve stimulation in anesthetized dogs. J Appl Physiol 34:489-494 (1973).

11. Wasserman, K., and A. Naimark. Effect of a closed glottis on pressure oscillations in the body plethysmograph. J Appl Physiol 17: 574-575 (1962).

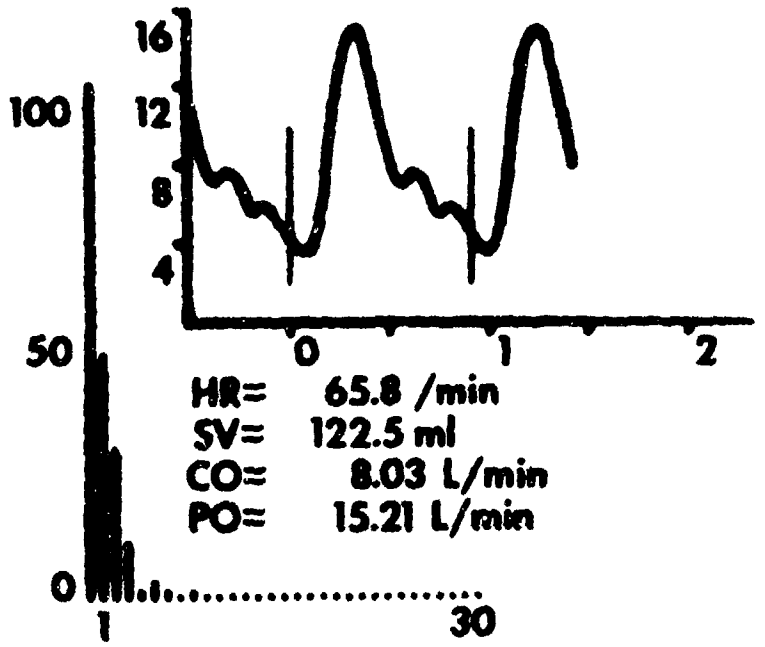

Figure 1. Computer display of the average pulmonary $\dot{Q}_C$ pulse from 6 supine normal subjects--together with the Fourier analysis. (The two vertical bars denote the R-R interval; the Y axis, the blood flow in liters per minute; and the X axis, the time in seconds. HR is the heart rate; SV, stroke volume; CO, mean cardiac output (mean pulmonary $\dot{Q}_C$); and PO, peak output. The bar graph adjacent to the display depicts the Fourier analysis; the Y axis, the percent of total harmonic content; and the X axis, the harmonics from 1 to 30.)

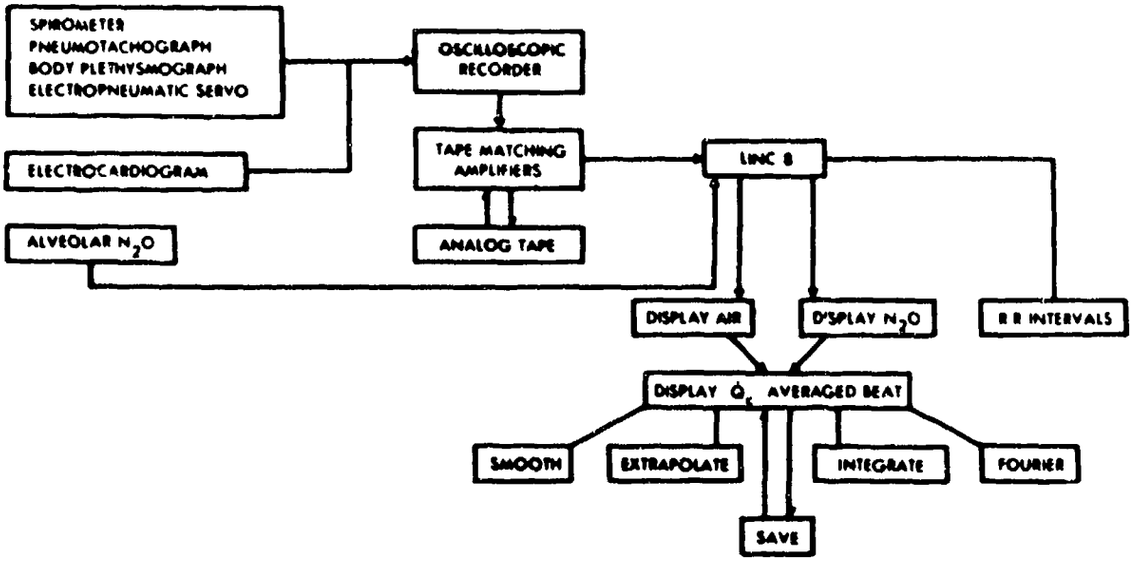

Figure 2. System for obtaining pulmonary $\dot{Q}_c$ measurements. (Block diagram)

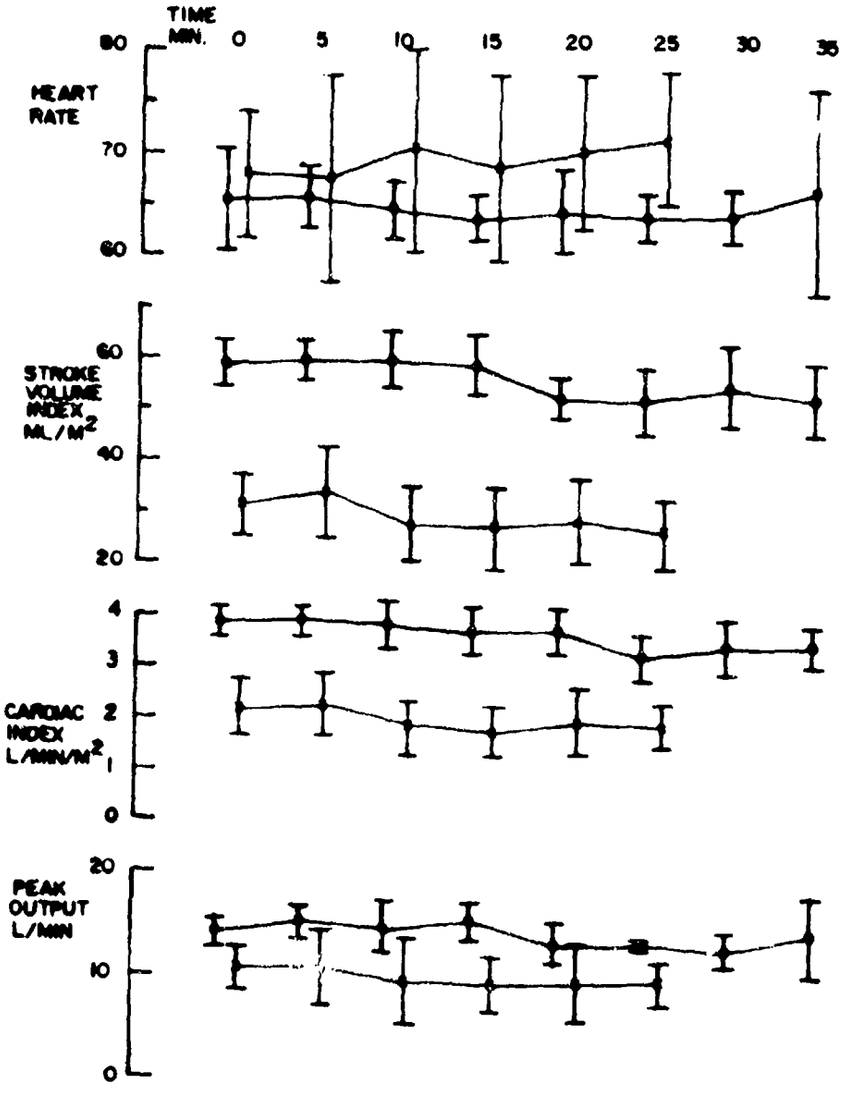

Figure 3. Reproducibility of N_2O plethysmographic data in normal subjects--supine (circles), and seated (crosses)--as a function of time.

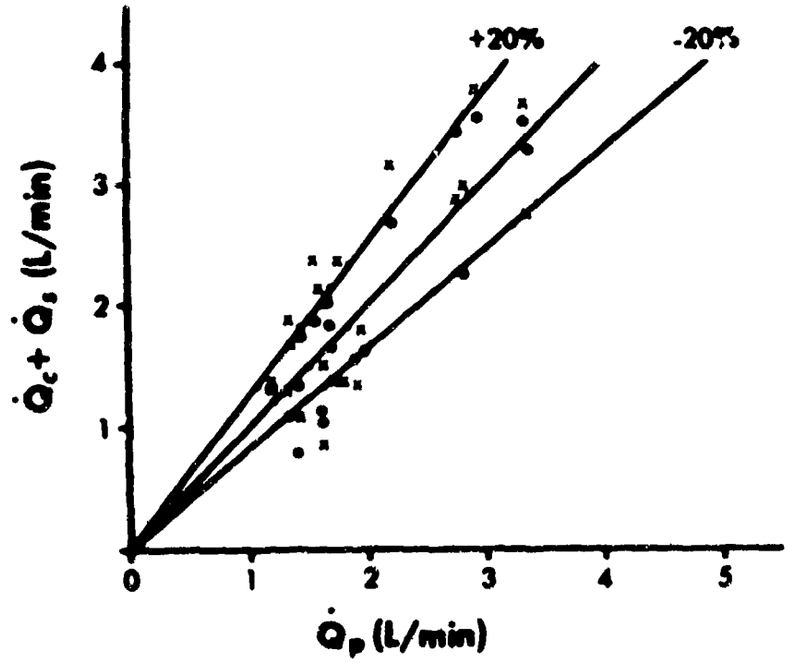

Figure 4. Comparison of N_2O plethysmographic (circles) and pneumotachographic (crosses) methods with simultaneous determined cardiac output by dye dilution ($\dot{Q}_p$) in anesthetized dogs. (Right-to-left intrapulmonary shunt blood flow has been added to the pulmonary $\dot{Q}_c$ estimate.)

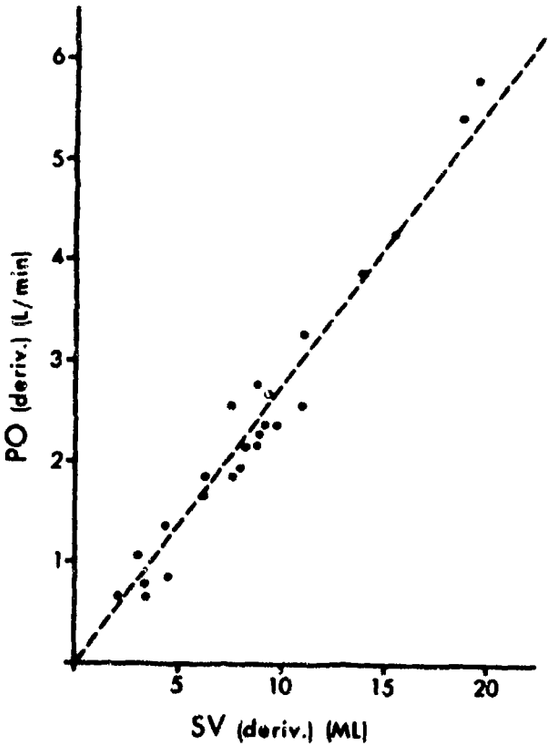

Figure 5. Peak pulmonary capillary blood flow (PO) plotted as a function of stroke volume (SV) in anesthetized dogs. (These values were based upon the plethysmographic determinations.)

-III-
(Part 3)

RE: SAM-TR-75-25
Section III (Part 3)

SUPPLEMENTARY INFORMATION ON: Laugh and Laughn User's Manual (including computer flow charts) concerning an inhouse computer program developed by Mt. Sinai Hospital.

In order for comprehensive information on this research to be readily accessible, microfiche have been made of the above-mentioned material. The microfiche are available through:

The Aeromedical Library
Documentation Section
Brooks AFB, Texas 78235

IV (Parts 1 and 2). EFFECTS OF TILTING AND USAF ANTI-G SUIT INFLATION ON PULMONARY CAPILLARY BLOOD FLOW ($\dot{Q}_C$)

PART 1: EFFECTS OF TILTING ON PULMONARY $\dot{Q}_C$

ABSTRACT

Graded tilting of 4 subjects in a body plethysmograph from 0° to 90° head-up tilt position caused a progressive fall in pulmonary $\dot{Q}_C$, stroke volume, and capillary pulse amplitude (CPA), and a rise in heart rate at each angle of tilt. Changes were slight at 30° and most pronounced in the 90° head-up posture. When the subjects were tilted back from 90° through 30° to supine position, the pattern of circulatory changes was similar at each angle of tilt. The $\dot{Q}_C$, peak systolic (PSF) and end-diastolic flows (EDF), and CPA were measured in 10 resting subjects in the supine and 90° vertical positions before, during, and after anti-G suit inflation, and immediately after isometric exercise. Passive tilting from the supine to 90° position caused a striking fall in $\dot{Q}_C$, stroke volume, PSF, and CPA in every subject, and normal pulsatility was no longer evident; neither fainting nor bradycardia occurred. These changes were greatly diminished by either inflation of the anti-G suit or isometric exercise. From all our data, a highly significant positive correlation between PSF and stroke volume was found both at rest and after exercise. Although the slope was similar, the regression equation for the exercise values lay above and to the left of the resting line. At rest, the changes were largely determined by the stroke volume which appears to be the major determinant of pulmonary capillary pulsatility under these conditions. During exercise, additional factors--such as a high peak inflow velocity into the pulmonary artery and/or a decrease in pulmonary arterial vasomotor tone--probably played a dominant role.

INTRODUCTION

With the advent of space flight, interest has been renewed in: the physiologic mechanisms involved in orthostatic tolerance to and following weightlessness; and a heightened need to develop practical and effective noninvasive methods for monitoring rapid circulatory changes in man. Traditionally, gravitational circulatory stress in man has been studied on the tilt table, since the upright tilt rapidly imposes a predictable set of circulatory changes (9, 17, 19, 21, 23, 24). It has been well established that the immediate cardiovascular responses to passive head-up tilting in normal subjects include an increased heart rate and diastolic arterial pressure, and a diminished stroke volume. Heart rate does not increase in proportion to the drop in stroke volume, and consequently the cardiac

output falls. At the same time, systolic pressure changes little, mean arterial pressure rises, and pulse pressure narrows. The physiologic events underlying these changes are complex and depend on many variables, such as the angle of the tilt, the length of time the subject remains at a given angle, and the use of invasive techniques which may evoke considerable psychic and physical stimulation leading to vasodepressor syncope. The orthostatic tolerance of tilted normal subjects is markedly diminished by the use of intravascular instrumentation, and also by psychic stimulation due to discomfort, fear, and anxiety associated with cardiac catheters and intra-arterial needles. In a large group of normal pilots under study, syncopal reactions to passive tilting were five times as frequent with invasive techniques as without them (21).

Although the qualitative response of the cardiac output to passive head-up tilting is indisputable, the magnitude of the fall has varied widely in different studies, ranging anywhere between 15% and 39% of control pretilt supine values (2, 11, 12, 20, 21, 23, 25). The reason for this wide scatter lies, in part, with the different techniques for measuring cardiac output and the different degrees of head-up tilt (ranging between 10° and 70°). Invasive measurements have not been previously reported beyond the 70° head-up tilt position, perhaps because of the fear that greater upright tilts might induce syncope. The invasive techniques for estimation of cardiac output are clearly undesirable, because indwelling catheters or needles may profoundly affect the hemodynamic status during orthostasis (21).

In the present investigation, we have used a tilt-table body plethysmograph (7) to study the effects of gravity on cardiac output and its related measurements in man. The technique is simple, accurate, noninvasive, atraumatic, and ideally suited to such experiments. Our purpose in this study was twofold: first, to determine the effects of 90° head-up tilt on cardiac output and stroke volume, and the change in these two parameters that results from inflation of an anti-G suit and mild exercise; and second, to establish the influence of gravitational stresses on pulmonary $\dot{Q}_c$ and its pulsatility. As Segal and McIlroy (16) previously reported, a change from the supine to the upright posture caused a reduction in the capillary flow pulse amplitude, which was attributed to a passive effect consequent upon the fall in stroke volume. It was of particular interest to extend these observations to the fully erect posture.

SUBJECTS AND METHODS

Fourteen healthy resting men, ages 22 - 39 yr (mean: 26 yr), were studied between 1 and 2 hr after a light lunch. Measurements were made

in a tilt-table body plethysmograph, the design and operation of which have been previously reported from our laboratory (7). Briefly, the pressure in the plethysmograph was regulated by a closed-loop electropneumatic servo system, so that the baseline pressure was always accurately reproducible immediately preceding each run when the servo was switched off. The chamber pressure was sensed by a differential pressure gage (Pace P90D $\pm$ 0.03 PSID) and electronically differentiated so that it could be calibrated as a flow. The differentiated pressure was then passed through a low-pass filter with a cutoff frequency of 9.5 Hz, and recorded on analog magnetic tape along with the electrocardiogram and alveolar N_2O concentration.

The subject first expired to residual volume, inspired rapidly to TLC with air, expired about 1 to 2 liters to clear the dead space, then slowly expired at a rate of 2 to 4 liters/min for 12 to 15 sec which he monitored by watching a damped microammeter connected to the output of an amplifier for the pneumotachograph signal. He then repeated this maneuver with inspiration of an 80% N_2O and 20% O_2 mixture. A continuous recording of alveolar N_2O concentration was made by sampling the gas concentration at the mouthpiece with an infrared analyzer (Godart, Instrumentation Associates, New York, N.Y.). These data were then processed by a LINC 8 digital computer (Digital Equipment Co., Maynard, Mass.).

Technical Procedures (In Part 1)

The purpose of the first part of the study was to determine the relation of the angle of tilting to the changes in cardiac output and heart rate, whether the length of time the subject remained at the given angle and the sequence of postural change (i.e., from recumbency to an upright position or vice versa) had any influence upon the tilt response. Measurements of pulmonary $\dot{Q}_C$, heart rate, stroke volume, peak systolic flow (PSF), and capillary pulse amplitude (CPA) derived from subtracting end-diastolic flow (EDF) from PSF were made in 4 subjects lying: first, in the supine; and then sequentially in the 30°, 60°, and 90° head-up tilt positions; and again after being returned to full recumbency (Fig. 1). After a 20-min rest period they were tilted straight up to the erect posture and similar measurements were repeated sequentially in the 90°, 60°, 30°, and supine positions. The time taken for the body plethysmograph to be tilted for 0° to 90° upright position was 40 sec. In each position measurements were made in duplicate, so that a total of 18 $\dot{Q}_C$ measurements were made in each subject. The time interval between each cardiac output measurement was 2.5 min; and the duration of the entire study was 90 min.

The concentration of N_2O in the exhaled breath was recorded immediately before each $\dot{Q}_c$ estimation and was always less than 1%.

Technical Procedures (In Part 2)

Part 2 of the study (the design of which will be evident from Fig. 2) was concerned with the physiologic effects of countermeasures upon the pronounced hemodynamic changes induced during a 90° head-up tilt from the supine position. Measurements of $\dot{Q}_c$ heart rate, stroke volume, and CPA were made in 10 subjects in the supine and 90° vertical head-up tilt positions, before, during, and after inflation of a standard USAF anti-G suit (inflation pressure was 100 mm Hg, achieved within 20 sec) and immediately after mild exercise performed in the upright and supine positions. The anti-G suit was inflated immediately before tilting to the 90° erect posture. Measurements were then made, in the upright position with the anti-G suit inflated, approximately 4 min after tilting--and 5 min after deflation. The anti-G suit was then reinflated while the subjects were upright, measurements being made after this maneuver and again when the anti-G suit was deflated. At the end of these procedures the subjects were returned to recumbency for a final set of measurements. Exercise consisted of repetitive flexion of the forearms against a variable resistance (attached to the footboard), while simultaneously stepping upwards and downwards on the toes for 30 sec, whereupon the air or control run was performed. The subject then repeated this exercise for a further 30 sec, and the nitrous oxide run was then recorded. No provision was made for estimating the load of work. All measurements at rest were made in triplicate and measurements immediately after exercise in duplicate, so that a total of 24 $\dot{Q}_c$ estimations were made in each of the 10 subjects. The interval between each cardiac measurement at rest was 5 min.

In 2 subjects, measurements of pulmonary $\dot{Q}_c$ were made after tilt to the 90° head-up position, and at 4-min intervals for another 20 min. After a further 20-min rest period for the subjects in the supine position, the anti-G suit was inflated in recumbency. In 3 other subjects, we tested the influence of the duration of inflation of the anti-G suit on cardiac output in the fully erect posture. Measurements of $\dot{Q}_c$ were made after each subject was tilted to the 90° position. The anti-G suit was then inflated (with the subject in this posture), and $\dot{Q}_c$ was measured at 4-min intervals for 20 min.

-IV-
(Part 1)

RESULTS

Effects of Angle of Tilt On $\dot{Q}_C$

The mean values of the 4 subjects undergoing graded tilting have been depicted in Figure 1. The cardiac output fell at all positions of head-up tilt. As the subjects were tilted from the supine posture through the 30°, 60°, and 90° head-up tilt positions, there was a progressive fall in $\dot{Q}_C$, stroke volume, PSF, and CPA, and a rise in heart rate during each angle of tilt. These changes were moderate between the supine and 30° tilt level, less marked between 30° and 60° positions, and most marked between 60° and 90° head-up posture. In this position the values for $\dot{Q}_C$, stroke volume, PSF, EDF, and CPA were virtually half the values observed in the supine position. On the average, the supine $\dot{Q}_C$ fell by: 19% between 0° and 30°, 24% between 0° and 60°, and 64% between 0° and 90° head-up tilt positions. All these changes were significant, being $P < .02$ between 0° and 30°; $P < .001$ for the remainder.

When the subjects were tilted back from 90° through 60° and 30° to the recumbent posture, the pattern of circulatory changes was similar at each angle of tilt. There was a progressive increase in $\dot{Q}_C$, stroke volume, PSF, EDF, and CPA, and a decrease in the heart rate; and, when the subjects reached recumbency, the values were similar to those observed initially in the pre-tilt supine posture. The changes were most marked between 0° and 90° tilt; but at each angle of tilt there was a definite measurable change, and in each subject the pattern of alteration during tilting was highly consistent. As in head-up tilting, we observed similar percentage changes and statistical significances in $\dot{Q}_C$ when the subjects were tilted back from 90° to recumbency. A significant positive correlation was found between stroke volume and PSF during these maneuvers.

Effects of Anti-G Suit Inflation On Upright Tilt

The mean values for 10 subjects before, during, and after anti-G suit inflation in the supine and 90° head-up tilt are shown in Figure 2, and some of the individual results are depicted in Figure 3. Inflation of the anti-G suit in the supine posture had no significant effect upon $\dot{Q}_C$, heart rate, stroke volume, PSF, and CPA. Passive tilting from the supine to the 90° head-up posture caused a striking fall in $\dot{Q}_C$ in every subject, the mean decreasing from 6.7 to 2.7 L/min. This difference was highly significant ($P < .001$), representing a reduction of 61% of the supine value for $\dot{Q}_C$ (Fig. 3). At the same time, there was a mean rise in heart rate of 24 beats/min (+ 43% of the supine value, $P < .001$), and a fall in stroke

volume in every subject. Stroke volume decreased from 103 to 31 ml, which was 71% less than the value in the supine posture ($P < .001$); PSF and CPA both fell on average by 62% of their supine values ($P < .001$); and pulmonary $\dot{Q}_C$ pulsatility was hardly recognizable. This response was measured twice and was highly reproducible (Fig. 2). Despite this marked fall in $\dot{Q}_C$, none of the subjects fainted or even developed presyncopal signs. All these changes were greatly reduced when the anti-G suit was inflated before passive tilting to the 90° posture. In the latter position, the fall in $\dot{Q}_C$, stroke volume, PSF, and CPA was considerably less, each representing approximately 30% of their supine values. In comparison, the same tilt without anti-G suit protection induced a fall in these variables which was twice as great as with the anti-G suit inflated. Nonetheless, even though the decreases in $\dot{Q}_C$, stroke volume, PSF, and CPA were greatly diminished by inflation of the anti-G suit, they were still all significantly different ($P < .01$) from their respective levels in the supine posture. In the 90° head-up tilt, in the face of a very low cardiac output and stroke volume, reinflation of the anti-G suit still caused a partial restoration of $\dot{Q}_C$ and its related measurements toward levels recorded in the supine posture. The values measured during both anti-G suit inflation periods were closely similar to each other.

The duration of the 90° head-up tilt through 20 min had no consistent effect upon $\dot{Q}_C$ and its related measurements. On the average, $\dot{Q}_C$ fell maximally almost immediately after assuming the 90° head-up tilt and remained depressed at a similar low level over the next 20 min. Similarly, after anti-G suit inflation in the upright posture, the cardiac output in general increased well above the preinflation level and did not alter materially over the 20-min period.

Effects of Exercise On the Tilt Response

The individual results of exercise performed in the upright and supine positions are illustrated in Figure 4. Mild exercise, performed for 1 min in the erect position, produced a greater reversal of the tilt response than did the inflated anti-G suit. Immediately after exercise in the 90° posture, the heart rate rose an average from 94 to 124 beats/min. There was a concomitant rise in $\dot{Q}_C$ from 2.9 to 6.9 L/min. Stroke volume increased from 32 to 57 ml, all these differences being highly significant ($P < .001$). At the same time there was marked increase in PSF and CPA. Exercise performed in the same manner in the supine position also caused large increases in $\dot{Q}_C$, PSF, and CPA; but, in contrast to exercise done in the upright position, stroke volume remained essentially unchanged in most of the subjects.

Relationships Between Stroke Volume (SV) and PSF

Taking all the data from the subjects at rest, with and without the inflated anti-G suit, revealed a highly significant correlation between SV and PSF ($r = 0.919$, $P < .001$). The regression equation for these data (Fig. 5) was:

$$\text{PSF L/min} = 3.3 + 0.094 \text{ SV ml.}$$

The relations between SV and PSF during exercise were also investigated (Fig. 5). We found that, as at rest, a significant positive relationship also existed between these variables both in the supine and upright posture, the supine values forming the lowest part of the curve and the upright values constituting the remainder ($r = 0.697$, $P < .01$). The regression equation (PSF L/min = 6.6 + 0.17 SV ml) lay well above and slightly to the left of the resting line. Thus, for any given value of SV, the PSF during exercise was substantially greater than at rest.

DISCUSSION

Unlike the results of Tuckman and Shillingford (23), those in the present investigation have demonstrated that the level of cardiac output in normal man is strongly influenced by the angle of passive tilting. We have shown that cardiac output and stroke volume fall significantly and progressively at each position of tilt between 0° and 90° in the head-up, and vice versa in the head-down positions. In contrast to these findings, these authors (using Coomassie Blue dye injected into a peripheral vein for measuring cardiac output with an ear oximeter) reported that, in normal man, the decreasing cardiac output associated with passive tilt to the upright position reached its maximum at 20°, with little further decrease between 20° and 60°, and with most of the decrease occurring between 10° and 20°. At the same time, however, the heart rate continued to increase and stroke volume decreased at all angles of tilt through 60°. Their subjects were not tilted beyond the 60° angle; and the percent difference in cardiac output between recumbency and 60° head-up tilt was -19%, which is similar to our findings for the same angle of tilt. Yet, the pattern of change in cardiac output at the intermediary angles of tilt contrasts sharply with the findings in the present study. Furthermore, even though the hydrostatic forces and cha es in heart rate and stroke volume continued to fall considerably on further tilting (beyond 20°), it seems surprising that the cardiac output in Tuckman and Shillingford's (23) study should not have changed more.

It might be argued that our measurements of pulmonary $\dot{Q}_C$ did not reflect true changes in cardiac output because of changes in intrapulmonary shunt fraction or distribution of ventilation during tilting; but this is unlikely for the following reasons: Bouhuys and van Lennep (4) showed that distribution of ventilation, as estimated from nitrogen washout curves, is uniform at 50° head-up tilt; and we have extended the observations in 5 subjects to a 90° head-up tilt. Arterial oxygen tension in nonsmokers in the erect position is not significantly different than in the supine, suggesting that a large increase in intrapulmonary shunt does not occur with postural change (22). In anesthetized dogs we have found that cardiac output, as estimated by simultaneous dye dilution and N_2O plethysmographic techniques, shows a magnitude of fall similar to that observed in the present experiments. Further, percent intrapulmonary shunt remains the same or diminishes. In numerous studies, cardiac output has been measured in fully upright man, either standing quietly (3, 5, 13, 15, 23) or suspended in a parachute harness (21); but none of these examples are comparable to man tilted passively on a tilt-table in the 90° position. While most studies (including the present investigation) have shown that, in the 60° or 70° head-up tilt position, cardiac output falls by 19% to 35% of the supine value, this study is the first in which measurements of cardiac output and pulmonary capillary pulsatility have been made in man tilted beyond the 70° upright position. In every subject a marked and consistent fall occurred in cardiac output beyond the 70° angle of tilt, the fall changing dramatically from an average of 25% (at 60° position) to 60% of the pretilt value (in the fully erect posture). This information suggests that, between 60° and 70° angle of tilt, hemodynamic changes are critical. The change from the supine to the upright position is accompanied by a partial redistribution of blood volume to the dependent parts of the body. It is generally accepted that this redistribution is the cause of the decrease of cardiac output--being associated with a fall in atrial pressure and a lower diastolic filling of the ventricles, and with a decrease in ventricular EDF volume, stroke volume, and central blood volume (17, 18). The results of our study suggest that, when normal man is tilted passively beyond the 60° position, the hydrostatic forces responsible for the gravitational pooling of blood become most pronounced--thus inducing the sudden and relatively huge fall in cardiac output.

In the 90° head-up tilt position, it is perhaps surprising that none of our subjects either developed presyncopal signs or fainted in the body plethysmograph. The reason is not known, but might lie in the fact that they were studied in the postprandial state and did not have vascular catheters in place (the subjects, therefore, experienced relatively little anxiety); these conditions led to heightened baroreceptor reflex activity, producing a marked increase in sympathetic tone which caused extensive peripheral

vasoconstriction and increased venous tone (1). It should, however, be stressed that the absence of fainting in this study may not reflect the frequency of fainting after simulated or actual "weightlessness." Further, in those subjects in whom cardiac output has been recorded during syncope, the magnitude of the fall in cardiac output was minimal but the systemic blood pressure fell precipitously (26).

The present results have demonstrated that a short duration of upright tilt does not cause further changes in cardiac output. After the subject is tilted to the upright position, the cardiac output falls immediately and does not appear to decrease more, at least over the ensuing 20 min--suggesting that the gravitational pooling and the concomitant compensatory peripheral vascular reflexes come into play almost immediately. Similarly, our results indicate that the level of cardiac output, while significantly influenced by inflation of the anti-G suit in the upright position, is unaffected by the duration of inflation. We have been unable to confirm the results of Gray et al. (8), who reported that the cardiac output rose immediately after anti-G suit inflation but returned rapidly to pretilt values within 5 min of inflation. Such a transient effect has never been measured in any of our subjects. The finding by Weissler et al. (25), of a 25% increase in cardiac output after acute anti-G suit inflation in normal subjects in the passively tilted 70° head-up position, compares favorably to a 31% increase in cardiac output in the 90° erect posture in our study. It is of interest that inflation of the anti-G suit in the sitting position does not significantly change cardiac output, although there is a significant small decrease in pulse rate. This result may be related to anti-G suit design because with the subject in the seated position there is a suggestion that the anti-G suit inflates from above downward, whereas this sequence of inflation is not as marked in the tilted position (14).

In all our subjects at rest, studied in supine and head-up tilt positions with and without anti-G suit inflation, a significant relationship existed between SV and PSF. This relationship is further evidence that the variables of posture and venous return influence pulmonary CPA indirectly, and that stroke volume plays the principal role (16). The fact that changes in stroke volume can explain the changes in CPA--both in the upright position (when the regional distribution of blood flow within the lung is uneven because of gravitational factors) and also in the supine position (when such regional differences are minimal--suggests that gravity per se in terms of pulmonary flow distribution has little or no effect on pulsatility. When the postural fall in stroke volume in vertical position is diminished by inflation of an anti-G suit, the postural change in pulsatility is also lessened, confirming that stroke volume is the major determinant of pulsatility under these conditions.

The present results allow comparison of pulmonary $\dot{Q}_C$ measurements with those reported previously (16). The slope of the regression lines for SV and PSF was remarkably similar in the two studies, considering that the design and mode of operation of the two body plethysmographs were quite different. In the present investigation, the values for SV and PSF fall even more in the 90° vertical position and lie on the lowest portion of the previously reported regression line (16), thus strongly suggesting that the same factors affecting CPA passively in seated man continue to operate when he assumes the erect posture.

Stroke volume was also significantly related to PSF immediately after exercise, performed in both supine and upright postures, and the slope of the regression line was remarkably similar to that obtained at rest; but it lay well above the latter when plotted on the same axes. Thus, in contrast to the resting relationship, the PSF was disproportionately greater for any given stroke volume immediately after exercise than at rest, and the CPA increased widely after exercise. This effect was due almost entirely to the large increase in PSF, which occurred in the face of a relatively small increase in systolic volume. The mechanism of the increase in CPA after exercise in both postures is not certain; but it may, in part, be due to a high peak in flow velocity of blood to the pulmonary arteries (10) and possibly to a decrease in pulmonary arterial vasomotor tone (6).

Finally, relatively narrow variation of the response of pulmonary $\dot{Q}_C$ to tilting procedures in normal subjects suggests that this test might be useful in determining the functional integrity of the circulatory system in patients with various cardiopulmonary abnormalities.

REFERENCES

1. Abel, F. L., J. H. Pierce, and W. G. Guntheroth. Baroreceptor influence on postural changes in blood pressure and carotid blood flow. Am J Physiol 205:360-364 (1963).

2. Allison, R. D., C. E. Lewis, and F. W. Rezek. Impedance plethysmograph study during a standardized tilt table procedure. Space Life Sci 2:361-393 (1970).

3. Bevegard, S., A. Holmgren, and B. Jonsson. The effect of body position on the circulation at rest and during exercise, with special reference to the influence on stroke volume. Acta Physiol Scand 49: 279-298 (1960).

4. Bouhuys, A., and H. J. van Lennep. Effect of body posture on gas distribution in the lungs. J Appl Physiol 17:38-42 (1962).

5. Chapman, C. B., J. N. Fisher, and B. J. Sproule. Behavior of stroke volume at rest and during exercise in human beings. J Clin Invest 39:1208-1213 (1960).

6. Donald, K. W., et al. The effect of exercise on the cardiac output and circulatory dynamics of normal subjects. Clin Sci 14:37-73 (1955).

7. Dougherty, R. L., et al. Body plethysmograph; a new body plethysmograph for cardiopulmonary studies in man. Analyzer 3:18-27 (1972).

8. Gray, S., III, et al. Acute and prolonged effects of G suit inflation on cardiovascular dynamics. Aerosp Med 40:40-43 (1969).

9. Hellebrandt, F. A., and E. B. Franseen. Physiological study of the vertical stance of man. Physiol Rev 23:20-55 (1943).

10. Karatzas, N. B., and G. J. De Lee. Propagation of blood flow pulse in the normal human pulmonary arterial system. Circ Res 25:11-21 (1969).

11. Lind, A. R., C. S. Leithead, and G. N. McNicol. Cardiovascular changes during syncope induced by tilting men in the heat. J Appl Physiol 25:268-276 (1968).

12. Naimark, A., and K. Wasserman. The effect of posture on pulmonary capillary blood flow in man. J Clin Invest 41:949-954 (1962).

13. Reeves, J. T., et al. Cardiac output response to standing and treadmill walking. J Appl Physiol 16:283-288 (1961).

14. Sackner, M. A., and R. Dougherty. Anti-G suit inflation on cardiac output of seated subjects. Riv Med Aeronaut Spaz (Roma) 46:264-266 (1973).

15. Segel, N., and J. M. Bishop. The circulatory effects of pronethalol with special reference to changes in heart rate and stroke volume during exercise. Clin Sci 29:363-373 (1965).

16. Segel, N., and M. B. McIlroy. Influence of respiration, stroke volume and heart rate on pulmonary capillary pulsatility. J Appl Physiol 26: 771-779 (1969).

17. Sjostrand, T. The regulation of the blood distribution in man. Acta Physiol Scand 26:312-327 (1952).

18. Sjostrand, T. Volume and distribution of blood and their significance in regulating the circulation. Physiol Rev 33:202-228 (1953).

19. Spodick, D. H., M. Meyer, and J. R. St. Pierre. Effect of upright tilt on the phases of the cardiac cycle in normal subjects. Cardiovasc Res 5:210-214 (1971).

20. Stead, E. A., Jr., et al. The cardiac output in male subjects as measured by the technique of right atrial catheterization. Normal values with observations on the effect of anxiety and tilting. J. Clin Invest 24:326-331 (1945).

21. Stevens, P. M. Cardiovascular dynamics during orthostasis and influence intravascular instrumentation. Am J Cardiol 17:211-218 (1966).

22. Strieder, D. J., R. Murphy, and H. Kazemi. Mechanism of postural hypoxemia in asymptomatic smokers. Am Rev Respir Dis 99:760-766 (1969).

23. Tuckman, J., and J. Shillingford. Effect of different degrees of tilt on cardiac output, heart rate and blood pressure in normal man. Br Heart J 28:32-39 (1966).

24. Wang, Y., R. J. Marshall, and J. T. Schepherd. The effect of changes in posture and of graded exercise on stroke volume in man. J Clin Invest 39:1051-1061 (1960).

25. Weissler, A. M., J. J. Leonard, and J. V. Warren. Effects of posture and atropine on the cardiac output. J Clin Invest 36:1656-1662 (1957).

26. Weissler, A. M., et al. Vasodepressor syncope; factors influencing cardiac output. Circulation 15:875-882 (1957).

FIGURES 1 - 5

for

Section IV: Part 1

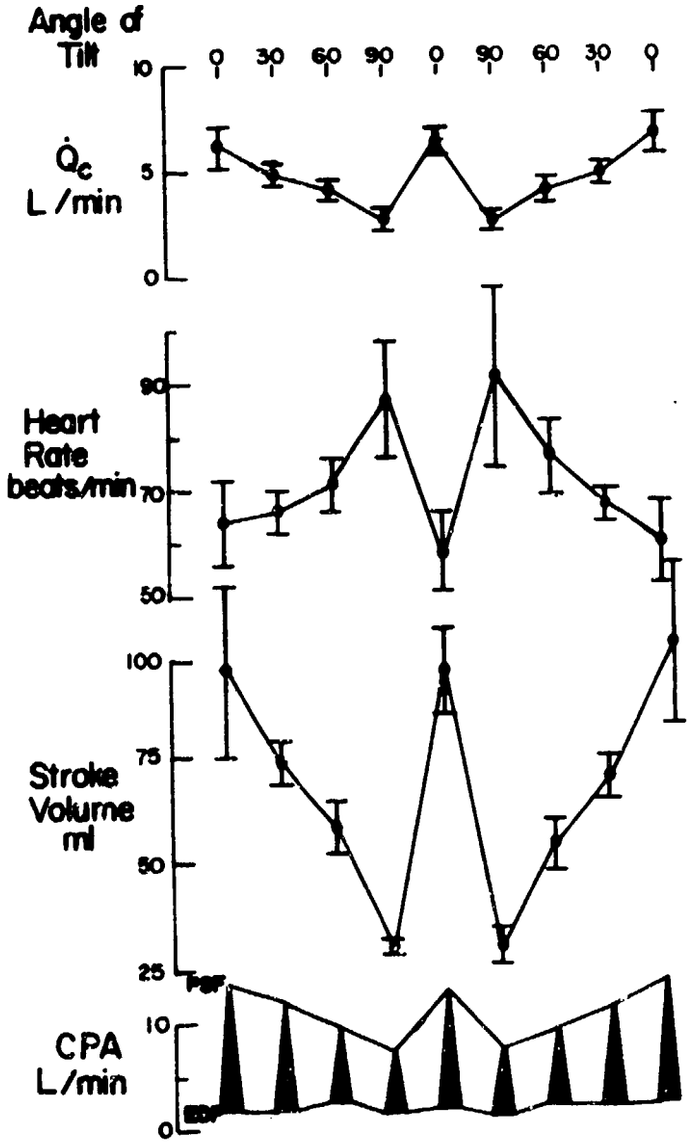

Figure 1. The effects--of tilting subjects from the supine (0^o) to the vertical position (90^c)--upon pulmonary capillary blood flow ($\dot{Q}_c$), heart rate, stroke volume, peak systolic flow (PSF) and end-diastolic flow (EDF), and capillary pulse amplitude (CPA). [Mean values in 4 normal subjects, SD, shown by vertical bars (I).]

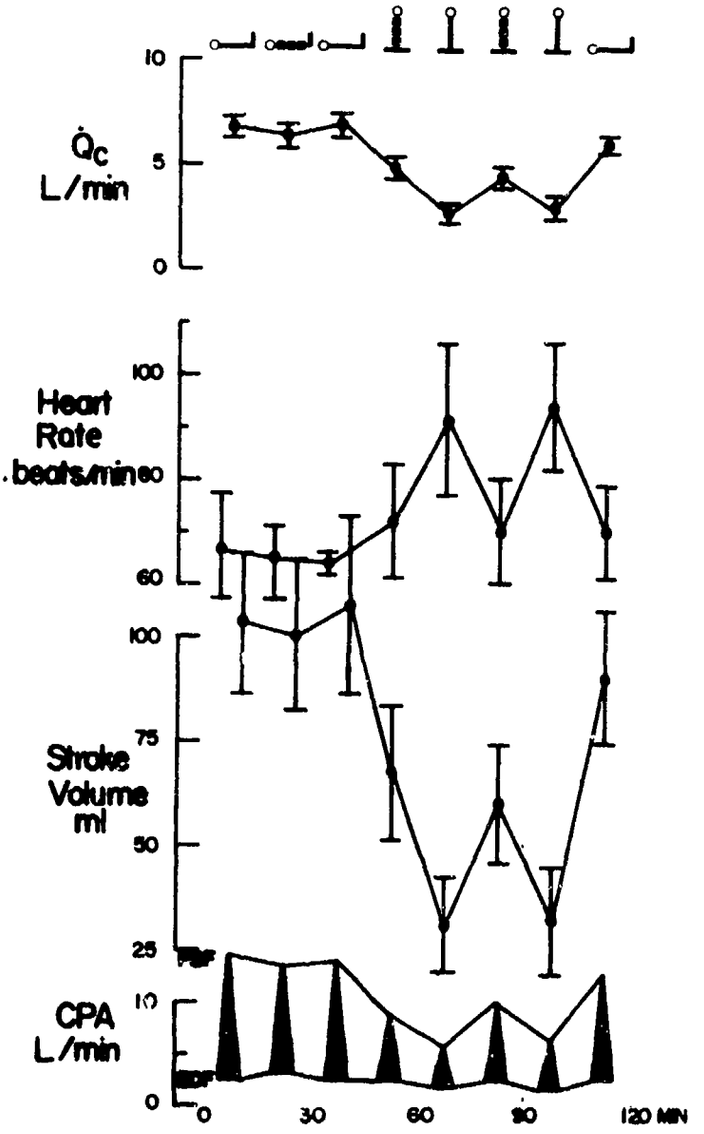

Figure 2. Mean values--for pulmonary $\dot{Q}_C$, heart rate, stroke volume, PSF and EDF, and CPA--in 10 normal subjects at rest in the supine and 90° head-up vertical postures before and during anti-G suit inflation ( ). [SD, shown by vertical bars (I).]

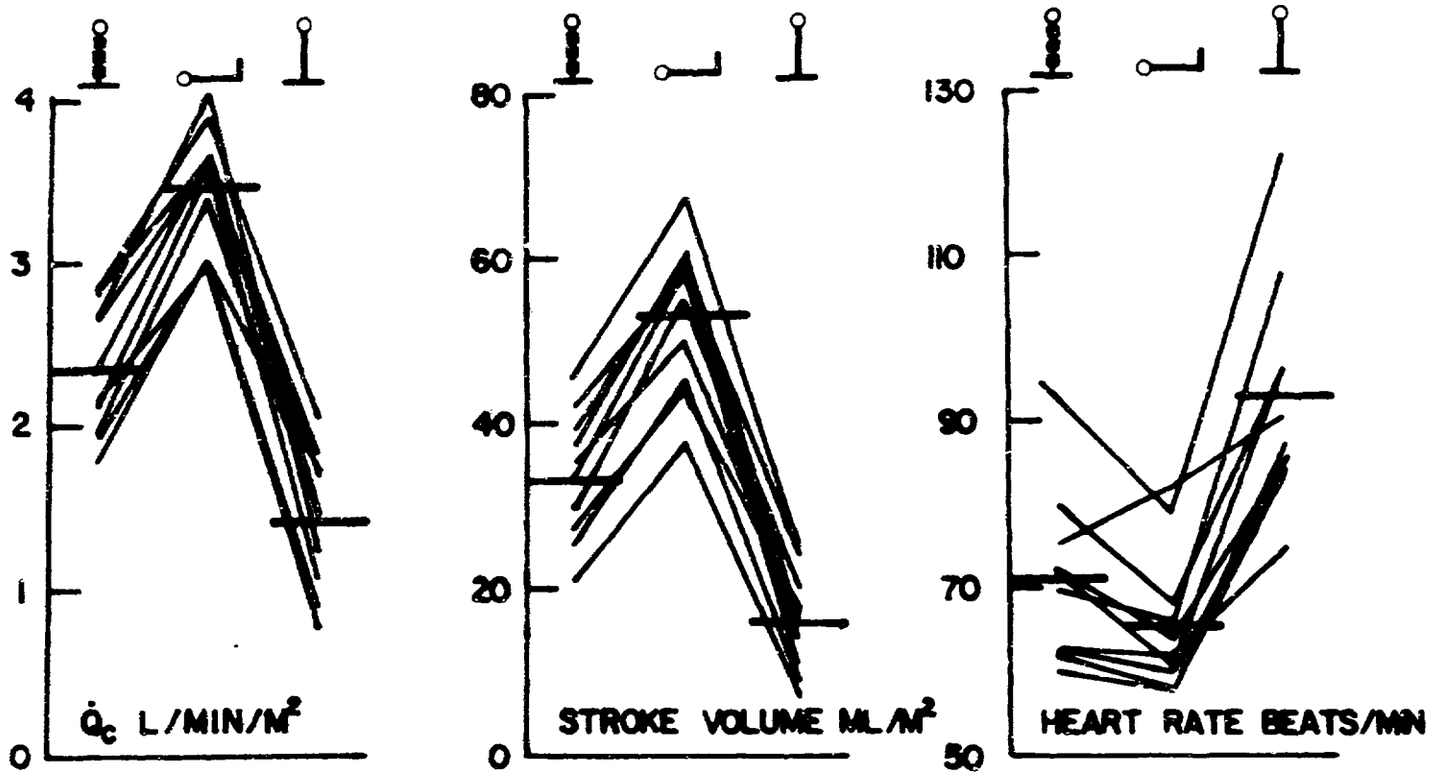

Figure 3. Individual results of $\dot{Q}_C$, stroke volume, and heart rate of subjects in the supine and vertical positions before ( ) and during anti-G suit inflation ( ).

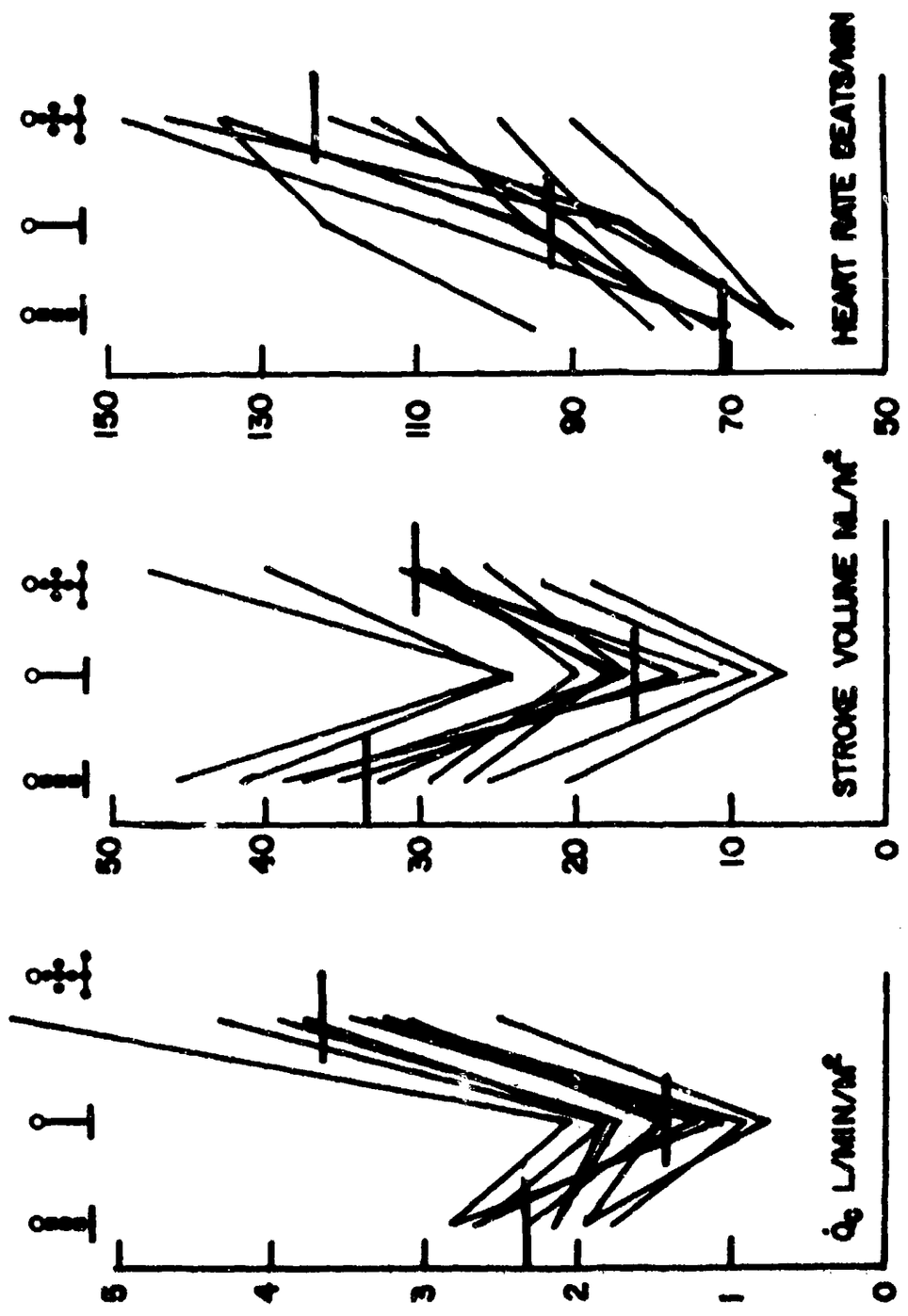

Figure 4. Individual results of pulmonary $\dot{Q}_C$, stroke volume, and heart rate of subjects in the vertical position before ( ), during anti-G suit inflation ( ), and immediately after exercise ( ).

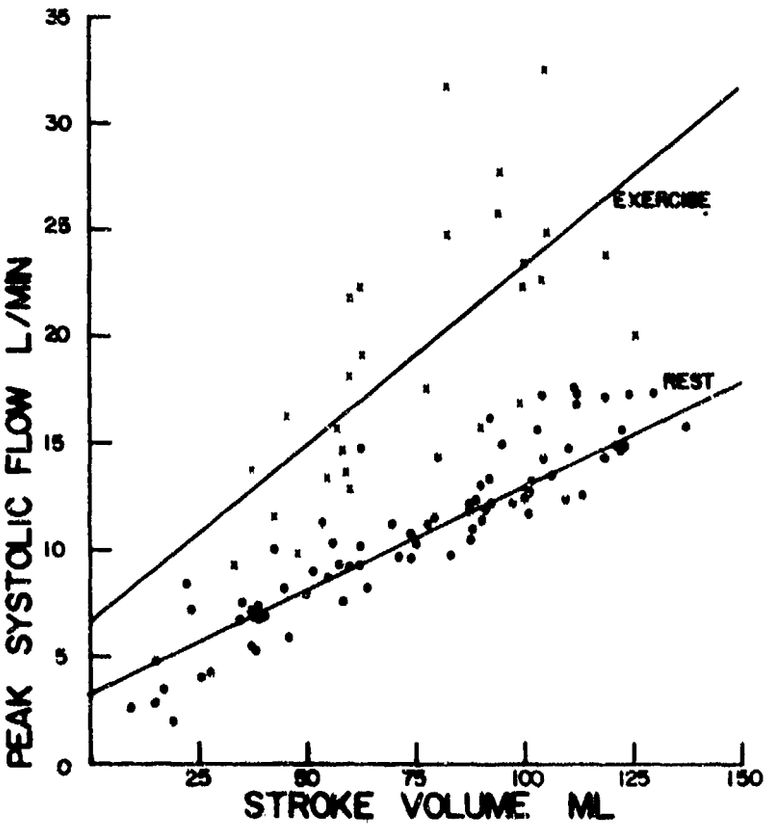

Figure 5. Relationship between individual values for stroke volume and peak systolic flow of subjects at rest (•) and during exercise (X) in the supine and 90° head-up vertical tilt positions.

PART 2: EFFECTS OF STANDARD ANTI-G SUIT ON CARDIAC OUTPUT OF SEATED SUBJECTS

ABSTRACT

The nitrous oxide plethysmographic technique was used to assess the effects of anti-G suit inflation on the cardiac output of seated human volunteers. No change in cardiac output, even with pressures as high as 6 psi, was induced by the inflation of the anti-G suit.

INTRODUCTION

The three reasons usually given for the increase in tolerance to acceleration application of anti-G suits include: rise in systemic arterial pressure; increase of venous return to the heart; and decrease in the vertical heart-to-head distance. In seated humans under +1 G_Z conditions, application of anti-G suits over a 5- to 10-sec period produces a rise in arterial and venous pressures accompanied by compensatory fall in heart rate (1, 2). In anesthetized dogs, pressure changes within the pulmonary circulation with inflations of an anti-G suit in the 1 - 5 psi range for 5 - 10 sec suggest that the suit produces an increase in venous return and probably an increase in intrathoracic blood volume (3). If venous return is increased by the anti-G suit, then cardiac output should increase as a function of Starling's Law of the Heart. In order to test this hypothesis, we measured cardiac output in seated normal volunteers under +1 G_Z conditions. We employed a modification of a bloodless nitrous oxide, body plethysmographic method which permitted us to measure cardiac output within 1 min post-inflation of the anti-G suit and at repeated intervals (4, 5).

METHODS

In turn, 10 normal male volunteers, ages 23 - 40 yr, donned a standard USAF anti-G suit. Each entered a vertical body plethysmograph, and serial measurements of pulmonary $\dot{Q}_C$ were made according to the following protocols.

In the first series of experiments the protocol was: (a) five control $\dot{Q}_C$ at 5-min intervals; (b) inflation of USAF anti-G suit at 2 psi followed by $\dot{Q}_C$ within 1 min, and 5, 15, and 20 min later; (c) deflation of anti-G suit followed by $\dot{Q}_C$ within 1 min, and 5, 15, and 20 min later; (d) subject left plethysmograph, lay supine for 5 min on the floor and the anti-G suit inflated at 2 psi; subject was lifted up by assistants and then walked four steps to the plethysmograph where he seated himself; $\dot{Q}_C$ was measured

within 1 min and 5, 10, 20, and 25 min later; and (e) deflation of anti-G suit followed by $\dot{Q}_C$ within 1 min, and 5, 10, 20, and 25 min later. In the second series of experiments, after the 5 control measurements, the anti-G suit was inflated and $\dot{Q}_C$ determined within 1 min, and 5, 10, 15, and 20 min later. The suit was then deflated in the sitting position and $\dot{Q}_C$ measured within 1 min, and 5, 10, and 15 min later. After the subject left the plethysmograph and lay supine for 5 min on the ground, he was lifted back into the plethysmograph without inflation of the anti-G suit. $\dot{Q}_C$ was measured, within 1 min, and 5 and 10 min later.

In the final series of experiments, the protocol for 8 subjects was: (a) two control $\dot{Q}_C$ at 5-min intervals; and (b) inflation of USAF anti-G suit at 6 psi, followed by $\dot{Q}_C$ within 1 min.

RESULTS

The effects of inflation of the anti-G suit with 2 psi in normal seated subjects are depicted in Figure 1. Inflation of the anti-G suit produced an average fall in heart rate of 7 beats/min ($P < .05$). The mean cardiac output of the 5 control runs was 3.99 L/min, SD 1.40. The cardiac output, postinflation, was: 3.55 L/min, SD 1.09 (P = NS); while the corresponding stroke volumes were: 57.8 ml, SD 20.4; 56.0 ml, SD 12.1, respectively (P = NS). After 20 min of anti-G suit inflation, the stroke volume showed a significant fall in the run immediately postdeflation, from 54.6 ml, SD 18.8, to 43.2 ml, SD 17.1 ($P < .02$). Neither heart rate nor cardiac output changes were of statistical significance; the former rose from 66 to 73 beats/min, and the cardiac output fell from 3.49 to 3.03 L/min.

When the anti-G suit was inflated in the supine position and the subject returned to the seated position for $\dot{Q}_C$ measurements, the following were observed. As compared with the five control runs with the subject in the seated position, heart rate slowed by 8 beats/min ($P < .05$), stroke volume increased from 57.8 to 92.5 ml ($P < .005$), and cardiac output rose from 3.99 to 5.79 L/min ($P < .001$).

The repeatability of the effects of the anti-G suit inflation can be noted in the study of 10 subjects approximately 3 months later (Fig. 2). As in the first series of experiments, the only significant change during anti-G suit inflation was a slowing of heart rate by 5 beats/min ($P < .02$). There was also a significant fall in stroke volume immediately after deflation of the anti-G suit. Changes in the seated subject's heart rate, stroke volume, and cardiac output--after rest in the supine position without inflating the anti-G suit--were similar to those when the suit was inflated.

There were no significant changes in heart rate, stroke volume, and cardiac output after immediate inflation and deflation of anti-G suit at 6 psi.

DISCUSSION

The bradycardia associated with inflation of the anti-G suit at +1 G_z in this study has also been observed by others (2). The bradycardia is probably due to depressor reflexes, originating in the carotid and aortic areas or thorax and abdomen, in response to the increase in arterial pressure produced by the suit. The response is blocked by the administration of tetraethylammonium chloride. It has been stated that the decrease in heart rate during suit inflation at +1 G_z may correlate with the protection offered by the suit to acceleration (2).

The fact that no significant increase occurred in stroke volume or cardiac output after inflation of the anti-G suit at 2 psi or 6 psi contrasts with our previous observations that the anti-G suit significantly affected hemodynamics in the passively tilted upright +1 G_z position. At a 90° tilt in 10 subjects--heart rate was 91.3 SD 14.5; stroke volume index 16.0 ml/M^2, SD 6.2; cardiac index 1.37 L/min/M^2, SD 0.40. After application of the anti-G suit at 2 psi, heart rate fell to 70.3, SD 9.6; stroke volume index rose to 32.2 ml/M^2, SD 8.1; cardiac index increased to 2.23 L/min/M^2, SD 0.48 ($P < .001$) (6). The failure of anti-G suit inflation in the seated position to increase the subject's cardiac output also occurred in the supine position (Table 1).

TABLE 1. EFFECT OF ANTI-G SUIT ON CARDIAC OUTPUT

			CARDIAC INDEX (L/min/M^2)	
Body position	Pressure (psi)	Subjects	Control	Anti-G suit
Sitting	2	20	2.12 ± 0.66	1.98 ± 0.70
Sitting	6	8	1.88 ± 0.41	1.99 ± 0.68
Supine	2	10	3.44 ± 0.39	3.29 ± 0.52
Supine	3	7	3.02 ± 0.41	2.98 ± 0.28
Standing	2	10	1.37 ± 0.40	2.23 ± 0.48
Standing	3	7	1.45 ± 0.27	1.76 ± 0.70

The discrepancy between the seated and supine positions as compared with the standing position might be related to the manner in which the anti-G suit inflates, or upon the amount of blood trapped in the lower half of the body at the +1 G_z positions. The standard USAF anti-G suit has abdominal, thigh, and leg bladders. For subjects in the seated position, it appears that the abdominal bladder might be pressurized slightly before the leg bladders. The inlet pressure tubing is situated at the abdominal bladder, and the leg bladders are inflated from tubings connected to the abdominal bladder. These connecting tubings might be partially crimped by the seated position and hence impede the rapid passage of air to the leg bladders. This impediment might produce a tourniquet effect on the lower extremities and hence cancel the increase or venous return produced by compression of the splanchnic and pelvic venous beds. We attempted to test this hypothesis by inflating the anti-G suit with the subject in the supine position and immediately making a measurement of the cardiac output while sitting. Although stroke volume and cardiac output showed significant increases after this maneuver, a sham experiment without inflating the anti-G suit produced similar results. This occurred because the subject had to take a few steps to climb back into the body plethysmograph, and therefore the hemodynamic alterations probably were due to exercise rather than the anti-G suit. Finally, it is possible that venous return is increased by the anti-G suit in the seated +1 G_z position; but, because of the curvilinearity of the Starling's Law of the Heart, the effective rise in filling pressure of the heart either does not produce a change which can be detected by our cardiac output method, or is masked by pain sensations induced by the inflated anti-G suit. Since the anti-G suit increases cardiac output in the standing position, where there is free egress of air to all the bladders, an anti-G suit should be designed for inflation upward from the calf to abdominal bladders; if an increase of cardiac output can be demonstrated in the seated position, this type of suit might afford more acceleration tolerance.

BIBLIOGRAPHY

1. Seiker, H. O., et al. A comparative study of two experimental pneumatic anti-G suits and the standard USAF G-4A anti-G suit. WADC Technical Report 52-317, Wright Air Development Center, Wright-Patterson AFB, Ohio, 1953.

2. Wood, E. H., and E. H. Lambert. Some factors which influence the protection afforded by pneumatic anti-G suits. J Aviat Med 23:218-228 (1952). [Now: Aviat Space Environ Med]

3. Lewis, D. H., and A. M. Stoll. The effects of external pressurization upon the cardiovascular system in dogs. I. Physiological aspects. NADC-MA-5709, Naval Air Development Center, Johnsville, Pa., 1957.

4. Lee, G. J. De, and A. B. DuBois. Pulmonary capillary blood flow in man. J Clin Invest 24:1380-1390 (1955).

5. Dougherty, R. L. Body plethysmograph: a new body plethysmograph for cardiopulmonary studies in man. Analyzer 3:18-27 (1972).

6. Segel, N., R. Dougherty, and M. A. Sackner. Effects of tilting on pulmonary capillary blood flow in normal humans. J Appl Physiol 35: 244-249 (1973).

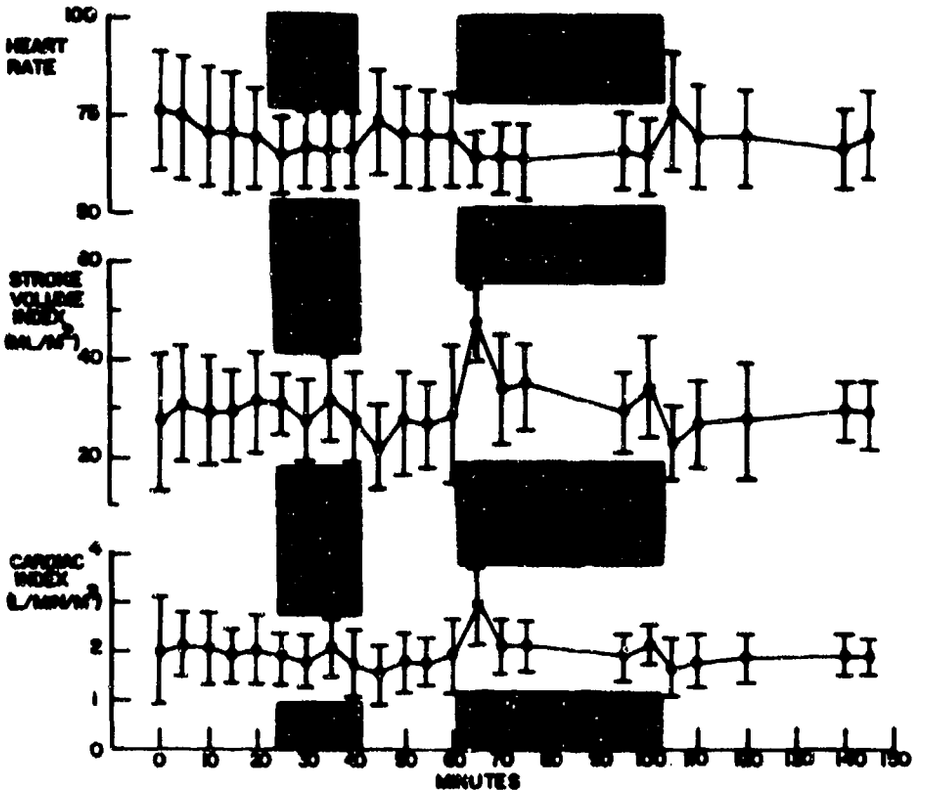

Figure 1. Heart rate, stroke volume index, and cardiac index plotted as a function of time in 10 normal subjects, pre- and postinflation of anti-G suit.

(Values are given for the mean and 1 SD. Nonshaded periods represent values in the seated position without inflation of the anti-G suit. The shaded period to the left represents values after anti-G suit inflation at 2 psi in the seated position. The shaded period to the right represents values in the seated position after anti-G suit inflation in the supine position.)

-IV-
(Part 2)

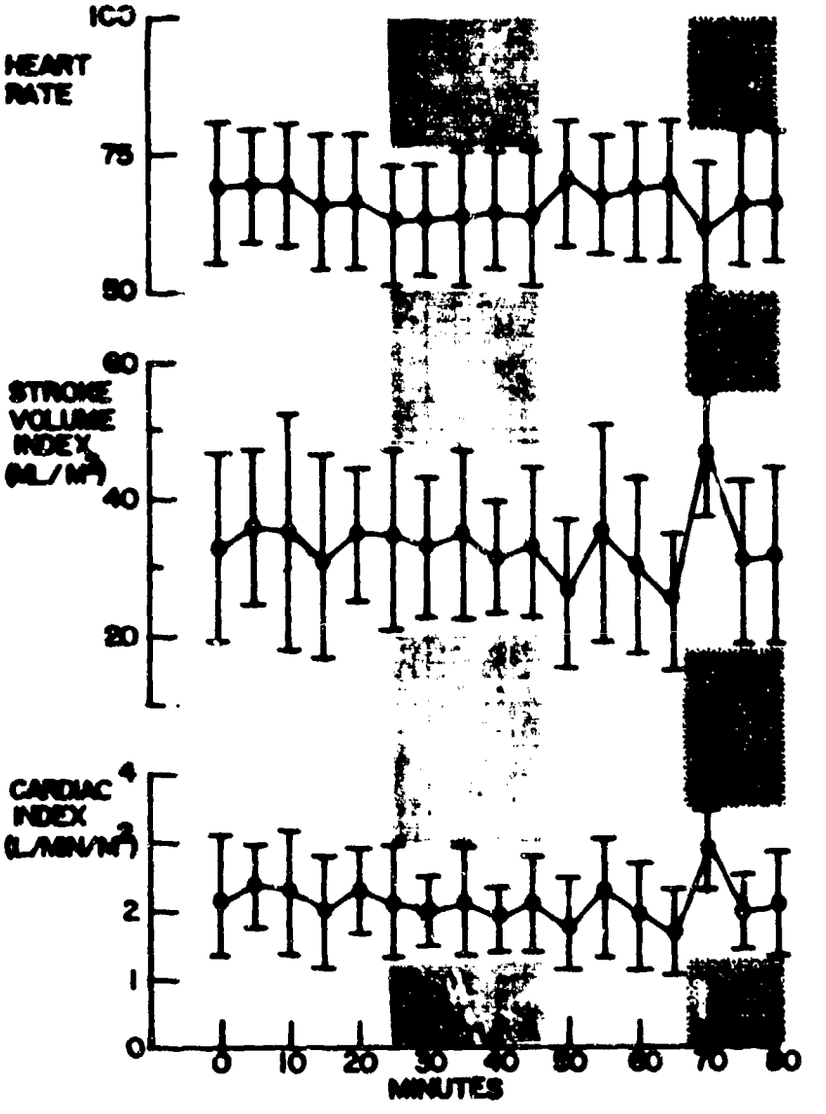

Figure 2. Heart rate, stroke volume index, and cardiac index plotted as a function of time in 10 normal subjects using inflated anti-G suit.

(Values are given for the mean and 1 SD. The shaded period to the left represents values after anti-G suit inflation at 2 psi with subject in the seated position. The shaded period to the right represents the seated position after "sham" inflation of the anti-G suit in the supine position.)

V. NONINVASIVE MEASUREMENTS OF PULMONARY AND SYSTEMIC CIRCULATION EFFECTS OF HYPOXIA

ABSTRACT

A noninvasive technique for calculation of mean pulmonary arterial pressure, using analysis of the pulmonary capillary blood flow pulse in conjunction with the phonocardiogram, was tested in 8 normal subjects breathing an hypoxic mixture. Only 2 of the 8 subjects showed the expected pulmonary arterial pressor effect of hypoxia. The apparent lack of sensitivity of this noninvasive technique is discussed and suggestions are made to improve it.

INTRODUCTION

In humans, the breathing of hypoxic mixtures is generally associated with an increase in pulmonary arterial pressure, although the response varies from subject to subject. Thus, in normal subjects, Daoud et al. (1) found that breathing a 10% O_2 in N_2 mixture caused a mean rise in pulmonary arterial pressure of 9 mm Hg above the control supine value of 15 mm Hg. This change was associated with a 33% increase in pulmonary arterial blood flow. Westcott et al. (2), using a 13% O_2 in N_2 mixture in 17 normal subjects, reported that median rise in pulmonary arterial pressure was 3.7 mm Hg. The extremes include one subject with a rise of only 0.3 mm Hg, and another with an increase of 19.1 mm Hg. No significant change occurred in pulmonary blood flow. Despite these variable responses to hypoxia, it was felt that breathing a hypoxic mixture might test the sensitivity of the method for noninvasive estimation of pulmonary arterial pressure (3, 4). This measure is determined from the analysis of the pulmonary capillary blood flow ($\dot{Q}_C$) pulse in conjunction with the phonocardiogram. The pulmonary arterial conduction time, the interval from the third component of the first heart sound (opening of the pulmonic valve) to the foot of the pulmonary $\dot{Q}_C$ pulse, is related by a curvilinear equation to mean pulmonary arterial pressure (4). The briefer the pulmonary arterial conduction time, the higher the mean pulmonary arterial pressure. Also examined, in addition to analysis of pulmonary $\dot{Q}_C$ during hypoxia, were other noninvasive parameters of circulatory function, the systolic time intervals of the carotid pulse (5), and peripheral blood flow in the arms and calves (6).

METHODS

The pulmonary $\dot{Q}_C$ during slow expiration was measured by the nitrous oxide plethysmographic technique (7). Lead II of the EKG and the high-frequency phonocardiogram from the pulmonic area were also recorded. The

second component of the second heart sound is known to correspond in time with the closure of the pulmonic valve, and the third component of the first heart sound corresponds with the opening of this valve.

From the pulmonary $\dot{Q}_C$ pulse and the phonocardiogram, the following variables were calculated: (a) the conduction time of the flow pulse from the pulmonic valve to pulmonary capillaries, measured as the time interval between the third vibration of the first heart sound and the foot of the pulmonary $\dot{Q}_C$ pulse; (b) the average acceleration of blood in the capillaries, computed from the difference between the flow rates at the foot and peak of the pulse divided by the time interval between these two points; (c) the percentage of stroke volume, stored in the pulmonary arterial tree during systole (systolic storage), is measured from the volume flow between the second component of the second heart sound and the third vibration of the first heart sound (diastolic volume), divided by the volume flow during the whole cardiac cycle, and expressed as a percentage (3); and (d) the mean pulmonary arterial pressure from an empirical equation based upon the pulmonary arterial conduction time (4).

The systolic time intervals of left ventricular systole were measured from simultaneous recordings of the EKG, phonocardiogram, and carotid pulse tracing. The carotid pulse was recorded through changes in electrical capacitance due to movement of an attached stretched latex diaphragm placed over the carotid artery. The total electromechanical systole (QS_2) is measured from the onset of ventricular depolarization to the first high-frequency vibrations of the aortic component of the second heart sound. The left ventricular ejection time (LVET) is measured from the beginning upstroke to the trough of the incisural notch on the carotid pulse tracing. The preejection phase (PEP) is derived by subtracting the LVET from QS_2. In the range of heart rate from 50 to 110 beats/min, these systolic time intervals are linearly related to heart rate and the values must be corrected if rate changes during a study (5). The ratio PEP:LVET appears to be independent of heart rate.

Blood flow to the forearm and calves was measured by mercury in Silastic strain gages (6).

Subjects

Eight normal male volunteers, ages 21 - 27 yr, gave informed consent for the study. They received financial remuneration for their participation. All worked in the Pulmonary Laboratory area and were familiar with the procedures used in the study.

Procedure

The subject rested within a horizontal body plethysmograph (8) for 20 min after the appropriate instrumentation had been applied. Control determinations of the hemodynamic parameters were made, and then the subject breathed a 10% O_2 in N_2 mixture through a demand valve. Measurements of pulmonary $\dot{Q}_c$, using a 10% O_2, 10% N_2, and 80% N_2O mixture, were made during the tenth and fifteenth minute after commencement of breathing the hypoxic mixture. At these times, systolic time intervals and peripheral blood flows were also obtained.

In 2 subjects, measurement of pulmonary $\dot{Q}_c$ were obtained in duplicate at predetermined thoracic gas volumes to permit calculation of mean pulmonary arterial pressure as a function of lung volume.

RESULTS

Pulmonary Capillary Blood Flow

The only significant changes in mean values during the breathing of the hypoxic mixture were a slight increase of heart rate and rises in cardiac output, peak output, and average acceleration (Table 1). The latter was measured as pulmonary $\dot{Q}_c$; but, since insignificant right-to-left intrapulmonary shunting occurs in normal subjects, it can be taken as cardiac output. Although conduction time shortened significantly after 15 min of hypoxia, there was no significant rise in pulmonary arterial pressure as calculated from the pulmonary arterial conduction time for the group as a whole. However, two subjects, Nos. 7 and 8, showed a calculated rise of 5.5 mm Hg and 7.9 mm Hg in pulmonary arterial pressure after 15-min exposure to the hypoxic mixture.

Systolic Time Intervals

Although there was a tendency toward shortening of the ratio PEP/LVET during hypoxia, no statistically significant changes in this function and other systolic time intervals were found (Table 2).

Peripheral Blood Flow

No significant change took place in forearm and leg blood flow during brief exposure to hypoxia (Table 3).

-V-

Influence of Lung Volume On
Calculated Pulmonary Arterial Pressure

There was a suggestion that calculated pulmonary arterial pressure was slightly higher at low than high lung volumes (Table 4).

DISCUSSION

The sensitivity of the noninvasive method for estimation of mean pulmonary arterial pressure in the present study appears to be poor. Although there is wide variability in the rise of directly measured pulmonary arterial pressure during the breathing of hypoxic mixtures, normal humans generally show a much larger increase than observed in the present study. Only 2 of the 8 subjects had a significant fall in pulmonary arterial conduction time with hypoxia leading to a rise in calculated pulmonary arterial pressure. Many factors might have given this disappointing result. First, it is possible that, by chance, 6 of the 8 subjects belonged to a group in which pulmonary vasoconstriction is minimally induced by hypoxia. (For example, Westcott et al. (2) observed that 3 of 17 normal subjects had less than a 2 mm Hg rise in pulmonary arterial pressure during the breathing of a hypoxic mixture.) Another contributing factor might have been the respiratory maneuver performed to obtain the measurement of pulmonary $\dot{Q}_C$. This vital capacity maneuver, which was used to inflate the lungs with the nitrous oxide mixture, might have transiently altered pulmonary vasomotor time. A third factor which must be considered was the lack of attention to making measurements at a fixed lung volume. After the hypoxia experiments were completed, this point was examined in 2 of the subjects, and it appears that calculated mean pulmonary arterial pressure is greater at higher than lower lung volumes. The calculation of mean pulmonary arterial pressure in humans is based upon data reported by Reuben (4, 9), who based his estimating equation on only 2 of 34 patients with mean pulmonary arterial pressures less than 15 mm Hg. Possibly, we were using an invalid equation over this low range of pulmonary arterial pressures. Lending support to this theory are the observations that Reuben et al. (10) made in anesthetized dogs. They found mean pulmonary arterial pressure during hypoxia rose from 12.9 to 20.8 mm Hg, while pulmonary arterial conduction time fell from 101 to 73 msec. Thus, for a rise in pulmonary pressure of 7.9 mm Hg, pulmonary arterial conduction time fell 17%. In the present study, after 15 min of hypoxia, pulmonary arterial conduction time fell 13% but calculated pulmonary arterial pressure increased only 2.3 mm Hg.

In order to validate the noninvasive estimate of pulmonary arterial pressure by analysis of pulmonary $\dot{Q}_C$ pulse, it will be necessary to avoid a vital capacity maneuver and to control lung volume at which the

measurements are made. Correlations with directly determined pulmonary arterial pressure are needed at the lower normal values of pressure.

The lack of change in the systolic time intervals and peripheral blood flow is not surprising in view of the paucity of central hemodynamic alterations obtained during brief exposure to hypoxia.

BIBLIOGRAPHY

1. Daoud, F. S., J. T. Reeves, and J. W. Schaeffer. Failure of hypoxic vasoconstriction in patients with liver cirrhosis. J Clin Invest 51: 1076-1080 (1972).

2. Westcott, R. N., et al. Anoxia and human pulmonary vascular resistance. J Clin Invest 30:957-970 (1951).

3. Karatzas, N. B., and G. J. De Lee. Propagation of pulmonary blood pulse in the normal human pulmonary arterial system. Circ Res 25:11-21 (1969).

4. Reuben, S. R. Wave transmission in the pulmonary arterial system in disease in man. Circ Res 27:523-529 (1970).

5. Weissler, A. M., W. S. Harris, and C. D. Schoenfeld. Bedside technics for the evaluation of ventricular function in man. Am J Cardiol 23:577-583 (1969).

6. Whitney, R. J. Measurement of volume change in human limbs. J Physiol 121:1-27 (1953).

7. Sackner, M. A., et al. Techniques of pulmonary capillary blood flow determinations. Bull Physiopathol Respir 9:1189-1202 (1973).

8. Dougherty, R. L., et al. A new body plethysmograph for cardiopulmonary studies in man. Analyzer 3:18-27 (1972).

9. Reuben, S. R. Compliance of the human pulmonary arterial system in disease. Circ Res 29:40-50 (1971).

10. Reuben, S. R., et al. Measurement of pulmonary arterial distensibility in the dog. Cardiovasc Res 4:473-481 (1970).

TABLE 1. ANALYSIS OF PULMONARY CAPILLARY BLOOD FLOW DURING 10% O_2 IN N_2 BREATHING

Subject	Heart Rate (beats/min)	Stroke Volume (ml)	Cardiac Output (L/min)	Peak Output (L/min)	Peak Output / Cardiac Output	Peak Output / Stroke Volume	Systolic Storage (%)	Average Acceleration ml/sec / msec	Conduction Time (msec)	Calculated Mean Pulm. Arterial Pressure (mmHg)	Total Pulm Vascular Resistance mmHg / L/min.
					Control						
1	64.6	118.0	7.61	11.72	1.53	0.099	75.4	6.8	206	13.3	1.75
2	61.4	108.4	6.64	10.84	1.63	0.100	80.2	5.8	216	12.4	1.87
3	47.2	164.0	7.70	13.31	1.73	0.081	81.4	6.3	216	12.4	1.61
4	64.5	71.1	4.61	7.81	1.74	0.110	78.8	4.3	206	12.9	2.80
5	63.3	106.4	6.72	11.08	1.65	0.140	69.0	5.5	178	15.0	2.23
6	63.6	121.9	7.72	11.95	1.55	0.098	75.8	6.7	232	11.5	1.49
7	54.7	102.9	5.61	10.45	1.87	0.102	80.5	7.0	174	15.4	2.74
8	55.7	150.1	8.34	15.84	1.91	0.106	81.2	9.8	202	13.2	1.58
Mean	59.4	117.8	6.87	11.62	1.70	0.100	77.8	6.5	204	13.2	2.01
SD	5.8	27.0	1.17	2.16	0.13	0.008	4.0	1.5	18	1.2	0.49
					10 Minutes						
1	75.9	90.7	6.87	8.93	1.32	0.098	74.4	6.7	176	15.2	2.21
2	70.1	107.5	7.58	14.59	1.94	0.136	83.7	11.3	197	13.5	1.79
3	60.4	143.2	8.65	13.53	1.56	0.094	75.6	9.6	237	11.3	1.30
4	68.8	66.5	4.56	8.50	1.86	0.128	85.0	6.3	205	13.0	2.85
	83.8	73.2	6.09	12.75	2.09	0.174	76.5	10.3	192	13.9	2.28
6	72.8	161.5	11.75	17.37	1.48	0.108	71.5	10.7	214	12.4	0.97
7	60.0	104.2	6.26	12.12	1.94	0.116	79.4	10.6	184	14.5	2.32
8	69.4	231.2	16.03	26.96	1.68	0.117	67.9	15.2	235	11.4	0.71
Mean	70.2*	122.2	8.45	14.34	1.73	0.120	76.8	10.1*	205	13.1	1.80
SD	7.2	51.1	3.49	5.47	0.25	0.025	5.4	2.6	21	1.3	0.70

TABLE 1. (CONTINUED)

Subject	Heart Rate (beats/min)	Stroke Volume (ml)	Cardiac Output (L/min)	Peak Output (L/min)	Peak Output / Cardiac Output	Peak Output / Stroke Volume	Systolic Storage (%)	Average Acceleration ml/sec / msec	Conduction Time (msec)	Calculated Mean Pulm. Arterial Pressure (mmHg)	Total Pulm Vascular Resistance mmHg / L/min.
				15 Minutes							
1	82.2	92.5	7.96	12.03	1.51	0.130	73.0	10.5	197	13.5	1.70
2	70.1	116.7	7.87	12.03	1.53	0.103	77.5	7.0	194	13.7	1.72
3	65.8	150.5	9.87	14.87	1.51	0.099	72.6	7.6	194	13.7	1.39
4	68.8	105.5	7.25	10.87	1.50	0.103	74.7	4.0	204	13.0	1.79
5	86.2	71.0	6.09	12.53	2.06	0.176	69.3	9.0	172	15.6	2.56
6	70.1	163.7	11.46	17.87	1.56	0.109	73.1	11.4	207	12.8	1.12
7	58.6	111.5	6.53	12.59	1.93	0.113	87.2	7.4	132	20.9	3.20
8	66.9	155.2	10.37	16.84	1.62	0.109	73.1	13.2	131	21.1	2.03
Mean	71.1*	120.8	8.42+	13.70+	1.65	0.118	75.1	8.8+	179+	15.6	1.94
SD	9.6	30.7	1.80	2.37	0.20	0.023	5.0	2.7	29	3.2	0.62

+ Difference from control P < .02
* Difference from control P < .01
# Difference from control P < .001

TABLE 2. EFFECTS OF 10% O_2 IN N_2 ON SYSTOLIC TIME INTERVALS IN 8 NORMAL SUBJECTS*

	Control		10 Min		15 Min	
	Mean	SD	Mean	SD	Mean	SD
QS_2+	-19	12	-23	19	-22	20
PEP+	-28	10	-20	27	-31	8
LVET+	11	9	8	17	11	18
PEP/LVET	0.246	0.034	0.236	0.034	0.234	0.030

*Control measurement and during breathing the hypoxic mixture for 10 and 15 min.

+Millisecond deviation from predicted values based upon heart rate (ref. 5).

TABLE 3. EFFECTS OF 10% O_2 IN N_2 BREATHING ON PERIPHERAL BLOOD FLOW IN NORMAL SUBJECTS

	Control	10 min	15 min
Forearm blood flow (ml/100 ml)			
No. of subjects	7	7	7
Mean	3.7	4.5	5.1
SD	1.0	2.3	2.2
P		>.05	>.05
Leg blood flow (ml/100 ml)			
No. of subjects	8	8	8
Mean	2.9	2.4	3.0
SD	1.6	1.1	2.0
P		>.05	>.05

TABLE 4. LUNG VOLUME AND PULMONARY ARTERIAL CONDUCTION TIME

Thoracic gas volume (L/BTPS)	Pulmonary arterial conduction time (msec)	Calculated $P_{\overline{PA}}$ (mm Hg)
	Subject 1	
4.00	254	10.6
3.40	260	10.4
2.70	221	12.0
	Subject 2	
4.00	268	10.1
3.40	264	10.2
4.40	254	10.6
2.40	251	10.7

VI. HEMODYNAMIC EFFECTS OF EPINEPHRINE AND TERBUTALINE IN MAN

ABSTRACT

The hemodynamic effects of subcutaneous epinephrine, 0.5 mg and 0.25 mg (an agent which stimulates alpha and beta adrenergic receptors), terbutaline 0.5 mg and 0.25 mg (an agent with more selective beta 2 activity), and normal saline in normal man were assessed by a double blind study using a modified latin squares design. Noninvasive circulatory techniques were employed because of the large number of measurements and the 5-hr duration of study for each agent. Instantaneous pulmonary capillary blood flow ($\dot{Q}_C$) by a nitrous oxide plethysmographic technique, systolic time intervals, and calf blood flow were measured. Studies were carried out in the supine position on alternate days in 10 normal volunteers. After a control period of 1 hr, the hemodynamic effects of these agents were studied over a 4-hr period. Epinephrine and terbutaline had qualitatively similar actions with peak hemodynamic responses of similar magnitude in equivalent doses. There was an increase in cardiac output mostly related to tachycardia rather than augmentation of stroke volume, a fall in systemic vascular resistance, an increase in calf blood flow, and no alteration in systolic time intervals. Terbutaline appeared to stimulate both beta-1 and beta-2 adrenergic receptors initially; but most of the effects 1 hr postinjection were predominantly beta-2 receptor stimulation, as indicated by a fall in systemic vascular resistance which was accompanied by tachycardia, while stroke volume remained at control levels. Evidence was also presented from analysis of the pulmonary $\dot{Q}_C$ pulse that both epinephrine and terbutaline probably produced pulmonary vasodilatation.

INTRODUCTION

Ahlquist (1) and Lands et al.(2) have distinguished three adrenergic receptor sites, designated as: alpha, beta-1, and beta-2. Alpha activity is marked by peripheral arterial constriction; beta-1, by positive chronotropic and inotropic effects on the heart, relaxation of small intestine and lipolysis of adipose tissue; and beta-2, by bronchodilatation, peripheral vasodilatation, and muscle glycogenolysis. The bronchodilator action of subcutaneous epinephrine, an agent commonly employed in status asthmaticus, lasts 3 to 4 hours (3) but the duration of its hemodynamic effects has not been studied. This agent displays both alpha and beta activity, as demonstrated by its effects on the peripheral vasculature (4). Small doses of epinephrine produce peripheral vasodilatation by beta-2 stimulation; large doses cause a transient rise in peripheral vascular resistance due to alpha stimulation which, with time, gives way to vasodilation as

the longer acting beta-2 effect predominates. In an effort to avoid the side effects of alpha and beta-1 stimulation that occur with epinephrine, several new compounds--terbutaline, salbutamol and orciprenaline--have been introduced into clinical practice as superior bronchodilator agents through more selective beta-2 receptor stimulation (5, 6). The purpose of the present study has been to compare the hemodynamic effects of subcutaneous epinephrine in normal man to those of one of the more selective beta-2 adrenergic stimulants, terbutaline. Since the study was designed to assess placebo effect and dose response of these agents, it would not have been feasible to carry out the hemodynamic evaluations by invasive techniques. Noninvasive methods were employed to estimate the effects of saline, epinephrine, and terbutaline on the systemic and pulmonary circulations and the heart. The measurement of instantaneous pulmonary $\dot{Q}_C$ by the nitrous oxide plethysmographic technique (7), along with the determination of pulmonary conduction time (8, 9), was chosen to evaluate effects of these agents on cardiac output and pulmonary vasomotor tone. Systolic time intervals from the carotid pulse tracing (10) were employed to indirectly assess myocardial contractility. The determination of systemic blood pressure by the Riva-Rocci method and calf blood flow by venous occlusion plethysmography (11) were used to investigate alternations in peripheral vasomotor tone.

METHODS AND PROCEDURES

Instantaneous pulmonary $\dot{Q}_C$ (beat-by-beat blood flow) during slow expiration was measured by the nitrous oxide plethysmographic technique (7). The mean capillary flow pulse was obtained by averaging all pulses obtained over a 10 - 15 sec determination with a digital computer. Lead II of the EKG and the high-frequency phonocardiogram from the pulmonic area were also recorded. The second component of the second heart sound is known to correspond in time with the closure of the pulmonic valve, and the third component of the first heart sound corresponds with the opening of this valve (8, 9). From the pulmonary $\dot{Q}_C$ pulse and the phonocardiogram, the following variables were calculated:

(a) The conduction time of the flow pulse from the pulmonic valve to pulmonary capillaries, measured as the time interval between the third vibration of the first heart sound and the foot of the pulmonary $\dot{Q}_C$; (b) the average acceleration of blood in the capillaries, computed from the difference between the flow rates at the foot and peak of the pulse divided by the time interval between these two points; (c) the percentage of stroke volume stored in the pulmonary arterial tree during systole (systolic storage)--this is measured from the volume flow between the second component of the second heart sound and the third vibration of

the first heart sound (diastolic volume), divided by the volume flow during the whole cardiac cycle expressed as a percentage (8); and (d) the mean pulmonary arterial pressure calculated from an empirical equation based upon the pulmonary arterial conduction time (9).

The systolic time intervals of left ventricular systole were measured from simultaneous recordings of the EKG, phonocardiogram, and carotid pulse tracing. The latter was recorded through changes in electrical capacitance due to movement of a stretched latex diaphragm placed over the carotid artery. The total electromechanical systole (QS_2) is measured from the onset of ventricular depolarization to the first high-frequency vibrations of the aortic component of the second heart sound. The left ventricular ejection time (LVET) is measured from the beginning upstroke to the trough of the incisural notch on the carotid pulse tracing. The pre-ejection phase (PEP) is derived by subtracting LVET from QS_2. In the range of heart rate from 50 to 110 beats/min, these systolic time intervals are linearly related to heart rate and the values must be corrected if rate changes during a study (10). Blood flow to the calf was measured by venous occlusion plethysmography, using mercury in silastic strain gages to measure volume changes (11). Systolic blood pressure was measured at the brachial artery by the Riva-Rocc. method, using Phase IV for diastolic pressure; mean blood pressure was calculated by adding one-third of the pulse pressure to the diastolic pressure.

Ten normal male volunteers, ages 21 - 40 years (mean age, 27 years) gave informed consent for the studies. They received financial remuneration for their participation. All worked in the Pulmonary Laboratory area and were familiar with the procedures used in the study. They arrived in the Laboratory at 8:00 a.m. in a fasting condition. The respective subject rested within a horizontal body plethysmograph (7) for 15 min after the appropriate instrumentation had been applied. This instrumentation consisted of a capacitance gage sensor for external carotid pulse tracings, a microphone for recording of heart sounds at the 3rd interspace along the left sternal border, electrocardiographic leads on the extremities, and mercury in silastic strain gage around the calf. Control measurements were made in duplicate at each point in time. The control values were obtained from the average at 60, 30, and 0.5 min before drug injection. The drugs tested were administered subcutaneously in a volume of 0.5 ml on a double blind basis according to a latin square experimental design. They included saline, epinephrine 0.5 mg, epinephrine 0.25 mg, terbutaline 0.5 mg, and terbutaline 0.25 mg. Testing was done on alternate days, beginning at 8:00 a.m. with the subject in a postabsorptive state. The data were treated statistically by means of a three-dimensional design of co-variance (ABS test) and critical differences calculated to

ascertain the probability of a difference among means being statistically significant (12). In addition, all subjects were also studied in the sitting position in a vertical body plethysmograph after subcutaneous injection of terbutaline 0.25 mg. These data were compared to the control measurements and the differences analyzed by means of Student's t-test.

RESULTS

Effects of Drugs on Hemodynamics Over Time in Supine Subjects

Saline--These data are summarized in Table 1. The control value was taken as the average of the three measurements before injection of the drug. The hemodynamic variables were quite stable over the duration of the study, with the exception of minor alterations in stroke volume, QS_2 interval, and the ratio of peak systolic blood flow (PSF) divided by stroke volume toward the end of the procedure.

Epinephrine 0.5 mg--This agent produced a maximum rise in heart rate of 17.5 beats/min above control value 30 min after drug injection (Table 2). The tachycardia persisted throughout the 4-hr duration of the study. Cardiac output increased 62% above control 30 min after drug administration. The rise in cardiac output was related to both tachycardia and increase in stroke volume. The stroke volume increased maximally, 27% above control 15 min after drug administration. After the initial rise in values, both cardiac output and stroke volume returned to control levels at 2 hr. Systolic blood pressure rose and diastolic pressure fell in the first hour after epinephrine injection, but mean blood pressure remained unchanged throughout the 4-hr duration of the test. The calculated systemic vascular resistance (mean blood pressure divided by cardiac output) fell 39% below control 15 min after drug administration and remained low through the first hour, while calf blood flow showed a concomitant increase. Except for lengthening of the QS_2 interval in the first hour, there was no change in the systolic time intervals when corrected for change in heart rate. PSF and the ratio of PSF divided by stroke volume were increased in the pulmonary capillaries for 4 hr and 2 hr, respectively, after epinephrine administration. There was a substantial increase in average acceleration of pulmonary $\dot{Q}_C$, and a significant fall in pulmonary arterial conduction time during the first hour after the epinephrine had been given. However, the control calculated value of mean pulmonary arterial pressure was not significantly affected by the drug, nor was the systolic storage of blood in the pulmonary capillaries.

Epinephrine 0.25 mg--In this dose, the agent produced a maximum rise in heart rate of 10.1 beats/min above the control value 30 min after

drug administration (Table 3). Tachycardia persisted throughout the 4-hr duration of the study. Cardiac output increased to a maximum of 49% above control 15 min after epinephrine had been administered. This increase in cardiac output was related to both tachycardia and increase in stroke volume. The stroke volume reached its maximum value, 28%, above control 15 min after drug administration. It fell to control values 1 hr after epinephrine administration. Systolic blood pressure rose and diastolic blood pressure fell the first hour after epinephrine injection; however, mean blood pressure remained unchanged throughout the 4-hr duration of the test. Calculated systemic vascular resistance fell 35% below control in the first 15 min after drug administration, and remained at a low level during the first hour of the study. Except for a slight lengthening of the QS_2 interval in the first 15 min and at the 2-hr measurement, there were no changes in PEP and LVET when corrected for changes in heart rate. No change in calf blood flow was detected by the venous occlusion plethysmography. PSF and the ratio of PSF divided by stroke volume increased in the first hour of the test. Average pulmonary capillary acceleration increased in the first 30 min and then fell to control values. The pulmonary arterial conduction time shortened, but this was statistically significant only at 30 min after drug administration. The calculated mean pulmonary arterial pressure and systolic storage of blood in the pulmonary capillaries were not affected by the drug.

Terbutaline 0.5 mg--The agent in this dosage produced a maximum rise in heart rate of 32 beats/min, 30 min after administration of the drug (Table 4). Tachycardia persisted throughout the 4-hr duration of this study. Cardiac output rose maximally 15 min after terbutaline administration to 85% above control. Stroke volume rose 30% above control after 15 min, and remained at an increased level over the first hour of the study and then fell to control levels. The systolic blood pressure remained elevated over the 4-hr duration of the study. The diastolic pressure fell over the first hour. There was no significant change in the mean blood pressure compared to the control values. Systemic vascular resistance fell 48% below control and remained low through the first 3 hr of the study. There was a concomitant increase in calf blood flow through this period. Except for minor changes in the QS_2 interval, PEP and LVET corrected for change in heart rate did not change over the 4-hr period of the study. PSF and the ratio of PSF divided by stroke volume were elevated throughout the entire 4-hr period of the study. Average pulmonary capillary acceleration increased during the first hour. Pulmonary arterial conduction time fell significantly throughout the first 2 hr of the study, but the calculated mean pulmonary arterial pressure did not change. The systolic storage of blood in the pulmonary capillaries was not affected by the drug.

Terbutaline 0.25 mg--A maximum rise in heart rate of 17.2 beats/min was reached 60 min after the drug was administered (Table 5). Tachycardia persisted throughout the entire 4-hr study period. The cardiac output rose 48% above control in the first 30 - 60 min after drug administration. There was a concomitant increase in stroke volume 14% above control which took place 15 min after terbutaline was administered, but the elevation of stroke volume persisted only through the first hour of the study. Systolic blood pressure remained elevated over the first 2 hr of the study, while diastolic blood pressure was lower than control values during the first hour after the drug had been administered. Mean blood pressure remained unchanged throughout the duration of the study. Systemic vascular resistance fell 36% below control 30 min after the drug was given, and remained low throughout the first 2 hr of the study. One hour after drug administration, calf blood flow showed a slight increase. Except for slight prolongation of the QS_2 interval in the first 30 min, there were no significant changes in PEP and LVET when corrected for changes in heart rate. PSF in the pulmonary capillaries and the ratio of PSF divided by stroke volume increased in the first and second hour of the study. There was also an increase in pulmonary $\dot{Q}_C$ acceleration and a fall in pulmonary arterial conduction time during the first hour. Calculated mean pulmonary arterial pressure and systolic storage of blood in the pulmonary capillaries were not affected by the drug.

Comparison of Epinephrine and Terbutaline on Systemic Hemodynamics in Supine Subjects

Epinephrine 0.5 mg vs. terbutaline 0.5 mg (Table 6)--Terbutaline produced a more rapid heart rate over the 4-hr study period than epinephrine. The cardiac output was significantly higher after terbutaline administration over the first 2 hours (Fig. 1), but there was no difference between the two agents in the quantitative rise in stroke volume. A fall in systemic vascular resistance was produced by both agents, but this effect persisted longer with terbutaline. The increase in calf blood flow produced by epinephrine was significantly greater than that produced by terbutaline 15 min after drug administration, but thereafter the increases in this parameter were the same. There were no statistical differences in systolic time intervals when the drugs were compared.

Epinephrine 0.25 mg vs. terbutaline 0.25 mg (Table 6)--Terbutaline produced a significantly faster heart rate over the first 3 hr than epinephrine. The initial increase in cardiac output produced by both agents was of similar magnitude; but the effect was more prolonged with terbutaline to 3 hr after its administration, whereas cardiac output returned to control

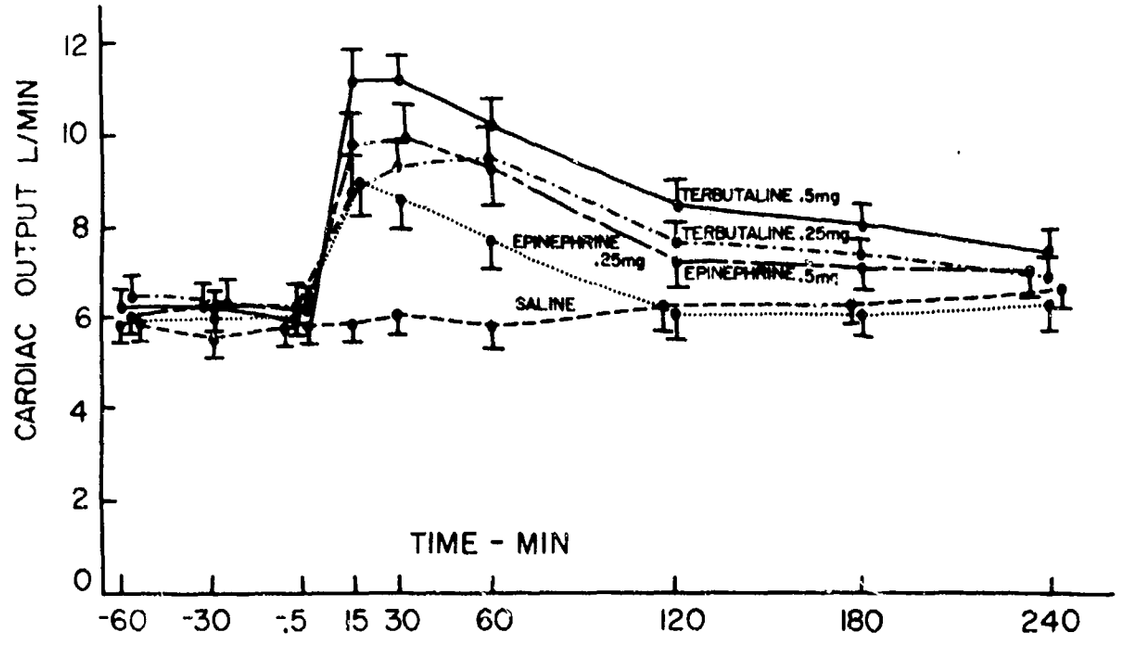

Figure 1. Effects of drugs on cardiac output. (The drugs were given immediately after the observations recorded at -0.5 min. The values indicate the mean and 1 SE. The increase of cardiac output induced by terbutaline is greater and more prolonged than an equivalent dose of epinephrine.)

levels at 2 hr after epinephrine administration. The changes in stroke volume were similar for both drugs. Systemic vascular resistance remained lower for terbutaline from the first through the fourth hour of the study when compared to epinephrine. At 1 hr after drug administration, terbutaline 0.25 mg caused a much larger increase in calf blood flow than epinephrine 0.25 mg; but, otherwise, differences in this parameter were slight. Systolic time intervals were not significantly affected by either of these drugs.

Comparison of Epinephrine and Terbutaline on Pulmonary Hemodynamics in Supine Subjects

Epinephrine 0.5 mg vs. terbutaline 0.5 mg (Table 7)--Although both drugs elevated the ratio of PSF, divided by stroke volume, this elevation was of much greater magnitude with terbutaline in the first 30- to 60-min period after drug administration than with epinephrine (Fig. 2). Also, terbutaline caused a greater increase in average acceleration of pulmonary capillary flow in the first 15 min after administration. There was no difference between the two drugs in their action on shortening of pulmonary arterial conduction in the first 1 - 2 hr after drug administration. The rises in calculated mean pulmonary arterial pressure were not statistically significant with time. When total pulmonary vascular resistance was calculated by dividing this value by cardiac output (Table 8), there appeared to be a similar diminution in total pulmonary vascular resistance with both epinephrine and terbutaline.

Epinephrine 0.25 mg vs. terbutaline 0.25 mg--There were few statistical differences between the two drugs at this dose among the various parameters of pulmonary circulation (Tables 7 and 8).

Effects of Terbutaline 0.25 mg on Hemodynamics in Seated Subjects

The heart rate, after terbutaline 0.25 mg, rose to a maximum of 11 beats above the control value 60 min after the drug was administered (Table 9). This tachycardia persisted throughout the 4-hr period of the study. Cardiac output increased 33% above control after 1 hr and then declined to control levels (Table 10). With the subject in the sitting position, no significant change occurred in stroke volume after terbutaline administration. The systolic blood pressure rose slightly during the first 30 min. No change occurred in diastolic mean blood pressure throughout the 4-hr period of the study. There was a 24% fall in systemic vascular resistance 1 hr after terbutaline 0.25 mg had been given. PSF in the pulmonary capillaries rose

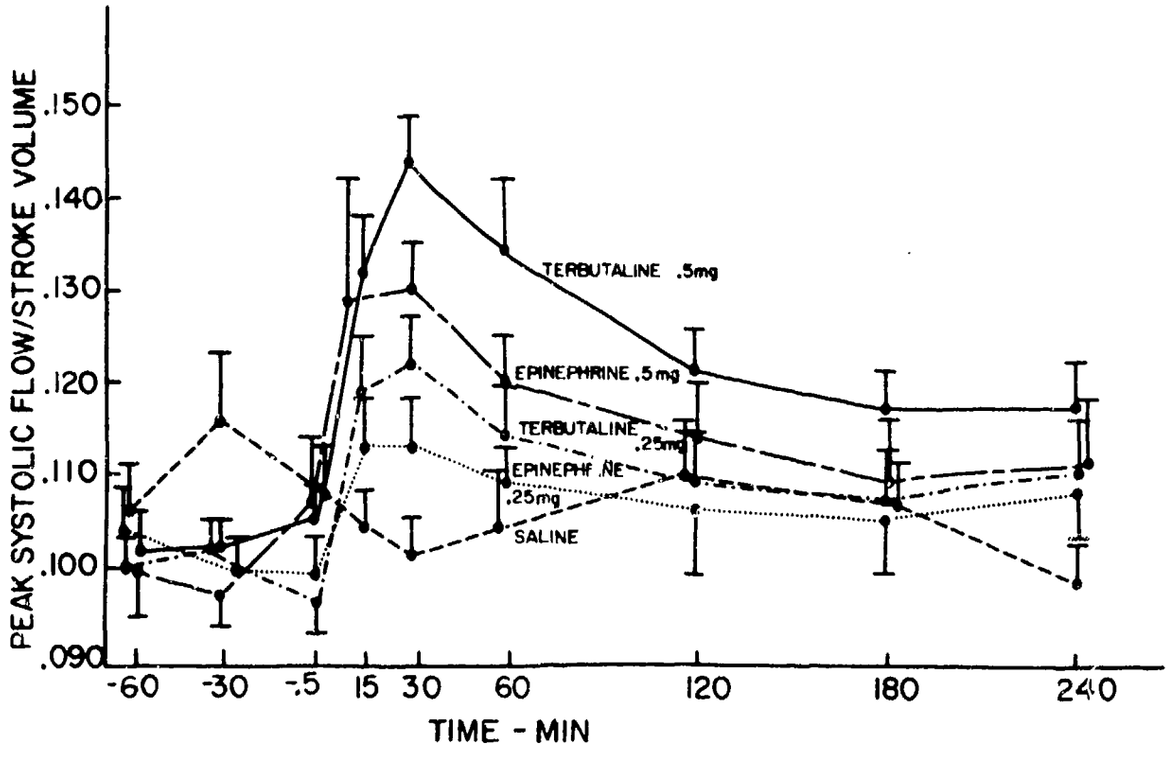

Figure 2. Effects of drugs on the ratio of PSF divided by stroke volume. (The drugs were given immediately after the observations recorded at -0.5 min. The values indicate the mean and 1 SE. This index of pulsatility of pulmonary $\dot{Q}_C$ was increased more by terbutaline than epinephrine in equivalent doses.)

slightly in the first 30 min, as did the ratio of PST divided by stroke volume (Table 11). There was a slight rise in average pulmonary acceleration of blood in the pulmonary capillaries through the first hour. A slight fall in pulmonary arterial conduction time occurred 30 min after the drug was given, but this parameter returned to normal values thereafter.

DISCUSSION

The bronchodilator effect of adrenergic agents can be explained through stimulation of beta-2 receptors, while cardiac effects--such as tachycardia, augmentation of stroke volume, and increase of myocardial contractility--may be attributed to stimulation of beta-1 receptors. Further, decrease in diastolic pressure and systemic vascular resistance are related to beta-2 receptor stimulation resulting from peripheral vasodilatation (1, 2, 4). A bronchodilator which would selectively stimulate the beta-2 receptors without causing stimulation of beta-1 receptors might mean an advance in the treatment of patients with bronchospasm because of the lack of cardiac side effects. However, the cardiac effects of these agents probably cannot be avoided, since tachycardia may not only be induced directly as a chronotropic action by beta-1 receptor stimulation but also indirectly because of a baroreceptor adjustment response to peripheral vasodilatation, a beta-2 receptor activity. Nevertheless, if beta-1 receptor stimulation were avoided, such agents might minimize undesirable cardiac side effects in patients with heart disease.

Cardioaccelerator Effects of Epinephrine and Terbutaline

Terbutaline produces a larger increase in heart rate over control values in the supine position than equivalent doses of epinephrine, although both agents show cardioaccelerative effects which last at least 4 hr after subcutaneous injection. Similar observations have been obtained over a 150-min period by Arner et al. (5). This tachycardia is associated with an increase in cardiac output which is generally greater and shows a longer duration of action for terbutaline than epinephrine. The effect is dose dependent and studies by Carlstrom and Westling (13) reveal an almost identical pattern of cardiac output response as demonstrated in the present study, although those authors used the indicator dilution method of measurement. The rise in cardiac output in the first hour with both epinephrine and terbutaline is dependent upon an increase in both heart rate and stroke volume. However, the increase in heart rate appears to be a more dominant factor. After the first hour, the cardiac output remains elevated with terbutaline, whereas it falls toward control levels at this time with epinephrine administration. The slight rise in pulse rate with the latter

is statistically significant, but the slight elevation in cardiac output is not. The late prolonged rise in cardiac output after terbutaline is solely related to the much greater tachycardia than epinephrine. The importance of heart rate in mediating the increase of cardiac output after terbutaline administration is further shown by the study carried out in the seated position. Here the entire rise in cardiac output can be explained by an increase in heart rate, since stroke volume is not altered over the 4-hr study period.

Because of tachycardia that may occur as an adjustment to peripheral vasodilatation, it is difficult to separate the magnitude of beta-1 and beta-2 receptor stimulation caused by a given agent. Stimulation of the beta-1 receptor sites in the heart is associated with an increase of myocardial contractility which may be reflected by an increase in stroke volume and heart rate. Both epinephrine and terbutaline injections produced these effects during the first hour of drug administration, but the cardioaccelerator effect was more pronounced. Furthermore, there was a considerable fall in systemic vascular resistance usually associated with an increase in calf blood flow. Thus, the observed effects might have been due to combined beta-1 and beta-2 receptor stimulation in the first hour after both epinephrine and terbutaline administration. In contrast to epinephrine, and as a dose-dependent phenomenon, the tachycardia persisted after the first hour with terbutaline in association with a stroke volume which had fallen to control values. After terbutaline, cardiac output still remained elevated up to 3 hours; but this increase was solely a function of the rapid heart rate. Systemic vascular resistance was also reduced below control levels and calf blood flow elevated above control levels. In the later stages of drug effect, the increase of cardiac output associated with a fall in systemic vascular resistance related solely to tachycardia suggests a pure beta-2 receptor stimulation secondary to peripheral vasodilatation. This finding has been further corroborated by the studies with the subject in the seated position in which the significant increase of cardiac output was due to tachycardia alone, since stroke volume was not altered from the control levels.

Systolic Time Intervals

The I.V. administration of epinephrine produces a significant shortening of PEP when corrected for heart rate, while LVET does not change (14, 15). Most of the shortening of the preejection period by beta adrenergic agents occurs after the first heart sound, thereby excluding changes in electromechanical delay as a major factor in the observed preejection period response. This effect is greater with equivalent doses of isoproterenol than epinephrine, the former having greater beta-1 stimulating activity.

Shortening of PEP appears to provide a more consistent reflection of the inotropic effects of the adrenergic stimulating agents than does shortening of LVET. The variable response in LVET, in these situations, may be related to the greater dependence of LVET on the alterations of stroke volume and afterload which accompany the positive inotropic effect of the catecholamines on the left ventricle. Thus, (a) increase in stroke volume due to enhanced ventricular filling is accompanied by lengthening of LVET and shortening of PEP, while usually QS_2 is unaltered; (b) transient increases in afterload induce prolongation of both LVET and PEP, whereas transient decreases in afterload lengthen LVET and shorten PEP; and (c) positive inotropic agents associated with little change in afterload are accompanied by shortening of QS_2, LVET, and PEP (16).

In the present study, no significant changes were observed in systolic time intervals with saline, epinephrine, and terbutaline administration. However, these agents were administered by s.c. injection, rather than I.V. infusion as in the studies reported by other workers (14, 15). Possibly, shortening of PEP occurred with epinephrine and terbutaline; but this effect might have been missed, since the first measurements were made 15 min after drug injection. It should be noted that, both with 0.5 mg doses of epinephrine and terbutaline, the PEP was shortened but the difference between the control value was just outside the range of statistical significance ($0.1 > P > .05$). The failure to demonstrate shortening of PEP later on in the study, while systemic vascular resistance was reduced with terbutaline, is further evidence that the observed hemodynamic effects might have been related to stimulation of beta-2 receptors of peripheral vessels. The data from the systolic time intervals and the cardiac output measurements did not separate beta-1 and beta-2 effects within the first hour after terbutaline administration.

Calf Blood Flow

Most of the studies of the effects of epinephrine on peripheral blood flow, reported in the literature, deal with either I.V. or intra-arterial (i.a.) infusions of this agent (17, 18). With I.V. infusions of epinephrine, there is a marked initial increase of forearm or calf blood flow, with a subsequent fall and secondary dilatation persisting throughout the infusion. With i.a. infusions, dilatation is transient; thereafter, depending upon the dose, blood flow either returns to control values or falls markedly. These results have been explained by the fact that epinephrine, while mostly a beta receptor stimulant, also has weak alpha effects. It is the latter action which produces vasoconstriction and diminution in peripheral blood flow. The present studies showed only vasodilator

effects, indicating that s.c. injection is more closely related to I.V. than i.a. infusions. Furthermore, the duration of vasodilatation appeared much briefer with epinephrine than with equivalent doses of terbutaline.

Effects of Epinephrine and Terbutaline on Pulmonary Circulation

Witham and Fleming (19) reported data on normal humans and patients with chronic lung diseases who were given 0.5 to 0.7 mg of epinephrine by injection I.M. during cardiac catheterization. In every case, mean pulmonary arterial pressure rose after the epinephrine injection. The average rise was 4 mm Hg, with a range of 2 to 8 mm Hg. The pulmonary arterial pressure rise usually began 1 - 2 min after injection I.M., reached a peak in 2 - 16 min, and gradually returned to basal levels in 20 min. In 1 subject, the pressure was elevated as long as 46 min. The cardiac output, as measured by the indicator dilution technique, reached its maximum 33% above control 0.5 to 11 min after injection of the epinephrine; this increase was similar to that obtained in the present studies.

Pulmonary arterial pressure may be calculated from pulmonary arterial conduction time as outlined by Reuben (9). He pointed out that the distensibility properties of the pulmonary arteries are of importance in determining the pattern of pulmonary $\dot{Q}_C$. The capillary flow pulse recorded by the nitrous oxide plethysmographic method represents the instantaneous summation of the flow pulse of all the capillaries engaged in gas exchange. If it is assumed that there is a matching of the length of the various vascular pathways to their conduction properties so that pulse wave velocity is effectively uniform through all of them, the time delay from pulmonic valve opening to the foot of the capillary flow pulse can be taken to represent the pulmonary arterial conduction time. From experimental data, Reuben (9) found a close correlation between pulmonary arterial conduction time, and directly determined pulmonary mean arterial pressure in humans. He showed that elevated pulmonary arterial pressure was associated with decreased distensibility of the pulmonary arterial tree, and vice-versa. Reuben (9) based his equation for predicting pulmonary arterial pressure from data obtained mostly on patients with pulmonary arterial hypertension. Only 2 of 21 subjects had a normal mean pulmonary arterial pressure of 15 mm Hg, while the remainder had pressures above this value. In 1 subject, the conduction time was 180 msec; in the other, 160 msec. Thus, a great deal of uncertainty exists in evaluating small changes in pulmonary arterial pressure in normotensive subjects indirectly from pulmonary arterial conduction times, although the method may be highly useful in screening

subjects with moderate-to-severe pulmonary hypertension where conduction times may be as low as 60 msec for a mean pulmonary arterial pressure of 47 mm Hg (9, 20).

In the present study, no statistically significant changes in calculated pulmonary arterial pressure were observed after either terbutaline or epinephrine injection, despite the significant shortening of pulmonary arterial conduction time. This result might have been due to (a) the insensitivity of Reuben's equation (9) to detect small changes of pulmonary arterial pressure in normotensive subjects, or (b) correctness of the estimating equation in predicting that no significant change in pulmonary arterial pressure occurred after administration of epinephrine and terbutaline. The control conduction times for our normal subjects ranged between 200 msec and 224 msec--values much higher than those for the patients reported by Reuben (9), who noted only 1 subject with a conduction time as high as 180 msec. However, Karatzas and Lee (21) reported 1 normal subject who had a heart rate of 57 beats/min and a pulmonary conduction time of 200 msec. Although conduction time is not purported to be pulse rate dependent up to 110 beats/min (9), the fact that a comparable conduction time in an individual with a pulse rate comparable to our subjects using a different plethysmographic system suggests that our data are valid. However, it may be necessary to calibrate each body plethysmographic system with subjects in whom directly measured pulmonary arterial pressures are obtained.

In dogs, acute elevation of mean pulmonary arterial pressure induced by hypoxia causes a fall in pulmonary conduction time from 100 to 83 msec for an increase in pressure of 6 mm Hg (22). This fall as a percentage of control is quite similar to what we found after terbutaline and epinephrine injections. Since the estimating equation of Reuben (9) is not linear, one cannot make direct comparisons of human and animal data. Possibly the equation of Reuben (9) may be appropriate, and no significant rises took place in pulmonary arterial pressure after drug injection. Such a finding would be consistent with the observations of Witham and Fleming (19), who demonstrated that directly determined pulmonary arterial pressure usually returns to control levels 20 min after epinephrine I.M. injection. Even though pulmonary arterial conduction times in the present study were significantly shortened in the first three observations--made 15, 30, and 60 min after drug injection--the data expected from the previous work by these investigators would indicate that pulmonary arterial pressure might be at control values at these time periods.

Thus, it is probable that either a slight or no rise in pulmonary arterial pressure takes place 15 min or later after terbutaline or epinephrine

injections. In association with the large increase in pulmonary $\dot{Q}_C$ brought about by both agents, calculated total pulmonary vascular resistance falls if it is assumed that there is little alteration of pulmonary venous pressure, thus suggesting that these agents have a pulmonary vasodilator action. Fur ..r, after epinephrine or terbutaline injections, the PSF is disproportionately greater for a given stroke volume than the control values, a situation analogous to exercise (23). This finding may be due to a decrease in pulmonary arterial vasomotor tone, or related to a high peak in flow velocity of blood to the pulmonary arteries (8, 24). This finding contrasts with those observed with administration of isoproterenol, in which the ratio of PSF divided by stroke volume is unchanged despite a significant increase in stroke volume (24).

The systolic storage volume is an index of the distensibility of the pulmonary arterial system and is partially pulse rate dependent. During tachycardia, the diastolic period of the cardiac cycle shortens and less time is available for capillary blood flow runoff during diastole. On the other hand, bradycardia is accompanied by a greater systolic storage due to the prolongation of diastolic runoff of blood flow into the pulmonary capillaries. The control values of systolic storage in our normal subjects are slightly higher than those reported by other workers (8, 21), but this might be accounted for by the slower resting heart rates in our subjects. Since no change occurs in systolic storage after epinephrine or terbutaline administration, despite tachycardia, these observations are consistent with an increase in distensibility of the pulmonary arterial system; for tachycardia might have been expected to cause a fall in systolic storage -- thus constituting further indirect evidence that both epinephrine and terbutaline might have pulmonary vasodilator effects.

REFERENCES

1. Ahlquist, R. P. A study of adrenotropic receptors. Am J Physiol 153:586-600 (1948).

2. Lands, A. M., et al. Differentiation of receptor systems activated by sympathomimetic amines. Nature 214:597-598 (1967).

3. Sackner, M. A., et al. Bronchodilator effects of terbutaline in asthma, chronic bronchitis and emphysema. Clin Pharmacol Ther 16:499-506 (1974).

4. Innes, I. R., and M. Nickerson. Drugs acting on postganglionic adrenergic nerve endings and structures innervated by them

(sympathomimetic drugs). In: Goodman, L. S., and A. Gilman (eds.). The pharmacologic basis of therapeutics, 4th ed., pp. 478-523. New York: Macmillan, 1970.

5. Arner, B., et al. Circulatory effects of orciprenaline, adrenaline, and a new sympathomimetic B-receptor-stimulating agent, terbutaline in normal human subjects. Acta Med Scan (Suppl) 512:25-32 (1970).

6. Harris, L. Comparison of cardiorespiratory effects of terbutaline and salbutamol aerosols in patients with reversible airways obstruction. Thorax 28:592-595 (1973).

7. Sackner, M. A., et al. Techniques of pulmonary capillary blood flow determination. Bull Physiopathol Respir 9:1189-1209 (1973).

8. Karatzas, N. B., and G. J. De Lee. Propagation of blood flow pulse in the normal human pulmonary arterial system; analysis of the pulsatile capillary flow. Circ Res 25:11-21 (1969).

9. Reuben, S. Wave transmission in the pulmonary arterial system in disease in man. Circ Res 27:523-529 (1970).

10. Weissler, A. M., R. P. Lewis, and R. F. Leighton. The systolic time intervals as a measure of left ventricular performance in man. In: Yu, P. N., and J. F. Goodwin (eds.). Progress in cardiology. Phila., Pa.: Lea & Febiger, 1972.

11. Whitney, R. J. Measurement of volume changes in human limbs. J Physiol 121:1-27 (1953).

12. Lindquist, E. F. Designs and analysis of experiments in psychology and education, pp. 93, 237, 238. Boston, Mass.: Houghton Mifflin, 1953.

13. Carlstrom, S., and H. Westling. Metabolic, circulatory and respiratory effects of a new sympathomimetic B-receptor-stimulating agent, terbutaline, compared with those of orciprenaline. Acta Med Scan (Suppl) 512:33-40 (1970).

14. Salzman, S. H., et al. Epinephrine infusion in man; standardization, normal response, and abnormal response in idiopathic hypertrophic subaortic stenosis. Circulation 43:137-144 (1971).

15. Harris, W. S., C. D. Schoenfeld, and A. M. Weissler. Effects of adrenergic receptor activation and blockade on the systolic preejection period, heart rate and arterial pressure in man. J Clin Invest 46:1704-1714 (1967).

16. Weissler, A. M., R. P. Lewis, and R. F. Leighton. The systolic time intervals as a measure of left ventricular performance in man. In: Yu, P. N., and J. F. Goodwin (eds.). Progress in cardiology pp. 155-181. Phila., Pa.: Lea & Febiger, 1972.

17. Ginsburg, J., and A. F. Cobbold. Effects of adrenaline, noradrenaline and isopropylnoradrenaline in man. In: Ciba Foundation Symposium: Adrenergic Mechanisms, pp. 173-189. Boston, Mass.: Little Brown, 1960.

18. Allwood, M. J., et al. Correlation of hemodynamic events during infusion of epinephrine in man. J Appl Physiol 17:71-74 (1962).

19. Witham, A. C., and J. W. Fleming. The effect of epinephrine on the pulmonary circulation in man. J Clin Invest 31:707-717 (1951).

20. Reuben, S. R.: Personal communication, 1973.

21. Karatzas, N., and G. J. De Lee. The effect of pulsatile capillary blood flow of gas exchange within the lungs: A consideration of some hydrodynamic factors which affect this pulsatility in man. Bull Physiopathol Respir 2:521-537 (1966).

22. Reuben, S. R., et al. Measurement of pulmonary arterial distensibility in the dog. Cardiovasc Res 4:475-481 (1970).

23. Segal, N., R. Dougherty, and M. A. Sackner. Effects of tilting on pulmonary capillary blood flow in normal man. J Appl Physiol 35:244-249 (1973).

24. Wasserman, K., J. Butler, and A. VanKessel. Factors affecting the pulmonary capillary blood flow pulse in man. J Appl Physiol 21:890-900 (1966).

TABLE 1. EFFECTS OF SALINE INJECTION ON HEMODYNAMICS

Time (min)	Heart Rate (beats /min)	Cardiac Output (L/min)	Stroke Volume (ml)	Systolic Blood Press. (mm Hg)	Diastolic Blood Press. (mm Hg)	Mean Blood Press. (mm Hg)	Systemic Vascular Resis. (mm Hg/L/min)	CS_2(msec) Corrected For Heart Rate	PEP(msec) Corrected For Heart Rate	LVET (msec) Corrected For Heart Rate	Calf Blood Flow (ml/100 ml)	Peak Sys. Flow (L/min)	Peak Sys. Flow : Stroke Volume	Average Pulm. Capill. Accel. (ml/sec/msec)	Systolic Storage (%)	Pulmonary Arterial Conduction Time (msec)	Calculated Mean Pulmonary Arterial Press. (mm Hg)
-60	58.7	5.89	103.6	124	79	94	16.0	-8	-14	-9	3.4	10.8	0.106	6.78	75.6	211	13
-30	58.1	5.54	96.7	124	81	95	17.1	-10	-19	-3	3.2	10.8	0.116	7.30	78.7	210	13
-0.5	57.6	5.72	101.1	124	80	94	16.4	-5	-24	7	3.8	10.7	0.108	6.95	77.2	210	12
15	57.8	5.82	101.7	125	80	95	16.3	-10	-22	-9	3.1	10.6	0.104	6.90	85.2	210	13
30	57.6	6.07	107.2	123	81	95	15.6	-11	-16	-8	4.0	10.8	0.101	6.70	81.7	208	13
60	57.7	5.74	101.0	124	82	96	16.7	-9	-24	-2	3.7	10.3	0.104	6.58	75.8	211	13
120	57.8	6.18	107.7	123	80	94	15.2	-14	-14	-11	3.6	11.5	0.110	7.43	77.6	216	12
180	57.7	6.20	109.2	123	80	94	15.2	-19*	-23	-8	3.2	11.5	0.107	6.48	78.7	217	12
240	57.7	6.64	117.6*	124	82	96	14.4	-17	-23	-6	3.2	11.4	0.098*	6.93	78.1	217	12

* $P < .05$ from mean control value.

+ $P < .01$ from mean control value.

TABLE 2. EFFECTS OF EPINEPHRINE 0.5 mg ON HEMODYNAMICS

Time (min)	Heart Rate (beats /min)	Cardiac Output (L/min)	Stroke Volume (ml)	Systolic Blood Press. (mm Hg)	Diastolic Blood Press. (mm Hg)	Mean Blood Press. (mm Hg)	Systemic Vascular Resis. (mm Hg/L/min)	QS_2 (msec) Corrected For Heart Rate	PEP(msec) Corrected For Heart Rate	LVET (msec) Corrected For Heart Rate	Calf Blood Flow (ml/100 ml)	Peak Sys. Flow (L/min)	Peak Sys. Flow/ Stroke Volume	Average Pulm. Capill. Accel. (ml/sec/ msec)	Systolic Storage (%)	Pulmonary Arterial Conduction Time (msec)	Calculated Mean Pulmonary Arterial Press (mm Hg)
-60	61.0	6.00	101.9	123	80	94	15.7	-20	-17	-17	3.1	10.0	0.100	5.9	75.7	210	13
-30	59.3	6.2[illegible]	107.6	124	80	94	15.0	-18	-21	-10	3.0	10.3	0.097	5.8	76.1	213	13
-0.5	60.1	6.16	105.9	124	79	93	15.1	-15	-22	-7	3.4	11.0	0.107	6.3	74.8	211	14
15	73.8‡	9.74*	133.6‡	142*	66*	91	9.3‡	-28*	-33	-9	4.8+	17.0*	0.129*	10.6*	73.6	184+	15
30	77.6*	9.95‡	128.7*	152‡	68*	96	9.6‡	-36‡	-38	-11	5.2*	16.6*	0.130*	11.5*	72.8	174‡	16
60	74.8*	9.30‡	125.8*	136*	73‡	94	10.1‡	-31+	-35	-11	4.6*	15.1‡	0.120‡	8.3+	72.4	180+	15
120	70.4*	7.21	105.6	127	78	94	13.0	-24	-24	-13	3.6	11.9*	0.114*	6.2	72.9	202	13
180	65.3+	7.12	110.9	126	78	94	13.2	-21	-26	-7	3.9	12.0*	0.109	6.6	75.1	215	13
240	63.8*	7.02	111.4	125	78	94	13.4	-22	-20	-15	3.2	12.1*	0.111	6.7	75.6	215	13

*p < .05 from mean control value

+p < .01 from mean control value

‡p < .001 from mean control value

TABLE 3. EFFECTS OF EPINEPHRINE 0.25 mg ON HEMODYNAMICS

Time (min)	Heart Rate (beats /min)	Cardiac Output (L/min)	Stroke Volume (ml)	Systolic Blood Press. (mm Hg)	Diastolic Blood Press. (mm Hg)	Mean Blood Press. (mm Hg)	Systemic Vascular Resis. (mm Hg/L/min)	QS_2(msec) Corrected For Heart Rate	PEP(msec) Corrected For Heart Rate	LVET (msec) Corrected For Heart Rate	Calf Blood Flow (ml/100 ml)	Peak Sys. Flow (L/min)	Peak Sys. Flow ÷ Stroke Volume	Average Pulm. Capill. Accel. (ml/sec/ msec)	Systolic Storage (%)	Pulmonary Arterial Conduction Time (msec)	Calculated Mean Pulmonary Arterial Press. (mm Hg)
-60	58.2	5.78	101.5	121	79	93	16.1	-12	-17	-7	3.4	10.0	0.104	6.5	78.4	204	14
-30	57.5	5.97	104.0	125	81	95	15.9	-12	-21	-3	3.3	10.3	0.099	5.9	77.4	205	13
-0.5	59.0	6.00	105.3	126	79	95	15.8	-8	-20	1	3.1	10.3	0.099	6.3	88.1	201	14
15	67.9*	8.81*	132.5*	132*	73*	92	10.4*	-25+	-27	10	3.8	14.7*	0.113*	9.3*	73.6	188	14
30	68.3*	8.66*	127.2*	130+	74+	92	10.6*	-17	-25	-6	3.5	14.3*	0.113*	9.3*	72.8	180*	15
60	66.4*	7.61*	114.9	131+	77	95	12.5+	-19	-23	-12	3.0	12.4*	0.109	7.0	76.0	189	14
120	62.3*	6.08	100.5	127	82	97	15.9	-26+	-29	-10	2.7	10.4	0.106	6.2	79.5	200	14
180	62.1*	5.94	97.2	127	83	97	16.3	-12	-29	-5	3.2	9.9	0.105	5.6	78.0	207	13
240	62.3*	6.13	99.1	126	81	96	15.7	-13	-21	-4	2.8	10.5	0.108	6.5	79.3	223*	12

*P < .05 from mean control value

+P < .01 from mean control value

*P < .001 from mean control value

TABLE 4. EFFECTS OF TERBUTALINE 0.5 mg ON HEMODYNAMICS

Time (min)	Heart Rate (beats /min)	Cardiac Output (L/min)	Stroke Volume (ml)	Systolic Blood Press. (mm Hg)	Diastolic Blood Press. (mm Hg)	Mean Blood Press.	Systemic Vascular Resis. (mmHg/l/min)	QS_2(msec) Corrected For Heart Rate	PEP(msec) Corrected For Heart Rate	LVET (msec) Corrected For Heart Rate	Calf Blood Flow (ml/100 ml)	Peak Sys. Flow (L/min)	Peak Sys. Flow / Stroke Volume	Average Fulm. Capill. Accel. (ml/sec/msec)	Systolic Storage (%)	Pulmonary Arterial Conductance Time(msec)	Calculat Mean Pulmonary Arterial Press. (mm Hg)
-60	59.5	6.13	106.6	124	75	91	14.8	-10	-16	-8	2.8	10.7	0.102	6.7	76.5	222	13
-30	58.5	6.19	108.1	124	80	94	15.2	-8	-15	-4	3.3	10.6	0.102	6.8	77.1	216	13
-0.5	57.0	5.81	104.4	125	81	95	16.4	-6	-15	-4	3.2	10.6	0.105	6.8	79.2	206	13
15	83.2‡	11.25‡	137.8‡	142‡	66‡	91	8.1‡	-31*	-34	-15	4.4+	17.9*	0.132‡	12.8‡	70.4	181*	15
30	90.9‡	11.16‡	125.8+	150‡	64‡	92	8.2‡	-17	-26	-7	4.9+	17.8‡	0.144‡	13.0‡	70.4	178*	15
60	86.1‡	10.25‡	121.1+	141*	71*	94	9.2‡	-17	-26	-10	5.1‡	15.7‡	0.134*	10.6*	70.7	180*	14
120	79.2‡	8.41‡	110.5	135*	78	97	11.5‡	-23+	-22	-6	4.6+	13.0‡	0.121*	7.5	73.9	191*	14
180	73.9‡	7.96‡	111.3	133‡	80	97	12.2+	-16	-24	-4	4.7+	12.8+	0.117+	6.1*	71.7	196	14
240	68.9‡	7.37+	108.5	130+	81	97	13.2	-23+	-28	-5	3.9	12.5+	0.117+	7.9	77.0	203	13

*P < .05 from mean control value

+P < .01 from mean control value

‡P < .001 from mean control value

TABLE 5. EFFECTS OF TERBUTALINE 0.25 mg ON HEMODYNAMICS

Time (min)	Heart Rate (beats /min)	Cardiac Output (L/min)	Stroke Volume (ml)	Systolic Blood Press. (mm Hg)	Diastolic Blood Press. (mm Hg)	Mean Blood Press. (mm Hg)	Systemic Vascular Resis. (mm Hg/L/min)	CS_2(msec) Corrected For Heart Rate	PEP(msec) Corrected For Heart Rate	LVET (msec) Corrected For Heart Rate	Calf Blood Flow (ml/100 ml)	Peak Sys. Flow (L/min)	Peak Sys. Flow: Stroke Volume	Average Pulm. Capill. Accel. (ml/sec/msec)	Systolic Storage (%)	Pulmonary Arterial Conduction Time (msec)	Calculated Mean Pulmonary Arterial Press. (mm Hg)
-60	59.9	6.46	108.3	127	82	97	15.0	-21	-19	-15	2.9	10.8	0.100	6.2	76.4	200	14
-30	59.4	6.41	109.0	128	81	95	14.8	-18	-21	-10	3.4	11.1	0.102	6.6	75.6	214	13
-0.5	58.3	6.24	108.6	130	81	97	15.5	-16	-29	-1	2.9	10.4	0.096	6.1	76.3	224	12
15	71.6‡	8.78‡	123.8*	139‡	66*	90	10.2‡	-36‡	-31	-21	3.1	12.7*	0.119‡	9.0*	74.5	186+	15
30	75.5‡	9.46‡	127.7*	140‡	68*	92	9.7‡	-35‡	-26	-22	3.5	15.4‡	0.122‡	9.8*	74.3	177‡	16
60	76.4‡	9.45‡	127.5+	140‡	72*	94	9.9‡	-23	-28	-15	4.6+	14.2‡	0.114+	9.2*	72.0	184+	15
120	71.3‡	7.62+	111.2	134+	80	98	12.9*	-27	-22	-19	3.5	11.9	0.109*	7.1	74.6	200	14
180	65.8‡	7.14	111.1	130	81	97	13.6	-24	-20	-16	3.4	11.6	0.107	6.5	76.1	197	15
240	64.4+	6.72	107.6	129	81	95	14.1	-28*	-23	-17	3.6	11.4	0.110*	6.8	76.5	200	14

* P <.05 from mean control value

+ P <.01 from mean control value

‡ P <.001 from mean control value

TABLE 6. EFFECTS OF TERBUTALINE AND EPINEPHRINE ON SYSTEMIC HEMODYNAMICS

Time after injection (min)	Terbutaline 0.5 mg	Epinephrine 0.5 mg	P*	Terbutaline 0.25 mg	Epinephrine 0.25 mg	P+
		(% compared to control)				
		Heart Rate				
15	+43	+23	<.001	+21	+17	<.05
30	+56	+29	<.001	+27	+17	<.001
60	+48	+24	<.001	+29	+14	<.001
120	+36	+17	<.001	+20	+8	<.001
180	+27	+9	<.001	+11	+7	< .05
240	+18	+7	< .01	+9	+6	NS
		Cardiac Output				
15	+86	+59	<.001	+38	+49	NS
30	+85	+62	< .05	+48	+46	NS
60	+70	+51	< .05	+48	+28	<.001
120	+39	+17	< .05	+20	+3	<.001
180	+32	+16	NS	+12	0	< .05
240	+22	+14	NS	+5	+4	NS
		Stroke Volume				
15	+30	+27	NS	+14	+28	NS
30	+18	+22	NS	+18	+23	NS
60	+14	+20	NS	+17	+11	NS
120	+4	0	NS	+2	-3	NS
180	+5	+6	NS	+2	-6	NS
240	+2	-1	NS	+6	-4	NS
		Systemic Vascular Resistance				
15	-48	-39	NS	-32	-35	NS
30	-47	-37	NS	-36	-37	NS
60	-41	-34	NS	-34	-21	<.05
120	-26	-15	< .05	-15	0	<.001
180	-23	-14	NS	-10	+2	< .05
240	-	-12	NS	-7	-1	< .05
		Calf Blood Flow				
15	+42	+50	NS	0	+15	NS
30	+50	+62	NS	+13	+ 6	NS
60	+65	+44	NS	+40	-9	< .01
120	+49	+12	NS	+13	-18	NS
180	+52	+22	NS	+ 8	-6	NS
240	+26	0	NS	+16	-14	NS

*Difference between terbutaline 0.5 mg and epinephrine 0.5 mg
+Difference between terbutaline 0.25 mg and epinephrine 0.25 mg

TABLE 7. EFFECTS OF TERBUTALINE AND EPINEPHRINE ON PULMONARY HEMODYNAMICS

Time after injection (min)	Terbutaline 0.5 mg	Epinephrine 0.5 mg	P*	Terbutaline 0.25 mg	Epinephrine 0.25 mg	P+
		(% compared to control)				
		Peak Systolic Flow/Stroke Volume				
15	+28	+28	NS	+20	+12	NS
30	+40	+29	<.01	+23	+12	NS
60	+30	+19	<.01	+15	+8	NS
120	+17	+10	NS	+13	+5	NS
180	+14	+8	NS	+8	+4	NS
240	+13	+10	NS	+11	+7	NS
		Average Acceleration Of Blood In Pulmonary Capillaries				
15	+88	+77	<.05	+43	+50	NS
30	+91	+92	NS	+56	+50	NS
60	+56	+38	NS	+46	+12	<.01
120	+10	+3	NS	+13	+10	NS
180	+19	+10	<.05	+3	+9	NS
240	+16	+12	NS	+8	+5	NS
		Pulmonary Arterial Conduction Time				
15	-16	-13	NS	-13	-7	NS
30	-17	-18	NS	-17	-11	NS
60	-16	-15	NS	-14	-7	NS
120	-11	-4	NS	-6	-2	NS
180	-9	+2	NS	-8	+2	NS
240	-6	+2	NS	-6	+10	<.05

*Difference between terbutaline 0.5 mg and epinephrine 0.5 mg
+Difference between terbutaline 0.25 mg and epinephrine 0.25 mg

TABLE 8. EFFECTS OF TERBUTALINE AND EPINEPHRINE ON TOTAL PULMONARY VASCULAR RESISTANCE

Time After Injection (min)	Terbutaline 0.5 mg	Epinephrine 0.5 mg	P*+	Terbutaline 0.25 mg	Epinephrine 0.25 mg	P*‡
	(% Compared to control)					
15	-36*	-28+	NS	-14	-24*	NS
30	-35*	-26+	NS	-18*	-18*	NS
60	-28*	-19*	NS	-19*	-14	NS
120	-18*	-8	NS	-9	4	.01
180	-13	-17*	NS	0	1	NS
240	-13	-6	NS	0	-10	.01

* Difference between mean control value with P < .05
\+ Difference between mean control value with P < .01
‡ Difference between mean control value with P < .001
*+ Difference between terbutaline 0.5 mg and epinephrine 0.5 mg
*‡ Difference between terbutaline 0.25 mg and epinephrine 0.25 mg

TABLE 9. EFFECTS OF TERBUTALINE 0.25 mg ON HEMODYNAMICS OF SUBJECTS IN SEATED POSITION

Time (min)	Heart Rate (beats /min)	Cardiac Output (L/min)	Stroke Volume (ml)	Systolic Blood Press. (mm Hg)	Diastolic Blood Press. (mm Hg)	Mean Blood Press. (mm Hg)	Systemic Vascular Resis. (mm Hg/L/min)	Peak Sys. Flow (L/min)	Peak Sys. Flow ÷ Stroke Volume	Average Pulmonary Capillary Acceleration (ml/sec/msec)	Pulmonary Arterial Conduction Time (msec)
-60	71.1	4.89	72.7	109	72	84	17.2	8.2	0.117	5.2	195
-30	73.0	5.03	71.9	109	74	86	17.1	8.2	0.116	5.0	200
-0.5	73.2	4.60	67.1	109	74	86	18.7	7.3	0.116	3.3	197
15	84.3*	6.32+	79.2	120*	72	88	13.9+	10.2*	0.133+	5.8*	181
30	86.9+	6.32‡	76.6	115*	72	86	13.6‡	10.0+	0.136*	6.6*	179*
60	87.4+	6.44+	77.2	113	74	87	13.5*	9.1	0.118	6.5*	191
120	83.2*	5.15	63.6	111	73	85	16.5	8.3	0.130*	5.6	186
180	80.9*	5.36	69.2	106	71	83	15.5	8.5	0.127	4.5	191
240	77.4+	5.34	72.0	110	71	84	15.7	9.0	0.126	6.7	206

* P <.05 from mean control value

\+ P <.01 from mean control value

‡ P <.001 from mean control value

TABLE 10. EFFECTS OF TERBUTALINE 0.25 mg ON SYSTEMIC HEMODYNAMICS OF SEATED SUBJECTS

Time Post-Injection (min)	Heart Rate	Cardiac Output	Stroke Volume	Systemic Vascular Resistance
	(% Control)			
15	116	131	112	78
30	117	131	108	77
60	120	133	109	76
120	112	106	90	93
180	112	111	98	88
240	107	110	102	89

TABLE 11. EFFECTS OF TERBUTALINE 0.25 mg ON PULMONARY HEMODYNAMICS OF SEATED SUBJECTS

Time Post-Injection (min)	Peak Systolic Flow / Stroke Volume	Average Acceleration of Blood in Pulmonary Capillaries	Pulmonary Arterial Conduction Time
	(% Control)		
15	115	126	92
30	117	143	91
60	102	141	97
120	112	122	94
180	109	98	97
240	109	145	104

VII (Parts 1 and 2). DIFFUSING CAPACITY, MEMBRANE DIFFUSING CAPACITY, CAPILLARY BLOOD VOLUME, AND CARDIAC OUTPUT MEASURED BY A REBREATHING TECHNIQUE

(PART 1)

ABSTRACT

A rebreathing method is described for estimation of membrane diffusing capacity (D_M), pulmonary capillary blood volume (V_C), pulmonary capillary blood flow ($\dot{Q}_C$), and pulmonary tissue volume. The method consists of rebreathing into a bag for a 15- to 25-sec period while continuously sampling C_2H_2, CO, O_2, He, and CO_2. The gas analysis is accomplished by using either a battery of individual physical gas analyzers or a mass spectrometer. Since the mass of CO and of N_2 are nearly identical, it is necessary to use a stable isotope $C^{18}O$, with the mass spectrometer technique. Diffusing capacity and pulmonary $\dot{Q}_C$ can be estimated with the battery of physical gas analyzers, but reproducible values of pulmonary tissue volume can be obtained only by means of the mass spectrometer. Comparisons of the rebreathing pulmonary $\dot{Q}_C$ technique with simultaneous indicator dilution techniques in anesthetized dogs have revealed fair agreement when the physical gas analyzers are employed, and good agreement when the mass spectrometer system is used. The rebreathing diffusing capacity method gives values which increase as a function of lung volume. Prebreathing of O_2 for 3 min before doing a diffusing capacity at an alveolar O_2 tension produces a 12% to 16% drop in cardiac output in normal seated human subjects. If this drop is not taken into account, spuriously high values of D_M and low values of V_C are calculated. Through this method, pulmonary V_C in dogs averaged 9.2 ml/kg--which is comparable to previous estimates obtained by an ether plethysmographic method. The rebreathing technique provides a rapid, reliable, noninvasive method for estimation of pulmonary hemodynamic parameters when gas analysis is carried out by the mass spectrometer.

INTRODUCTION

Pulmonary capillary blood volume and membrane diffusing capacity (D_M) are commonly obtained from analysis of multiple measurements of the 10-sec breath-holding diffusing capacity of the lung (D_L) for carbon monoxide (CO) at different alveolar O_2 tensions (1). D_M is based upon the solution of the equation relating the reciprocal of the diffusing capacity ($1/D_{CO_{SB}}$) to the reciprocal of the rate of uptake of CO by the blood ($1/\theta$). [Note: $1/D_{CO_{SB}}$ = the reciprocal of the membrane diffusing capacity, carbon monoxide, single breath technique.] The difficulties

of the method limit its potential usefulness. Deviations of $1/D_{CO_{SB}}$ as a linear function of $1/\theta$ necessitate doing a least squares fit of several determinations, because analysis of only two points may cause imprecision (2). Investigation of the transient effects of drugs, postural changes, or exercise is not possible; for each determination cannot be repeated until at least 3 min have elapsed, in order to allow time for clearance of the test gases from the lungs. Finally, it is common to encounter obviously erroneous results (such as negative values of D_M), particularly in patients with moderate-to-severe obstruction airway disease. These spurious results are mainly due to inaccuracies in estimating the effective breath-holding time of pulmonary exposure to CO, because of uncertainty in selecting the onset and end of this period. It is implicit in the calculation of the single breath test that the exponential disappearance of CO from the lung passes through unity at time equal to zero. Even when the same criteria are applied to the measurement of the onset and end of breath-holding time, however, construction of a CO disappearance curve (from repeated single breath maneuvers with varying breath-holding times) reveals that the curve may pass through unity at times that vary ± 1 sec in normal subjects, and vary more in patients with pulmonary disorders (Fig. 1). Nevertheless, under these conditions, the slope of the CO disappearance curve is equivalent to the ratio of diffusing capacity/alveolar volume, and is influenced neither by the value of the intercept nor by the effective breath-holding times. Comparisons of the values for diffusing capacity, obtained in this manner, to the standard 10-sec breath-holding calculation indicate that the diffusing capacity may be in error by as much as 40% in patients with obstructive lung disease (3). The construction of CO disappearance curves at two levels of alveolar oxygen tension should lead to more precise estimates of pulmonary V_C and D_M, but takes about 1 to 2 hours to complete and is obviously impractical for routine clinical use or for evaluation of physiologic and pharmacologic stimuli. Therefore, we turned to the rebreathing method described by Lewis et al. (4, 5). With a battery of rapidly responding gas analyzers or a mass spectrometer and on-line computer data processing, it is possible to obtain a curve of CO disappearance within minutes of 15- to 25-sec rebreathing of CO and He in air mixture. The test can be repeated within a few minutes, while breathing an oxygen mixture to permit calculation of V_C and D_M. Further, the addition of acetylene to the test gas mixture allows the estimation of cardiac output ($\dot{Q}c$) (6). A description and the reproducibility of this method for measurements of diffusing capacity and cardiac output constitute a major part of the presentation in this paper.

-VII-
(Part 1)

In order to measure diffusing capacity at a high alveolar oxygen tension (~ 600 mm Hg) as a prerequisite for estimation of D_M and V_C, some laboratories advocate breathing 100% O_2 for approximately 5 min before the actual measurements of D_L. However, as estimated by dye dilution methods, the breathing of 100% O_2 may produce as much as a 13% fall in cardiac output (8, 9). If this fall also occurs during measurement of D_L at a high alveolar oxygen tension, then a spurious result might be obtained, since D_L is a function of cardiac output (7, 10). Indeed, Johnson et al. (7) recognized that, during exercise, corrections had to be applied to D_L at the high alveolar oxygen tension to allow for differences in Q_C at the two levels of oxygenation. In view of the previous reports of depression of resting cardiac output by O_2 breathing, we felt that an investigation of possible differences in cardiac output during determination of diffusing capacity at high and low in alveolar oxygen tension was necessary in order to assess the effect on calculation of resting D_M and V_C.

METHODS

Procedure in Humans

The methods used in the present study were based upon the rebreathing procedure described by Lewis et al. (4) and Lawson (10). Instead of using an initial and final reading of helium concentration as the former did--or a small number of discrete samples of gas concentrations as the latter did--our initial studies involved the continuous sampling of all test gases by a battery of rapid responding physical analyzers. Further on-line data processing was carried out with a small digital computer. Trace concentrations of acetylene were also included in the test mixture to permit calculation of the cardiac output during the rebreathing period (6, 10). In the apparatus used in these studies (Fig. 2), the subject breathed through a common port to four optional pathways (Rudolph 4-way valve, Warren E. Collins, Braintree, Mass.). These pathways led: (1) to room air; (2) to an oxygen demand valve; (3) to a CO_2 absorber; and thence (4) to a 6-liter rubber anesthesia bag containing the test gas mixtures. The bag was filled to a predetermined volume from a giant syringe with a mixture consisting of: either 0.4% CO, 0.5% C_2H_2, 10% He, 21% O_2, and balance N_2; or 0.4% CO, 0.5% C_2H_2, 10% He, and balance O_2. The tubing to the physical gas

---

EDITOR'S NOTE: The rebreathing technique described here in detail (in "Procedure In Humans") was also used in report section VIII (in "Rebreathing Technique," p. 168, par. 2).

analyzers was arranged on a manifold, and the output from the CO, C_2H_2, and CO_2 infrared analyzer was returned to the rebreathing bag to maintain bag volume constant. The return of the rapid paramagnetic oxygen analyzer (Godart, Instrumentation Associates, N.Y.) could not be led to the bag, because its outflow was contaminated by room air. Hence, the O_2 was analyzed for only two or three brief periods during the rebreathing maneuver. Helium was measured by a rapid responding catharometer (Godart) and its output was bled to room air because of its contamination with oil. These procedures caused an approximate fall in bag volume of about 75 ml which was neglected in the computations.

After the bag was filled with the test mixture to a predetermined volume, the subject expired to residual volume through the room-air port, the mouthpiece was turned into the bag containing the test mixture containing a balance of N_2 (vide supra). He rebreathed into the bag for 15 - 25 sec, usually at a rate of 25 cycles/min, in time to a breathing stimulator (Somanetics, Calif.) while endeavoring to just empty the bag on each inspiration. At the end of this period, he breathed room air or O_2 from a demand valve for 3 - 4 min, expired to residual volume and rebreathed from a test mixture in which O_2 was substituted for N_2. Before and after these two runs, the back pressure for CO in the blood was measured by a rebreathing method using the port connected to the CO_2 absorbers and rubber anesthesia bag (11).

Procedure in Dogs

In anesthetized dogs, the rebreathing setup was similar to that employed for humans, except that a 1.5-liter giant syringe was used to deliver the test mixture by pumping at the rate of 25 - 30 times/min. During the rebreathing procedure, a simultaneous estimation of cardiac output was obtained by the indicator dilution method employing indocyanine green via catheters placed in the pulmonary and carotid arteries. Right-to-left shunt was determined by a standard technique during the breathing of 100% O_2 (12). In addition to the rebreathing procedure using a battery of physical gas analyzers, as in the human studies, a mass spectrometer (MGA-1100, Perkin-Elmer, Pomona, California) was used in some of the animal experiments. The test mixture consisted of 0.3% $C^{18}O$ (Miles Labs.; Res. Div., Kankakee, Ill.; or, Liquid Carbonic Corp. Chicago, Ill.) 0.5% C_2H_2, 10% He, 21% O_2, and balance N_2. The mass spectrometer sampled at the rate of 15 ml/min, and its output was vented to atmosphere.

-VII-
(Part 1)

Procedure in Data Processing

Analog signals from the physical gas analyzers or mass spectrometer were matched to the computer input of ± IV by means of a matching amplifier system (UMA, Electronics For Medicine, Inc., White Plains, N.Y.). These data were processed (Fig. 3) on-line by means of a program written for a small digital computer system: LINC 8 (Digital Equipment Co., Maynard, Mass.). The sampling rate for the analysis of the test gases was 7 points/sec, each point being corrected for helium dilution. The disappearance of CO and acetylene was calculated and displayed according to the method of Cander and Forster (13). The computer shifted each analog gas signal from the physical gas analyzer back in time relative to the helium tracing, because each analyzer had a different response time. It used the 50% rise time of the analyzer output, as measured when the rebreathing mixture along with added CO_2 was suddenly turned into the gas analysis network. CO_2 and O_2 were measured in order to correct the catharometer readings, since the helium estimation was sensitive both to changes in CO_2 and O_2 concentrations. None of these corrections were necessary when the mass spectrometer was used. Alveolar CO values were corrected for back pressure of CO in blood by assuming that the buildup occurred as a linear function of the number of tests.

After the data were collected, the program selected the start point of the calculation of the CO and C_2H_2 disappearance curves on the basis of minimal oscillations of the He tracing. Alternately, the user could initiate the starting point on the display by teletype instructions. The data were then analyzed after inputting the following data from the teletype: (1) alveolar CO for back pressure measurement; (2) temperature; (3) weight; (4) apparatus dead space; (5) hemoglobin; and (6) bag or syringe volume. The program then displayed the CO and C_2H_2 disappearance curves on the cathode ray oscilloscope of the computer, using a least squares fit. The program corrected for the start time by forcing the CO disappearance curve to intercept at unity. This time shift was then used to shift the C_2H_2 disappearance curve to display its intercept at time zero, a value which is a function of pulmonary tissue volume (13). This volume was to be used in calculation of the cardiac output; but, in preliminary studies, we found that the physical gas analyzers system did not give a reproducible value for the intercept--probably because corrections for the response times of the analyzer were imperfect. Therefore, we employed a value of 450 ml for pulmonary tissue volume in humans, and 250 ml in dogs as a constant correction. However, the mass spectrometer method in dogs gave reproducible values for the

intercept of the acetylene disappearance curve because of the uniform fast response times of the detectors; and hence this value of pulmonary tissue volume was employed in calculation of cardiac output (13).

Studies in Humans

In 11 normal nonsmoking subjects--10 men and 1 woman, ages 23 to 41 yr (mean: 28 yr)--the following studies utilizing the rebreathing technique were carried out using the battery of physical gas analyzers. For each set of experiments, the volume of the test mixture was taken as approximately 4, 3, and 2 liters. After resting in the seated position about 5 min, the subject performed the following maneuvers at intervals of 3 - 4 min: (a) rebreathing the test mixture containing 21% O_2; (b) breathing 100% O_2 for 3 - 4 min, followed by rebreathing the test mixture containing 90% O_2 and immediately determining back pressure of CO in the blood; (c) breathing 100% O_2 for 3 - 4 min, followed by rebreathing the test mixure containing 90% O_2; and (d) rebreathing the test mixture containing 21% O_2. These experiments permitted calculation of diffusing capacity, cardiac output, O_2 consumption, and alveolar volume in duplicate for three alveolar volumes.

In three of these subjects, pulmonary D_M and V_C were calculated from diffusing capacity at a single alveolar volume measured at two alveolar O_2 tensions at 15, 25, and 40 respirations/min.

In another group of 9 normal nonsmoking subjects--7 men and 2 women, ages 19 - 41 yr (mean: 25 yr)--the following studies of the rebreathing technique were carried out using the battery of physical gas analyzers. The volume of the test mixture was taken as 3 or 4 liters. After resting in the seated position about 5 min, the subject performed the following maneuvers at 3- to 4-min intervals: rebreathing the test mixture containing 21% O_2; taking three deep breaths of O_2 immediately followed by rebreathing the test mixture containing 90% O_2; and breathing 100% O_2 for 3 min, then rebreathing the test mixture containing 90% O_2, followed immediately by estimating back pressure of CO in the blood.

Studies in Mongrel Dogs

Mongrel dogs were anesthetized with pentobarbital, 25 mg/kg, and intubated with a cuffed endotracheal tube. Cardiac catheters were placed within the carotid artery and within the pulmonary artery via the external jugular vein. In 7 dogs, the rebreathing technique was

carried out using the battery of physical gas analyzers; and, in 5 dogs, the mass spectrometer was employed. Three to four sequential tests were done with each method. Simultaneous measurements of cardiac output were made by injection of indocyanine green into the pulmonary artery and sampling blood from the carotid artery by means of a densitometer. In 3 of the dogs in whom the mass spectrometer was employed, 0.25 mg terbutaline was given I.V. in order to effect an increase in cardiac output to provide further comparisons between the rebreathing and dye dilution methods.

RESULTS

Human Studies

A display of the CO and acetylene disappearance curves from the cathode-ray oscilloscope of the small digital computer is depicted in Figure 4. In all subjects, these experimental data could be fitted with a single exponential equation.

Effects of respiratory frequency--There was no significant difference in diffusing capacity, D_M, pulmonary V_C, and pulmonary $\dot{Q}_C$ in 3 subjects when alveolar volume was constant and breathing frequency adjusted to 15, 25, and 40 breaths/min.

Reproducibility--Mean duplicate measurements of diffusing capacity and pulmonary $\dot{Q}_C$ at two different pulmonary capillary O_2 tensions and three alveolar volumes are listed in Table 1. The percent SD of the mean of these two determinations was less than 5.1%.

Effects of lung volume on rebreathing parameters--As alveolar volume was increased by using a larger volume of the test gas mixture, O_2 consumption, and diffusing capacity and pulmonary $\dot{Q}_C$ also increased (Table 2). This increase occurred during the runs when either air or oxygen was prebreathed. Both the diffusing capacity and pulmonary $\dot{Q}_C$ were significantly lower during the runs obtained at the high pulmonary capillary O_2 tension.

Effects of breathing oxygen on pulmonary $\dot{Q}_C$--At a given lung volume, the pulmonary $\dot{Q}_C$ after breathing 100% oxygen f[or] 3 - 4 min was 12% - 16% lower than that obtained on air breathing (Fig. 5). Since there is almost no intrapulmonary right-to-left shunting of blood in normal subjects, the pulmonary $\dot{Q}_C$ can be equated with cardiac output.

The mean calculated cardiac index for all the determinations in the first group of 11 normal seated subjects was: for breathing air, 2.25 L/min/M^2, SD 0.13; and for breathing oxygen, 1.95 L/min/M^2, SD 0.20 ($P < .01$). In the second group of normal subjects, no decrease occurred in pulmonary $\dot{Q}_C$ at this high level of pulmonary capillary O_2 tension if the prebreathing period was limited to 3 breaths (Table 3).

Effects of lung volume on ratios of diffusing capacity: blood flow and diffusing capacity: alveolar volume--In general, the ratio of diffusing capacity to blood flow did not change over the three lung volumes studied (Table 4). The ratio of diffusing capacity to alveolar volume declined with increased lung volume.

Effects of lung volume on D_M and pulmonary V_C--If the actual values of diffusing capacity obtained at the low and high pulmonary capillary O_2 tensions are used to calculate D_M and V_C, then apparently D_M increases at the rate of 13 ml/min x mm Hg per liter alveolar volume while pulmonary V_C remains unchanged (Table 5). However, if it is assumed that diffusing capacity is proportional to pulmonary $\dot{Q}_C$, then diffusing capacity must be increased about 4% at the high pulmonary capillary O_2 tension to account for the depressant effect of O_2 breathing on cardiac output. When this correction is applied, D_M increased 8.5 ml/min x mm Hg per liter of alveolar volume, while V_C increased 6.2 ml per liter of alveolar volume over the range of lung volumes studied (Table 5). The effect of depression of cardiac output by O_2 upon estimation of D_M and V_C where no correction is applied to diffusing capacity is shown in Table 3. Prebreathing O_2 for 3 min caused a fall in cardiac output of 16%, but prebreathing O_2 for 3 breaths did not significantly affect cardiac output. D_M is lower and V_C higher in the estimate using 3 breaths of O_2 than using 3 min of O_2 breathing. Thus, prebreathing oxygen for 3 min may give spuriously low values of pulmonary V_C and spuriously high values of D_M.

Animal Studies

Physical gas analyzer technique--Data from 7 dogs are listed in Table 6. Diffusing capacity averaged 0.7 ml/min x mm Hg/kg; and pulmonary $\dot{Q}_C$, 0.064 L/min/kg. Comparison of the pulmonary $\dot{Q}_C$ measurements to the cardiac output estimated by indicator dilution minus the intrapulmonary shunt is depicted in Figure 6. There is a tendency for the acetylene rebreathing method to give lower values for blood flow than the indicator dilution method, although most values fall within 20% of the line of identity.

Mass spectrometer technique--The display from the cathode-ray oscilloscope of the digital computer of the CO and C_2H_2 disappearance curve is shown in Figure 7. Diffusing capacity averaged 0.8 ml/min x mm Hg/kg; and pulmonary $\dot{Q}_C$, 0.107 L/min/kg (Table 7). Shown in Figure 8 is a comparison of the pulmonary $\dot{Q}_C$ measurements to the cardiac output estimated by the indicator dilution method. These values tended to cluster about the line of identity. The diffusing capacity as a function of body weight for both the physical gas analyzers and the mass spectrometer method is shown in Figure 9.

The mass spectrometer technique gave fairly reproducible values of pulmonary tissue plus capillary blood volume (Table 7). If it is assumed that pulmonary V_C is 1.9 ml/min x mm Hg/kg (14), then the calculated pulmonary tissue volume ranges from 6.0 to 11.6 ml/kg, mean 9.2 ml/kg.

DISCUSSION

The rebreathing method for estimation of diffusing capacity (D_L) and pulmonary $\dot{Q}_C$ with on-line data processing by a small digital computer is rapid and reproducible. Since a complete CO disappearance curve is obtained (rather than a single value of uptake of CO as in the single breath method), it is not subject to errors in estimating the effective breath-holding time which might give rise to spurious results (3). Further, there is evidence that the rebreathing D_L value is not as affected by uneven distribution of ventilation as are the steady-state methods (4, 15, 16). The employment of a mass spectrometer has the following advantages over analysis of the alveolar gases by a battery of individual physical gas analyzers: rapid response time; less volume needed for analysis, thereby permitting studies at much lower lung volumes; and ability to obtain measurements of pulmonary tissue plus capillary blood volume. However, the stable isotope $C^{18}O$ must be used as the test gas rather than naturally occurring CO, because its mass nearly coincides with that of nitrogen (17). This isotope is much more costly than CO.

Effects of Respiratory Frequency On Rebreathing Method

The equation for estimating D_L from the rate of fall in CO concentration during rebreathing is strictly valid only if the rate of rebreathing is infinitely fast. However, as Lewis et al. (4) have shown and as we have confirmed, breathing frequencies above 15/min do not influence the calculated diffusing capacity--thus indicating that in normal subjects the

method is not affected by a wide range of respiratory rates. Furthermore, estimates of D_M, pulmonary V_C, and pulmonary $\dot{Q}_C$ also appear to be independent of respiratory frequency.

Effect of Lung Volume On Rebreathing Method

Values of the single breath diffusing capacity have been shown by several investigators to increase as a function of lung volume (18, 19, 20). The present study, as well as that of Lewis et al. (4), indicates that this observation also holds true for the rebreathing technique. Lawson (10) has shown that the higher values of the single breath D_{CO} measured at TLC and the rebreathing D_{CO} at large tidal volumes, at rest and during exercise, disappear or become minimal when the measurements are made at the same lung volume. [Note: $D_{CO_{RB}}$ = diffusing capacity, carbon monoxide, rebreathing technique.] Our values of $D_{CO_{RB}}$ breathing air correspond quite closely to those obtained by other authors at similar lung volumes--present study: 29.6, SD 5.2; Lewis et al. (4): 27.3; and Lawson (10): 27.7, SD 4.4.

The O_2 consumption during rebreathing at 54% TLC of 431 ml/min is similar to the value of 406 ml/min found by Lewis et al. (4). This value is considerably above the calculated basal levels and probably is related to the considerable exercise of the respiratory muscles caused by the rebreathing procedure. The level falls to 328 ml/min at 36% TLC since the work of breathing at smaller tidal volumes is much less. The values of pulmonary $\dot{Q}_C$ appear to increase slightly as a function of lung volume, but this increase cannot be completely accounted for by the change in oxygen consumption.

Estimates of Pulmonary $\dot{Q}_C$

The mean value of pulmonary $\dot{Q}_C$ determined by the acetylene rebreathing method of 2.25 L/min/M^2, SD 0.13 of subjects in the seated position is similar to values of 2.12 L/min/M^2, SD 0.66 that we obtained in 20 normal subjects by the nitrous oxide plethysmographic technique (21). The studies in anesthetized dogs revealed fair agreement between simultaneously determined estimations of indicator dilution pulmonary $\dot{Q}_C$ corrected for shunt using the physical gas analyzers, and good agreement using the mass spectrometer for gas analysis. The reason for this discrepancy is not completely clear: the estimate of pulmonary $\dot{Q}_C$, using the physical gas analyzers, appeared to be systematically too low. This finding could have been in part related to: the small volumes of test mixture that had to be used in the dog, leading to imperfect mixing in the analyzer circuit

because of the large capacity of the circuit; PPB might have altered the observed concentrations of CO, since the detector cells are pressure sensitive; and assumption of an incorrect pulmonary tissue volume. These considerations did not hold when the mass spectrometer was employed wherein there was much better agreement between it and the measurements of blood flow by the indicator dilution method.

Effects of O_2 Breathing On Cardiac Output

The present study confirms previous observations that O_2 breathing decreases cardiac output (8, 9). Furthermore, this effect is seen within 3 - 4 min after initiation of O_2 breathing. Daly and Bondurant (8) concluded that the effect was a result of vagus-dependent decrease in heart rate and a rate-dependent decrease in cardiac index, but the possibility of a lesser direct myocardial effect of hyperoxia could not be excluded. Recently, Ishikawa et al. (22) found that 5 min of O_2 breathing produced falls in various myocardial contractility indices. These falls were similar even when the heart rate was maintained constant by cardiac pacing, and suggested that O_2 breathing diminished myocardial contractility directly.

Rebreathing Estimates of D_M and Pulmonary V_C

The calculation of D_M and V_C from estimations of diffusing capacity and two alveolar O_2 tensions assumes that no hemodynamic alterations occurred between the two determinations. This point was recognized by Johnson et al. (7) who had to take it into account when they calculated D_M and V_C during exercise. When $\dot{Q}_C$ was not constant at both levels of oxygenation, measurements of D_{CO} at the high alveolar oxygen tensions were adjusted to the same levels of $\dot{Q}_C$ measured at the low O_2 tensions by extrapolation of a graph relating diffusing capacity and blood flow for that individual at high O_2 tensions. The fall in cardiac output if O_2 is prebreathed introduces a spurious error into the calculations (as demonstrated in Tables 3 and 5). If the correction for the depressant effect of O_2 on cardiac output is not applied, it appears that D_M increases at the rate of 13 ml/min x mm Hg/L alveolar volume, while V_C remains unchanged. When the correction is applied, then D_M increased 8.5 ml/min x mm Hg/L alveolar volume, while V_C increased 6.2 ml/L alveolar volume. To obviate the need for these corrections, it is preferable in the estimation of D_M and V_C to prebreathe only 3 breaths of O_2 before obtaining the diffusing capacity at the high level of alveolar O_2 tension.

The effect of lung volume on D_M and V_C, using the single breath method of analysis, has been reported by other authors (19, 20). Both Hamer (19) and Miller and Johnson (20) found that D_M increased by

8.4 ml/min x mm Hg/L alveolar volume in normal subjects, a value close to ours when the correction for the depressant effect of O_2 breathing was taken into account. Hamer (19) reported a fall in V_C with increasing lung inflation; and Miller and Johnson (20), no change. In the present investigations, a slight rise was found. Miller and Johnson (20) pointed out that a doubling of lung volume will cause a 26% increase in the diameter of the alveoli, and that these vessels must be stretched correspondingly. When a rubber tube is stretched by this amount, the luminal volume of this tube increases only 3%. Miller and Johnson (20) suggested that lung capillaries behave in the same way as rubber tubes, so that stretching the alveolar surface has a negligible effect on alveolar volume. We previously found that D_M increased 9.7 ml/min x mm Hg/L alveolar volume, while V_C remained unchanged using the steady-state method (23). The reason why the rebreathing method gives higher values of V_C with increase of lung volume than do the steady-state or single breath method may be simply the inexactitude of making the measurements; for only a 4% increase in diffusing capacity at the high O_2 tension alters the results from no change in pulmonary V_C to an increase of 6.2 ml/L alveolar volume. Alternately, it may be related to the increased alveolar CO_2 which occurs during the rebreathing procedure, owing to the increased work of breathing which is a function of the larger tidal volumes necessary to measure diffusing capacity at a greater lung volume. Rankin, McNeill, and Forster (24) showed that increased alveolar CO_2 increased V_C in normal humans; and perhaps this is the explanation for the increase of V_C with increased lung volume during the rebreathing procedure.

Rebreathing D_M in Anesthetized Dogs

The D_M in anesthetized dogs, as determined by the single breath method, has been reported as 0.84 ml/kg. The rebreathing method gave slightly lower values of 0.77 ml/kg. This might be related to the lower values of alveolar volume at which the rebreathing procedure was carried out.

Pulmonary Tissue Volume in Anesthetized Dogs

In 5 normal human subjects, Cander and Forster (13) measured the rates of disappearance of SF_6, N_2O. C_2H_2, diethyl ethyl, and acetone from the alveolar air during breath-holding, after a single deep inspiration of a mixture of one of these gases and 15% He. They found that SF_6 is so insoluble that there is no significant change in its concentration relative to He. Ether and acetone are so soluble that they dissolve in the tissues around the dead space during inspiration and evaporate during

expiration, preventing the accurate estimation of alveolar concentration. N_2O and C_2H_2 showed: a rapid (less than 1.5 sec) initial fall in relative alveolar concentration; and an exponential, more gradual decrease. The former presumably results from the solution of the foreign gas in the pulmonary parenchymal tissues and capillary blood, and can be used to calculate this volume; the latter is used to calculate the pulmonary $\dot{Q}_C$. The disadvantage of their method is that repeated breath-holds must be carried out in order to construct a disappearance curve for C_2H_2 and N_2O, and similar hemodynamic status must be assumed for each data point. The rebreathing procedure offers several theoretical advantages: the C_2H_2 disappearance curve can be obtained over 15 sec; repeated measurement of pulmonary tissue and capillary blood volume are easy to make; there is no need to assume the same hemodynamic status. Unfortunately, both in our human and animal work, it was impossible to estimate a reproducible intercept of the acetylene disappearance curve using the physical gas analyzers. This failure was the result of using analyzers with differing slow response times; but this did not prove a problem when the mass spectrometer was employed, because all the detector sites had uniformly rapid response times. The mean value of pulmonary tissue volume in 5 dogs, calculated by subtracting an assumed value of V_C of 1.9 ml/kg (24) from the intercept value obtained, was 9.2 ml/kg. This estimate compares favorably to previous values obtained in anesthetized dogs, of 8.6 ml/kg, using a plethysmographic method which involved measuring the volume of ether evolved in the lungs after injection of liquid ether into the pulmonary artery (25).

REFERENCES

1. Roughton, F. J. W., and R. E. Forster. Relative importance of diffusion and chemical reaction in determining rate of exchange of gases in the human lung, with special reference to the true diffusing capacity of pulmonary membrane and volume of blood in the lung capillaries. J Appl Physiol 11:290 (1957).

2. McNeill, R. S., J. Rankin, and R. E. Forster. The diffusing capacity of the pulmonary membrane and the pulmonary capillary blood volume in cardiopulmonary disease. Clin Sci 17:465 (1958).

3. Spicer, W. S., Jr., R. L. Johnson, Jr., and R. E. Forster, II. Diffusing capacity and blood flow in different regions of the lung. J Appl Physiol 17:587 (1962).

4. Lewis, B. M., et al. The measurement of pulmonary diffusing capacity for carbon monoxide by a rebreathing method. J Clin Invest 38:2073 (1959).

5. Lewis, B. M., et al. The effects of body position, ganglionic blockage and norepinephrine on the pulmonary capillary bed. J Clin Invest 39:1345 (1960).

6. Grollman, A. The cardiac output of man in health and disease. Springfield: Charles C Thomas, 1932.

7. Johnson, R. L., Jr., et al. Pulmonary capillary blood volume, flow and diffusing capacity during exercise. J Appl Physiol 15:893 (1960).

8. Daly, W. J., and S. Bondurant. Effects of oxygen breathing on the heart rate, blood pressure, and cardiac index of normal man resting, with reactive hyperemia, and after atropine. J Clin Invest 41:126 (1962).

9. Eggers, G. W. N., et al. Hemodynamic responses to oxygen breathing in man. J Appl Physiol 17:75 (1962).

10. Lawson, W. H., Jr. Rebreathing measurements of pulmonary diffusing capacity for CO during exercise. J Appl Physiol 29:896 (1970).

11. Sackner, M. A., et al. Effect of lung volume on steady-state pulmonary membrane diffusing capacity and pulmonary capillary blood volume. Am Rev Respir Dis 104:408 (1971).

12. Berggren, S. M. The oxygen deficit of arterial blood caused by nonventilating parts of the lung. Acta Physiol Scand [Suppl] 2 (1942).

13. Cander, L., and R. E. Forster. Determination of pulmonary parenchymal tissue volume and pulmonary capillary blood flow in man. J Appl Pnysiol 14:541 (1959).

14. Cree, E. M., J. F. Benfield, and H. K. Rasmussen. Differential lung diffusion, capillary volume and compliance in dogs. J Appl Physiol 25:186 (1968).

15. Lewis, B. M., et al. Effect of uneven ventilation on pulmonary diffusing capacity. J Appl Physiol 16:679 (1961).

16. Lewis, B. M., and B. Bork. An analog computer analysis of regional diffusing capacity in airflow obstruction. J Appl Physiol 22:1137 (1967).

17. Wagner, P. D., R. W. Mazzone, and J. B. West. Diffusing capacity and anatomic dead space for carbon monoxide ($C^{18}O$). J Appl Physiol 31:847 (1971).

18. Cadigan, J. B., et al. An analysis of factors affecting the measurement of pulmonary diffusing capacity by the single breath method. J Clin Invest 40:1495 (1961).

19. Hamer, N. A. J. Variations in the components of the diffusing capacity as the lung expands. Clin Sci 24:275 (1963).

20. Miller, J. M., and R. L. Johnson, Jr. Effect of lung inflation on pulmonary diffusing capacity at rest and exercise. J Clin Invest 45:493 (1966).

21. Sackner, M. A., and R. Dougherty. Anti-G suit inflation on cardiac output of seated subjects. Riv Med Aeronaut Spaz (Roma) 46:264-266 (1973).

22. Ishikawa, K., et al. Fall in myocardial contractility following 100% oxygen breathing in patients with and without coronary artery disease. Abstract Circulation IV:180 (1973).

23. Sackner, M. A., et al. Effects of lung volume on steady state pulmonary membrane diffusing capacity and pulmonary capillary blood volume. Am Rev Respir Dis 104:408 (1971).

24. Rankin, J., R. S. McNeill, and R. E. Forster. Influence of increased alveolar CO_2 tension on pulmonary diffusing capacity for CO in man. J Appl Physiol 15:543 (1960).

25. Sackner, M. A., et al. Pulmonary arterial blood volume and tissue volume in man and the dog. Circ Res 34:761 (1974). [USAFSAM Editor's Note: Consult report section IX for related information.]

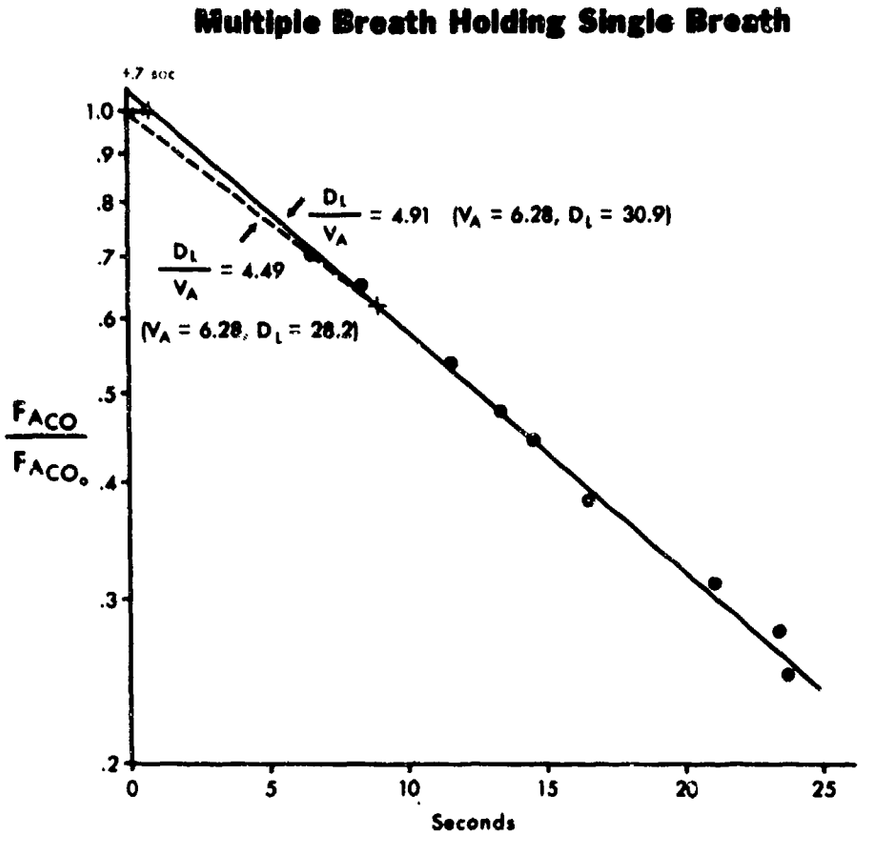

Figure 1. CO disappearance curve, in a normal subject, obtained by multiple breath-holding tests.

(The closed circles = individual data points; the cross = another data point which might be used to calculate a single breath diffusing capacity in which breath-holding varies between 8 and 12 sec. The hatched line = the slope used for calculation of the latter, since the zero intercept is assumed to be unity. Because the value at unity is actually + 0.7 sec, the standard calculation underestimates diffusing capacity by 9%.)

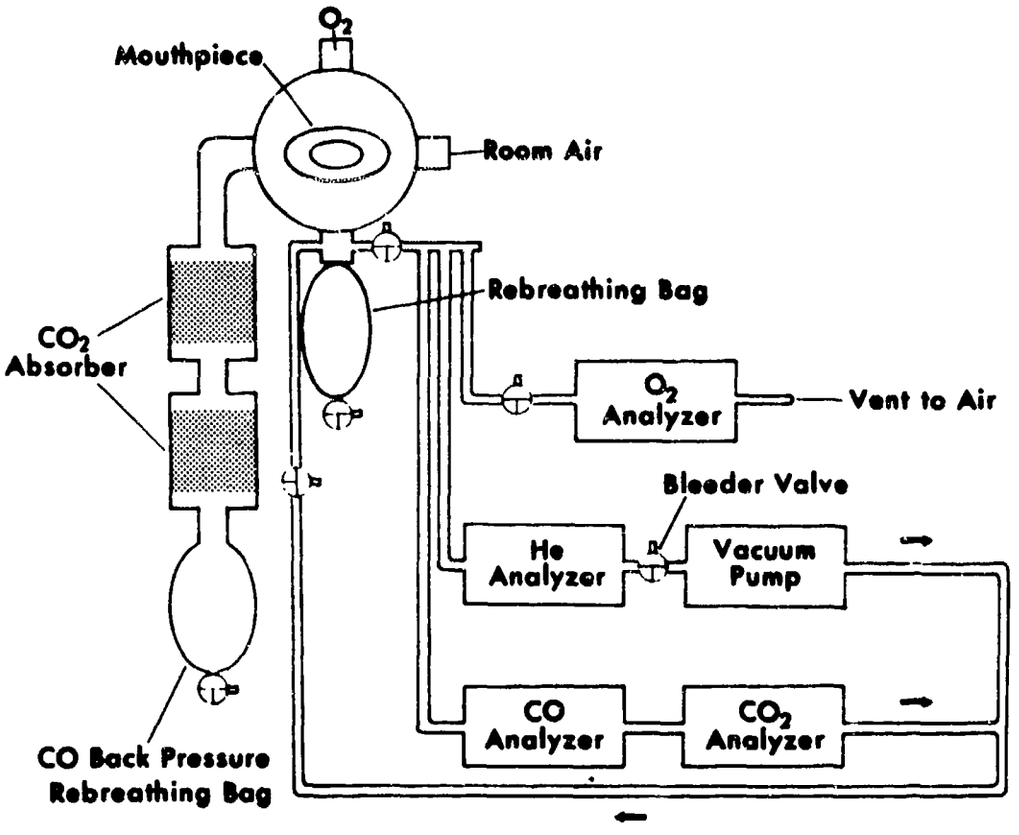

Figure 2. Set-up for estimation of rebreathing diffusing capacity and cardiac output by means of physical gas analyzers. (Schematic diagram)

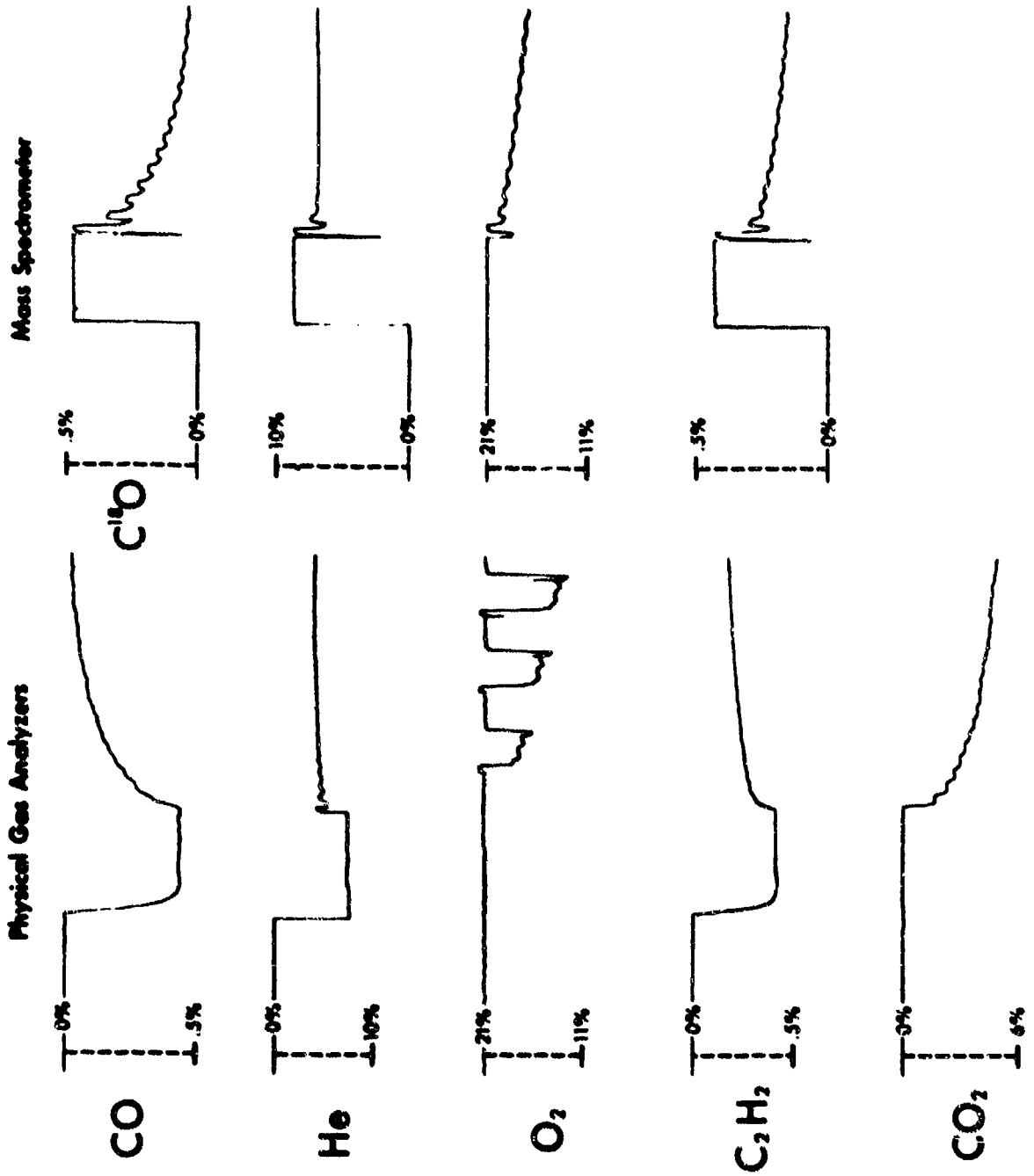

[Figure 3. (Legend on facing page)]

Figure 3 (on facing page). Analog signals from physical gas analyzers and mass spectrometer during air breathing.

(The total run comprises 25 sec. On the left panel, the differences in response times among the physical gas analyzers are clearly shown; in part, this is also related to delay in transit time to the analyzers because of differences in connecting tubing. The damping of the various signals in the physical gas analyzer system contrasts with the oscillations on the mass spectrometer signals due to the rebreathing maneuver. The polarity of the signals from the two systems is reversed except for the O_2 tracing. The latter is sampled intermittently in the physical gas analyzer system and continuously in the mass spectrometer system. The slight fall in He concentration, after complete mixing of the lung and rebreathing bag has been achieved, is due to the change in concentrations of O_2 and CO_2 effects on the He recording; but this does not occur in the mass spectrometer recording, and hence CO_2 is not measured in this system.)

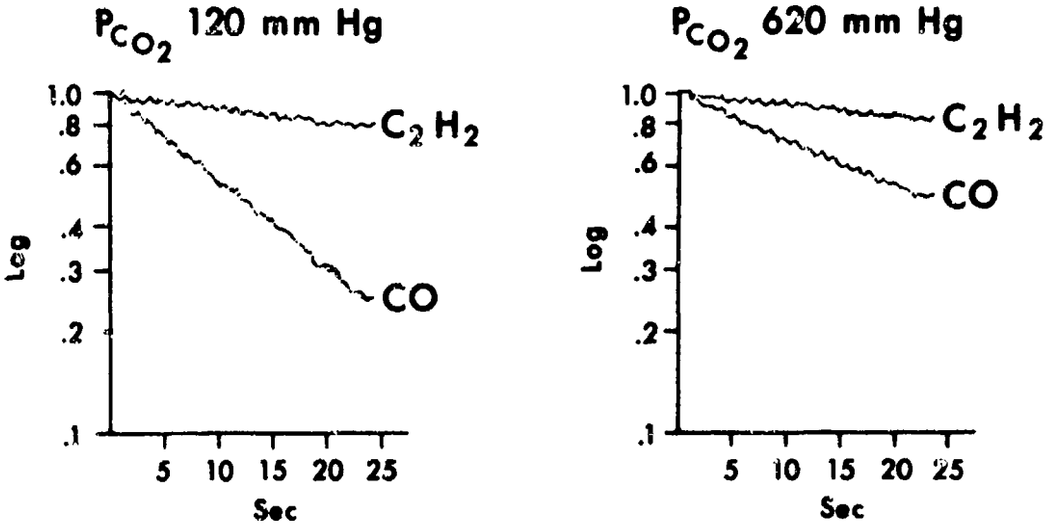

Figure 4. Representative computer-derived display of CO and acetylene disappearance curves at pulmonary capillary O_2 tensions of 120 and 620 mm Hg, using the physical gas analyzers.

(The ordinate represents the log concentration of the test gases corrected for He dilution divided by the initial alveolar gas concentration; the abscissa, the time of rebreathing in seconds. There is a much steeper disappearance slope of CO during air than during O_2 breathing, and hence a higher diffusing capacity.)

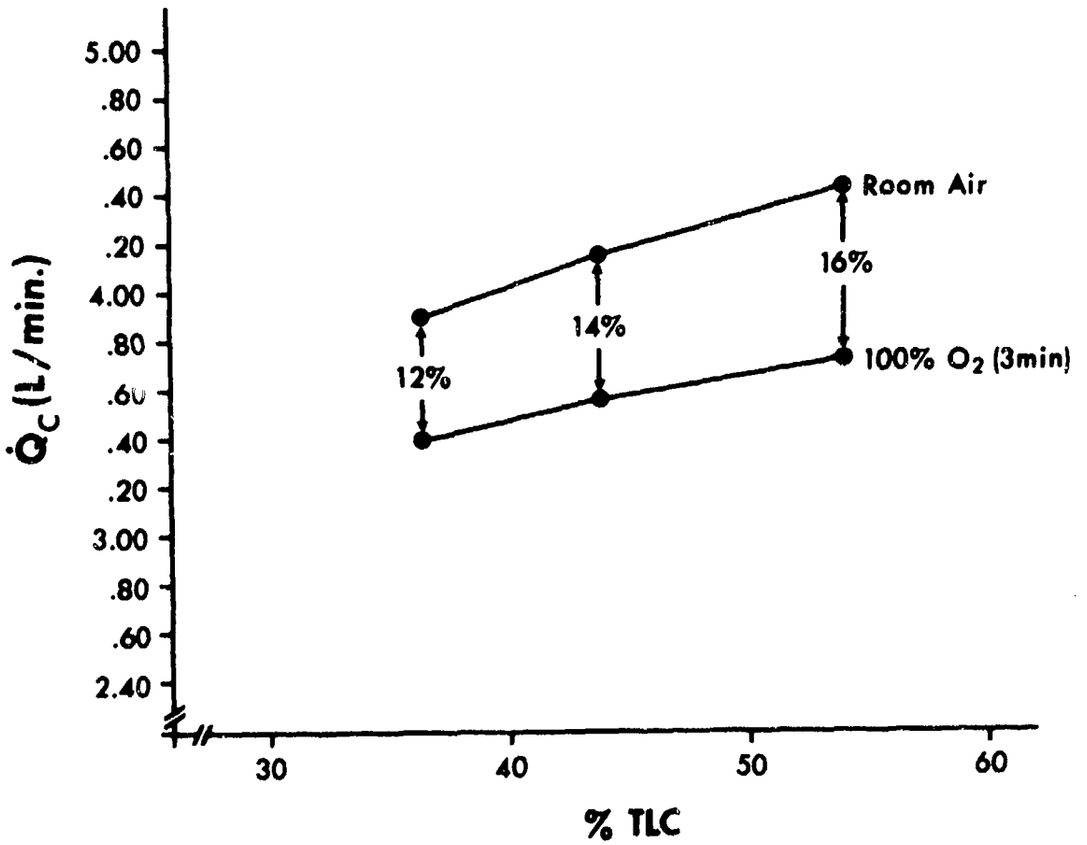

Figure 5. Effects of 3 min O_2 breathing on pulmonary $\dot{Q}_C$ (cardiac output) in normal seated subjects.

(At any given lung volume, O_2 suppresses cardiac output.)

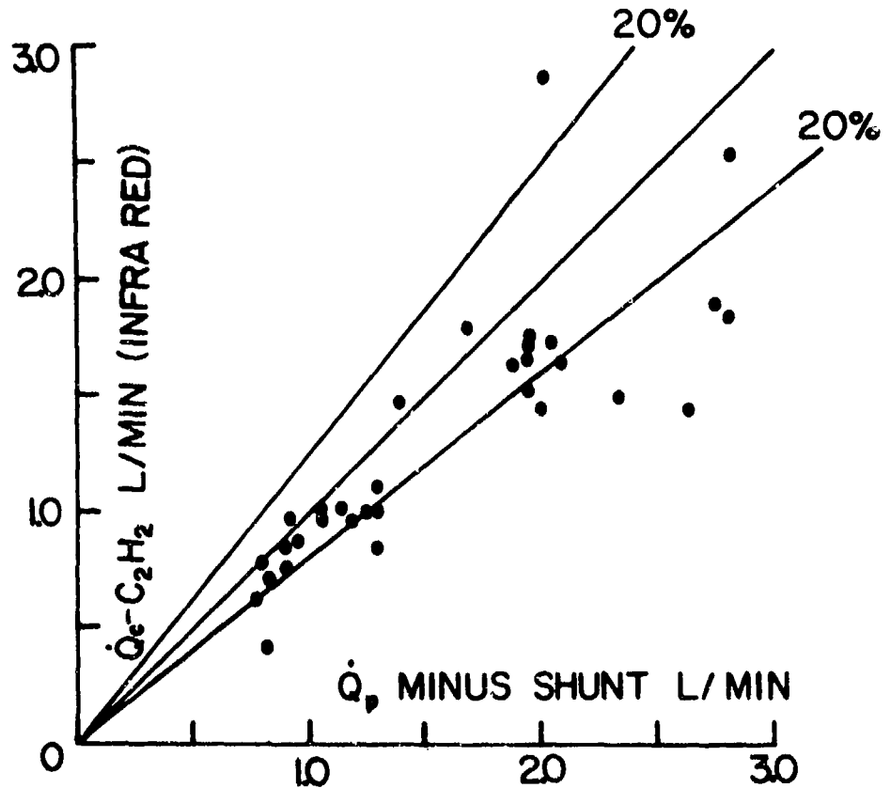

Figure 6. Comparison, in anesthetized dogs, of pulmonary $\dot{Q}_C$ by acetylene rebreathing using physical gas analyzers vs. pulmonary $\dot{Q}_C$ by indicator dilution method minus calculated shunt.

(In 10 of 32 observations, the physical gas analyzer system underestimated blood flow by more than 20%.)

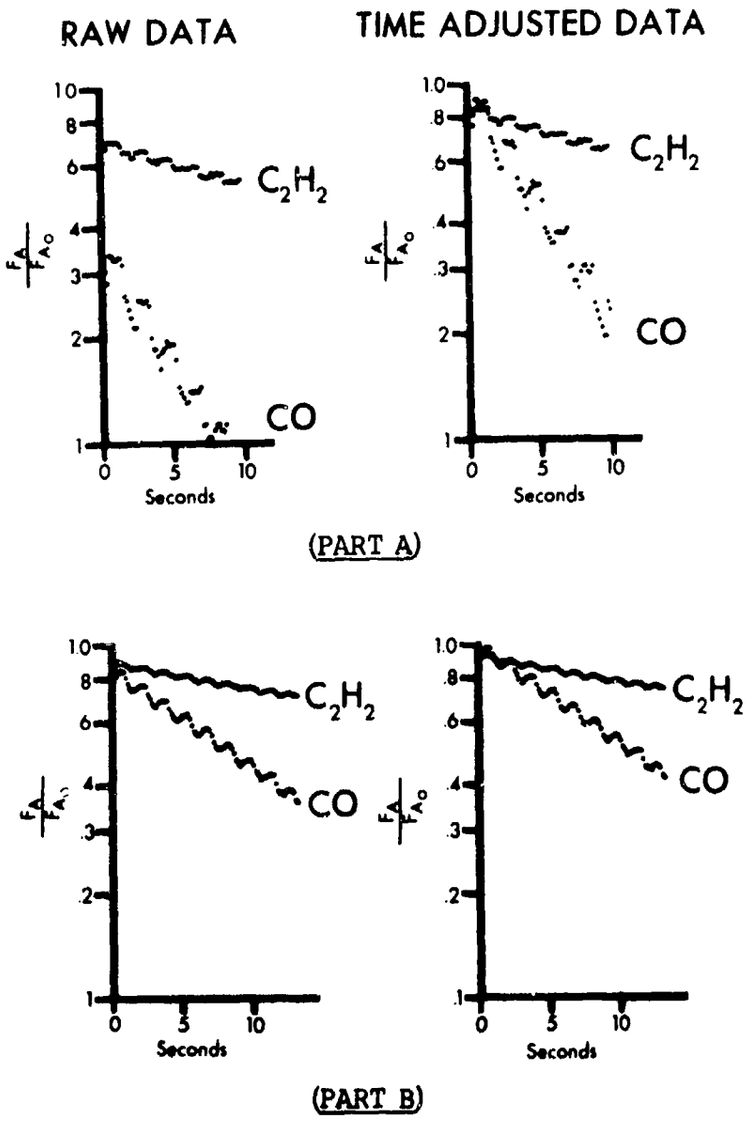

Figure 7 (Parts A and B). Representative mass spectrometer displays from oscilloscope of small digital computer.

(Note, in Part A, the failure of the CO disappearance curve to intercept at zero time in the raw data display and the low values of the C_2H_2 disappearance curve. After the computer has adjusted the CO disappearance curve to intercept at a value of unity zero time--in Part B--the C_2H_2 intercept is displaced upward to the true value, since the former indicates a correct zero time.)

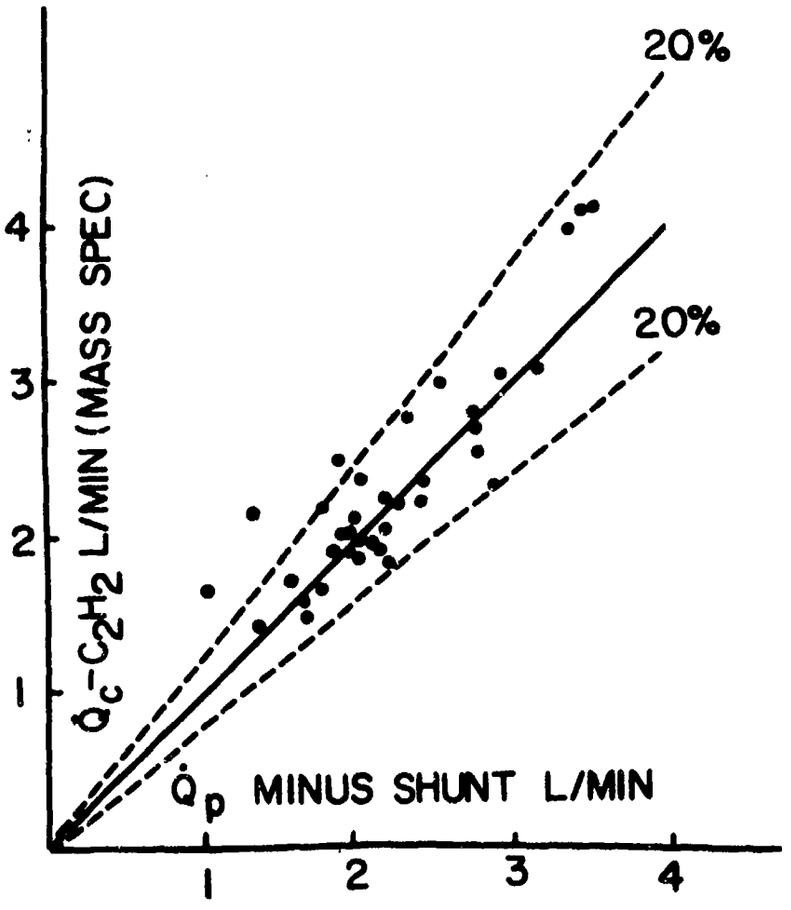

Figure 8. Comparison, in anesthetized dogs, of pulmonary $\dot{Q}_c$ by acetylene rebreathing, using mass spectrometer vs. pulmonary $\dot{Q}_c$ by indicator dilution method minus calculated shunt.

(In 3 of 36 observations, the mass spectrometer overestimated blood flow by more than 20%.)

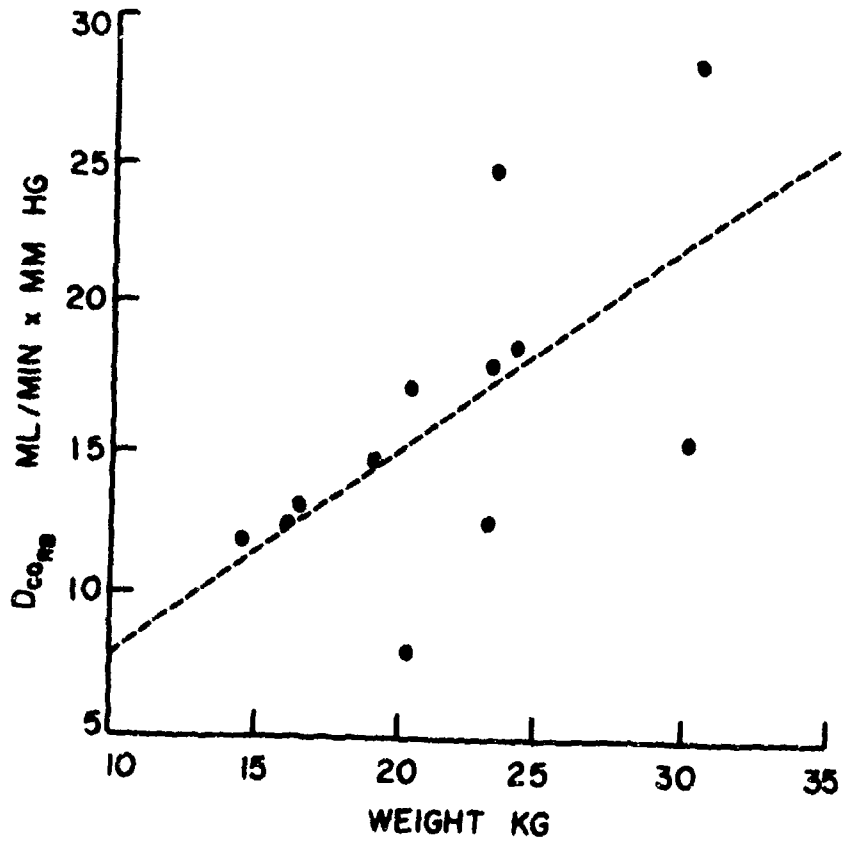

Figure 9. Rebreathing diffusing capacity vs. body weight in anesthetized dogs.

(The estimating equation is $D_{CO_{RB}} = 0.795 + 0.711 \times kg$ ($r = 0.625$).)

TABLE 1. REPRODUCIBILITY OF $D_{CO_{RB}}$ AND $\dot{Q}c_{RB}$*

Lung Volume+	54%TLC			44%TLC			36%TLC		
$D_{CO_{RB}}$ (ml/mmHg) x min)	1	2	%Variation from man	1	2	%Variation from man	1	2	%Variation from man
Prebreathing air ($P_{C_{O_2}}$ = 116 mmHg)									
Mean	30.2	28.9	4.4	26.1	27.0	2.7	23.2	22.6	3.5
SD	5.4	5.0		4.4	5.0		3.6	3.5	
Prebreathing O_2 ($P_{C_{O_2}}$ = 607 mmHg)									
Mean	14.2	14.0	3.3	12.7	13.0	2.9	11.3	11.6	4.0
SD	3.1	2.5		2.1	2.3		1.6	2.2	
$\dot{Q}c_{RB}$ (L/min)									
Prebreathing Air									
Mean	4.70	4.23	5.0	4.40	3.96	5.1	3.97	3.82	4.6
SD	0.55	0.37		0.39	0.26				
Prebreathing O_2									
Mean	3.85	3.64	3.4	3.64	3.52	4.0	3.52	3.23	4.4
SD	0.62	0.62		0.61	0.43		0.30	0.30	

Note: 1 and 2 in column headings refer to duplicate measurements (i.e., measurement 1 compared with measurement 2 under the same tensions of O_2 and alveolar volumes).

* 11 normal subjects.

+ Lung volume equals residual volume plus one-half volume of test gas mixture as percent TLC.

TABLE 2. VALUES ESTIMATED BY REBREATHING METHOD*

Lung Volume	54%TLC Mean	54%TLC SD	p*+	44%TLC Mean	44%TLC SD	p*‡	36%TLC Mean	36%TLC SD
Alveolar Volume (LSTPD)+	5.32	0.82	<.001	4.47	0.42	<.001	3.21	0.65
Oxygen Consumption (ml/min STPD)‡	431	52	<.02	367	75	<.02	328	46
$D_{CO_{RB}}$ (ml/min x mm Hg)								
Prebreathing air (P_{CO_2} = 116mmHg)	29.6	5.2	<.001	26.6	4.7	<.01	22.9	3.6
Prebreathing O_2 (P_{CO_2} = 607mmHg)	14.1	2.8	<.01	12.9	2.2	<.02	11.5	1.9
$Q_{C_{RB}}$ (L/min)								
Prebreathing air	4.47	0.46	<.05	4.18	0.38	<.02	3.90	0.45
Prebreathing O_2	3.75	0.62	<.05	3.64	0.52	<.02	3.38	0.30

*11 Normal subjects

+Residual volume plus bag volume

‡During $D_{CO_{RB}}$ prebreathing air

*+Probability of difference between means at 54% TLC and 44% TLC

*‡Probability of difference between means at 44% TLC and 36% TLC

TABLE EFFECTS OF PREBREATHING OXYGEN ON D_M AND V_C

Subject	AIR				AS O_2				3 MINUTES O_2				3 BREATHS O_2		3 MINUTES O_2	
	V_A (L. BTPS)	P_{CO_2} (mmHg)	$D_{CO_{RB}}$ $\left(\frac{ml}{min \times mmHg}\right)$	$\dot{Q}c_{RB}$ (L/min)	V_A (L. BTPS)	P_{CO_2} (mmHg)	$D_{CO_{RB}}$ $\left(\frac{ml}{min \times mmHg}\right)$	$\dot{Q}c_{RB}$ (L/min)	V_A (L. BTPS)	P_{CO_2} (mmHg)	$D_{CO_{RB}}$ $\left(\frac{ml}{min \times mmHg}\right)$	$\dot{Q}c_{RB}$ (L/min)	D_M $\left(\frac{ml}{min \times mmHg}\right)$	VC (ml)	D_M $\left(\frac{ml}{min \times mmHg}\right)$	VC (ml)
1	5.10	112	25.9	3.56	5.15	442	16.1	3.88	4.90	584	13.3	3.49	46.2	81.5	49.6	75.0
2	5.48	115	28.8	4.10	5.56	422	17.4	4.55	5.43	603	12.6	3.72	59.5	78.1	78.8	63.8
3*	4.05	130	17.4	3.60	3.92	482	9.3	5.77	3.77	559	8.4	3.54	47.2	41.2	48.0	40.0
4	5.07	127	19.7	4.28	5.15	426	10.8	3.39	5.11	538	8.8	3.00	66.8	41.3	84.4	37.8
5	4.95	121	27.3	5.33	5.05	431	14.1	5.96	4.69	563	13.2	3.34	107.0	52.6	67.8	65.6
6	4.84	127	26.1	5.60	4.98	461	18.1	5.81	5.08	581	16.9	4.57	39.5	113.9	37.8	125.2
7	5.09	127	24.4	5.15	5.32	434	16.1	5.99	4.94	579	9.7	4.20	42.9	83.8	159.8	42.5
8*	4.00	126	21.0	3.73	3.94	415	12.9	3.27	3.67	582	10.2	3.16	46.2	56.5	50.2	53.0
9	5.28	123	27.2	5.68	5.05	435	13.8	3.24	5.04	563	11.6	3.16	119.0	50.9	110.1	52.2
Mean	4.87	123	24.2	4.24	4.90	439	14.3	4.43	4.74	572	11.6	3.58	63.8	66.6	76.3	61.8
SD	0.48	5.72	3.70	0.64	0.56	19.7	2.79	1.12	0.58	17.7	2.54	0.49	27.6	22.9	36.4	25.4

* Female Subjects

TABLE 4. EFFECTS OF LUNG VOLUME ON $D_{CO_{RB}}/\dot{Q}_{c_{RB}}$ AND $D_{CO_{RB}}/V_A$

	54% TLC			44% TLC			36% TLC	
	Mean	SD	P*	Mean	SD	P+	Mean	SD
$D_{CO_{RB}}/\dot{Q}_{c_{RB}}$								
Prebreathing Air (P_{CO_2} = 115 mmHg)	0.0064	0.0010	NS	0.0064	0.0010	NS	0.0060	0.0012
Prebreathing O_2 (P_{CO_2} = 607 mmHg)	0.0036	0.0006	NS	0.0036	0.0006	<.02	0.0032	0.0005
$D_{CO_{RB}}/V_A$								
Prebreathing Air (P_{CO_2} = 116 mmHg)	5.59	0.67	<.001	6.45	0.86	<.01	7.20	1.02
Prebreathing O_2 (P_{CO_2} = 607 mmHg)	2.77	0.34	<.001	3.38	0.56	<.001	4.13	0.85

* Probability of difference between means at 54% TLC and 44% TLC.

\+ Probability of difference between means at 44% TLC and 36% TLC.

TABLE 5. EFFECTS OF LUNG VOLUME ON D_M AND V_C*

Lung Volume+	54%TLC	44%TLC	36%TLC
D_M(ml/mmHg x min)			
Actual	71.3	56.3	43.9
Assuming $D_L \simeq \dot{Q}_c$‡	59.4	51.5	41.5
V_C (ml)			
Actual	71.8	71.4	70.0
Assuming $D_L \simeq \dot{Q}_c$‡	83.8	77.0	71.1

*11 normal subjects.
+Lung volume equals residual volume plus one-half volume of test gas mixture as %TLC.
‡Correction amounts to 4% increase of D_L at high pulmonary capillary O_2 tension.

TABLE 6. REBREATHING METHOD USING PHYSICAL GAS ANALYZERS

Dog	Wt (kg)	Alveolar Volume (L. BTPS)	Oxygen Consumption (ml STPD/min)	Pulmonary Capillary Oxygen Tension (mm Hg)	Diffusing Capacity (ml/min x mm Hg)	Pulmonary Capillary Blood Flow (L/min)
1	16.4	1.69 (0.02)*	100 (6)	134 (4)	13.0 (0.6)	1.46 (0.41)
2	24.1	2.11 (0.01)	82 (4)	132 (1)	18.7 (0.6)	1.11 (0.10)
3	20.4	0.95 (0.09)	69 (16)	128 (5)	8.0 (0.4)	1.01 (0.20)
4	14.5	1.32 (0.02)	86 (14)	125 (4)	11.8 (0.4)	0.77 (0.05)
5	23.2	1.41 (0.01)	112 (12)	115 (3)	12.6 (0.1)	1.74 (0.03)
6	19.1	1.50 (0.02	89 (14)	122 (2)	14.6 (0.1)	1.56 (0.05)
7	30.4	2.00 (0.02)	156 (23)	127 (0.4)	28.6 (0.4)	1.92 (0.20)

*Values in parentheses, in body of table, represent standard error.

TABLE 7. REBREATHING METHOD USING MASS SPECTROMETER

Dog	Wt (kg)	Alveolar Volume (L. BTPS)	Oxygen Consumption (ml STPD/min)	Pulmonary Capillary Oxygen Tension (mmHg)	Diffusing Capacity (ml/min x mmHg)	Pulmonary Tissue Plus Capillary Blood Volume (ml)	Pulmonary Capillary Blood Flow (L/min)
1	20.4	1.28 (0.01)*	93 (0.03)	139 (4)	17.2 (0.4)	276 (17)	2.07 (0.06)
2	30.2	1.42 (0.02)	101 (5)	124 (0.8)	15.4 (0.2)	239 (17)	2.19 (0.09)
3	16.0	1.39 (0.01)	98 (17)	130 (4)	12.4 (0.2)	205 (16)	1.70 (0.08)
4	23.2	1.44 (0.01)	114 (8)	123 (6)	18.1 (0.4)	226 (14)	2.30 (0.07)
5	23.2	1.66 (0.02	210 (36)	113 (2)	24.8 (1.3)	269 (37)	3.78 (0.20)

*Values in parentheses, in body of table, represent standard error.

RE: SAM-TR-75-25
Section VII (Part 2)

SUPPLEMENTARY INFORMATION ON: "Flow Charts--Rebreathing Procedure."

In order for comprehensive information on this research to be readily accessible, microfiche have been made of the above-mentioned material. The microfiche are available through:

The Aeromedical Library
Documentation Section
Brooks AFB, Texas 78235

VIII. EFFECTS OF MODIFIED ANTI-G SUIT ON CARDIAC OUTPUT AND DIFFUSING CAPACITY

ABSTRACT

Cardiac output and diffusing capacity (D_L) during air and oxygen (O_2) breathing were measured in 10 human volunteers, in the seated position, breathing air or 100% O_2. Application of the standard USAF anti-G suit and a modified USAF anti-G suit were compared in these subjects. The standard suit tended to fill from the abdominal bladder downward--whereas the modified suit filled upward in sequence the leg bladders, thigh bladders, and abdominal bladder. The design of the modified type was based on previous studies which revealed that inflation of the standard suit did not produce an increase in cardiac output in subjects in the seated +1 G_z position. In the present studies, the modified suit produced significant increases in both cardiac output and D_L during air breathing. Cardiac output was unchanged when the subject breathed 100% O_2, although a slight rise in D_L occurred. These studies suggest that an anti-G suit capable of inflating from below upward might be more beneficial in protection against acceleration maneuvering than the standard USAF anti-G suit. However, even the modified suit did not improve cardiac output during O_2 breathing, a condition which causes suppression of cardiac output of 12% to 16%. These studies further suggest that careful attention has to be directed to inspired O_2 concentration during accelerated maneuvering testing of anti-G suits.

INTRODUCTION

The reasons usually given for the increase in tolerance during application of anti-G suits include: rise in systemic arterial pressure; increase of venous return to heart; and decrease in vertical heart-to-head distance. In seated humans under +1 G_z conditions, application of anti-G suits over a 5- to 10-sec period produces a rise in systemic arterial and venous pressures accompanied by a compensatory fall in heart rate (1, 2). Furthermore, the inflation of an anti-G suit produces substantial rises of pressure in the pulmonary circulation, accompanied by an increase in D_L of the lung (3, 4). When human volunteers are passively tilted from the supine to the 90° head-up position, there is a striking fall in cardiac output from a mean of 6.7 to 2.7 liters/min. Inflation of the standard USAF anti-G suit, before tilt or after the 90° head-up tilt, produces a partial restoration of cardiac output to 4.5 liters/min (5). As we previously reported, these data indicated that the anti-G suit either improved venous return or prevented trapping of blood in the pelvic region and lower extremities. Accordingly, we studied the suit's effect on human volunteers in the seated +1 G_z position and found that, although the inflation of the standard USAF

anti-G suit caused a slight fall in heart rate, no effect on cardiac output occurred (6). This anti-G suit consists of an abdominal bladder, thigh bladders, and leg bladders joined together by tubings but with the inlet tubing located at the level of the abdominal bladder. We postulated that the failure to increase in cardiac output in the seated position might be related to: crimping of the connecting tubings to the thigh and leg bladders in the seated position, thereby causing a tourniquet effect on the lower extremities which would cancel the increase of venous return produced by compression of the splanchnic and pelvic venous beds; or the venous return was increased by the inflation of the anti-G suit in the seated +1 G_z position but, because of the curvilinearity of Starling's Law Of The Heart, the effective rise in filling pressure did not produce a sufficiently detectable change or was masked by effects of pain sensations. For these reasons, we decided to test an anti-G suit which inflated upwards from the calf bladder to the abdominal bladder. We measured D_L and cardiac output by a rebreathing procedure during both air and O_2 breathing (7). Systolic time intervals were measured from analysis of an external carotid artery pulse tracing, phonocardiogram, and EKG (8).

METHODS

Modified Anti-G Su[i]t

The modified suit was constructed by severing the tubing connection around the abdominal, thigh, and calf bladders and bringing separate pressure lines from a reservoir chamber (50-gal steel drum) so that the individual bladders could be filled by a hand-operated toggle switch. The bladders could be filled in sequence from below upwards at 3 psi in about 15 sec.

Rebreathing Technique

The method used in this study has already been described in detail in report section VII (in "Procedure in Humans," p. 135, par. 1, to p. 136, par. 2).

Data processing was conducted on-line by means of a small digital computer system (LINC 8, Digital Equipment Co., Maynard, Mass.). The disappearance of CO and C_2H_2 was calculated and displayed according to the method of Cander and Forster (10). From these curves, diffusing capacity, and cardiac output were calculated.

Systolic Time Intervals

The systolic time intervals of left ventricular systole were measured from simultaneous recordings of the EKG, phonocardiogram, and carotid pulse tracing. The latter was recorded through changes in electrical capacitance due to movement of an attached stretched latex diaphragm placed over the carotid artery. The total electromechanical systole (QS_2) is measured from the onset of ventricular depolarization to the first high-frequency vibrations of the aortic component of the second heart sound. The left ventricular ejection time (LVET) is measured from the beginning upstroke to the trough of the incisural notch on the carotid pulse tracing. The pre-ejection phase (PEP) is derived by subtracting the LVET from QS_2. In the range of heart rate from 50 - 110 beats/min, these systolic time intervals are linearly related to heart rate and the values must be corrected if rate changes during a study (8).

Procedure

Either the standard or the modified anti-G suit was donned by the volunteer, who then rested in the sitting position for 7 min. A rebreathing test was done, and the volunteer then rested for 3 min. The anti-G suit was inflated to 3 psi, a procedure which took 15 - 20 sec, and the rebreathing test immediately performed. The anti-G suit was deflated and the subject rested for 7 min. He then breathed 100% O_2 from a demand valve for 3 min, rebreathed O_2 through a CO_2 absorber for 3 min to enable a determination of back pressure for CO in the blood, and then breathed 100% O_2 from a demand valve. A rebreathing procedure with a high O_2 concentration in the test mixture was carried out and followed by breathing O_2 from a demand valve for 3 min. The anti-G suit was inflated, and this was immediately followed by a rebreathing test. The anti-G suit was removed and the procedure repeated with the anti-G suit which had not been used in the first series of tests.

RESULTS

Standard USAF Anti-G Suit

The effects of the inflation of the standard suit are summarized in Table 1. Presented in Figure 1 are the observations on heart rate, stroke volume index, and cardiac output index--during both air and O_2 breathing--using the standard and the modified suits. With the standard USAF anti-G suit, there was a 4% increase in $D_{CO_{RB}}$ on air breathing (P = NS) and a 6% increase with O_2 breathing ($P < .05$). The ratio $D_L:V_A$ significantly increased with inflation of the anti-G suit (Fig. 2). During inflation of

the anti-G suit, the systolic time intervals showed the following: Q - S_2 interval, no change; LVET, slight prolongation; and PEP, slight shortening (Fig. 3).

Modified USAF Anti-G Suit

The effects of the inflation of the modified suit are summarized in Table 2. During both air and O_2 breathing, heart rate was unchanged. During air breathing, however, there was a 9% increase in stroke volume ($P < .02$) and a 12% increase in cardiac output ($P < .01$) (Fig. 1). Although similar changes took place during O_2 breathing, the differences were not statistically significant. Diffusing capacity increased 14% during air breathing ($P < .01$) and 8% during O_2 breathing ($P < .02$). The ratios D_L:V_A also showed a significant increase (Fig. 2). During inflation of the anti-G suit, the systolic time intervals showed the following: Q - S_2, no change; LVET, slight prolongation; and PEP, no change (Fig. 3).

DISCUSSION

The physiologic action of anti-G suits has been the subject of intense investigation (11). One explanation for their beneficial effect is that, by applying pressure to the lower limbs and abdomen, these devices tend to keep the transmural pressure of the blood vessels in these parts constant, thereby preventing pooling of blood and transudation of fluid when the internal pressure is increased by acceleration. The quantity of blood which can collect in these vessels is, however, relatively small during the brief exposure to the high degrees of acceleration occurring at the time that the suits are beneficial in preventing symptoms. The protective effects of the anti-G suit can be explained if a reduction takes place in the hydrostatic distance between the heart and brain. However, radiographs indicate that this reduction, although it does occur, accounts for only 0.2 G of the overall protection provided by anti-G suits.

The application of external pressure to the torso increases systemic blood pressure which is of great importance in protecting cerebral blood flow and raising the threshold for acceleration. On the arterial side of the circulation, external pressure increases the resistance to inflow of blood, although this is achieved by a decrease in arteriolar transmural pressure. At the same time, compression of the veins forces blood from the capacity vessels back into the general circulation, increases venomotor tone, and diminishes the space available for blood pooling. It has been postulated that the more efficient garments produce a larger increment of thoracic blood volume through this mechanism. Their greater protection lies in the larger rise of systemic blood pressure resulting from this increment.

Howard (11) explained the protective action of anti-G suits in terms of their initial and late effects. The early, or short-term, protection results from a combination of minor elevation of the diaphragm and compression of the legs. The former decreases the vertical distance between the heart and brain; the latter raises the peripheral arteriolar resistance. In the late stages of a long exposure to acceleration, the compression of the legs acts to prevent or reduce the collection of blood in the capacity vessels of the limbs, thus helping to maintain cardiac output at a time when it would be otherwise falling further.

The present study clearly demonstrates that a modified USAF anti-G suit which inflates from below upward is, in its hemodynamic effects, superior to the standard USAF anti-G suit. This modified suit significantly increases pulmonary $\dot{Q}_C$ and D_L of the lung during air breathing when the subject is in the +1 G_z seated position. Although similar changes take place during O_2 breathing, the increase in pulmonary Q_C is not statistically significant. The modified anti-G suit cannot completely overcome the suppressant action of O_2 breathing on cardiac output, an effect which amounts to a 12% to 16% decrease (7).

The modified anti-G suit in which the application of pressure is from below upwards is more efficient in milking blood from the extremities into the venous system, with the following beneficial results. The larger rise in diffusing capacity, a measure which is proportional to pulmonary V_C when the modified anti-G suit is applied, probably reflects a larger increment in thoracic blood volume, and this might allow a greater rise in systemic blood pressure, thus affording greater acceleration protection during its early stages. On the other hand, the increase in cardiac output by the increased venous return should give better G protection during the later phase of G exposure. These effects have only been studied under +1 G_z conditions, however; and such a suit must undergo testing on the centrifuge where high accelerative forces can be applied.

Increases in stroke volume due to enhanced ventricular filling are accompanied by a lengthening of the LVET and abbreviation of the PEP while, in general, QS_2 interval remains unchanged. Transient increases in after-load induce prolongation of both LVET and PEP (8). Both the rise in systemic pressure and increase in stroke volume induced by inflation of the anti-G suit tend to lengthen LVET, whereas PEP is shortened by one factor and lengthened by another. In the present study, the lengthening of LVET with anti-G suit inflation was the only consistent finding observed in the systolic time intervals.

The D_M and pulmonary V_C could not be calculated from the measurements of diffusing capacity at the high and low alveolar O_2 tensions

because of the inability to ensure an identical hemodynamic state between the two determinations--owing to the design of the experimental protocol. We were interested in whether the suppressant effects of O_2 on cardiac output could be overcome with the modified anti-G suit; but this did not prove to be the case, and suggested that the inspired O_2 concentration might also play a role in limiting tolerance to accelerative maneuvering.

BIBLIOGRAPHY

1. Seiker, H. O., et al. A comparative study of two experimental pneumatic anti-G suits and the standard USAF G-4A anti-G suit. WADC Technical Report 52-317, Wright Air Development Center, Wright-Patterson AFB, 1953.

2. Wood, E. H., and E. H. Lambert. Some factors which influence the protection afforded by pneumatic anti-G suits. J Aviat Med 23:218-228 (1952). [Now: Aviat Space Environ Med]

3. Ross, J. C., T. H. Lord, and G. D. Ley. Effect of pressure-suit inflation on pulmonary-diffusing capacity. J Appl Physiol 15:843-848 (1960).

4. Ross, J. C., et al. Influence of pressure suit inflation on pulmonary diffusing capacity in man. J Appl Physiol 17:259-262 (1962).

5. Segal, N., R. Dougherty, and M. A. Sackner. Effects of tilting on pulmonary capillary blood flow in normal man. J Appl Physiol 35:244-249 (1973).

6. Sackner, M. A., and R. Dougherty. Anti-G Suit inflation on cardiac output on seated subjects. Riv Med Aeronaut Spaz (Roma) 46:264-266 (1973).

7. Sackner, M. A., et al. Diffusing capacity, membrane diffusing capacity, capillary blood volume and cardiac output measured by a rebreathing technique. Submitted for publication (1974). [USAFSAM Editor's Note: Consult report section VII for related information.]

8. Weissler, A. M., R. P. Lewis, and R. F. Leighton. The systolic time intervals as a measure of left ventricular performance in man. In: Yu, P. N., and J. F. Goodwin (eds.). Progress in cardiology, pp. 155-181. Phila., Pa.: Lea & Febiger, 1972.

9. Lewis, B. M., et al. The measurement of pulmonary diffusing capacity for carbon monoxide by a rebreathing method. J Clin Invest 38:2073-2086 (1959).

10. Cander, L., and R. E. Forster. Determination of pulmonary parenchymal tissue volume and pulmonary capillary blood flow in man. J Appl Physiol 14:541-551 (1968).

11. Howard, P. The physiology of positive acceleration. In: Gillies, J. A. (ed.). A textbook of aviation physiology, pp. 551-687. Oxford: Pergamon Press, 1965.

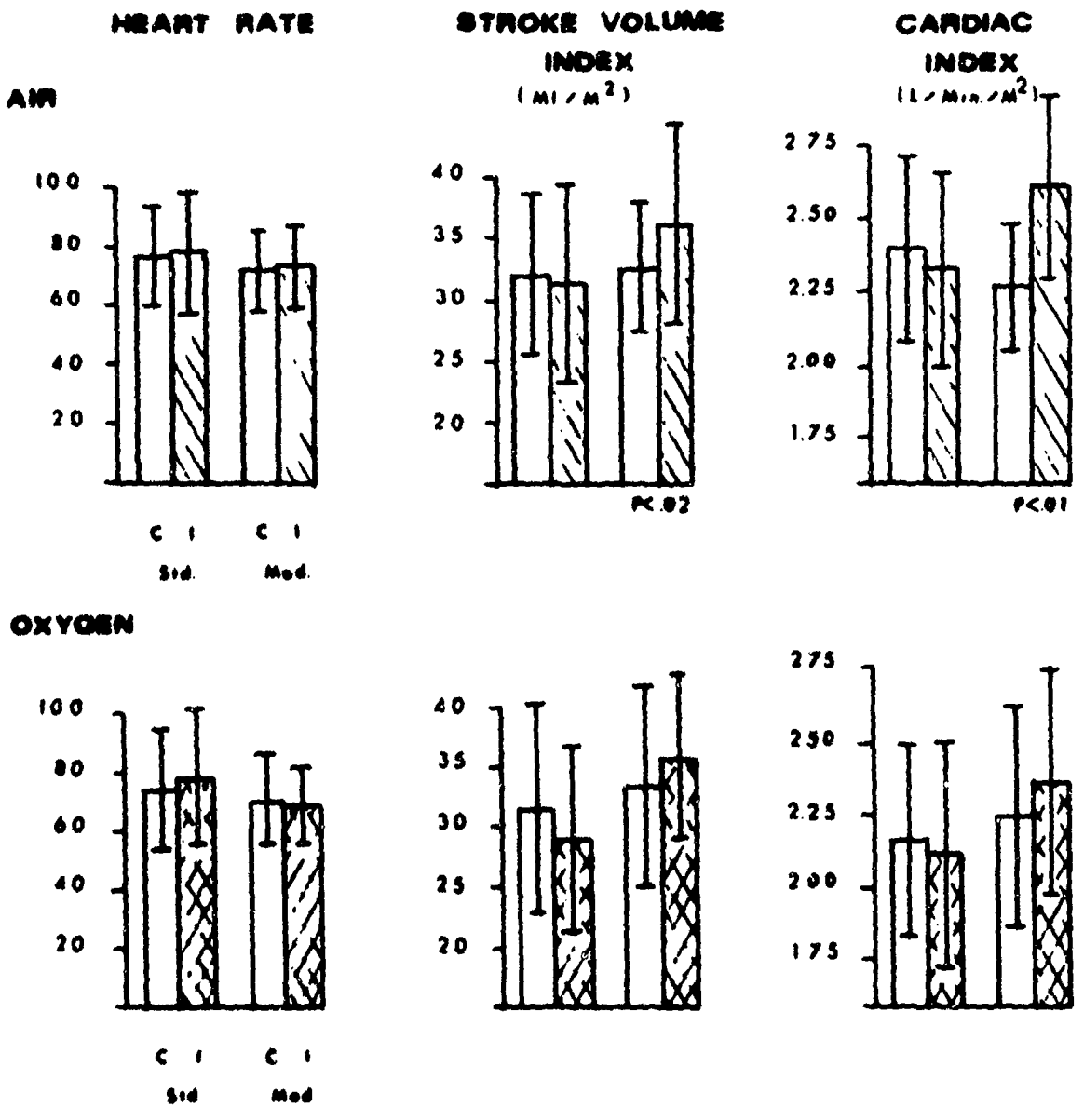

Figure 1. Changes in heart rate, stroke volume index, and cardiac index pre- (C) and postinflation (I) of the standard and of the modified anti-G suits.

[For each set of observations, the data are shown for: the standard anti-G suit (Std), on the left; the modification (Mod), on the right.]

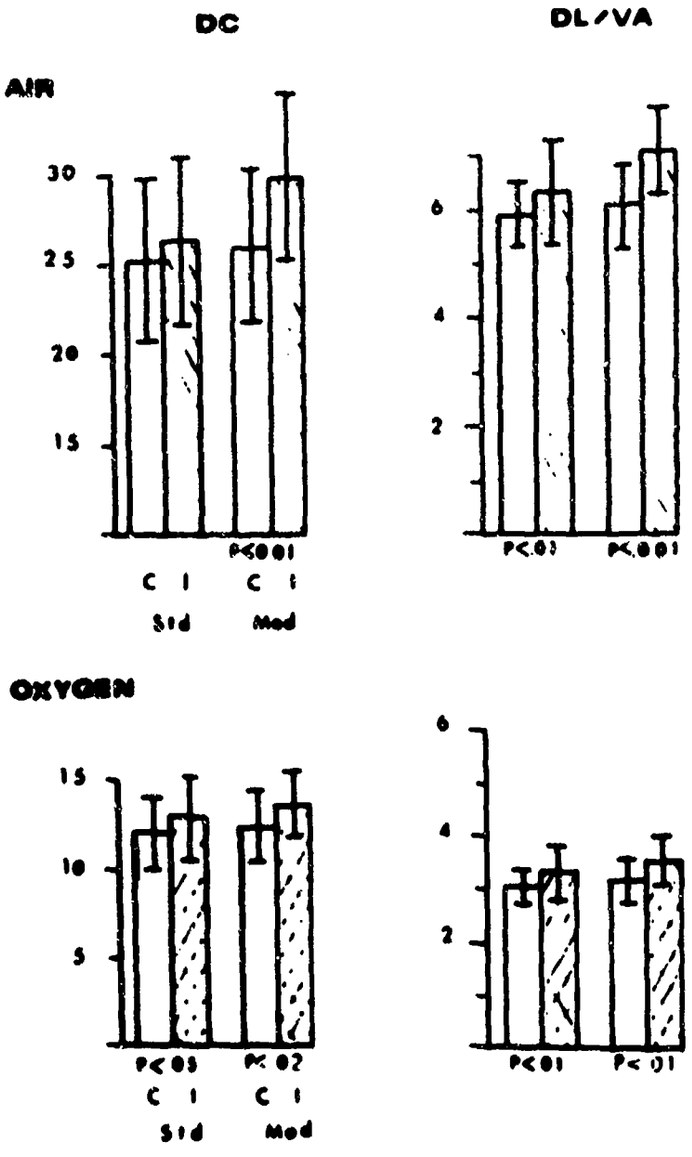

Figure 2. Changes in diffusing capacity (DC) and the ratio of D_L:V_A pre- (C) and postinflation (I) of the standard (Std) and modified (Mod) anti-G suits.

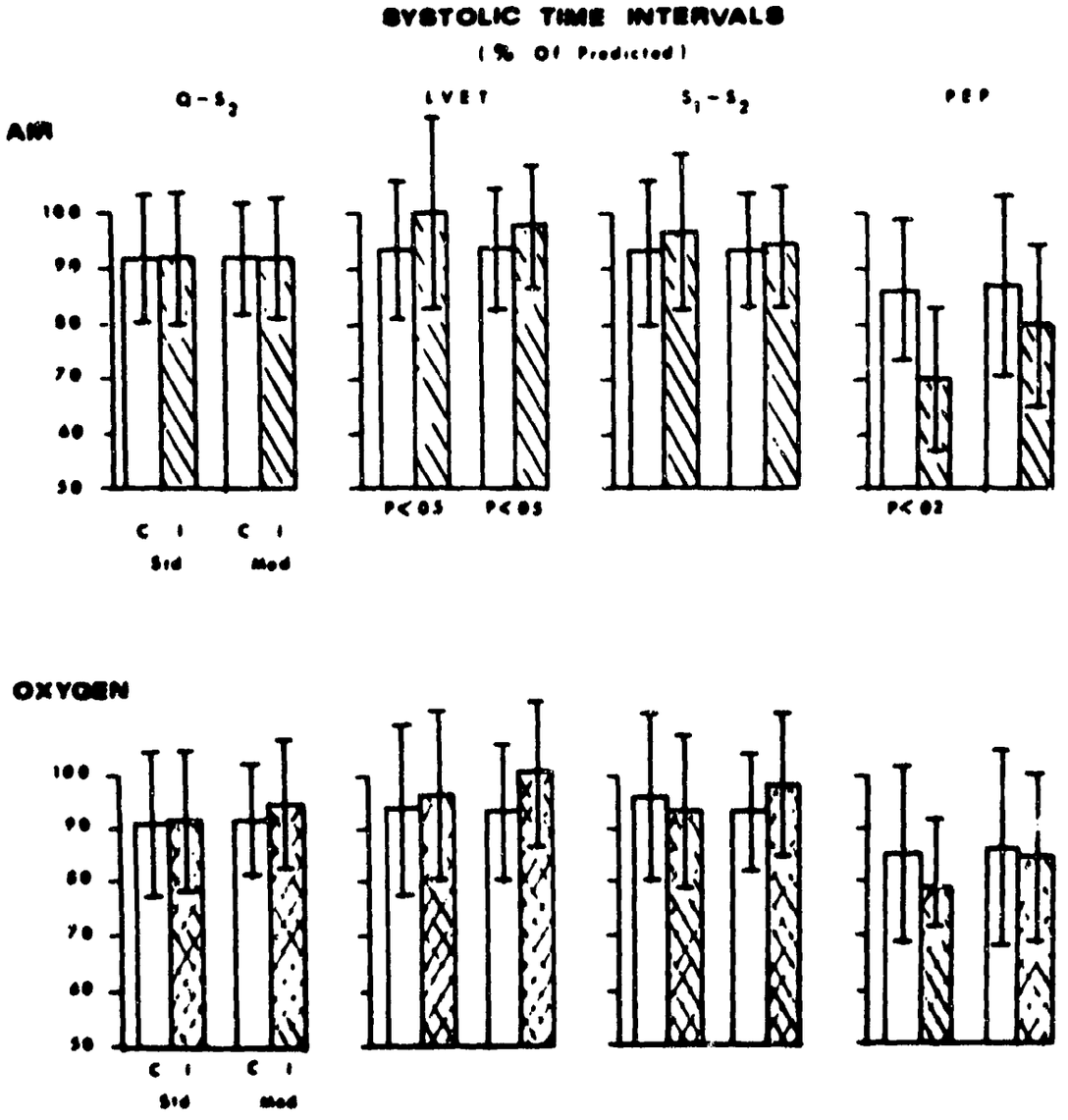

Figure 3. Systolic time intervals heart rates are plotted as a percentage of predicted values for the heart rate; and the changes, pre- (C) and postinflation (I), of the standard (Std) and of the modified (Mod) anti-G suits are depicted.

TABLE 1. EFFECTS OF INFLATION OF STANDARD USAF ANTI-G SUIT

Subject	Control: Heart Rate (Beats/min)	Cardiac Output (L/min)	Stroke Volume (ml)	Alveolar Volume (L.BTPS)	Oxygen* Consumption (ml/min STPD)	$P_{c}O_2$ (mmHg)	$D_{CO_{RB}}$ (ml/min x mmHg)	Anti-G Suit Inflated: Heart Rate (Beats/min)	Cardiac Output (L/min)	Stroke Volume (ml)	Alveolar Volume (L.BTPS)	Oxygen* Consumption (ml/min STPD)	$P_{c}O_2$ (mmHg)	$D_{CO_{RB}}$ (ml/min x mmHg)
							Air Breathing							
1	79.6	4.75	59.7	4.05	454	116	22.0	83.1	4.53	54.5	3.94	357	123	21.1
2	63.2	4.94	78.2	4.18	386	128	26.1	51.9	4.12	79.4	3.99	351	122	27.2
3	92.3	5.75	62.3	4.66	494	117	29.5	108.0	5.52	51.1	4.43	304	119	31.2
4	71.4	4.56	63.9	5.06	366	126	26.5	81.2	4.13	50.9	4.96	320	126	25.3
5	58.8	3.78	64.3	3.34	260	113	22.2	63.3	4.13	65.2	3.44	239	112	26.8
6	100.8	3.93	39.0	4.33	325	118	28.5	89.6	3.84	42.9	4.22	312	113	29.5
7	105.3	4.17	39.6	3.67	344	114	18.7	106.2	4.28	40.3	3.66	316	108	19.7
8	67.4	4.81	71.4	5.30	378	120	33.5	68.2	4.91	72.0	5.18	473	114	33.6
9	55.3	4.13	74.7	3.67	272	117	19.3	45.4	3.63	79.8	3.55	303	115	20.1
10	68.3	5.06	74.1	4.26	335	109	27.3	73.3	5.52	75.3	4.02	344	104	29.6
Mean	76.2	4.59	62.7	4.25	356	118	25.4	77.0	4.46	61.1	4.14	332	116	26.4
SD	16.7	0.57	13.0	0.59	60	5	4.5	19.8	0.62	14.3	0.55	57	7	4.6
							Oxygen Breathing							
1	73.0	3.69	50.5	3.71		578	10.1	76.5	3.78	49.4	3.68		569	9.9
2	55.0	3.94	71.6	3.92		612	12.2	57.7	3.65	63.3	3.65		591	12.3
3	81.5	4.60	56.4	4.04		561	12.9	90.9	4.06	44.7	3.68		581	14.6
4	78.5	3.41	43.7	4.76		557	12.3	87.6	2.99	34.1	4.85		572	12.9
5	58.8	3.61	61.4	3.25		592	11.8	58.0	4.01	69.1	3.22		591	13.5
6	104.3	3.91	37.5	4.07		607	12.9	96.3	3.23	33.5	3.87		602	11.8
7	104.3	4.25	40.7	3.61		575	9.2	107.1	5.10	47.6	3.72		590	11.3
8	55.1	4.86	88.2	5.32		597	16.6	69.8	5.08	72.8	5.17		592	17.6
9	43.9	3.68	83.8	3.44		600	9.4	55.4	3.53	63.7	3.42		600	9.9
10	72.9	5.49	75.3	3.77		582	12.4	67.6	5.07	75.0	3.70		596	13.0
Mean	72.7	4.14	60.9	3.99		586	12.0	76.7	4.05	55.3	3.91		588	12.7
SD	19.4	0.62	17.2	0.59		18	2.0	17.1	0.74	14.7	0.59		11	2.2

*Could only be calculated during air breathing.

TABLE 2. EFFECTS OF INFLATION OF MODIFIED USAF ANTI-G SUIT

Subject	Control: Heart Rate (Beats/min)	Cardiac Output (L/min)	Stroke Volume (ml)	Alveolar Volume (L,BTPS)	Oxygen* Consumption (ml/min STPD)	P_{C_2} (mmHg)	$D_{CO_{RB}}$ (ml/min x mmHg)	Anti-G Suit Inflated: Heart Rate (Beats/min)	Cardiac Output (L/min)	Stroke Volume (ml)	Alveolar Volume (L,BTPS)	Oxygen* Consumption (ml/min STPD)	P_{C_2} (mmHg)	$D_{CO_{RB}}$ (ml/min x mmHg)
						Air Breathing								
1	78.9	4.56	57.8	4.05	375	124	23.6	84.3	5.18	61.-	4.07	336	121	24.9
2	61.9	4.07	65.8	3.96	308	122	24.8	56.1	4.11	73.3	3.92	265	127	27.7
3	95.8	4.53	47.3	5.00	628	120	28.5	91.6	4.86	53.1	4.72	367	114	33.8
4	65.4	4.83	73.9	5.12	475	126	27.8	79.2	5.42	68.4	5.00	414	121	30.9
5	62.5	4.19	67.0	3.54	323	120	26.2	61.3	4.61	75.2	3.54	404	117	30.0
6	90.2	4.02	44.6	4.25	340	122	30.9	95.2	4.69	49.3	4.30	376	114	33.4
7	70.6	4.24	60.1	3.74	32[illegible]	114	19.8	71.9	5.72	79.6	3.98	390	106	25.3
8	66.8	5.15	77.1	5.51	402	120	33.5	65.4	5.45	83.3	5.50	343	121	38.3
9	50.2	3.77	75.1	3.56	331	106	18.3	51.4	4.02	78.2	3.63	290	112	21.8
10	68.2	5.00	73.3	4.10	340	109	27.5	74.3	5.77	77.7	3.99	403	105	30.8
Mean	71.1	4.44	64.2	4.28	385	118	26.1	73.1	4.98	69.9	4.27	359	116	29.7
SD	13.0	0.43	11.0	0.65	94	6	4.4	14.0	0.60	11.1	0.59	46	7	4.6
						Oxygen Breathing								
1	74.3	3.73	50.2	3.69		550	10.5	68.8	3.91	56.8	3.88		574	11.2
2	73.9	3.86	52.2	3.69		570	10.2	46.2	4.03	87.2	3.74		595	13.6
3	98.0	4.64	49.4	4.24		565	13.1	79.8	5.39	67.5	4.09		571	15.3
4	60.7	5.18	85.3	4.88		584	14.8	81.9	5.06	61.8	4.56		560	14.[illegible]
5	58.8	3.63	61.7	3.15		603	12.8	56.4	3.87	68.6	3.15		602	14.[illegible]
6	96.0	3.69	38.4	4.00		615	14.[illegible]	65.9	3.41	39.7	3.82		623	13.1
7	62.8	4.69	74.7	3.70		585	10.[illegible]	60.3	4.78	79.3	3.60		593	11.8
8	56.5	5.19	91.9	5.51		605	15.[illegible]	66.3	4.94	74.5	5.14		605	15.9
9	43.7	3.38	77.3	3.54		581	8.[illegible]	50.8	3.46	78.0	3.46		576	10.3
10	69.8	5.05	72.3	3.79		590	13.1	75.0	5.69	75.3	3.78		589	13.8
Mean	69.5	4.32	65.3	4.02		585	12.3	67.1	4.50	68.9	3.92		589	13.5
SD	16.2	0.69	16.7	0.80		19	2.9	12.9	0.72	12.8	0.54		18	1.8

*Could only be calculated during air breathing.

IX (Parts 1 and 2). PULMONARY ARTERIAL BLOOD VOLUME AND TISSUE VOLUME IN MEN AND DOGS

(PART 1)

ABSTRACT

The pulmonary arterial circulation time after injection of an ether in alcohol solution just beyond the pulmonic valve was determined in conscious man by an established body plethysmographic technique [Feisal, Soni, and DuBois, in J Clin Invest 41:390 (1962)], and in anesthetized man by a newly developed pneumotachographic method. The latter was compared to simultaneously determined estimates in the anesthetized dog by the plethysmographic technique, and showed good agreement. Aspects of corrective factors to improve the accuracy of these methods (such as taking into account the right-to-left intrapulmonary shunt and the uptake of ether gas from the alveoli into the blood while ether gas is being evolved from the initial injection) were evaluated from the animal experiments. In 5 humans with normal pulmonary arterial pressures, pulmonary arterial blood volume estimated by these methods was 172 ml, SD 22 ml. Estimates of pulmonary tissue volume, both in dogs and man, were much larger than values reported by others for tritiated water space of the lungs--and more in keeping with previously published postmortem estimates of the total water content of the lungs.

INTRODUCTION

In 1962, Feisal et al. (1) described a body plethysmographic method to obtain, in anesthetized apneic dogs: the pulmonary arterial circulation time, the pulmonary arterial blood volume, lung density, and tissue volume. Their method was based upon the principle that ether gas could be detected as it arrived at the pulmonary capillaries by a rise in plethysmographic pressure after it had been injected as a solution above the pulmonic valve. The method was subsequently employed to measure aspects of the pulmonary circulation not readily obtainable by other techniques: e. g., in conjunction with injections of bicarbonate and of lactic acid to measure intrapulmonary reaction times of these compounds (2, 3); to estimate the size of gas exchange vessels within the lung (4); and to demonstrate the effects of breathing hypoxic mixtures on the mechanical properties of large pulmonary arterial vessels (5). However, the method has not been heretofore applied to humans. The purposes of the present investigation were: (a) to determine the feasibility of ether plethysmographic method in conscious man; (b) to describe a modification of this

technique, using a pneumotachograph, and to compare its accuracy with that of the standard plethysmographic method in anesthetized dogs; and (c) to determine the feasibility of the pneumotachographic method in anesthetized man.

METHODS AND PROCEDURES

Ether Plethysmographic Method

The following deals with the collection and processing of data for the ether plethysmographic method. For the comparison between the ether plethysmographic and ether pneumotachographic methods (vide infra), an anesthetized dog is enclosed within an airtight chamber, the body plethysmograph (BOX); and 0.5 - 2 ml of an ethyl ether in alcohol solution 1:4 is flushed in rapidly with 3 - 8 ml of saline into the pulmonary artery. The same procedure is employed for conscious humans; but, instead of remaining apneic, they expire slowly at a relatively constant flow rate of 2 - 3 L/min--with the aid of a visual monitor connected to the output of a Fleisch pneumotachograph--because of the difficulty in remaining relaxed with an open glottis in an apneic position. This maneuver imposes a steady ramp signal on the plethysmographic tracing and is easily separated from the signal after ether injection. There is an initial rise in BOX pressure as a result of the saline flush; BOX pressure is calibrated as a volume, and the volume of saline injected is recovered completely in the wave form of the BOX pressure (Fig. 1). After the saline flush, a slow rise in BOX pressure is caused by the entry of gaseous ether into the alveoli until a peak is reached. As blood with a decreasing concentration of ether continues to flow into the capillaries, the capillary to alveolar ether gradient is reversed, and ether diffuses from the alveoli back into the blood--producing a fall in BOX pressure at a rate depending upon the solubility of ether in blood, the partial pressure gradient for ether, and the pulmonary $\dot{Q}_C$.

The pulmonary arterial circulation time (pulmonic valve to pulmonary capillaries) is measured as follows: The median transit time is the period measured between the time at which the rise of BOX pressure caused by the injection volume reaches half its maximal value, and the time at which the rise of BOX pressure caused by the appearance of ether gas in the alveoli reaches half its peak value. The rationale for this estimate of circulation time has been explained, as follows, by Feisal et al. (1): There is a scatter of arrival times of ether at the capillaries related to different rates of flow to different parts of the lung. The mid-volume point of the rise in BOX pressure corresponds to the time of arrival of half the ether at the capillaries. If ether is uniformly mixed with the blood,

the concentration of ether in all branches of the pulmonary artery will be equal; and the arrival of half the ether indicates the arrival of half the blood at the capillaries. The measurement of median transit time is more rapid and easy to obtain manually than the mean transit time, a parameter which might be more accurate if the evolution of ether behaved as a cumulative frequency motion. For the mean transit time, it is necessary to perform the following operation on the ether curve:

$$\text{mean transit time} = \frac{\int_o^\infty t d^{rr}}{\int_o^\infty dV}$$

in which t = time, and dV = an element of the volume of ether at any point in time. Because this analysis is more time consuming, Feisal et al. (1) did not use it since their preliminary studies suggested that the results of both median and mean transit times were similar. They also pointed out that pressure-time curve after ether injection is not a true cumulative frequency, because ether returns to the blood before peak plethysmographic pressure is reached.

The return of ether to the blood before its peak evolution can be taken into account by correcting for the elapsed time, the degree of pressure change and rate constant of the descending curve after peak BOX pressure: The peak ether volume is delineated, and a least squares fit on the descending curve is performed to obtain its slope. The ether curve is translated as follows:

$V'(t) = V(t) - m(t-t_i)$ for $t-t_i \rightarrow t_{max}$ in which $V'(t)$ = the translated function; $V(t)$ = original ether curve; m = the slope; t = time; t_i = initial time of inscription of ether curve; and t_{max} = the time of peak ether volume. This correction is additive to the actual volume of ether measured. Since the volume of ethyl ether gas evolved is a function of the ratio of alveolar volume/pulmonary capillary plus tissue volume (1), this correction sets a lower limit to the estimate of pulmonary tissue volume. Another correction which must be considered is the amount of right-to-left intrapulmonary shunting of blood. The larger the shunt, the less the volume of ether evolved; and failure to allow for this correction results in an overestimate of pulmonary tissue volume. In the present investigation, the significance of these correction factors is systematically examined.

-IX-
(Part 1)

Ether Pneumotachographic Method

This ether pneumotachographic method was developed in order to study apneic subjects on respirators or under anesthesia, and is based upon a technique described by Wasserman and Comroe (6) and later modified by our group (7). It has been used to estimate nitrous oxide uptake as a prerequisite for calculating pulmonary Q_C. During apnea, the chest becomes analogous to the BOX and, with a sensitive pneumotachograph at the airway, the evolution of ether gas is detected as a rise in expiratory air flow superimposed on the cardiogenic oscillations (Fig 1). Such oscillations of flow are synchronous with the heart beat and are as much as 7 to 15 times larger than the peak flow, due to evolution of ether gas. Filtering of these oscillations might be best accomplished by a low-pass digital filter with a sharp cutoff, since the period of oscillations is much faster than the period of ether evolution. However, because of core restrictions in our small digital computer, and after preliminary trials of several approaches to eliminate the cardiogenic oscillations from the record, we found that the most reproducible method was to use the cardiogenic oscillation immediately preceding ether injection as a template to subtract the oscillatory content beat-by-beat throughout the ether evolution. The resultant flow curve was integrated to give the volume of ether gas evolved and pulmonary arterial circulation time computed, as in the analysis of BOX records. It was impossible to employ the pneumotachographic method in conscious subjects; for reproducible baseline cardiogenic flow oscillations could not be obtained, owing to incomplete relaxation of the thorax.

Data Processing

A program was written which runs on both a standard LINC 8 digital computer with 4K of core and on an updated version, the PDP 12 (Digital Equipment Co., Maynard, Mass.). Analog signals are put into the computer by means of analog-to-digital converters: 1) signal from an injection apparatus (Cordis Injector, Cordis Corp., Miami, Fla.) which delivers saline to flush the ether solution into the pulmonary artery; 2) EKG; and 3) flow signal from the pneumotachograph, or volume signal from the body plethysmograph. The program calculates the mean and median pulmonary arterial circulation time and displays the ether curve. The program allows the user to enter digital values of the volume of liquid ethyl ether injected, alveolar volume, and pulmonary V_C into the computer--thus permitting calculations of lung density and pulmonary tissue volume as described by Feisal et al. (1). However, the partition coefficient for

ether in lung tissue in the present study is taken as 12 (8, 9), rather than 15.5 as used by these authors. Right-to-left intrapulmonary shunt was determined during 100% O_2 breathing; and this shunt fraction was subtracted from the volume of liquid ethyl ether injected in order to correct for volume of ether solution not arriving at the alveolocapillary membrane. It is possible to examine the raw data at various points in the program before finalizing the display (Fig. 2).

Comparison of Ether Plethysmographic and Pneumotachographic Methods on Animals

Twenty-three mongrel dogs, each weighing 13 - 30 kg, were anesthetized with sodium pentobarbital (25 mg/kg). They were intubated with a cuffed endotracheal tube, and catheters were placed within the pulmonary and carotid arteries and a peripheral vein. Of these animals, 10 were paralyzed with intermittent administration of succinyl choline chloride and ventilated with a Harvard Respirator. In 5 of these 10 animals, marked sinus arrhythmia was observed; and it was necessary to introduce a bipolar electrode into the right atrium for pacing the heart at a regular rate. In 13 other dogs, ventilation was supported by means of transvenous phrenic nerve stimulation (PNS) (10). Cardiac pacing was not required in these animals because marked sinus arrhythmia was not encountered. In 7 animals, measurements were obtained of both pulmonary arterial and left atrial pressures, and cardiac output was estimated by the dye dilution method utilizing indocyanine green.

The animal was enclosed within a body plethysmograph which had an internal volume of 170 liters (11). Plethysmographic pressure was sensed by a differential pressure gage (DP 45 $\pm$ 1 in. water, Validyne Corp., Northridge, Calif.). The frequency response of the chamber was flat to 21 Hz. Flow at the airway during apnea was sensed through a #00 Fleisch pneumotachograph connected to a differential gage (DP 45 $\pm$ 1 in. water, Validyne Corp.) which was situated within the body plethysmograph. The frequency response of the pneumotachographic system was flat to 14 Hz. After calibration of the plethysmograph and pneumotachograph, 0.5 - 2 ml of 1:4 ether in alcohol solution was instilled into a cardiac catheter whose tip was positioned just above the pulmonic valve. A baseline was established of both plethysmographic pressure and pneumotachographic flow for 2 - 3 sec during apnea; and the ether solution was flushed into the pulmonary artery by means of 3 - 8 ml saline solution through a Cordis Injector triggered to deliver the saline just after the inscription of the R wave of the EKG. The data were recorded on magnetic tape and analyzed off-line on a LINC-8 digital computer which was not

situated in the same building as the Animal Laboratory. (The data could have been analyzed on-line, if the computer had been nearby.)

Ether Circulation Time in Patients

After their informed consent for the procedure had been obtained, 3 conscious subjects were studied by the ether plethysmographic method; and 3 anesthetized subjects, by the ether pneumotachographic method. The same type of gages utilized in the animal experiments were employed. The frequency response of the human chamber was flat to 19 Hz. A cardiac catheter was placed under fluoroscopic control just above the pulmonic valve. The catheter had a sealed tip and multiple proximal side holes in order to minimize its recoil after the injection of fluid. The accuracy of its position was checked by gently withdrawing from the pulmonary artery until the right ventricular pressure curve was recorded, and then advancing until the pulmonary arterial pressure tracing was obtained. This position was not rechecked until the end of the procedure. Cardiac output was measured by the nitrous oxide plethysmographic and the nitrous oxide pneumotachographic methods, in the conscious and anesthetized subjects, respectively (12, 13). Alveolar volume was measured by the plethysmographic method (14) in the conscious subjects and by a rapid He rebreathing technique (11) in anesthetized subjects. Pulmonary V_C was estimated from CO disappearance curves obtained with multiple breath-holding times at two different alveolar oxygen tensions (15). Student's t-test was used to check for statistical significance of differences between means.

RESULTS

Comparison of Ether Plethysmographic and Pneumotachographic Methods on Dogs

In 60 simultaneous determinations from 16 dogs, only ten percent of mean transit times by the pneumotachographic method varied by more than 10% from the plethysmographic determinations (Fig. 3). On the other hand, thirteen percent of the pneumotachographically determined ether volumes varied by more than 20%, and seventeen percent by more than 10% from the plethysmographic estimation (Fig. 4). In two successive measurements within a period of 3 min, both pulmonary arterial circulation time (using either mean or median transit times) and volume of ether (evolved by either method) had less than 10% variation from the mean value for the respective method. For example, 35 sequential pairs of median transit time determinations showed a mean of: 0.98 sec,

SD 0.36 for the first trial; and 0.98 sec, SD 0.36 for the second trial. The difference between the trials, disregarding algebraic sign, was: 0.08 sec, SD 0.08.

The pulmonary arterial median transit time by the plethysmographic technique of 1.22 sec, SD 0.44 (110 determinations from 28 dogs) was consistently less in paired observations than the mean transit time of 1.29 sec, SD 0.48 ($P < .001$). The correction of the ether curve, by adding to it the ether gas evolved as a function of the rate constant of the descending curve following peak BOX pressure, gave the following results: In 70 determinations from 10 dogs, the mean transit time rose from 1.44 sec, SD 0.42, to 1.51 sec, SD 0.67 ($P < .001$); and the median transit time, from 1.36 sec, SD 0.42, to 1.43 sec, SD 0.58 ($P < .001$). The volume of ether by the BOX method evolved before correction for loss to the blood was: 8.9 ml, SD 2.8; and after correction, 9.9 ml, SD 3.5 ($P < .001$).

In 6 dogs, there were no significant changes in either pulmonary arterial circulation time or volume of ether gas evolved as measured by the plethysmographic method, whether the measurement was made with an open or occluded airway at the FRC position.

Pulmonary Tissue Plus Capillary Volume in Dogs

Of the 17 animals measured, duplicate values for pulmonary tissue plus capillary volume varied by less than 10% in 14 animals, and by less than 15% in the remaining 3. Listed in Table 1 are: the values for the sum of pulmonary tissue plus capillary volume for the first 10 dogs studied in whom the volume of ether evolved was corrected for right-to-left intrapulmonary shunting, and the rate constant of the ether redissolving in the blood after peak volume was reached. A value for pulmonary V_C, calculated from previously published values for dogs (16), was subtracted from the combined pulmonary tissue plus capillary volume in order to estimate tissue volume alone. Values for pulmonary tissue volume were quite variable, ranging from 4.2 to 12.2 ml/kg, with a mean of 8.3 ml/kg. In these first 10 dogs in which pulmonary tissue volume was measured, pulmonary arterial pressure was within normal limits. In order to exclude a hemodynamic factor for the variability of pulmonary tissue volume measurements, both pulmonary arterial and left atrial pressures as well as cardiac output were measured in another group of 7 dogs (the data of the final 7 dogs in Table 1). All these parameters were within normal limits and the variability of pulmonary tissue volume did not differ from the first 10 animals.

-IX-
(Part 1)

Pulmonary Arterial Blood Volume and Tissue Volume in Man

The injection of ethyl ether in alcohol solution into the pulmonary artery of the conscious subjects did not produce subjective symptoms, other than the taste of ethyl ether at about the time the peak evolution of ethyl ether was being recorded. None of the subjects coughed. Pulmonary arterial pressure was not affected by the injection in both the conscious and anesthetized patients. Representative computer processed displays of ether circulation times for both the plethysmographic and pneumotachographic methods are shown in Figures 5 and 6, respectively. Values for the 6 patients are summarized in Table 2. In 5 of the 6 subjects with normal pulmonary arterial pressures at rest, the volume of the pulmonary arterial tree ranged from 135 to 198 ml, with a mean of 172 ml. This volume was only 90 ml in a patient with primary pulmonary hypertension confirmed by both cardiac catheterization and lung biopsy. This patient also had a pulmonary tissue volume much larger than the other subjects. In the subjects with normal pulmonary arterial pressures, lung densities ranged from 0.07 to 0.22 gm/ml; and combined pulmonary capillary plus tissue volume, from 221 to 438 ml, with a mean of 330 ml (200 ml/M^2 BSA).

DISCUSSION

Pulmonary Arterial Blood Volume

The injection of ethyl ether dissolved in alcohol into the pulmonary artery of man appears to be a safe procedure. We injected 0.2 - 0.4 ml ethyl ether in alcohol, whereas Fraser et al. (17) used 0.1 - 0.2 ml ethyl ether and followed it with a saline flush to detect right-to-left intracardiac shunts. No ill effects were observed in 109 patients undergoing the latter procedure. However, the normal subjects generally coughed after ethyl ether injection into the pulmonary artery. The studies of Feisal et al. (1) suggest that the cough in their patients might be related to formation of bubbles of ether gas in the blood when the liquid is injected which does not occur when the ethyl ether is dissolved in alcohol.

This report describes the first estimates of pulmonary arterial blood volume in man from ether circulation time determinations. Values in our 5 subjects with normal pulmonary arterial pressures ranged from 135 to 198 ml, with a mean of 172 ml; in one subject with pulmonary hypertensio the value was only 90 ml. This diminution in the latter corresponded to the generalized narrowing of pulmonary arterial vessels, as seen in lobar arteries and smaller arteries on chest roentgenogram and by histologic

examination of the lung biopsy. It is of interest that preliminary reports of the determination of pulmonary arterial transit time, by employment of scans to measure the activity of radio-iodinated macro-aggregated serum albumin from the opening of the pulmonic valve to the periphery of the lung, are in close agreement with the present studies both in dogs and humans. Indeed, Lewis and Herrera (18) compared the scanning technique in dogs to the ether plethysmographic method and found that 20 of 25 determinations fell within 20% of a line of identity. The authors further found that the average pulmonary arterial blood volume in man ranged from 149 to 215 ml, with a mean of 182 ml (19). Since the method of Lewis and Herrera (18, 19) depends upon injection of the tracer into the right atrium and does not involve enclosing the subject within a body plethysmograph, that method may be more practical to use if only pulmonary arterial circulation time--and not an estimate of pulmonary tissue volume--is desired. Indeed, the complexity of enclosing volunteer patients within a body plethysmograph with a catheter in the pulmonary artery has caused us to abandon the method in conscious humans. The detection of ether gas evolution by measurement of flow at the airway with a sensitive pneumotachograph eliminates the need for a body plethysmograph, but cannot be used in conscious subjects because we have been unable to train them to relax the chest during apnea while the glottis is held open. However, this method is ideal for use in anesthetized humans, and also should be applicable to patients on mechanical respirators who often have a Swan-Ganz catheter in the pulmonary artery for monitoring the pressure within this vessel. The method can be used in mild but not marked cases of sinus arrhythmia, and cannot be employed when atrial fibrillation or ectopic beats are present.

Pulmonary Tissue Volume

It is difficult to compare our values for pulmonary tissue volume in man to those reported by others for its determination by inspiration of soluble gases (20, 21), or for estimates of pulmonary extravascular water space by the indicator dilution technique using tritiated water (22). We did not measure pulmonary V_C in all our subjects, a prerequisite for calculating pulmonary tissue volume from the space measured by the ether method. Further, only 1 of our subjects had a normal cardiopulmonary system, although 4 of the remaining 5 with cardiac disease had normal pulmonary arterial pressures at rest. The pulmonary tissue volume determined by ether injection appears to lie between the value for the space measured by the indicator dilution tritiated water method (22) and the larger volume found by analysis using inspiration of soluble gases (20, 21). In one of our subjects with primary pulmonary hypertension,

the combined pulmonary tissue plus capillary volume was about twice the mean value of the rest of the group. This finding might have been related to the low output cardiac failure which was present in this patient.

The variability in duplicate measurement of pulmonary tissue plus capillary volume by the ether plethysmographic method is approximately the same as that for determination of the pulmonary extravascular water space determined by the tritiated water indicator dilution technique. The variability cannot be accounted for by the presence of hemodynamic pulmonary edema, and its explanation is uncertain. Correlation between its value and that obtained by morphometry will have to be undertaken. The latter gives a pulmonary extravascular water content in dogs of 3.5 ml/kg body weight (23) which is slightly less than one-half the value of pulmonary tissue volume by the ether plethysmographic method (Table 1). Since the tritiated water dilution technique estimates only about 50% of the water content of the lungs at autopsy (23), it appears that the ether plethysmographic method may more closely reflect the total water content of the lungs. This view is consistent with data obtained in man from the transient uptake of nitrous oxide by a plethysmographic method which gives values for pulmonary tissue volume (21) about twice that reported for the tritiated water indicator dilution studies (22).

Ether Circulation Time

As reported by Feisal et al. (1) and confirmed in the present study, the mean transit time for ether solution from the pulmonic valve to the capillaries is slightly greater than the median transit time. Further, these authors pointed out that some ether may return to the blood before peak pressure is reached; and, consequently, the ether curve should be corrected for pressure decay at every point as a function of elapsed time, the degree of pressure change, and the rate constant of the descending curve. They stated that both these corrections involved an improvement in accuracy to 5% and that the routine use of these corrections did not justify the longer method of calculation. In the present study, we found that these corrections cannot be neglected. The mean pulmonary arterial transit time was about 6% longer than the median transit time, and the correction for pressure decay added another 5% to the mean transit time. Therefore, failure to take these corrections into account results in underestimating pulmonary arterial blood volume by 11%.

-IX-
(Part 1)

Lung Density

The mean value of lung density of 0.16 gm/ml determined in our 10 dogs was lower than the mean value of 0.23 gm/ml found in 12 dogs by Feisal et al. (1). This difference was both the result of our choosing a smaller value for the partition coefficient of ethyl ether and of taking into account the right-to-left intrapulmonary shunt. The density of the lung in humans was generally less than in dogs, because the lung volume was proportionally much larger than the tissue volume. We do not have an explanation for this apparent structural difference between human and canine lungs.

REFERENCES

1. Feisal, K. A., J. Soni, and A. B. DuBois. Pulmonary arterial circulation time, pulmonary arterial blood volume and the ratio of gas to tissue volume in the lungs of dogs. J Clin Invest 41:390-499 (1962).

2. Feisal, K. A., M. A. Sackner, and A. B. DuBois. Comparison between the time available and the time required for CO_2 equilibration in the lung. J Clin Invest 42:24-28 (1963).

3. Soni, J., K. A. Feisal, and A. B. DuBois. The rate of intrapulmonary gas exchange in living animals. J Clin Invest 42:16-23 (1963).

4. Sackner, M. A., K. A. Feisal, and D. N. Karsch. Size of gas exchange vessels in the lung. J Clin Invest 43:1847-1855 (1964).

5. Sackner, M. A., D. H. Will, and A. B. DuBois. The site of pulmonary vasomotor activity during hypoxia or serotonin administration. J Clin Invest 45:112-121 (1966).

6. Wasserman, K., and J. H. Comroe, Jr. A method for estimating instantaneous pulmonary capillary blood flow in man. J Clin Invest 41:401-410 (1962).

7. Greenberg, J. J., et al. Preoperative and postoperative cardiac output determinations using an instantaneous pulmonary capillary blood flow method. Ann Thorac Surg 72:629-648 (1971).

8. Bachofen, H., and L. E. Farhi. Simple manometric apparatus for measuring partition coefficients of highly soluble gases. J Appl Physiol 30:136-139 (1971).

9. Cander, L. Solubility of inert gases in human lung tissue. J Appl Physiol 14:538-540 (1959).

10. Wanner, A., and M. A. Sackner. Transvenous phrenic nerve stimulation in anesthetized dogs. J Appl Physiol 34:489-494 (1973).

11. Avery, W. G., and M. A. Sackner. A rapid measurement of functional residual capacity in paralyzed dog. J Appl Physiol 33:515-518 (1972).

12. Dougherty, R. L., et al. Body plethysmograph; a new body plethysmograph for cardiopulmonary studies in man. Analyzer 3:18-27 (1972).

13. Sackner, M. A., et al. Techniques of pulmonary capillary blood flow determinations. Bull Physiopathol Respir 9:1189-1202 (1973).

14. DuBois, A. B., et al. A rapid plethysmographic method for measuring thoracic gas volume; a comparison with nitrogen washout method for measuring functional residual capacity in normal subjects. J Clin Invest 35:322-327 (1956).

15. Miller, J. M., and R. L. Johnson, Jr. Effect of lung inflation on pulmonary diffusing capacity at rest and exercise. J Clin Invest 45:493-500 (1966).

16. Cree, E. M., R. R. Benfield, and H. K. Rasmussen. Differential lung diffusion, capillary volume and compliance in dogs. J Appl Physiol 25:186-190 (1968).

17. Fraser, R. S., et al. The identification of right to left shunts in the central circulation by the injection of ether. Circulation 24:1224-1226 (1961).

18. Lewis, M. L., and C. E. Herrera. Effect of alveolar hypoxia on canine pulmonary artery blood volume. Clin Res 18:486 (1970) (Abstract).

19. Herrera, C. E., and M. L. Lewis. Human pulmonary arterial volume. Clin Res 19:511 (1971) (Abstract).

20. Cander, L., and R. E. Forster. Determination of pulmonary parenchymal tissue volume and pulmonary capillary blood flow in man. J Appl Physiol 14:541-551 (1959).

21. Sackner, M. A., K. A. Feisal, and A. B. DuBois. Determination of tissue volume and carbon dioxide dissociation slope of the lungs in man. J Appl Physiol 19:374-380 (1964).

22. Turino, G. M., et al. The volume of extravascular water of the lung in normal man and in disease. Bull Physiopathol Respir 7:1161-1179 (1971).

23. Levine, O. R., R. B. Mellins, and A. P. Fishman. Quantitative assessment of pulmonary edema. Circ Res 27:414-426 (1965).

-IX-
(Part 1)

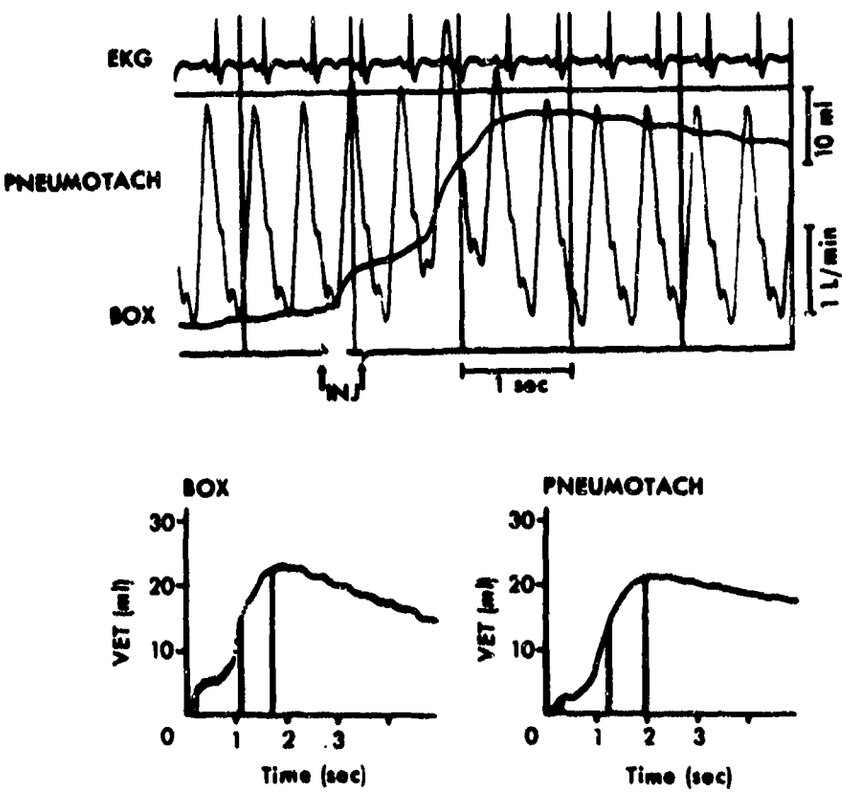

Figure 1. Comparison of ether plethysmographic and pneumotachographic techniques in anesthetized apneic dogs.

[For key to Fig. 1, see facing page]

-IX-
(Part 1)

-- Key to Figure 1 --

(The upper tracing shows the raw data; the lower two tracings, the final display from the cathode ray oscilloscope of the LINC 8 digital computer. The upper analog record shows the: EKG; pneumotachographic [PNEUMOTACH] tracing of flow at the endotracheal tube with the flow calibration; plethysmographic [BOX] pressure calibrated as a volume; and time of injection [INJ] of saline to flush ether solution into the pulmonary artery. The record shows an initial rise due to saline injection. Then, there is a second rise in both volume within the plethysmograph and flow at the airway, due to evolution of ether gas followed by a decay as ether gas redissolves into the pulmonary capillary blood. The computer displays show a record of the evolution of ether gas. The first vertical line at the left indicates the end of the injection period; the second, the mid-volume point of ether gas evolution; and the final, the peak volume point. In this example, the following data were obtained: For the BOX record--median transit time, 0.96 sec; mean transit time, 1.00 sec; volume of ether, 19.3 ml, and lung density, 0.09. For the pneumotachographic record--median transit time, 0.99 sec; mean transit time, 1.09 sec; volume of ether, 18.9 ml, and lung density, 0.10.)

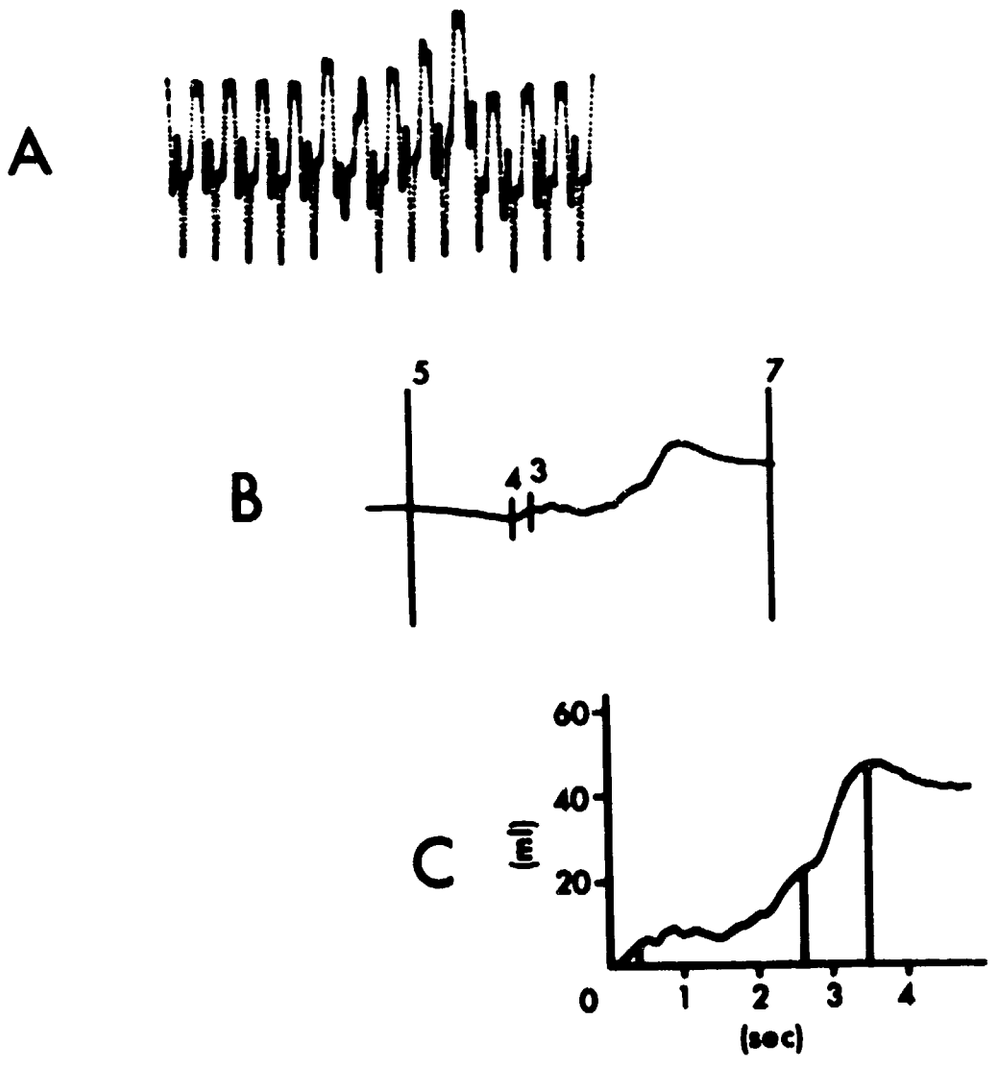

Figure 2. Computer display of an ether pneumotachographic tracing from a 68-year-old woman with tetanus, curarized and controlled by a mechanical ventilator.

(Tracing A shows the oscillations produced by the heartbeat with the superimposed waves due to injection of saline and evolution of ether gas. Tracing B shows a volume record after first subtracting a template of the oscillation preceding the saline injection and then integrating the flow signal. The vertical lines denote the beginning of the base line computation--5, injection period--4,3, and the end of the run--7, as chosen by the computer program. The final display, C, shows the volume of the saline flush and ether gas evolved on the Y axis, and time in seconds on the X axis.)

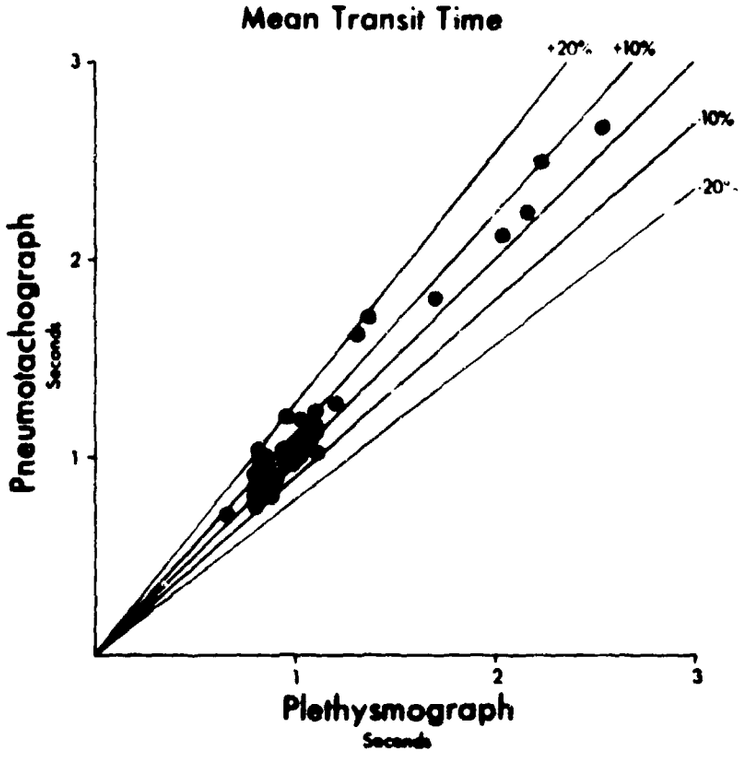

Figure 3. Comparison of 60 simultaneous determinations, from 16 dogs, of mean transit time from the pulmonic valve to the capillaries by the ether pneumotachographic and plethysmographic methods.

(There appear to be less than 60 points, because of the superimposition of points grouped about the 1-sec value.)

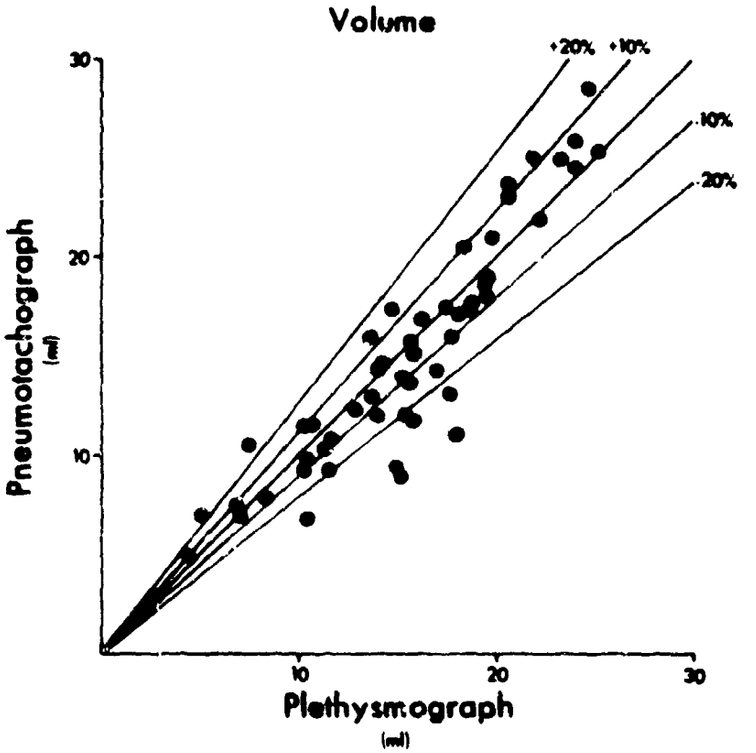

Figure 4. Comparison of 60 simultaneous determinations, from 16 dogs, of volume of ether evolved by the ether pneumotachographic and plethysmographic methods.

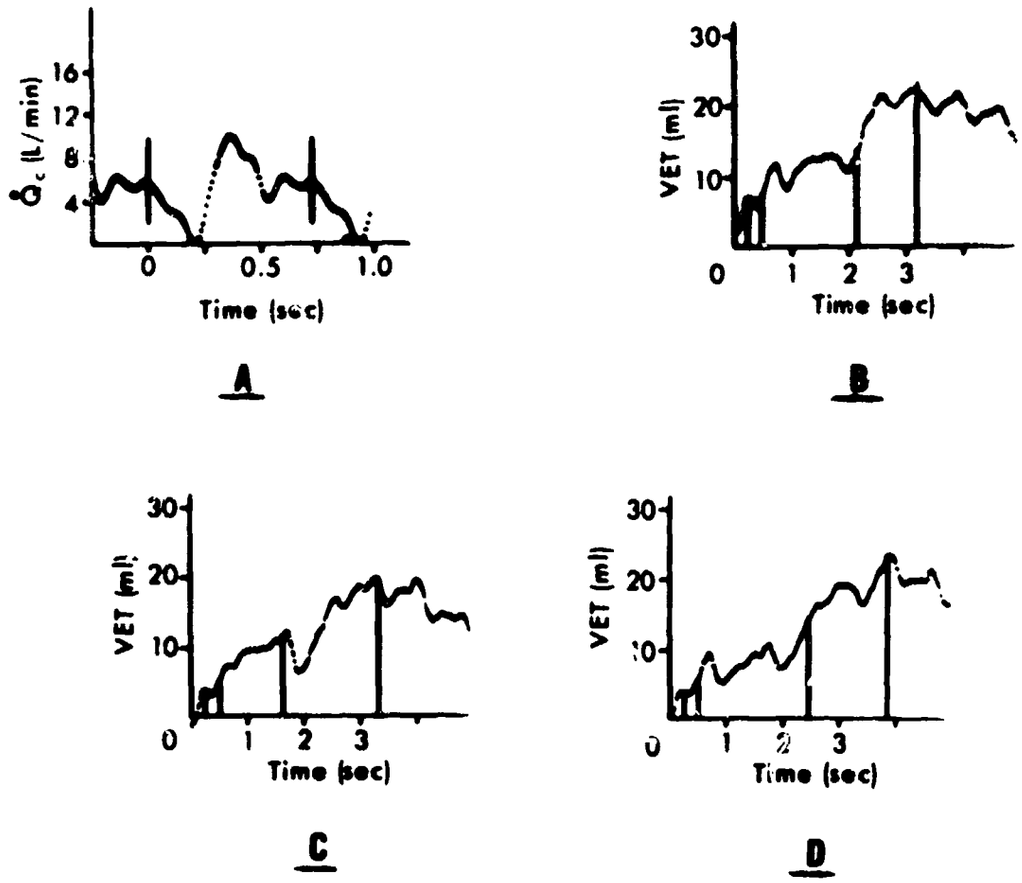

Figure 5. Pulmonary $\dot{Q}_C$ as determined by the nitrous oxide plethysmographic method (tracing A), and ether circulation time in a patient (JG, Table 2) with a functional systolic murmur (tracings B, C, and D).

(For the display of the average pulmonary $\dot{Q}_C$ pulse, the two solid vertical lines denote one R-R interval of the EKG. In this subject, the dye dilution estimate of cardiac output immediately after the nitrous oxide plethysmographic determination of 5.31 L/min was 5.17 L/min. For the display of ether circulation times, the first vertical bar indicates mid-injection point; the second bar, the end of injection; the third bar, the mean transit time; and the fourth bar, the peak ether volume. The short mean transit time in the run of the upper right panel is due to a markedly negative pulsation resulting from a ventricular extrasystole.)

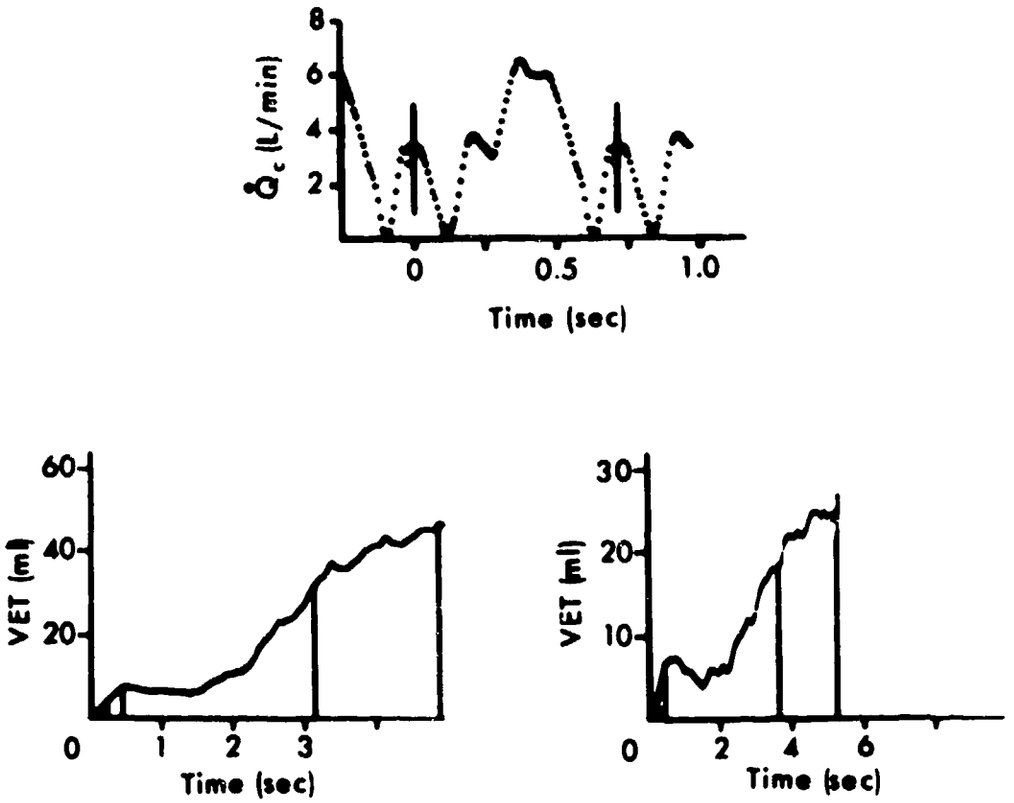

Figure 6. Pulmonary $\dot{Q}_C$ as determined by the nitrous oxide pneumotachographic method (top tracing), and ether circulation time in a patient (AD, Table 2) undergoing coronary bypass surgery (two lower tracings).

(Both time and volume calibrations are different on the two ether circulation times because the computer made adjustments to obtain the optimal display. Although the volume of ether solution injected varied by a factor of two [i.e., 2 ml of 1:4 ether in alcohol solution in the left panel, and 1 ml in the right panel], there was close correspondence in the results obtained [mean transit time 2.93 sec and 3.43 sec, respectively; and pulmonary tissue plus capillary blood volume, 389 ml and 365 ml, respectively].)

TABLE 1. PULMONARY TISSUE VOLUME IN DOGS

Dog (No.)	Weight (kg)	Lung Density (gm/ml)	$V_T + V_C$ (ml)	V_C* (ml[calc])	V_T (ml)	V_T/kg (ml/kg)
1	15.9	0.18	145	30	115	7.2
2	13.6	0.18	98	26	72	5.2
3	16.4	0.20	119	31	88	5.4
4	20.5	0.16	180	39	141	6.9
5	20.4	0.23	270	39	231	11.3
6	30.0	0.22	382	57	325	10.8
7	26.0	0.13	304	49	255	9.8
8	16.0	0.27	226	30	196	12.2
9	19.1	0.14	117	36	81	4.2
10	16.3	0.16	195	31	164	10.0
11	27.3	0.29	432	52	380	13.9
12	24.1	0.17	172	46	126	5.2
13	21.4	0.15	159	41	118	5.5
14	27.3	0.17	217	52	165	6.0
15	23.2	0.23	274	44	230	9.9
16	20.4	0.17	256	39	217	10.6
17	15.9	0.18	140	30	110	6.9
Mean	20.8	0.19	216	40	177	8.3
SD	4.7	0.04	91	9	84	2.8

*Based on calculation of 1.9 ml/kg (ref. 16).

TABLE 2. PULMONARY ARTERIAL BLOOD AND TISSUE VOLUME IN MAN*

Subject	Age (yr)	Diagnosis	Method	Mean Transit Time (sec)	V_{PA} (ml)	$\dot{Q}_c$ (L/min)	LD (gm/ml)	$V_T + C$ (ml)	V_C (ml)	V_T (ml)
		Normal Pulmonary Arterial Pressure								
JG	29	Functional Systolic Murmur	[illegible]	[illegible]	102	[illegible]	[illegible]	[illegible]	[illegible]	[illegible]
DR	21	Postop. Pulmonic Valvulotomy	[illegible]	[illegible]	19?	6.03	[illegible]	[illegible]	[illegible]	[illegible]
AV	59	Coronary Artery Disease	[illegible]	[illegible]	167	[illegible]	0.07	[illegible]		
AD	63	Coronary Artery Disease	[illegible]	3.18	[illegible]	[illegible]	[illegible]	377		
SF	66	Tetanus	[illegible]	1.94	135	4.18	0.2?	[illegible]	4?	[illegible]
Mean				2.1?	172	[illegible]	0.12	[illegible]		
SD				.57	22	1.53	0.05	[illegible]		
		Pulmonary hypertension								
BK	62	**Primary pulmonary hypertension**	[illegible]	1.35	93	2.30	[illegible]	[illegible]	[illegible]	

***Mean transit time = pulmonary arterial circulation time; V_{PA} = volume of blood in pulmonary arterial tree; $\dot{Q}_c$ = pulmonary capillary blood flow; LD = lung density; and $V_T + C$ = pulmonary tissue plus capillary blood volume.**

RE: SAM-TR-75-25
Section IX (Part 2)

SUPPLEMENTARY INFORMATION: Ether (concerning a program written to process waveforms obtained during the measurement of pulmonary arterial circulation time).

In order for comprehensive information on this research to be readily accessible, microfiche have been made of the above-mentioned material. The microfiche are available through:

The Aeromedical Library
Documentation Section
Brooks AFB, Texas 78235

X. EFFECTS OF LUNG INFLATION AND TRANSMURAL PULMONARY ARTERIAL PRESSURE ON PULMONARY ARTERIAL BLOOD VOLUME IN INTACT DOGS

ABSTRACT

The isolated effects of alterations of lung inflation and transmural pulmonary arterial pressure (P_{TM})--pressure difference between intravascular and pleural pressure--on pulmonary arterial blood volume (V_{PA}) were investigated in anesthetized intact dogs. Using transvenous phrenic nerve stimulation, changes in P_{TM} at a fixed transpulmonary pressure (P_{TP}) were produced by the Mueller maneuver, and increases in P_{TP} at relatively constant P_{TM} by a Quasi-Valsalva maneuver. Also, both P_{TM} and P_{TP} were allowed to change during open airway lung inflation. The V_{PA} was determined during these three maneuvers by multiplying pulmonary blood flow by pulmonary arterial mean transit time obtained by an ether plethysmographic method. During open airway lung inflation, mean (± SD) P_{TP} increased by 7.2 (± 3.7) cm H_2O, and P_{TM} by 4.3 (± 3.4) cm H_2O, for a mean increase in V_{PA} by 26.2 (± 10.7 ml). A pulmonary arterial compliance term ($\Delta V_{PA}/\Delta P_{TM}$) calculated from the Mueller maneuver was 3.9 ml/cm H_2O; and an interdependence term ($\Delta V_{PA}/\Delta P_{TP}$) calculated from the Quasi-Valsalva maneuver was 2.5 ml/cm H_2O for a 19% increase in lung volume, and 1.2 ml/cm H_2O for an increase in lung volume from 19% to 35%. These findings indicate that in normal anesthetized dogs near FRC for a given change in P_{TP} and P_{TM}, the latter results in a greater increase of V_{PA}.

INTRODUCTION

Although numerous investigations have dealt with the effect of lung inflation on total pulmonary blood volume (7, 18) and pulmonary vascular resistance (19, 22), only a few such studies have been reported on the pulmonary arterial blood volume alone. Macklin's (13) experiments on dog lungs indicated that lung inflation had a squeezing effect on capillaries and simultaneously increased the capacity of the arteries and veins. These findings were later confirmed by Howell et al. (10), who also demonstrated two vascular compartments in excised dog lungs. They found that with a rise in transpulmonary pressure: a volume, probably representing the capillaries, decreased--whereas a volume, probably representing the arterial and venous segment, increased. From a mathematical model, supported by experiments in excised lung lobes, Lloyd (12) reported that pulmonary arterial conductance was highest at an intermediate lung volume and showed a decrease as the lungs were deflated or inflated from that position. He related these changes to alterations in arterial geometry which were independent of alveolar pressure. Recently, Benjamin et al. (2) demonstrated in excised dog

lungs a high degree of interdependence between lung inflation and pulmonary vascular diameters, suggesting that expansion of intrapulmonary arteries is equally related to lung inflation and increases in intravascular arterial pressure. None of these investigations have been carried out in intact animals. The ether plethysmographic technique for estimation of pulmonary arterial circulation time combined with measurement of pulmonary blood flow permits calculation of pulmonary arterial blood volume (V_{PA}) in intact animals (6, 17). In the present study, we used this method in anesthetized dogs in conjunction with induced respiratory maneuvers through transvenous phrenic nerve stimulation (20) to assess the contributions of transmural pulmonary arterial pressure (P_{TM}) and transpulmonary pressure to V_{PA}.

THEORETICAL CONSIDERATIONS

Due to the presence of elastic tissue attachments within the lung, the pressure volume characteristics of one portion of the lung are influenced by the state of inflation of adjacent portions. This phenomenon is called interdependence. Thus, the change in the volume of the pulmonary artery (ΔV_{PA}) is dependent both upon the change in distending pressure of the pulmonary artery (ΔP_{TM}), which can be approximated by subtracting pleural pressure from intravascular pressure ($P_{TM} = P_{PA} - P_{Pl}$), and upon the change in transpulmonary pressure (ΔP_{TP}), or:

$$\Delta V_{PA} = K_1 \Delta P_{TM} + K_2 \Delta P_{TP} \qquad \text{(Eq. 1)}$$

If P_{TM} can be changed while keeping lung volume constant, ΔP_{TP} becomes zero, and equation (1) reduces to:

$$\Delta V_{PA} = K_1 \Delta P_{TM} \qquad \text{(Eq. 2)}$$

Rearranged,

$$K_1 = \frac{\Delta V_{PA}}{\Delta P_{TM}} \qquad \text{(Eq. 3)}$$

which is the expression for pulmonary arterial compliance. Conversely, lung inflation without changing transmural arterial pressure ($\Delta P_{TM} = 0$) results in an interdependence term between P_{TP} and V_{PA}:

$$K_2 = \frac{\Delta V_{PA}}{\Delta P_{TP}} \qquad \text{(Eq. 4)}$$

The magnitude of K_2, therefore, is an index of the degree of interdependence between lung inflation and expansion of the pulmonary arterial tree, and determines how much V_{PA} changes for a given change in lung volume.

METHODS

Experimental Setup

Ten mongrel dogs, each weighing between 14.5 and 33 kg, were anesthetized with pentobarbital, 25 mg/kg of body weight. They were intubated with a cuffed orotracheal tube and placed in the lateral decubitus position in a 170-liter constant volume body plethysmograph (1). The endotracheal tube was connected to the central port of a 5-way valve which was attached to the inside of the aluminum door, thus allowing operation of the valve from the outside by a sealed knob. Two ports were open to the inside of the body plethysmograph: one port was occluded; and one port led through the door to the outside room air which the animal breathed when the body plethysmograph was sealed. A 12 F mushroom catheter was inserted through an intercostal space on the midchest level on the free side of the laterally positioned dog for measurement of intrapleural pressure. The catheter was connected to a differential gage (Statham PM 131, $\pm$ 2.5 PSI, Puerto Rico) and referenced to the atmosphere through an opening in the door. Mouth pressure was determined at the upstream end of the endotracheal tube with a strain gage. Ventilation was controlled by transvenous phrenic nerve stimulation (PNS) with an American Electronic Laboratories pulse generator (21). A 7 F catheter with sideholes was placed through a jugular vein into the pulmonary artery with the tip located immediately distal to the pulmonic valve. This catheter was led through the door to an Automatic Injector (type 97-E-7, Cordis Corporation, Miami, Fla.). A 5 F catheter tip manometer (PC-350, Millar Instruments, Houston, Texas) was also placed within the pulmonary artery. The left atrium was catheterized with a 7 F catheter, using a retrograde approach from a femoral artery. The left atrial pressure was measured by a strain gage (Statham P-23) located outside of the plethysmograph and referenced to the mid-chest level. Catheters were also placed within the carotid artery and a peripheral leg vein. After systemic heparinization with 50 mg heparin sulphate, blood was withdrawn with a roller pump (Holter Company, Extracorporeal Medical Specialty, Inc., King of Prussia, Pa.), at a rate of 25 ml/min through the door of the plethysmograph and thence through a densitometer (model 103 TR, Gilford Instrument, Oberlin, Ohio) to be continuously returned to the peripheral vein. Thus, indicator dilution curves were obtained without causing a change in plethysmographic pressure. A partially closed clamp was placed around the tubing downstream of the roller pump in order to reduce the possibility of micro-aero embolism (9). A 4-lead EKG was continuously recorded.

All signals were simultaneously recorded on an Electronics for Medicine Oscilloscopic Recorder (DR 12, White Plains, N.Y.) and on analog magnetic tape (Technical Measurement Corporation, New Haven, Conn.). A LINC 8 digital computer (Digital Equipment Co., Maynard, Mass.) was used for data processing.

Pulmonary blood flow and pulmonary arterial mean transit time were determined simultaneously by injecting 1 ml cardio-green dilution and 0.2 cc ether in 0.8 cc alcohol as a bolus using the Automatic Injector. The latter was triggered from the R-wave of the EKG without a time delay so that the injection occurred at the beginning of systole. Pulmonary blood flow was calculated by the indicator-dilution method (8). The pulmonary arterial mean transit time after ether injection into the pulmonary artery was obtained (17). The V_{PA} was calculated as the product of pulmonary arterial mean transit time and pulmonary blood flow. P_{TM} was obtained from the sum of mean intravascular pressure and intrapleural pressure.

For the determination of thoracic gas volume (V_{TG}) by the body plethysmographic technique (5), the airway was occluded and panting simulated by rapid PNS (21).

Experimental Procedure

The following breathing maneuvers were performed to separate the influence of lung inflation and P_{TP} on V_{PA}: (a) Open airway--V_{PA} was determined during apnea at FRC, at half inspiration and at full inspiration. Half and full inspiration were achieved by continuous stimulation of the phrenic nerve for 10 - 15 sec, with adjustment of the output voltage to obtain optimal changes in transpulmonary pressure. After the ether circulation time had been recorded, the V_{TG} was measured. (b) Mueller maneuver--Following occlusion of the airway, runs were made at FRC without PNS, and at FRC with half optimal and then with full optimal voltage while continuous PNS was carried out. The V_{TG} was measured after each run to confirm that no air leaks had developed in the system. (c) Quasi-Valsalva maneuver--After a control run at FRC, the airway was occluded at either half or full inspiration, and immediately followed by cessation of PNS. In this maneuver, an increased lung volume was obtained with a positive airway pressure because of passive compression by the chest wall which relaxed during general anesthesia. As in the other respiratory maneuvers, V_{TG} was determined after each run.

Statistical differences between means were assessed by Student's t-test.

RESULTS

In Table 1 are listed the mean values, for all 10 dogs, of P_{TP}, P_{TM}, and V_{PA}. Mean values are shown separately for FRC, half and full inspirations. Although large standard deviations for all these parameters determining pulmonary interdependence indicate marked individual variations between dogs, the changes which occurred during the different breathing maneuvers were significant, except for those which we attempted to maintain constant (namely, P_{TM} during the Quasi-Valsalva maneuver, and P_{TP} during the Mueller maneuver). The only unexpected nonsignificant change was encountered for V_{PA} between FRC and half inspiration during the Mueller maneuver. Maximum mean increase in V_{PA} was: 17.9 ml for the Quasi-Valsalva maneuver, and 19.5 ml for the Mueller. Mean V_{PA} increased more (i.e., 26.2 ml) during open airway inflation when both P_{TP} and P_{TM} were allowed to increase. This maneuver produced a 43% increase in V_{PA} with half inspiration, and a 62% increase with full inspiration.

Shown in Table 2 are the mean values for V_{TG}, mean pulmonary arterial pressure (P_{PA}), mean left atrial pressure (P_{LA}), pulmonary blood flow ($\dot{Q}_{PA}$), and pulmonary vascular resistance (PVR). Comparable changes in V_{TG} were obtained during open airway inflation (0.35 L) and the Quasi-Valsalva maneuver (0.28 L). As expected, no significant changes occurred in V_{TG} during the Mueller maneuver. There was no significant change in $\dot{Q}_{PA}$ and PVR within or among different breathing maneuvers.

Figure 1 demonstrates the absence of a correlation between V_{PA} and bodyweight, FRC or lung tissue and pulmonary capillary blood volume ($V_T + V_C$) in the 10 dogs; therefore V_{PA} could not be normalized to those parameters. Shown in Figure 2 are the relative changes of mean V_{PA} as a function of mean P_{TM} (Fig. 2a) and mean P_{TP} (Fig. 2b) during the Mueller and Quasi-Valsalva maneuvers, respectively. When $\%\Delta V_{PA}$ is plotted against ΔP_{TP} (Fig. 2b): the curve produced by the Quasi-Valsalva maneuver, where the volume of the arterial tree expands during lung inflation with only minimal changes in P_{TM}, is slightly less steep than the curve produced by the Mueller maneuver (Fig. 2a) which allows changes in P_{TM} at a fixed lung volume. Figure 2b therefore represents the degree of interdependence between lung inflation and expansion of the pulmonary artery, whereas Figure 2a shows the distensibility curve of the pulmonary artery. In both graphs, the curve of the open airway inflation is also included and is visibly steeper than that produced by either the Mueller or the Quasi-Valsalva maneuver. This change is expected, because P_{TM} as well as P_{TP} change concomitantly.

K_1 and K_2 were calculated for each dog from the Mueller and Quasi-Valsalva maneuvers. Since P_{TM} changed slightly in most dogs during Quasi-Valsalva maneuvers and P_{TP} also showed minimal changes during the Mueller maneuver, equations 3 and 4 could not be employed for the calculations. Equation 1 was therefore applied to both maneuvers, so that two equations with two unknowns (K_1, K_2) were obtained which permitted calculation of values for the two constants. K_1 (= 3.9 ml/cm H_2O, SD 3.0), representing compliance of the pulmonary artery, was derived from full inspiration only because half inspiratory effort during the Mueller maneuver did not produce a significant increase in V_{PA}. However, mean K_1--calculated between FRC and half inspiratory effort--was 4.1 ml/cm H_2O, thus suggesting that the pressure volume curve of the pulmonary arterial system was linear over this range. The interdependence term, K_2, was calculated separately between FRC and half inspiration and half inspiration and full inspiration. Interdependence had the tendency to decrease as the lung was inflated from FRC over half (+ 0.12 L) to full (+ 0.28 L) inspiration. Mean K_2 decreased from 2.5 ml/cm H_2O (SD 4.7) for half inspiration to 1.2 ml/cm H_2O (SD 2.9) for between half to full inspiration. The difference between these two values was not significant, however.

Mean ΔV_{PA} calculated from K_1 and K_2 (Eq. 1) was: 16.3 ml (SD 17.2), for half inspiration; and 20.1 ml (SD 13.0), for full inspiration. These values were slightly lower than the actually measured ΔV_{PA} during open airway inflation, where ΔV_{PA} was: 19.3 ml, for half inspiration; and 26.2 ml, for full inspiration.

DISCUSSION

In this investigation we have separated the influence of P_{TM} and P_{TP} on V_{PA} in intact animals. The three different breathing maneuvers permitted independent or concomitant changes of the pressure parameters. The Mueller maneuver produced significant changes in P_{TM} without allowing P_{TP} to change. On the other hand, the Quasi-Valsalva maneuver--which created a mild positive intrathoracic pressure at higher lung volumes by passive compression of the relaxed chest wall against the closed airway--resulted in an essentially unchanged P_{TM}, although P_{TP} increased with lung inflation. Finally, during open airway lung inflation, both P_{TP} and P_{TM} changed simultaneously. Thus, the relationship between P_{TM} and V_{PA} on the one hand and P_{TP} and V_{PA} on the other permitted calculation of a static pulmonary arterial compliance term ($\Delta V_{PA}/\Delta P_{TM}$) and an interdependence term ($\Delta V_{PA}/\Delta P_{TP}$), from which changes in V_{PA} during open airway inflation could be predicted. The fact that the calculated changes in V_{PA} were fairly close to the actually measured changes during open

airway inflation supports the finding that the volume of the pulmonary artery is governed by both the elastic recoil of the lung itself and the elastic recoil of the pulmonary artery. The lack of a more perfect agreement between predicted and actual ΔV_{PA} might have been caused by changes in the elastic properties of the pulmonary artery and the lung during the course of the experiment. Further, the relative contributions of P_{TM} and P_{TP} were markedly different. For half inspiration, mean K_1 was 3.9 ml/cm H_2O and mean K_2 was 2.5 ml/cm H_2O, indicating that for 1 cm H_2O increase in P_{TP} or P_{TM}, the V_{PA} should increase by 3.9 ml or 2.5 ml, respectively.

Our experimental design did not allow the exploration of a wide range of lung volumes, and the mean increase of lung volume during maximum inspiration with PNS was only 0.35 L. As already pointed out, possibly because of this small change in lung volume, we did not find an interdependence constant to be significantly lower at full than at half inspiration, although a higher degree of interdependence at lower lung volumes had been reported by Benjamin et al. (2).

Also, we inflated the lungs with FRC with an approximate P_{TP} of 4 cm H_2O to approximately 10 cm H_2O, whereas the interdependence constant of Benjamin et al. (2) was determined during deflation from 10 to 0 cm H_2O. Since their data suggested that interdependence increased with lung deflation as lung collapse was approached, our slope of K_2 during inflation from FRC did not include that portion of the curve with a high degree of interdependence.

The compliance of the pulmonary arterial tree (K_1 = 3.9 ml/cm H_2O) in these experiments was much greater than that reported by Reuben et al. (15). Those authors computed compliance from the systolic storage increment and the concomitant pulmonary arterial distending pressure, and found the pulmonary arterial compliance to be 1.4 ml/cm H_2O. They determined dynamic compliance in contrast to our quasi-static measurements. Also, the vascular volume changes in the present experiments were much greater than the systolic storage volume changes considered by Reuben et al. (15). Although K_1 was lower for half inspiration than full inspiration, the difference between the two was not statistically significant. Since V_{PA} did not increase significantly between FRC and half inspiratory effort in the Mueller maneuver, we calculated K_1 only between FRC and full inspiratory effort, assuming a linear pressure volume curve of the pulmonary artery in these ranges of P_{TM}.

A possible artifact could have been introduced into our experiments by the development of hypoxia, leading to increased pulmonary arterial vasomotor tone. We did not monitor arterial blood gases during the experiments; but previous experiences with transvenous PNS indicated that, up to 6 hours, no hypoxia or metabolic acidosis develops in dogs whose respiration is maintained by this technique of ventilatory support (21). The occurrence of hypoxia, during the runs which were made during apnea, was suggested by a slight gradual rise in mean pulmonary arterial pressure. However, this rise was less than 1 cm H_2O at the time when the ether and indicator dilution curves were inscribed (within 5 - 10 sec of breath-holding).

Furthermore, vasomotor tone may have been influenced by pentobarbital anesthesia. In his studies on the canine systemic circulation, Cox (4) indicated that pentobarbital affects the responsiveness of vascular smooth muscle of catecholamines; and it is conceivable that similar phenomena occur in the pulmonary circulation. The influence of a rapid injection of an ether in alcohol mixture on pulmonary arterial vasomotor tone is also unknown. The possible effects of hypoxia, pentobarbital anesthesia, and ether in alcohol injection on pulmonary arterial compliance and pulmonary interdependence were, however, of minor significance--as indicated by the fact that PVR was not affected throughout the experiment period. The validity of the ether injection method in measuring pulmonary arterial mean transit time has been previously documented. Sackner et al. (16) showed that, when ether is mixed with alcohol in the ratio of 1:4, only about 9% evolves before the capillaries--and the rest over the first 1/100 of the capillary length--so that only an insignificant segment of the capillaries is included when V_{PA} is calculated from the product of ether mean transit time and $\dot{Q}_{PA}$. Also, we demonstrated in preliminary experiments that the simultaneous injection of ether and cardiac green did not alter either of the two curves. The addition of intrapleural pressure to intravascular arterial pressure in order to obtain true distending pressu has been justified by Burton and Patel (3). Although extra-pulmonary vessels are surrounded by intrapleural pressure, it is not quite clear how far intrapleural pressure influences intrapulmonary arteries. Therefore, our P_{TM} probably only applies to extrapulmonary segments of the pulmonary artery.

In the present study, some inaccuracy in absolute transmural pressure was also introduced by estimating intrapleural pressure with a mushroom catheter located in the upper side of the dog who was situated in the lateral decubitus position. However, we considered this technique acceptable, since we were interested in changes rather than absolute

values of intrapleural pressure. Another inaccuracy may have been produced by the fact that the distribution of intrapleural pressures was changed by the Mueller and possibly the Quasi-Valsalva maneuvers, due to deformations of the chest wall (20). Considering the pulmonary arterial tree as a lumped system, the position of the pressure-probe in the main pulmonary arteries resulted in an overestimation of mean intravascular pressure, since the smaller branches have lower values. This error is minimized by the fact that these small vessels contribute only a small fraction of the total V_{PA} (16) and that probably most volume changes take place in the major vessels. Only minimal changes of $\dot{Q}_{PA}$, heart rate, and PVR were associated with the open airway, the Mueller and Quasi-Valsalva maneuvers indicating little alteration in cardiac output and vasomotor tone in our experiments. The absence of a significant change in cardiac output during the Mueller maneuver has been previously demonstrated in man (11). The fact that we did not find an expected decrease in cardiac output during the Quasi-Valsalva maneuver (11) may have been due to the relatively small positive intrathoracic pressures produced by this maneuver. Since we were only interested in the variability of V_{PA} which is part of the expanded portion (10) of the pulmonary circulation, the influences of lung inflation and negative or positive airway pressures on the compressed portion (10)--which is probably represented by the pulmonary capillaries--did not have to be considered.

A wide scatter of values for K_1 and K_2 was evident in our experiments. Between FRC and full inspiration, for instance, K_1 ranged from 0.9 to 10.2, and K_2 from -3.0 to 11.3. It is probable that at least some of these variations were due to differences in vasomotor tone.

Our data support Mead's model of pulmonary interdependence (14) and confirm in vivo previous reports on the close relationship between lung inflation and V_{PA} (2, 10). It appears that in normal intact anesthetized dogs near FRC for the same increase in P_{TP} or P_{TM}, the latter results in a greater increase in V_{PA}. An interesting field for future investigations would be these relationships in disease states (such as pulmonary arterial hypertension, pulmonary edema, and emphysema) in which either the elastic recoil of the pulmonary arterial system or the lung is altered.

REFERENCES

1. Avery, W. G., and M. A. Sackner. A rapid measurement of functional residual capacity in paralyzed dogs. J Appl Physiol 33:515-518 (1972).

2. Benjamin, J. J., et al. Pulmonary interdependence in excised dog lobes. J Appl Physiol [Submitted for publication.]

3. Burton, A. C., and D. J. Patel. Effect on pulmonary vascular resistance of inflation of the rabbit lungs. J Appl Physiol 12:239-246 (1958).

4. Cox, R. H. Influence of pentobarbital anesthesia on cardiovascular function in trained dogs. Am J Physiol 223:651-659 (1972).

5. DuBois, A. B., et al. A rapid plethysmographic method for measuring thoracic gas volume: a comparison with a nitrogen washout method for measuring functional residual capacity in normal subjects. J Clin Invest 31:40-50 (1952).

6. Feisal, K. A., J. Soni, and A. B. DuBois. Pulmonary arterial circulation time, pulmonary arterial blood volume, and the ratio of gas to tissue volume in the lungs of dogs. J Clin Invest 41:390-400 (1962).

7. Frank, N. R., E. P. Radford, Jr., and J. L. Whittenberger. Static volume-pressure interrelations of the lungs and pulmonary blood vessels in excised cats' lungs. J Appl Physiol 14:167-173 (1959).

8. Hamilton, W. F., et al. Studies on the circulation IV. Further analysis of the injection method, and of changes in hemodynamics under physiological and pathological conditions. Am J Physiol 99:534-551 (1932).

9. Hannemann, R. E., and R. G. Barile. Bubble formation in the roller infusion pump. Am J Dis Child 125:706-708 (1973).

10. Howell, J. B. L., et al. Effect of inflation of the lung on different parts of pulmonary vascular bed. J Appl Physiol 16:71-76 (1961).

11. Kawakami, Y., H. A. Menkes, and B. DuBois. A water filled body plethysmograph for the measurement of pulmonary capillary blood flow during changes of intrathoracic pressure. J Clin Invest 49:1237-1251 (1970).

12. Lloyd, T. C., Jr. Analysis of the relation of pulmonary arterial or airway conductance to lung volume. J Appl Physiol 23:887-894 (1967).

13. Macklin, C. Evidences of increase of the capacity of the pulmonary arteries and veins of dogs, cats, rabbits during inflation of the freshly excised lung. Rev Can Biol [Montreal] 5:199-232 (1946).

14. Mead, J., T. Takishima, and D. Leith. Stress distribution in lungs: A model of pulmonary elasticity. J Appl Physiol 28:596-608 (1970).

15. Reuben, S. R., et al. Measurement of pulmonary arterial distensibility in the dog. Cardiovasc Res 4:473-481 (1970).

16. Sackner, M. A., K. A. Feisal, and D. N. Karsch. Size of gas exchange vessels in the lung. J Clin Invest 43:1847-1855 (1964).

17. Sackner, M. A., et al. Pulmonary arterial blood volume and tissue volume in man. Circ Res 34:761-9 (1974). [USAFSAM Editor's Note: Consult report section IX for related information.]

18. Sarnoff, S. J., and E. Berglund. Pressure-volume characteristics and stress relaxation in the pulmonary vascular bed of the dog. Am J Physiol 171:238-244 (1952).

19. Thomas, L. J., Jr., Z. J. Griffo, and A. Roos. Effect of negative pressure inflation of the lung on pulmonary vascular resistance. J Appl Physiol 16:451-456 (1961).

20. Vu-Dinh, M., et al. Reversal of pleural pressure gradient by electrophrenic stimulation. Fed Proc 33:440 (1974).

21. Wanner, A., and M. A. Sackner. Transvenous phrenic nerve stimulation in anesthetized dogs. J Appl Physiol 34:489-494 (1973).

22. Whittenberger, J. L., et al. Influence of state of inflation of the lung on pulmonary vascular resistance. J Appl Physiol 15:878-882 (1960).

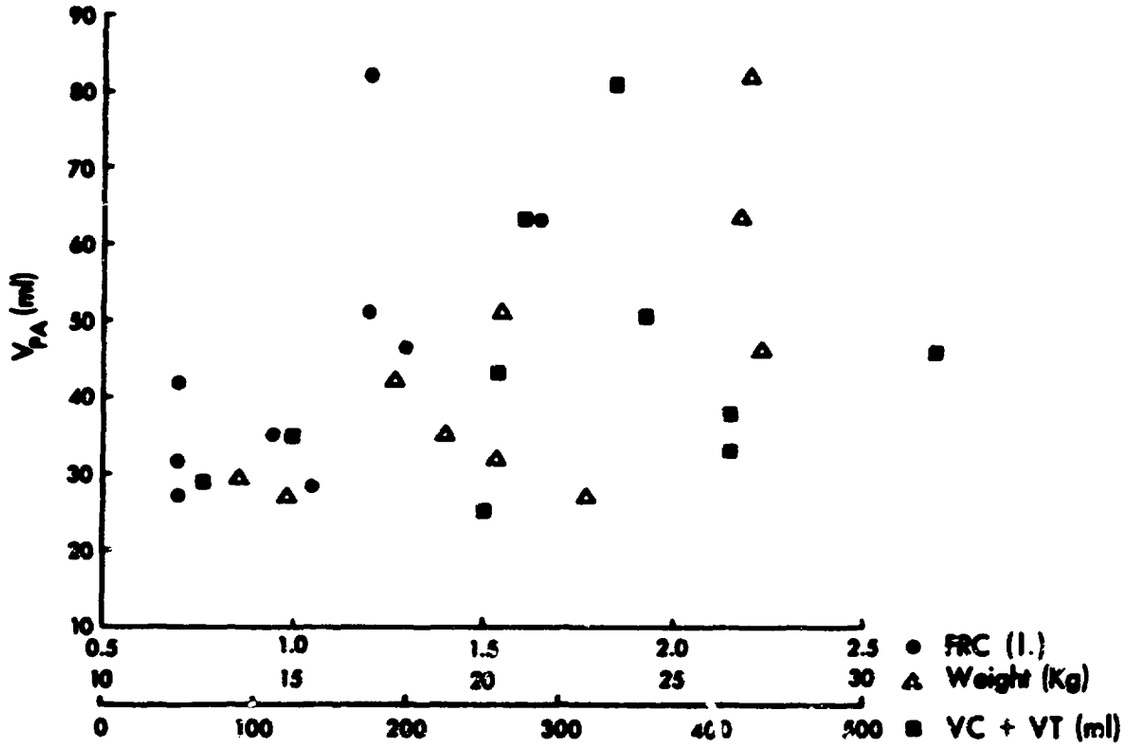

Figure 1. Pulmonary arterial blood volume (Vp_A) at FRC related to FRC lung tissue and pulmonary capillary blood volume ($V_T + V_C$) and body weight in 10 dogs.

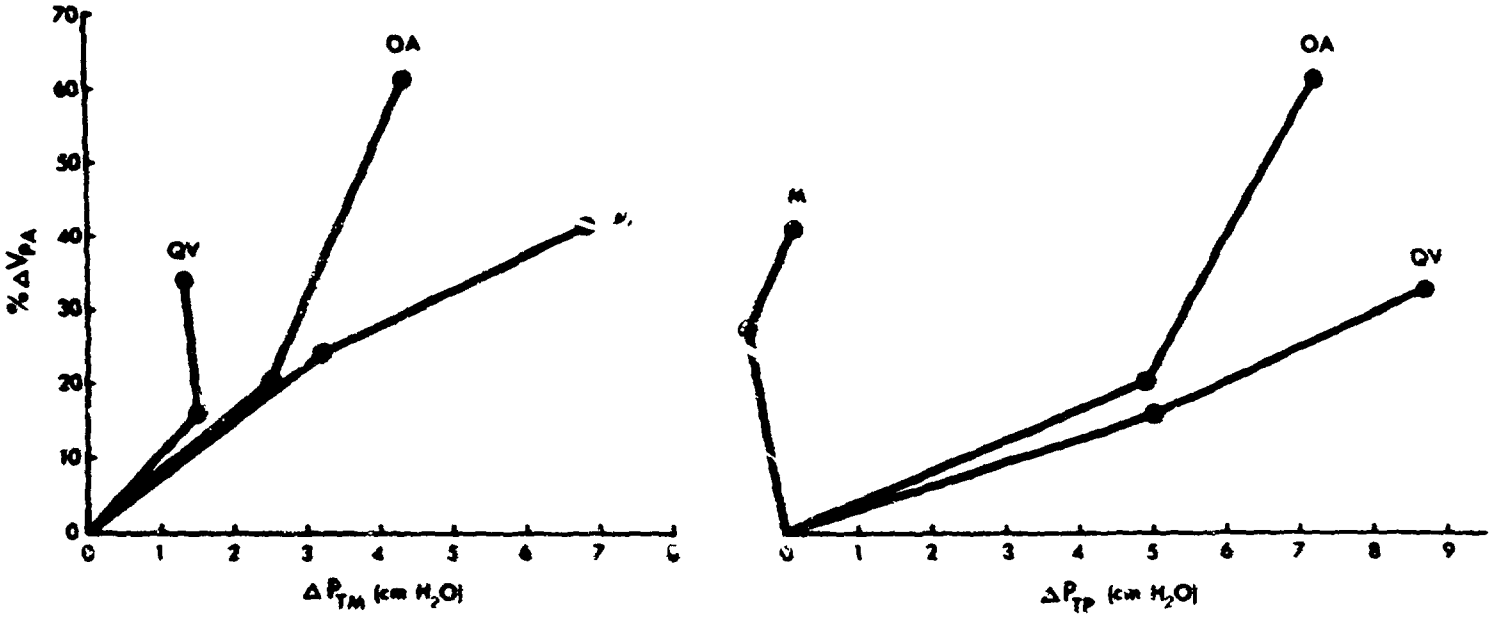

(Plot a) (Plot b)

Figure 2. Relative changes, in 10 dogs, of mean V_{PA} ($\%\Delta V_{PA}$) as a function of mean ΔP_{TM} (plot a: left) and mean ΔP_{TP} (plot b: right).

(M = Mueller maneuver; QV = Quasi-Valsalva maneuver; and OA = open airway lung inflation.)

TABLE 1. MEAN VALUES (± SD) FOR TRANSPULMONARY PRESSURE (P_{TP}), TRANSMURAL PULMONARY ARTERIAL PRESSURE (P_{TM}) AND PULMONARY ARTERIAL BLOOD VOLUME (V_{PA}) IN 10 DOGS DURING DIFFERENT BREATHING MANEUVERS

Parameter	FRC	Half Inspiration	P*	Full Inspiration	P+
		OPEN AIRWAY INFLATION MANEUVER			
P_{TP} (cmH_2O)	4.6 ± 1.7	9.5 ± 2.3	< .001	11.9 ± 3.6	< .001
P_{TM} (cmH_2O)	22.5 ± 3.9	25.0 ± 3.7	< .001	26.8 ± 3.4	< .01
V_{PA} (ml)	42.3 ± 19.5	60.6 ± 27.5	< .001	68.5 ± 24.7	< .001
		MUELLER MANEUVER			
P_{TP} (cmH_2O)	4.1 ± 1.5	3.6 ± 2.4	> .05	4.2 ± 3.4	< .05
P_{TM} (cmH_2O)	23.3 ± 4.9	26.5 ± 3.5	< .01	30.1 ± 5.2	< .001
V_{PA} (ml)	47.0 ± 18.3	58.4 ± 19.8	> .05	66.5 ± 18.5	< .001‡
		QUASI-VALSALVA MANEUVER			
P_{TP} (cmH_2O)	3.3 ± 2.3	8.3 ± 3.0	< .001	12.0 ± 4.8	< .001
P_{TM} (cmH_2O)	25.2 ± 4.6	26.7 ± 4.9	> .05	26.5 ± 5.0	> .05
V_{PA} (ml)	52.9 ± 26.3	61.6 ± 29.5	> .05	70.8 ± 33.9	< .02

* Significance of means between FRC and half inspiration.

\+ Significance of means between half inspiration and full inspiration.

‡ Significance of means between FRC and full inspiration.

TABLE 2. MEAN VALUES (± SD) FOR THORACIC GAS VOLUME (V_{TG}), MEAN PULMONARY ARTERIAL PRESSURE ($\bar{P}_{PA}$), MEAN LEFT ATRIAL PRESSURE ($\bar{P}_{LA}$), PULMONARY BLOOD FLOW ($\dot{Q}_{PA}$) AND PULMONARY VASCULAR RESISTANCE (PVR) IN 10 DOGS DURING DIFFERENT BREATHING MANEUVERS

Parameter	FRC	Half Inspiration	P*	Full Inspiration	P+
		OPEN AIRWAY INFLATION MANEUVER			
V_{TG} (L)	1.0 ± 0.3	1.2 ± 0.2	<.001	1.3 ± 0.2	<.001
$\bar{P}_{PA}$ (cmH_2O)	18.2 ± 3.2	15.9 ± 3.8	<.001	14.5 ± 3.4	>.05
$\bar{P}_{LA}$ (cmH_2O)	6.0 ± 2.9	3.6 ± 3.5	>.05	3.2 ± 3.4	>.05
$\dot{Q}_{PA}$ (L/min)	2.9 ± 1.8	2.6 ± 1.8	>.05	2.4 ± 1.7	>.05
PVR (cmH_2O/L/min)	7.3 ± 5.5	6.6 ± 2.8	>.05	8.1 ± 5.7	>.05
		MUELLER MANEUVER			
V_{TG} (L)	1.0 ± 0.3	1.1 ± 0.3	>.05	1.1 ± 0.3	>.05
$\bar{P}_{PA}$ (cmH_2O)	19.8 ± 4.6	11.5 ± 5.2	<.01	6.4 ± 7.6	<.01
$\bar{P}_{LA}$ (cmH_2O)	7.1 ± 3.5	-0.9 ± 6.9	<.001	-8.1 ± 9.8	<.01
$\dot{Q}_{PA}$ (L/min)	3.0 ± 1.7	3.0 ± 1.6	>.05	2.9 ± 1.8	>.05
PVR (cmH_2O/L/min)	5.0 ± 3.1	5.8 ± 3.1	>.05	4.5 ± 2.3	>.05
		QUASI-VALSALVA MANEUVER			
V_{TG} (L)	1.1 ± 0.2	1.2 ± 0.3	<.001	1.4 ± 0.3	<.001
$\bar{P}_{PA}$ (cmH_2O)	21.5 ± 4.3	25.6 ± 4.1	<.001	26.2 ± 4.3	>.05
$\bar{P}_{LA}$ (cmH_2O)	8.0 ± 4.5	10.0 ± 5.4	<.01	10.6 ± 5.6	>.05
$\dot{Q}_{PA}$ (L/min)	3.2 ± 2.4	3.1 ± 2.0	>.05	2.8 ± 1.8	>.05
PVR (cmH_2O/L/min)	5.6 ± 3.8	6.3 ± 4.5	>.05	7.0 ± 4.5	>.05

* Significance of means between FRC and half inspiration.

+ Significance of means between half inspiration and full inspiration.

XI. DISTRIBUTION OF VENTILATION DURING DIAPHRAGMATIC BREATHING (16)

ABSTRACT

This study was designed to assess the effectiveness of voluntary diaphragmatic breathing on distribution of ventilation as measured by a nitrogen washout procedure and Gamma camera imaging of the lung with radioactive xenon. In 11 patients with chronic obstructive lung disease, diaphragmatic breathing did not alter the indices of distribution calculated from analysis of the nitrogen washout curve. In 5 of 8 normal subjects, Gamma camera imaging with radioactive xenon revealed that initiation of inspiration by a diaphragmatic breathing maneuver directed the initial inspirate toward the lower zones--in contrast to thoracic breathing which directed it to the upper zones. In none of 5 patients with chronic obstructive lung disease was there a difference in topographic distribution of the initial inspirate from residual volume between the diaphragmatic and thoracic breathing maneuvers. The present study suggests that, in patients with chronic obstructive lung disease, good movement of the upper abdominal wall (as can be accomplished by diaphragmatic breathing exercises) has little, if any, effect on favoring distribution of inspired air to the bases.

INTRODUCTION

Diaphragmatic breathing exercises, as taught by physical therapists, have long been advocated in the rehabilitation of patients with chronic obstructive lung disease. Their effect is difficult to measure objectively and, in fact, the benefit of breathing exercises is often ascribed to psychologic support rather than alteration of physiologic state. Recently, we found that the distribution of ventilation of inspired air in normal subjects was not altered by diaphragmatic breathing when the subject breathed at resting lung volume or when the chest was restricted with a binder (1). Furthermore, the volume of "air trapped" within the lung by the application of the binder was not diminished by diaphragmatic breathing. However, when a breath was initiated from residual volume by a diaphragmatic maneuver, and closing volumes measured, 2 of 15 normal subjects developed a negative deflection on the single breath nitrogen test at the point of airway closure, suggesting that air might have been directed preferentially into the lower zones. The reversal of the sequential ventilatory pattern in the 2 subjects was thought to be related to their ability to sustain the diaphragmatic maneuver over a greater part of the vital capacity than the other subjects. The purpose of the study was twofold: (a) to ascertain whether diaphragmatic breathing might improve distribution of ventilation in patients with obstructive lung diseases; and (b) to document, by Gamma camera imaging the lung with radioactive xenon, whether diaphragmatic

breathing initiated from residual volume position could preferentially direct the initial inspirate to the lower zones.

SUBJECTS, MATERIALS, AND METHODS

The normal subjects comprised 8 laboratory workers--5 men and 3 women--ages 23 to 40 yr (mean: 28 yr). The patient population consisted of 8 men and 3 women, ages 44 to 66 yr (mean: 58 yr). The diagnoses were based upon clinical features and pulmonary function tests: (a) bronchial asthma, 4 cases; (b) emphysema, 5 cases; and (c) chronic bronchitis, 2 cases.

Diaphragmatic Breathing

All subjects were instructed in diaphragmatic breathing by a physical therapist who did not use a mechanical measuring device. They were taught diaphragmatic breathing while sitting, relaxed, with the dominant hand applying pressure over the midrectus area and the nondominant hand resting on the midsternal region. Upon inspiration, the subject was told to watch his lower hand rise while the upper hand remained absolutely still. During expiration, he was told to cause the hand on the abdominal area to sink down slowly while keeping the upper thorax completely still, all the while watching and feeling to see that his upper hand did not move. Initially, the subject practiced diaphragmatic breathing in this fashion while looking at both hands with the therapist applying gentle pressure to the abdominal region. When the subject mastered breathing in this manner, the tactile, auditory, and visual stimuli were removed. Then he practiced diaphragmatic breathing without any sensory clues until he could perform this maneuver at will.

Distribution of Ventilation

For the measurement of nitrogen washout curves in the patients, mercury in silastic strain gages were placed about the upper chest, the lower chest, and the abdomen. These gages were calibrated for length by stretching with a ruler arrangement. The patients breathed 100% oxygen to an end tidal oxygen concentration of less than 1%--first with normal spontaneous breathing and then with diaphragmatic breathing, being coached to keep respiratory rate and tidal volume similar during the two maneuvers. The end-tidal concentrations of nitrogen as a function of accumulated ventilation were displayed as a semilogarithmic plot, after correction of nitrogen concentration for nitrogen eliminated from blood and tissue by a small digital computer (LINC 8, Digital Equipment Company, Maynard, Mass.). In 5 subjects, the mixed expired concentration of nitrogen as a

function of accumulated ventilation was also analyzed. The computer calculated indices of the uniformity of ventilation: pulmonary nitrogen clearance delay; the ventilation to slow space ($\dot{V}_{A_1}/L_1$), and fast space ($\dot{V}_{A_2}/L_2$) rations; and fraction of slow space volume L_1/L_T, and fast space volume L_2/L_T (2, 3). The computer also calculated: the lung clearance index (LCI)--the total ventilation of oxygen required to reduce end-tidal N_2 concentration to 2% divided by FRC in liters; and the mixing ratio--the ratio of observed to ideal number of breaths required to reduce end-tidal N_2 to 2%, where the ideal value of LCI is based upon various values of FRC, tidal volume, and dead space in a uniformly ventilated space (4). Finally, dev w was calculated by adding the products of (the difference between measured and ideal w for each compartment) x (the fraction of alveolar ventilation going into each compartment) (5). All patients were trained within 6 hr and then performed the nitrogen washout procedure. In three of the groups, instruction was continued twice a week for 1-hr sessions and the nitrogen washout was repeated 3 weeks later.

Radioactive Xenon Distribution Measurements

Both the group of normal subjects and 5 of the patients with obstructive lung disease underwent this procedure. The studies were carried out with subjects in the seated position, and were a modification of the method of Dollfuss et al. (6) for determining regional ventilation. A Gamma camera was positioned over the lungs posteriorly, such that the right lung fell within the imaging field. The subject breathed from a circuit in which it was possible to inspire room air, or oxygen from a demand valve, or to rebreathe into a spirometer filled with oxygen. At the mouthpiece was placed a pneumotachograph with a differential pressure transducer whose output was led to a strip recorder so that the subject could monitor his inspiratory flow rate. The subject breathed oxygen from the demand valve for 3 min, expired to residual volume, and initiated inspiration with either a thoracic or diaphragmatic maneuver while keeping inspiratory flow rate constant at 0.5 L/sec. At the beginning of the maneuver, a bolus of 5 ml air containing 10 - 15 mc ^{133}Xe was injected from a syringe into the mouthpiece. When the level of total lung capacity (TLC) was reached by the subject, the breath was held and an image of gamma ray activity was recorded by a Gamma camera-computer system (7). He then expired to resting lung volume into the spirometer and rebreathed rapidly and deeply for 2-3 min to obtain an equilibrated distribution of xenon. He again inspired to TLC and held his breath for a second Gamma camera recording. The computer recordings of xenon activity as a function of anatomic position were later analyzed to obtain the topographic distribution of the inspired xenon. Two thoracic and two diaphragmatic initiated breathing maneuvers were performed on each subject.

RESULTS

Distribution of Ventilation in Obstructive Lung Disease

The mean respiratory frequency during spontaneous breathing was 15.5/min, SD 3.8; and, during diaphragmatic breathing, 13.8/min, SD 2.9 (P = NS). The mean tidal volume during spontaneous breathing was 576 ml, SD 238 ml; and, during diaphragmatic breathing, 679 ml, SD 256 ml (P = NS). The FRC level of the spirometer tracing did not significantly change when diaphragmatic breathing was employed. The analog tracing of the excursions of the chest and abdomen in a representative patient are shown in Figure 1. The values of excursions for the entire group of patients are depicted in Figure 2. Only the change in abdominal movement between normal (1.35 cm, SD 0.42 cm) and diaphragmatic breathing (2.52 cm, SD 1.09 cm) is significant ($P < .01$). There were no alterations with diaphragmatic breathing in any of the indices of distribution measured (Table 1). The values for pulmonary

TABLE 1. INDICES OF DISTRIBUTION

Index *	Normal breathing Mean	Normal breathing SD	Diaphragmatic breathing Mean	Diaphragmatic breathing SD
Mixing ratio	2.13	0.92	2.02	0.76
Lung clearance index	9.84	3.95	9.20	3.29
dev w	0.077	0.036	0.079	0.040
Pulmonary N_2 clearance delay	57.8	34.0	50.7	19.5
V_{A_1}/L_1	0.564	0.232	0.587	0.256
V_{A_2}/L_2	3.296	1.839	3.468	2.129
L_1/L_T	0.758	0.113	0.738	0.119
L_2/L_T	0.242	0.105	0.262	0.119

*V_A/L = alveolar ventilation per lung volume, and L_n/L_T = fraction of space; subscript 1 = slow space, and subscript 2 = the fast space.

nitrogen clearance delay, when mixed expired concentration as a logarithmic function of accumulated ventilation in 5 subjects in whom it was measured, did not differ from the results obtained using end-tidal nitrogen concentrations--although the values of this index were higher for both normal and diaphragmatic breathing when it was calculated for mixed expired concentration (Fig. 2).

Topographic Distribution of Bolus of ^{133}Xe Inspired at Residual Volume Position

Data from a representative experiment in a normal subject is shown in Figure 3. A schematic diagram (Fig. 4) depicts the topographic distribution of the radioactive gas in normal subjects after thoracic and diaphragmatic initiated inspirations. In 5 of the 8 normal subjects, the diaphragmatic maneuver shifted ventilation from the top toward the bottom of the lungs. In the remainder, no change occurred in topographic distribution of ventilation with diaphragmatic breathing. In none of the 5 patients with obstructive lung disease was there a difference in topographic distribution of ventilation between thoracic and diaphragmatic initiated inspiration from residual volume position (Fig. 5).

DISCUSSION

Diaphragmatic breathing exercises are widely employed as a rehabilitative procedure in the treatment of chronic obstructive lung disease. If diaphragmatic breathing were truly effective, it might alter the distribution of ventilation as measured by a nitrogen washout test. However, in the patients with chronic obstructive lung disease, in the present study, there was no difference between normal spontaneous breathing and diaphragmatic breathing among indices of distribution. These findings are similar to those we previously reported in normal subjects (1). They are also consistent with the lack of change in regional tidal volume and ^{133}Xe washout measurements in normal subjects when the relative contributions of rib cage and abdomen to the tidal volume are varied (8). Thus, if diaphragmatic breathing has a physiologic basis in patient care, it might be related to diminution in the work of breathing but not to improvement in distribution of ventilation.

When an erect normal subject inspires slowly from the residual volume position to TLC, most of the initial inspirate is distributed to the upper zones; this is mainly due to the gradient of pleural pressure from top to bottom caused by the effects of gravity. At residual volume position, the pleural pressure at the top of the lung is negative with respect to

atmospheric pressure--while at the bottom, it is slightly positive. This gradient promotes patency of upper zone and closure of lower zone airways. Until the pleural pressure becomes negative at the bottom of the lungs as the level of lung volume changes from residual volume toward FRC, the upper zones receive most of the inspirate. Thereafter, most of the air is delivered to the lower zones as inspiration proceeds to TLC (6, 9). As we previously showed, in some normal subjects, initiation of inspiration using a diaphragmatic maneuver can cause a reversal in sequential emptying of gas in the lung as determined by a single breath nitrogen test (1). Similar findings have been observed by Onstad et al. (10) using ^{133}Xe as the test marker for closing volume. The evidence that diaphragmatic breathing can alter the usual topographic distribution of ^{133}Xe at residual volume position was obtained in the present study using a Gamma camera, and by Onstad et al. (10) with scintillation counters. The diaphragmatic breathing maneuver produced a diversion of the initial inspirate away from the upper to the lower zones in about half our subjects. Onstad et al. (10) calculated a ventilation index as a fraction of counts from a region after bolus injection of ^{133}Xe divided by the fraction of counts from the same region after rebreathing. This index had a mean value of 1.40 and 0.80 at the top and bottom of the lungs, respectively, for thoracic initiated inspiration; and 1.14 and 1.04 for diaphragmatic initiated inspiration. In our study using the Gamma camera, we could not readily calculate this index; but the change in top to bottom concentration, in those subjects in whom diaphragmatic breathing altered the topographic distribution of inspirate, was qualitatively similar.

In the absence of a pneumothorax, the shape of the lungs conforms to the shape of the chest wall and the diaphragm. D'Angelo et al. (11) noted that changes in the local elastic recoil, at the same relative height and lung volume accompanying posture, induce changes in the shape of the chest wall and lungs of animals. Onstad et al. (10) compared the shape of the thorax by chest roentgenography when 2 liters air were inspired from residual volume by either a thoracic or diaphragmatic initiated maneuver. A definite lengthening of the thoracic cage with the diaphragmatic maneuver was apparent when the chest roentgenograms were compared. This finding indicated that depression of the diaphragm favors expansion of the lower zones and restricts expansion of the upper zones. The downward expansion of the upper zones during a diaphragmatic maneuver might be limited by fixation or attachment at the hila. In addition to the regional deformation of the chest cage produced by a diaphragmatic breathing maneuver, it has recently been demonstrated that diaphragmatic tonus may also affect the pleural pressure gradient. Continuous stimulation of phrenic nerve roots in the intact dog provokes a diaphragmatic contraction which reverses the normal apex to basal pleural pressure gradient in the erect position (12).

Although a diaphragmatic initiated maneuver from residual volume position was effective in diverting ventilation from the upper to the lower zones in normal subjects, it had no effect in patients with chronic obstructive lung disease. This finding suggests that such patients, who have an initial depressed diaphragm, may have little influence over its movement despite good excursions of the abdominal wall. In this connection, Wade (13) found that movement of the anterior abdominal wall may not indicate the extent of diaphragmatic movement in normal subjects. However, he made these measurements above FRC and did not study diaphragmatic breathing at residual volume position. Our observations suggest that diaphragmatic breathing might be useful under conditions in which the resting lung volume is close to the residual volume level; e.g., erect subjects who are obese; patients with cirrhosis and ascites; and pilots with an inflated anti-G suit during acceleration maneuvering (14, 15). Under such circumstances, pulmonary blood flow is preferentially distributed to the lower zones whereas ventilation is preferentially distributed to the upper zones of the lung, thus causing hypoxemia due to right-to-left intrapulmonary shunting of blood. Because the diaphragms are elevated above the normal at FRC position in these conditions, diaphragmatic breathing might be effective and promote a better match of ventilation to perfusion.

REFERENCES

1. Shearer, M. D., et al. Lung ventilation during diaphragmatic breathing. Phys Ther 52:139 (1972).

2. Fowler, W. S., E. R. Cornish, and S. S. Kety. Lung function studies. VIII Analysis of alveolar ventilation by pulmonary N_2 clearance curves. J Clin Invest 31:40 (1952).

3. Briscoe, W. A., and A. Cournand. Uneven ventilation of normal and diseased lungs studied by an open-circuit method. J Appl Physiol 14:284 (1959).

4. Edelman, N. H., et al. Effect of respiratory pattern on age differences in ventilatory uniformity. J Appl Physiol 24:49 (1968).

5. Rusher, J. L., P. J. Stoll, and C. Lenfant. Exercise-induced hyperpnea and uniformity and efficiency of pulmonary ventilation. J Appl Physiol 28:63 (1970).

6. Dollfuss, R. E., J. Milic-Emili, and D. V. Bates. Regional ventilation of the lung, studied with boluses of ^{133} Xenon. Respir Physiol 2:234 (1967).

7. Watson, D. D., and J. P. Nelson. A computer system for nuclear medicine at Mount Sinai Hospital. USAEC Conf. - 710415 (1971).

8. Bake, B., A. R. Fugl-Meyer, and G. Grimby. Breathing patterns and regional ventilation distribution in tetraplegic patients and in normal subjects. Clin Sci 42:117 (1972).

9. Milic-Emili, J., et al. Regional distribution of inspired gas in the lung. J Appl Physiol 21:749 (1966).

10. Onstad, G. D., J. E. Wilson, III, and M. A. Sackner. Redistribution of regional distribution ventilation by selective diaphragmatic inhalation. (In preparation)

11. D'Angelo, E., et al. Topography of the pleural surface pressure in rabbits and dogs. Respir Physiol 8:204 (1970).

12. Minh, V. D., and K. M. Moser. Diaphragmatic tonus: a third factor in determining the pleural pressure gradient. Clin Res 21:278 (1972).

13. Wade, O. L. Movements of the thoracic cage and diaphragm in respiration. J Physiol 124:193 (1954).

14. Holley, H. S., et al. Regional distribution of pulmonary ventilation and perfusion in obesity. J Clin Invest 46:475 (1967).

15. Glaister, D. H. The effect of positive centrifugal acceleration upon the distribution of ventilation and perfusion within the human lung, and its relation to pulmonary arterial and intraesophageal pressures. Proc Roy Soc (Series B: Biol) 168:311 (1967). [Now: Proc Roy Soc Lond]

16. Sackner, M. A., et al. Distribution of ventilation during diaphragmatic breathing in obstructive lung disease. Am Rev Respir Dis 109:331 - 337 (1974).

FIGURES 1-5

for

Section XI

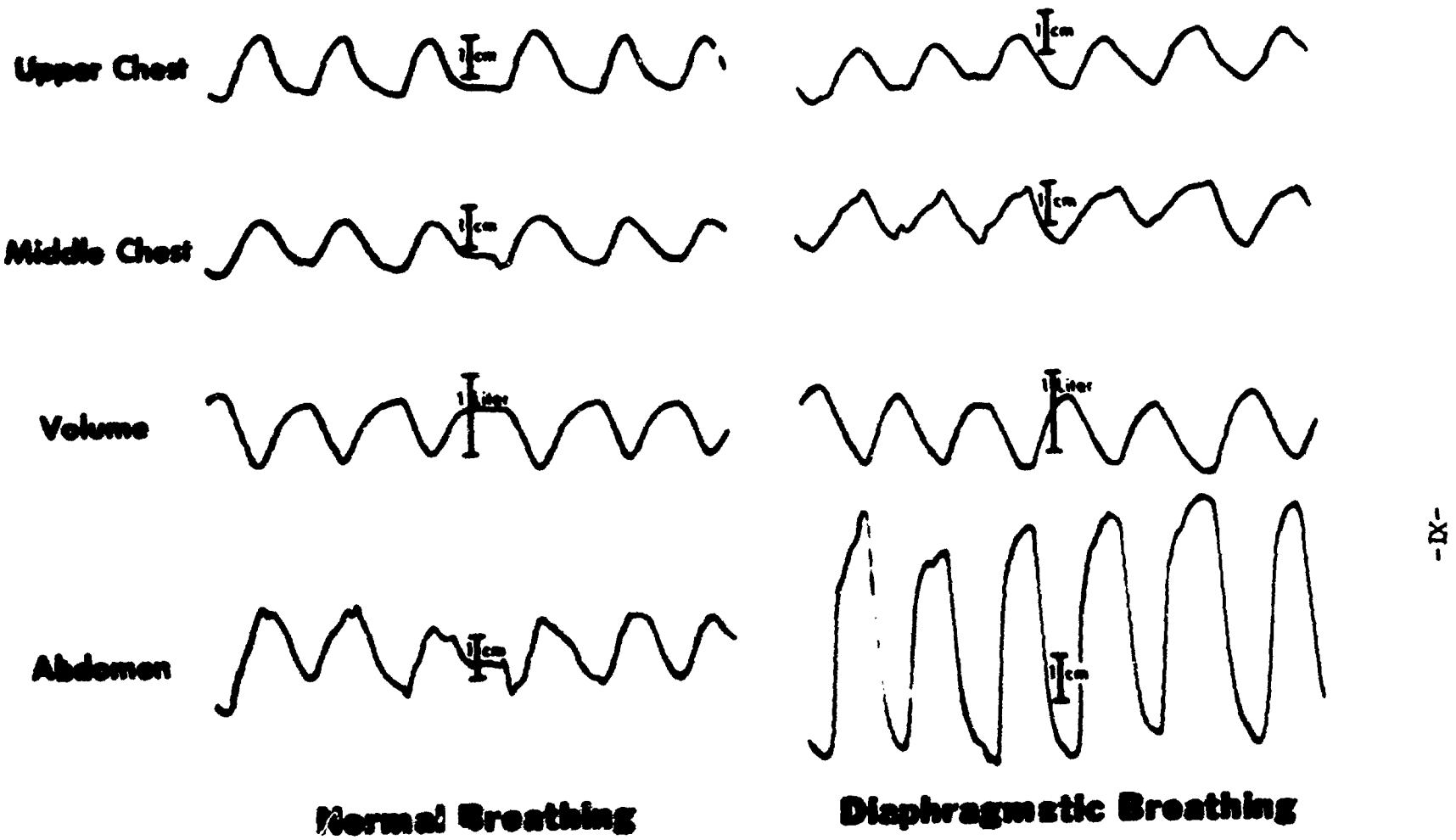

Figure 1. Analog tracings showing deflections from the Hg in silastic strain gages placed about the upper chest, middle chest, and abdomen during normal and diaphragmatic breathing in patients with chronic obstructive lung disease. (The deflections are upward for inspiration, and downward for expiration--whereas, for the volume tracing from the spirometer, the reverse is true. Diaphragmatic breathing produces large excursions in abdominal movement with little alteration in thoracic movements.)

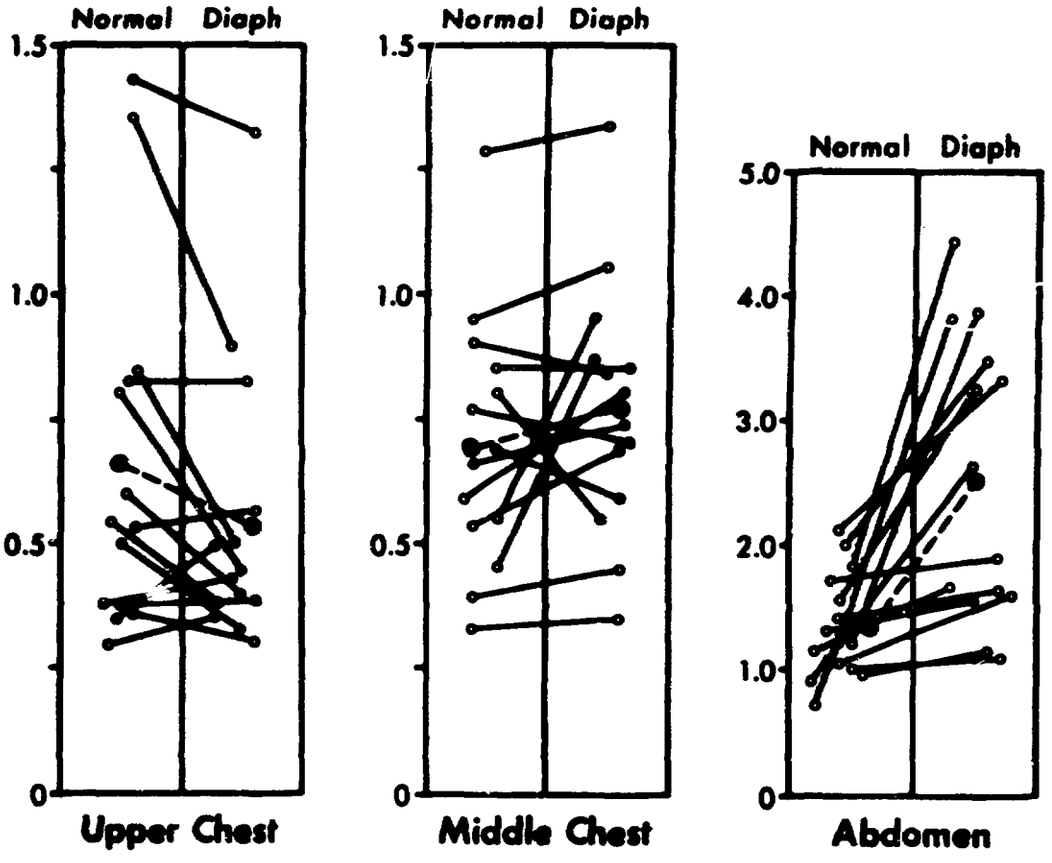

Figure 2. Excursions of thorax and abdomen for normal and diaphragmatic breathing in patients with chronic obstructive lung disease.

(The deflections are calibrated in centimeters, and the solid circles indicate the mean values for the group. Only the abdominal movement changes during diaphragmatic breathing are significant. Note: Calibration scale is four times less than the thoracic calibration scale.)

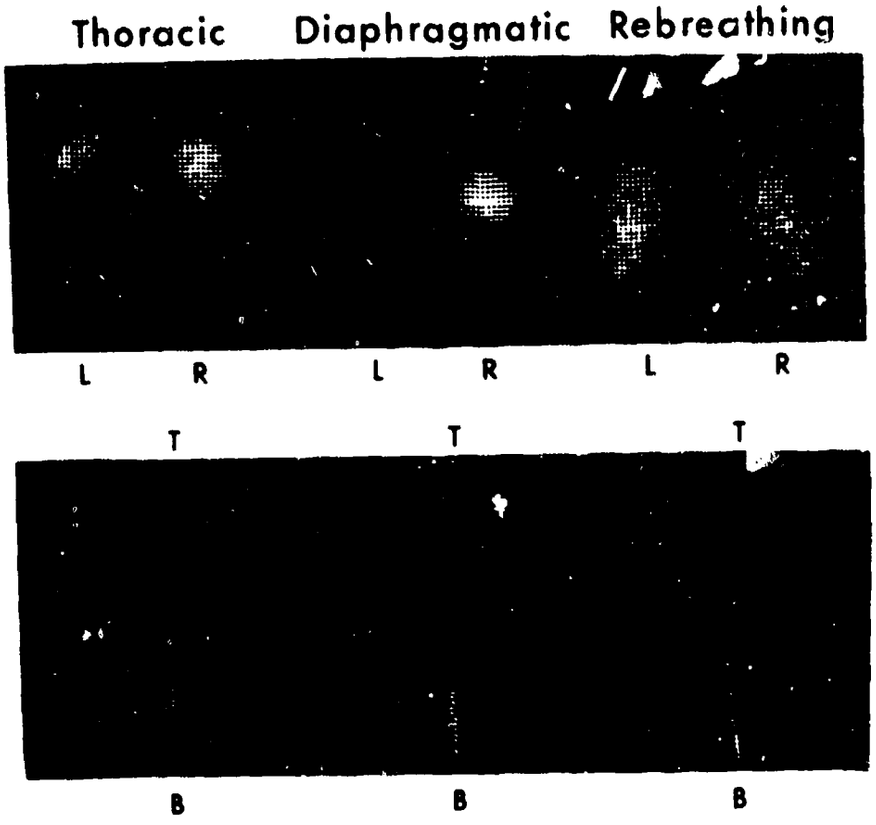

Figure 3. Computer display of radioactivity in a normal subject after inspiration of a bolus of ^{133}Xe from residual volume position.

(The upper strip depicts the lung scan at TLC: after a thoracic initiated maneuver, after a diaphragmatic initiated maneuver, and after rebreathing to equilibration throughout the lungs. R signifies the right lung: and L, the left lung. The lower strip shows the relative radioactivity from top, T, to bottom, B, measured along a vertical strip through the middle of the right lung. Increased radioactivity is shown as a deflection to the left. When the bolus of ^{133}Xe is inspired by a thoracic initiated maneuver, the peak is seen in the upper quarter of the lung--whereas, with a diaphragmatically initiated maneuver, the peak moves to about halfway down the lung. The dimensions of the entire lung are seen after the rebreathing maneuver.)

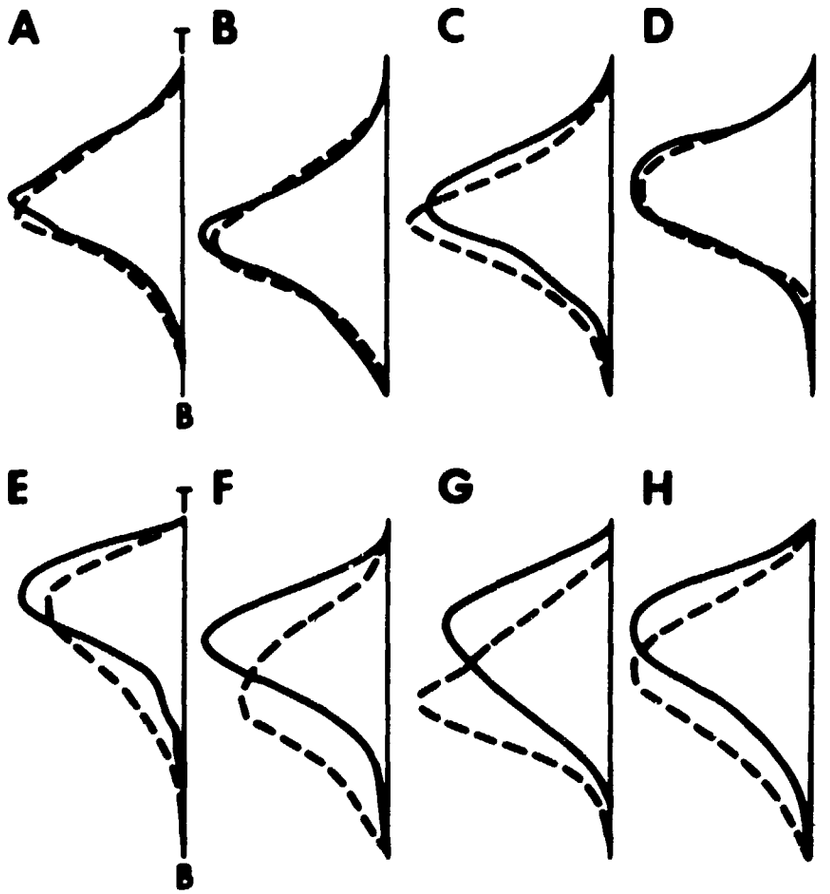

Figure 4. Topographic distribution of ventilation in 8 normal subjects (A to H) after inspiration from residual volume position with a thoracic initiated (solid line) and a diaphragmatic initiated maneuver (hatched line). [Schematic diagram]

(In 5 of the subjects--C, E, F, G, H--the diaphragmatic maneuver appeared to shift ventilation from the top, T, toward the bottom, B, of the lungs.)

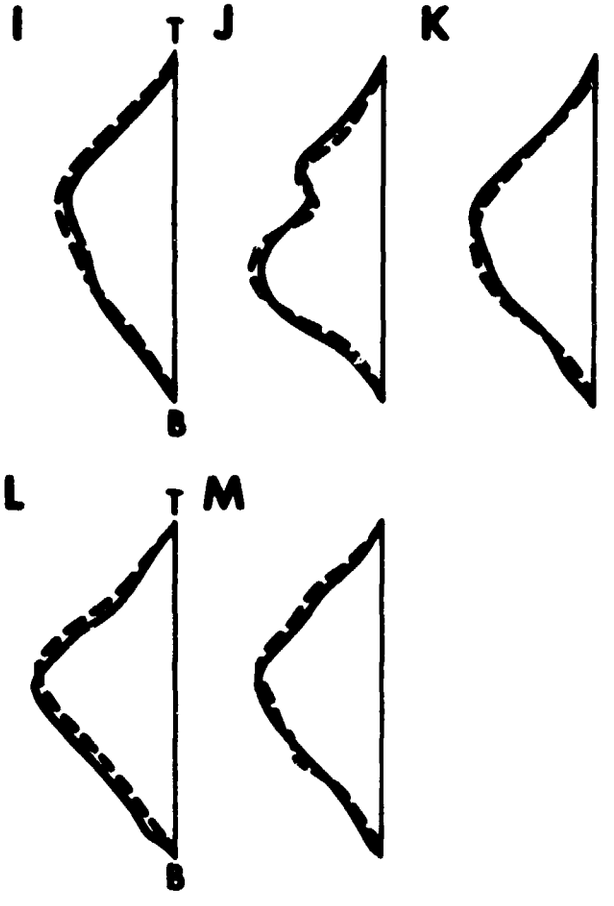

Figure 5. Topographic distribution of ventilation, in 5 patients (I to M) with chronic obstructive lung disease, after inspiration from residual volume position with a thoracic initiated (solid line) and a diaphragmatic initiated maneuver (hatched line). [Schematic diagram]
(In all 5 patients, there was no discernible difference in topographic distribution between the two maneuvers. T = top, and B = bottom, of the lungs.)

XII (Parts 1 and 2). RELATIONSHIP BETWEEN FREQUENCY DEPENDENCE OF LUNG COMPLIANCE AND DISTRIBUTION OF VENTILATION

PART 1

ABSTRACT

The empirical association (already demonstrated) between frequency dependence of lung compliance and distribution of ventilation, the latter determined by the N_2 washout technique, was confirmed by establishing a mathematical link between the two tests. Assuming a two-compartment system with known compliances and making corrections for Pendelluft and common dead-space mixing effects, the ratio of dynamic to static compliance (C_{dyn}/C_{st}) for any respiratory frequency can be calculated from the compartmental analysis of the N_2 washout at a single respiratory frequency. Using these equations, a good correlation was found between calculated and measured C_{dyn}/C_{st} in a mechanical lung model, in dogs with artificially induced bronchial obstruction, and in young smokers or young nonsmokers after carbachol inhalation. Finally, a two-compartment N_2 washout was demonstrated in 10 young healthy smokers at one or two respiratory frequencies whereas a single exponential curve was shown by all 10 normal controls. These findings indicate that the noninvasive N_2 washout test is capable of predicting C_{dyn}/C_{st} and at the same time gives a direct measure of gas distribution. Further, this test appears to be a highly sensitive method for the detection of "small airway disease."

INTRODUCTION

As already convincingly demonstrated in the electrical analog of the lung (1) as well as in human experiments (2), unequal time constants among parallel pulmonary units produce frequency dependence of lung compliance. Defares and Donleben (3) deduced that unequal time constants lead to uneven ventilation when the ratios of compartmental tidal volumes to respective compartmental volumes are different. A tendency toward a rate dependent decrease in dynamic lung compliance was demonstrated by Chiang (4), in healthy adolescents, with nonuniform distribution of ventilation as measured by an N_2 washout technique. Ingram and Schilder (5) found that distribution of ventilation became more uneven as dynamic lung compliance (C_{dyn}) decreased with increasing respiratory rates in smokers and patients with mild obstructive lung disease. Recently, Chiang (6) established that the mechanical time constant for the whole lung was closely related to a time constant derived from analysis of the N_2 washout

curve. Thus, frequency dependence of lung compliance appears to be associated with rate dependent changes in distribution of ventilation. If it is possible to predict frequency dependence of lung compliance from analysis of the N_2 washout curve, then the latter test can be substituted for the difficult, time-consuming, and invasive lung compliance test, the present standard for detection of small airway disease (2).

The dual purpose of the present investigation was: (a) to develop a mathematical two-compartment analog of the lung to relate the equations of Otis and his associates (1) for dynamic lung compliance to those of Fowler et al. (7) for N_2 washout; and (b) to test these equations while simultaneously measuring dynamic compliance and N_2 washout in a mechanical analog of the lung, in dogs with mechanically induced bronchial obstruction, in humans with pharmacologically induced bronchoconstriction, and in young smokers.

THEORETICAL CONSIDERATIONS

The relationship between frequency dependence of lung compliance, or any appreciable decrease in dynamic compliance with increasing breathing frequency and uneven distribution of ventilation has been investigated by Defares and Donleben (3). They demonstrated that frequency dependence of lung compliance is not always associated with uneven distribution of ventilation at a given respiratory rate; for frequency dependence of compliance is a reflection of differences in impedance of parallel compartments in the lung and therefore, of differences in the tidal volumes of these compartments. The criteria for uneven distribution of ventilation include not only the distributions of compartmental tidal volumes, but also the distribution of compartmental volumes, or, for the two-compartment model:

$$\frac{V_{T_1}}{V_1} = \frac{V_{T_2}}{V_2} \qquad \text{(Eq. 1)}$$

in which $V_1 = n_1 V_L$ and $V_2 = n_2 V_L$ (n_1 and n_2 are the fractional volumes of the compartments, and V_L is the lung volume). To clarify, we will consider the following situations: (a) The elastic properties of the lung are normal (i.e., $C_1/V_1 = C_2/V_2$, $C_1 = n_1 C_{st}$, and $C_2 = n_2 C_{st}$, where C_1 and C_2 are the compartmental compliances, and C_{st} is the static compliance of the lung) and the compartmental RC time constants are

equal; (b) normal elastic properties, but unequal compartmental time constants; (c) altered elastic properties of the lung ($C_1/V_1 \neq C_2V_2$) and unequal time constants; and (d) altered elastic properties and equal time constants.

In the first situation (a), which describes the normal healthy lung, distribution of ventilation will be uniform and lung compliance will not change with respiratory frequency. In the second case (b), frequency dependence of lung compliance due to unequal time constants will be associated with uneven distribution of ventilation, as detected by the multiple breath N_2 washout at all respiratory frequencies. This is probably the case in the majority of patients with early obstructive airway disease. The third case (c) is a special one in which frequency dependence of lung compliance will be present due to unequal time constants, but distribution of ventilation may be uniform at a single respiratory frequency. However, uneven distribution of ventilation will occur at all other respiratory frequencies [as illustrated in Figure 1, in which this case (View A) is compared to that (View B) of normal elastic properties with unequal time constants]. Finally, the fourth case (d) is the uncommon occurrence of a corresponding change in airway resistance to match the change in compartmental compliance due to altered elastic properties in such a way as to make the RC time constants equal. In this fourth situation, the distribution of ventilation may be uneven while lung compliance is not frequency dependent. However, this situation is not probable enough to warrant further consideration.

Therefore, for all practical purposes, uneven distribution of ventilation should be associated with frequency dependence of lung compliance--whereas even distribution of ventilation, determined at a single breathing frequency, could indicate: absence of frequency dependence of compliance, or the special case of frequency dependence of lung compliance with altered elastic properties of the compartments. Consequently, to be certain that lung compliance is not frequency dependent, the N_2 washout analysis must be performed at two frequencies, at least. If at both frequencies the N_2 washout curves are single exponentials, it may be assumed that distribution is even for all frequencies and that the dynamic lung compliance is not frequency dependent. A single exponential curve at one frequency but not at another will indicate frequency dependence of compliance with altered compartmental elastic properties, unless the single exponential curve is due to lack of sensitivity of the N_2 washout method at lower frequencies, or trapping of gas at higher frequencies. The dynamic compliance is a precise indicator of distribution of ventilation only when the compartmental volumes are known. However, in the

presence of unequal time constants where T_2/T_1 is above a threshold value of approximately ten, uneven distribution of ventilation can be demonstrated regardless of compartmental volume by the N_2 washout procedure if multiple breathing frequencies are employed. In this mathematical treatment we have assumed Otis' two-compartment model of the lung (1) for simplicity (Fig. 1: View C); but the treatment is readily extended to an n-compartmental model.

Otis et al. (1) assumed a two-compartment model of the lung and derived expressions for the dynamic lung compliance and for the tidal volumes of the 2 compartments. These expressions, rearranged, are:

$$C_{dyn} = \frac{W^2 (T_2C_1 + T_1C_2)^2 + (C_1 + C_2)^2}{W^2 (T_1^2C_2 + T_2^2C_1) + (C_1 + C_2)} \qquad \text{(Eq. 2)}$$

$$V_{T_1} = V_T Z_T/Z_1 \qquad \text{(Eq. 3)}$$

$$V_{T_2} = V_T Z_T/Z_2 \qquad \text{(Eq. 4)}$$

in which $W = 2\pi \times$ frequency; C_1, C_2 = compartmental compliances; T_1, $T_2 = R_1C_1$; R_2C_2 = compartmental RC time constants; Z_T = total impedance of the lung; Z_1, Z_2 = compartmental impedances; and V_T = tidal volume. Now, since:

$$Z = (R^2 + 1/W^2C^2)^{1/2} = \frac{1}{C} (T^2 + 1/W^2)^{1/2}, \qquad \text{(Eq. 5)}$$

equations 3 and 4 can be written:

$$\frac{V_{T_1}}{V_T} = \frac{1/C_2 \left(T_2^2 + 1/W^2\right)^{1/2}}{\left(\frac{T_1^2 + 1/W^2}{C_1^2} + \frac{T_2^2 + 1/W^2}{C_2^2} + 2\,\frac{T_1T_2 + 1/W^2}{C_1C_2}\right)^{1/2}} \qquad \text{(Eq. 6)}$$

$$\frac{V_{T_2}}{V_T} = \frac{1/C_1 \left(T_1^2 + 1/W^2\right)^{1/2}}{\left(\frac{T_1^2 + 1/W^2}{C_1^2} + \frac{T_2^2 + 1/W^2}{C_2^2} + 2\,\frac{T_1T_2 + 1/W^2}{C_1C_2}\right)^{1/2}} \qquad \text{(Eq. 7)}$$

If we assume that the elastic properties of the two compartments are the same (as is probably true for healthy subjects and those with early obstructive airway disease), then $C_1 = n_1 C_{st}$, and $C_2 = n_2 C_{st}$ (Fig. 1: View B). Therefore, now equations 2, 6, and 7 can be reduced to:

$$\frac{C_{dyn}}{C_{st}} = \frac{w^2 (n_2 T_1 + n_1 T_2)^2 + 1}{w^2 (n_2 T_1^2 + n_1 T_2^2) + 1} \qquad \text{(Eq. 8)}$$

$$\frac{V_{T_1}}{V_T} = \frac{n_1 (T_2^2 + 1/w^2)^{1/2}}{\left[(n_2 T_1 + n_1 T_2)^2 + 1/w^2\right]^{1/2}} \qquad \text{(Eq. 9)}$$

$$\frac{V_{T_2}}{V_T} = \frac{n_2 (T_1^2 + 1/w^2)^{1/2}}{(n_2 T_1 + n_1 T_2)^2 + 1/w^2}^{1/2} \qquad \text{(Eq. 10)}$$

From equations 9 and 10--if the ratios V_{T_1}/V_T and V_{T_2}/V_T are known for a given respiratory frequency, and the fractional volumes n_1 and n_2 are known--the two equations can be solved simultaneously for T_1 and T_2 into equation 8, and varying w, the rationalized dynamic compliance can be predicted as a function of frequency.

The analysis of the N_2 washout curve (7) gives data which with certain assumptions yield values for the fractional volumes, and a close approximation of the ratios V_{T_1}/V_T and V_{T_2}/V_T. The latter are based upon the ratios of the compartmental alveolar ventilations to the total alveolar ventilation, $\dot{V}_{A_1}/\dot{V}_A$ and $\dot{V}_{A_2}/\dot{V}_A$. If the dead space of the lung is evenly distributed and the tidal volume is large relative to the compartmental dead space these ratios approximate the ratios of the tidal volumes, or:

$$\frac{V_{T_1}}{V_T} = \frac{\dot{V}_{A_1}}{\dot{V}_A} \quad : \quad \frac{V_{T_2}}{V_T} = \frac{\dot{V}_{A_2}}{\dot{V}_A} \qquad \text{(Eq. 11)}$$

The values for alveolar ventilation of the two compartments as derived by the analysis of Fowler et al. (7) are not entirely accurate. The bidirectional gas transfer between compartments due to Pendelluft and common dead space mixing is responsible for an underestimation of the ventilation

of the "fast" compartment, and a slight overestimation of the ventilation of the "slow" compartment. In order to obtain more accuracy in the determination of the ratios $\dot{V}_{A_1}/\dot{V}_A$ and $\dot{V}_{A_2}/\dot{V}_A$, appropriate corrections must be applied. Safonoff and Emmanuel (8) reported that the error in the ventilation of the slow compartment is minimal and can be neglected in the range of interest. They estimated that the volume of gas transfer due to Pendelluft and common dead space mixing is approximately 60% of the tidal volume of the slow compartment (see Part 2: A). Thus:

$$V_T = V_{T_1} + V_{T_2} - V_p \qquad \text{(Eq. 12)}$$

where V_P = the volume of gas transfer due to Pendelluft and common dead space mixing. But $V_P = 0.60 \times V_{T_2}$, where V_{T_2} is the tidal volume of the "slow" compartment. Then:

$$V_T = V_{T_1} + 0.4\, V_{T_2} \qquad \text{(Eq. 13)}$$

Now, since $\dot{V}_A = (V_T - V_D) \times \text{freq.}$, or, $V_T = \dot{V}_A/f + V_D$:

$$\dot{V}_A/f + V_D = \dot{V}_{A_1}/f + V_{D_1} + 0.40 \quad \frac{\dot{V}_{A_2}}{f} + V_{D_2} \qquad \text{(Eq. 14)}$$

which reduces to:

$$\dot{V}_A + (V_D - V_{D_1} - 0.40\, V_{D_2})\, f = \dot{V}_{A_1} + 0.40\, \dot{V}_{A_2} \qquad \text{(Eq. 15)}$$

If it is assumed that $(V_D - V_{D_1} - 0.40\, V_{D_2}) \ll V_T$, then:

$$\dot{V}_A \simeq V_{A_1} + 0.40\, \dot{V}_{A_2}; \qquad \text{(Eq. 16)}$$

and, since the error in $\dot{V}_{A_2}$ can be neglected (8), this approximation can be used to correct the ventilation of the fast compartment, $\dot{V}_{A_1}$:

$$\dot{V}_{A_1} = \dot{V}_A - 0.40\, \dot{V}_{A_2} \qquad \text{(Eq. 17)}$$

By substituting the corrected values for the ventilation ratios into equations 9 and 10, along with the frequency at which these ratios were determined, T_1 and T_2 can be solved. The solutions are:

$$T_1 = \frac{\left\{ B\left[\frac{(Y^2 + 4P)^{1/2} - Y}{2}\right] + A \right\}^{1/2}}{n_2} \qquad \text{(Eq. 18)}$$

$$T_2 = \frac{\left[\frac{(Y^2 + 4Z)^{1/2} - Y}{2}\right]^{1/2}}{n_1}$$

in which:

$$A = \frac{\dot{V}_{A_2}^2}{W^2}\left(\frac{n_1^2}{\dot{V}_{A_1}^2} - \frac{n_2^2}{\dot{V}_{A_2}^2}\right)$$

$$P = \left(\frac{\dot{V}_{A_2}}{\dot{V}_{A_1}}\right)^2$$

$$Y = \frac{A + \left(\frac{n_1^2\,\dot{V}_A}{\dot{V}_{A_1}^2\,W^2} - \frac{1}{W^2} - A\right)\left(\frac{B}{2} - \frac{\dot{V}_A^2}{2\dot{V}_{A_1}^2} + \frac{1}{2}\right)}{B - \left(\frac{B}{2} - \frac{\dot{V}_A^2}{2\dot{V}_{A_1}^2} + \frac{1}{2}\right)^2}$$

$$B = \frac{\left(\frac{n_1^2\,\dot{V}_A^2}{\dot{V}_{A_1}^2\,W^2} - \frac{1}{W^2}\right)^2}{B - \left(\frac{B}{2} - \frac{\dot{V}_A^2}{2\dot{V}_{A_1}^2} + \frac{1}{2}\right)^2}$$

Substituting these values for T_1 and T_2 into equation 8 enables us to generate a plot of rationalized dynamic compliance vs. frequency. The accuracy of the approximation of $V_p/V_{T_2} = 0.60$ is presented in Part 2:A (of report section XII); and a complete derivation of the expressions for T_1 and T_2 is given in Part 2:B.

METHODS

Model Experiments

Frequency dependence of N_2 washout and dynamic compliance were determined in a two-compartment mechanical model (Fig. 2). It consisted of two equally sized (500 ml each) Plexiglas cylinders whose two open ends were covered with a latex membrane. The tension of these membranes was so adjusted that the static pressure-volume curves of the two compartments were identical. The two cylinders were connected in parallel through a 1/2-in. brass Y-connector. The dead space of each compartment was 7 ml. The downstream end of the Y-connector was connected via a #0 Fleisch-pneumotachograph (with a Validyne DP-7 transducer, Northridge, Calif.) which had a linear output to a flow rate of 18 L/min, to a 4-way valve. This system was determined to be dynamically balanced below 3 Hz; that is, there was no measurable output when the distal end of the pneumotachograph was occluded and the proximal end driven by a sinusoidal pressure source. The common dead space was 19 ml. The system was driven with a volume-limited piston-type pediatric respirator (Bournes, Riverside, Calif.). Static pressure in the system was recorded in the common dead space with a differential gage (Validyne DP-9) referenced to ambient pressure. All pressure transducers used demonstrated a common mode rejection ratio of greater than 64 dB below 3 Hz. At frequencies up to 90/min with flow rates in the range used in this experiment, no phase shift was detected in this system. The displaced volume was obtained by electrical integration of expiratory flow (#0 Fleisch Pneumotachograph) in the expiratory line of the respirator. N_2 concentration was determined (Nitralyzer, Model 505, Med. Science, St. Louis) at the downstream end of the common dead space. All signals were recorded on a Grass recorder (Model 78B, Quincy, Mass.).

The model was ventilated with a constant volume of 70 ml/cycle at 20, 40, and 60 cycles/min, and the ratio of inflation to deflation time was maintained at 1:1. Graded resistances made of small parallel

catheters were placed in the upstream end of the dead space of one compartment. These resistances were linear over the range of flow rates encountered in the experiments.

The tests were conducted as follows: First, the model was ventilated with room air until a stable preinflation pressure was reached. At this point, the system was occluded by turning the 4-way valve and 100% O_2 was introduced into the respirator, thereby providing an inspiratory N_2 concentration of less then 0.3%. After 5 - 10 cycles, during which time the inspiratory lines of the respirator were cleared of N_2, the 4-way valve was again turned and the N_2 washout of the system was started. The test was terminated when the preinflation N_2 concentration was below 1%. Dynamic compliance was determined during the N_2 washout, and a static pressure-volume curve was obtained by a stepwise inflation and deflation of the whole system with a giant syringe.

Animal Experiments

Ten mongrel dogs, each weighing between 12 kg and 30 kg, were: anesthetized with sodium pentobarbital, 50 mg/kg; intubated with a cuffed orotracheal tube; and suspended in the prone position. Ventilation was controlled by a Harvard Animal Respirator with a fixed tidal volume of 0.2 - 0.4 liters, adjusted according to the weight of the dog and an inspiration to expiration ratio of 1:1. A balloon catheter, as described by Milic-Emili et al. (9), was placed in the lower esophagus; and transpulmonary pressure was estimated with a differential gage (DP-9 Validyne) by referencing esophageal pressure to mouth pressure. At frequencies up to 90/min, and with flow rates in the range used in the experiments, no phase shift was detected in this system. Between the inspiratory and expiratory part of the respirator and the T-adaptor at the downstream end of the endotracheal tube, two 3-way valves were incorporated so that the dog's airway could be occluded at any instant of the respiratory cycle. A dynamically balanced Fleisch #0 pneumotachograph, connected to a Validyne DP-7 transducer, was inserted between the endotracheal tube and the T-adaptor to obtain points of zero flow for the calculation of dynamic compliance. Nitrogen concentration was measured upstream of the T-adaptor with a rapidly responding analyzer (Nitralyzer, Med. Science, St. Louis). Expiratory flow was recorded from the expiratory line of the breathing system, with a dynamically balanced Fleisch #1 pneumotachograph which was linear, to flow rates of 60 L/min. Flow was electrically integrated to obtain tidal volume. All signals were recorded on a Grass Polygraph recorder (Model 78B,

Quincy, Mass.). The delivery of pure oxygen and the experimental procedure was identical to that described for the model experiments. The experiment was started when a stable end-expiratory volume level was obtained. For the dynamic compliance measurements, care was taken that the end-expiratory and end-inspiratory pressure remained on the linear portion of the static pressure-volume curve.

N_2 washout and dynamic compliance measurements were performed at respiratory frequencies of 20, 30, 40, and 50/min, before and after partial obstruction of one main bronchus. The obstruction consisted of a metal tube, 2 mm in diameter and 10 mm in length, surrounded by an inflatable cuff. It was placed, with a bronchoscopic forceps, in the right or left main bronchus immediately distal to the carina. Its location was ascertained by bronchofiberscopy. The cuff was inflated and the proximal end of the cuff catheter was occluded with a plugged needle which was stuck through the rubber adaptor of the endotracheal tube. Frequent tracheal suctioning was performed in order to prevent plugging of the obstruction with bronchial secretions. Before each run, the dog was given a deep breath by occluding the expiratory line. Static pressure-volume curves were obtained by stepwise inflation to 1.0 L above FRC and deflation to FRC of the lung with a calibrated giant syringe, after sighing the dog to 1.0 L above FRC.

Human Experiments

Three sets of experiments were conducted with human volunteers from whom informed consent was obtained. Two of these experiments were designed to determine the relation between the dynamic lung compliance calculated from the N_2 washout curves and the actually measured dynamic lung compliance (Groups A and B), while the third experiment (Group C) was to compare a number of commonly used pulmonary function tests for the detection of early lung disease between young healthy smokers and nonsmokers. All subjects were selected solely on the basis of their smoking history.

Nine healthy nonsmokers, ages 21 to 35 years (Group A), with normal routine pulmonary function tests (described in the following), performed N_2 washouts at respiratory frequencies of 60 and 75/min. Dynamic lung compliance measurements (at 20, 40, and 60 breaths/min.) and quasi-static pressure-volume plots of the lung were obtained by the esophageal balloon catheter technique (9). Transpulmonary pressure was measured

with a Validyne DP Differential transducer with a common mode injection ratio of greater than 64 dB below 3 Hz, and flow was measured by a dynamically balanced #1 Fleisch pneumotachograph connected to a Validyne DP-7 transducer. A slow inspiratory vital capacity maneuver followed by a slow expiratory vital capacity maneuver were done immediately before and after N_2 washout and dynamic compliance determinations, in order to ensure identical volume histories. These tests were performed in the control state and immediately after inhalation of 15 - 30 breaths of 1.5% carbachol delivered through a D-30 generator (10). N_2 washouts at two different frequencies and dynamic lung compliance were also obtained in 9 healthy young smokers, ages 21 to 42 years (Group B), with normal routine pulmonary function tests. Finally, 10 young healthy nonsmokers and 10 smokers, ages 18 to 42 years (Group C), were selected for estimation of distribution of ventilation by N_2 washout at 60 and 75 breaths/min. The smokers continued to smoke on the experiment day, but not within one hour prior to the study. Routine pulmonary function studies were performed on all, and the following parameters were determined: The displaceable lung volumes were measured with a spirometer and FRC and airway resistance (panting at 1 to 2 Hz up to 0.5 L/sec inspiratory flow rate) with a body plethysmographic technique (11, 12). Single breath diffusing capacity (13), single breath nitrogen test (14), closing volume and flow volume curves (15) were also obtained.

N_2 washout was carried out with a breathing system analogous to the one used for the animal experiments. The nitrogen and volume signals were also displayed on an oscilloscope in order to guide the subject in maintaining an approximately constant end-expiratory volume throughout the test. A breath simulator (Model 700, Somanetics Inc., La Jolla, Calif.) providing respiratory frequencies up to 110 breaths/min was used, and the subject was asked to follow the simulated breath sounds.

Data Analysis

Dynamic compliance was calculated conventionally by dividing the volume change by the system pressure change (model experiments) or transpulmonary pressure change (animal and human experiments) between points of zero flow from end inspiration to the beginning of the following inspiration. Static compliance was calculated on the deflation leg of the static pressure volume curve between pressure limits which were recorded during measurement of dynamic compliance. The N_2 washout curves were analyzed on-line or from analog magnetic tape on a small digital computer (LINC 8, Digital Equipment Co., Maynard, Mass.) using either expiratory flow

(model and animals) or tidal volume (humans) (16). End-tidal N_2 concentration was plotted against time (model and dogs) and against cumulative expiratory volume (humans), and expressed as N_2 clearance delay as described by Fowler et al. (7). Corrections for the excretion of tissue nitrogen were made according to Simmons and Hemingway (17) in dogs and Bouhuys (18) in humans. Another correction was made for the N_2 signal delay which was determined prior to the experiments. A computer program, written in FOCAL, was used to calculate frequency dependence of lung compliance from the compartmental analysis of the nitrogen washout curve.

RESULTS

Model Experiments

Frequency dependence of N_2 clearance delay (NCD) and dynamic compliance expressed as the ratio of dynamic compliance (C_{dyn}) and static compliance (C_{st})--the latter obtained from the slope of the static pressure-volume curve at the particular system pressure--are shown in Figure 3 for the different unilateral obstructions (A = 5, B = 90, C = 275, and D = 740 cm H_2O/Lsec). The ratio of C_{dyn}/C_{st} decreased as NCD increased. With the high grade obstruction, NCD returned to 0% at high frequencies when the tidal volume of the slow compartment became equal to or less than its dead space. Since effective ventilation of the slow compartment was minimal, the N_2 was washed out as a single exponential curve. When the cycling frequency was reduced after completion of the washout, a second exponential curve was obtained indicating ventilation of the previously trapped gas in the slow compartment. It is also of interest that, in our mechanical analog with equal compartmental volumes, the return to a single exponential curve occurred when C_{dyn}/C_{st} approached 0.5. Using the equations which relate the time constants of the model to expected N_2 washout, a good experimental fit was obtained. As depicted in Figure 4, the theoretically predicted curves for obstructions A, B, C, and D compared well with the experimentally determined curves at frequencies of 20, 40, and 60/min. The difference between any two points was always less than 20%. Similarly, a good agreement was demonstrated between C_{dyn}/C_{st} calculated from the N_2 washout curve and the C_{dyn}/C_{st} actually measured (Fig. 5). The prediction was more accurate when a N_2 washout at a high respiratory frequency was used for the calculation.

Animal Experiments

No frequency dependence of C_{dyn} and a single compartment N_2 washout was found in all 10 dogs before unilateral bronchial obstruction; but, following partial obstruction of one main bronchus, frequency dependence of C_{dyn} and N_2 washout took place in a manner similar to that in the model experiment. Good agreement was found between C_{dyn}/C_{st} calculated from the N_2 washout at 50 breaths/min and C_{dyn}/C_{st} actually measured (Fig. 6). Eighty-five percent of the points fell within $\pm$ 15% of the line of identity. As might be predicted, the ratio C_{dyn}/C_{st} leveled off at a volume of 0.5 in this model where the FRC of the obstructed and unobstructed lungs could be assumed to be approximately equal, and the distribution of inspired air within each lung even. With this type of obstruction and respiratory frequencies up to 50/min, we never observed a single compartment indicating trapping of the obstructed lung.

Human Experiments

Group A - All 9 subjects in this group of nonsmokers exhibited no frequency dependence of C_{dyn} and a single exponential N_2 washout curve at 60 and 75 breaths/min in the control state, whereas the inhalation of carbachol produced definite changes in these two tests (Table 1: Group A). A good correlation was demonstrated between calculated C_{dyn}/C_{st} and actually measured C_{dyn}/C_{st} in all subjects at respiratory frequencies of 20, 40, 60/min (Fig. 7).

Group B - The 9 young smokers selected for this group had frequency dependence of C_{dyn} and exhibited two compartments in at least one of their N_2 washout curves (Table 1: Group B). Correlations between calculated and measured C_{dyn}/C_{st} at frequencies of 20, 40, and 60/min (Fig. 8) were similar to Group A after carbachol administration. The smoking history in these subjects ranged from 1 - 40 pack-years.

Group C - The anthropometric characteristics, smoking history, symptoms, and the results of the routine pulmonary function tests of the 10 nonsmokers and 10 smokers are listed in Tables 2 and 3. Predicted normal values were taken from Bates et al. (19) and DuBois et al. (12). The two groups were matched with regard to age; the mean age of the smokers was 27.3 years (range 18-42) and of the nonsmokers 28.3 years (range 22-35). Of the smokers, 7 were asymptomatic, and, of the 3 who gave a history of morning cough with sputum production, 1 also stated he experienced mild exertional dyspnea in the morning. None of the

nonsmokers had respiratory symptoms. All the tests which are conventionally used to detect airway obstruction were within normal limits in both smokers and nonsmokers (Tables 2 and 3). Figure 9 compares, in smokers and nonsmokers, the single breath nitrogen test, maximal flow at 50% vital capacity and closing volume. Although the differences were not significant for the single breath nitrogen test and closing volume, the maximum expiratory flow at 50% of vital capacity was significantly less in smokers (2.15 L/sec $\pm$ 0.65) than nonsmokers (3.25 L/sec $\pm$ 1.20) ($P < .05$).

Distribution of ventilation, as determined by the N_2 washout technique, was even at respiratory rates of 60 and 75/min in the 10 nonsmokers. The NCD was 0% in all of them, indicating that one compartment was present. On the other hand, all 10 smokers had two compartments in their N_2 washout curves at one respiratory rate, at least. In 7 smokers, an uneven distribution of ventilation was demonstrated at both respiratory rates.

DISCUSSION

In the present investigation, a good correlation was established between calculated C_{dyn}/C_{st} and actually measured C_{dyn}/C_{st} in a two-compartment mechanical model, in mechanically ventilated dogs with partial obstruction of one main bronchus, in young subjects with artificially induced airway obstruction (carbachol), and in asymptomatic young smokers. In the lung model and in dogs, in the presence of unequal time constants, distribution of ventilation expressed as NCD increased as C_{dyn} decreased with increasing frequency, thus confirming the experimental findings of Ingram and Schilder (5) in humans. Our human data were insufficient for this comparison; for our experimental design was to predict C_{dyn}/C_{st} from N_2 washout curves, and these curves were determined only at higher frequencies to allow greater accuracy. In the human experiments where C_{st} was determined from the deflation leg of the static pressure-volume curve for comparison with C_{dyn}, systematic overestimation of frequency dependence of compliance could be expected because of the difference in volume history. However, the lack of frequency dependence of compliance in normals indicated that this overestimation was slight. Furthermore, the degree of such an error would be expected to decrease with increasing respiratory frequency.

The influence of Pendelluft, which goes through a maximum and returns to a minimum at high frequencies if the time constants are sufficiently different, and of the common dead space on alveolar mixing

appeared to be significant when C_{dyn}/C_{st} was to be calculated from the compartmental analysis of the N_2 washout curve. According to Safonoff and Emmanuel (8), these effects result in an underestimation of the alveolar ventilation of the fast compartment and minimal overestimation of the ventilation of the slow compartment. However, using their experimentally obtained correction factor to convert the apparent ventilation of the fast compartment to its actual alveolar ventilation, our calculated C_{dyn}/C_{st} correlated well with the measured C_{dyn}/C_{st}. Since this is only an approximate correction factor (8), and the effects of Pendelluft and common dead space mixing become minimal as the difference between the compartmental alveolar ventilation increases, it is not surprising that the accuracy of the predicted C_{dyn}/C_{st} is better at higher respiratory frequencies (see Part 1: A in this report section). A further theoretical objection to equating the compartmental to total tidal volume ratio (V_{T_1}/V_T) with the compartmental to total alveolar ventilation ratio ($\dot{V}_{A_1}/\dot{V}_A$) is the presence of common (V_D) and compartmental dead spaces (V_{D_1}, V_{D_2}) which have to be subtracted from the tidal volumes for the calculation of alveolar ventilation:

$$\frac{\left(V_{T_1} - V_{D_1}\right) \times f}{\left(V_T - V_D\right) \times f} = \frac{\dot{V}_{A_1}}{\dot{V}_A}$$

Since V_{T_1}/V_T changes with both increasing respiratory frequencies and increasingly uneven compartmental time constants, but V_{D_1} and V_D are more or less of constant value, an error is introduced into equation 15. However, if the distribution of dead spaces approximates the distribution of tidal volumes, or,

$$\frac{V_{D_1}}{V_D} \cong \frac{V_{T_1}}{V_T}$$

then the dead space effect can be neglected. This assumption is probably applicable in the case of small airway disease.

While the expectation was that the theoretical predictions based on a two-compartment system would hold true in the lung model and in dogs with partial obstruction of one lung whose gas mixing appears to be ideal because of extensive collateral ventilation (19), there was also a close

correlation between calculated and measured C_{dyn}/C_{st} in the human lung. Since our analysis requires normal elastic properties of the two compartments, it is mostly applicable to healthy subjects or those with minimal lung disease. These relationships can be expected to be less ideal in more advanced lung disease with differences in elastic properties among various lung units.

Woolcock et al. (2, 20) introduced frequency dependence of lung compliance as a test for small airway obstruction and indicated that frequency dependence of C_{dyn} is associated with frequency dependence of distribution of ventilation [subsequently confirmed by others (4, 5)]. Based on Ingram and O'Cain's (21) study on frequency dependence of C_{dyn} in asymptomatic smokers, we expected to find a difference in N_2 washout at high respiratory frequencies between our young smokers and nonsmokers. While the nonsmokers had a single exponential N_2 washout curve, all 10 smokers revealed two compartments at one or both measured respiratory frequencies. Our finding, that all nonsmokers had a single exponential curve, contrasts with that of Bouhuys (22) who found a mean NCD of 29% in young subjects from 24 to 34 years of age at normal respiratory rates. From these data, however, it is not quite clear whether smokers were included as normal subjects.

In our subjects, of two other tests which have been employed to detect small airway obstruction, the closing volume (23) showed no significant difference between nonsmokers and smokers, whereas maximum expiratory flow at 50% of vital capacity was significantly lower in smokers than in nonsmokers. However, the scatter of data in this test minimizes the selection of individual young smokers with small airway obstruction. In contrast, the NCD was 0% in all nonsmokers and deviated from 0% in all young smokers at a higher respiratory frequency.

A number of theoretical and technical reasons can be incriminated for the observed slight discrepancies between calculated and measured C_{dyn}/C_{st} in these smokers. First, the influence of boundary diffusion on alveolar mixing was not taken into account. It is evident that diffusion of gases takes place between the dead space and gas exchange units, and that this diffusion factor decreases as frequency is increased. Although Roos et al. (24) indicated that boundary diffusion may have a significant effect on alveolar mixing, the factor was neglected in our analysis because we had no way to quantitate it. The assumption of Otis' (1) model--which neglected such factors as parallel airway compliance (25), and assumed sinusoidal inputs--may have introduced some error in the

calculations. A further assumption in the mathematical considerations was that time constants were not altered with changes in respiratory frequencies. In the mechanical model and possibly also in the obstructed animals, the type of resistance used ensured linearity at all frequencies, and the monitoring of the system pressure established the corresponding static compliance for all changes in lung volume. However, in the human lung with a large number of uneven time constants, all the resistances cannot be assumed to be linear nor can all the compliances be operating on the linear portion of the static pressure-volume curve at all frequencies. Consequently, at higher frequencies, certain units may already be excluded from the ventilation when others have still decreasing alveolar ventilation as a function of frequency. Further, a slight increase in FRC during the run may have occurred despite careful monitoring of the end expiratory volume level and, consequently, have produced an artifactual slow compartment. Slight changes in tidal volumes had probably little effect on the distribution of ventilation, since N_2 concentration was plotted against cumulative expired volume. Finally, the extrapolation of a two-compartment system to the abnormal lung with a large number of uneven time constants must introduce some degree of inaccuracy. An examination of Table 1, in fact, shows that the fractional compartmental volume did not remain the same for the two breathing frequencies in all subjects. Also, the ratio of $\dot{V}_{A1}/\dot{V}_{A2}$ did not increase with frequency in all cases. The arbitrary fitting of a two-component curve to the N_2 washout in a multi-compartment system with a continuum of time constants could have resulted in the situation where individual compartments with intermediate time constants would be included either in the slow or fast compartment, depending on respiratory frequency. As a consequence of these inconsistencies, the values for the compartmental time constants were not accurately reproducible. In addition to the inaccuracy introduced by the fitting of a two-component curve to the washout data, in the normals after carbachol the short action of the drug could have caused a change in the degree of airway obstruction between the two N_2 washout determinations. This seemed to be the case, as the data on this group were less consistent than those on the healthy smokers. Despite these considerations, experimental data in the lung model as well as in dogs and humans indicated a good correlation between calculated (from N_2 washout curves) and actually measured C_{dyn}/C_{st}. These correlations were made at frequencies under 60/min in order to minimize inertial effects.

The N_2 washout method performed at higher respiratory frequencies appears to be an excellent screening test for the detection of mild

unevenness of distribution of ventilation occurring in early lung disease. Considering the possible discrepancies between frequency dependence of compliance and distribution of ventilation, the N_2 washout technique which measures directly gas distribution and indirectly C_{dyn}/C_{st} may be preferable to the conventional determination of dynamic compliance.

REFERENCES

1. Otis, A. B. Mechanical factors in distribution of pulmonary ventilation. J Appl Physiol 8:427-443 (1956).

2. Woolcock, A. J., N. J. Vincent, and P. T. Macklem. Frequency dependence of compliance as a test for obstruction in the small airways. J Clin Invest 48:1097-1105 (1969).

3. Defares, J. G., and P. G. Donleben. Relationship between frequency-dependent compliance and unequal ventilation. J Appl Physiol 15:166-169 (1960).

4. Chiang, S. T. Distribution of ventilation and frequency-dependence of dynamic lung compliance. Thorax 26:721-726 (1971).

5. Ingram, R. H., and D. P. Schilder. Association of a decrease in dynamic compliance with a change in gas distribution. J Appl Physiol 23:911 (1967).

6. Chiang, S. T. Relationship between the time constants of R, C networks and nitrogen washout in the respiratory system. Aerosp Med 42:1270-1274 (1971).

7. Fowler, W. S., E. R. Cornish, Jr., and S. S. Kety. Lung function studies VIII. Analysis of alveolar ventilation by pulmonary N_2 clearance curves. J Clin Invest 31:40-50 (1952).

8. Safonoff, I., and C. E. Emmanuel. The effect of pendelluft and dead space on nitrogen clearance: Mathematical and experimental models and their application to the study of the distribution of ventilation. J Clin Invest 46:1683-1693 (1967).

9. Milic-Emili, J., et al. Improved technique for estimating pleural pressure from esophageal balloons. J Appl Physiol 19:207-211 (1964).

10. DuBois, A. B., and L. Dautrebande. Acute effects of breathing inert dust particles and of carbachol aerosol on the mechanical characteristics of the lungs in man. Changes in response after inhaling sympathomimetic aerosols. J Clin Invest 37:1746-1755 (1958).

11. DuBois, A. B., et al. A rapid plethysmographic method for measuring thoracic gas volume: A comparison with a nitrogen washout method for measuring functional residual capacity in normal subjects. J Clin Invest 31:40-50 (1952).

12. DuBois, A. B., S. Y. Botelho, and J. H. Comroe, Jr. A new method for measuring airway resistance in man using a body plethysmograph: Values in normal subjects and in patients with respiratory disease. J Clin Invest 35:327-335 (1956).

13. Ogilvie, C. M., et al. A standardized breath holding technique for the clinical measurement of the diffusing capacity of the lung for carbon monoxide. J Clin Invest 36:1-16 (1957).

14. Comroe, J. H., Jr., and W. S. Fowler. Lung function studies VI. Detection of uneven alveolar ventilation during a single breath of oxygen. A new test of pulmonary disease. Am J Med 10:408-413 (1951).

15. Hyatt, R. E., D. P. Schilder, and D. L. Fry. Relationship between maximum expiratory flow and degree of lung inflation. J Appl Physiol 13:331-336 (1958).

16. Sackner, M. A., and N. D. Atkins. Pulpac: An on-line data processing system for pulmonary function testing. Am Rev Respir Dis 105:1013 (1972).

17. Simmons, D. H., and A. Hemingway. Functional residual capacity and respiratory nitrogen excretion in dogs. J Appl Physiol 8:95-101 (1955).

18. Bouhuys, A. Influence of tissue nitrogen elimination on analysis of pulmonary nitrogen clearance curves. Acta Physiol Pharmacol Neerl [Amsterdam] 8:431-436 (1959).

19. Bates, D. V., P. T. Macklem, and R. V. Christie. Respiratory function in disease, pp 92-93. Philadelphia, Pa.: W. B. Saunders Co., 1971.

20. Brown, R., et al. Physiological effects of experimental airway obstruction with beads. J Appl Physiol 27:328-335 (1969).

21. Ingram, R. H., Jr., and C. F. O'Cain. Frequency dependence of compliance in apparently healthy smokers versus nonsmokers. Bull Physiopathol Respir 7:195-210 (1971).

22. Bouhuys, A. Pulmonary nitrogen clearance in relation to age in healthy males. J Appl Physiol 18:297-300 (1963).

23. McCarthy, D. S., et al. Measurement of "closing volume" as a simple and sensitive test for early detection of small airway disease. Am J Med 52:747-753 (1972).

24. Roos, A., H. Dahlstrom, and J. P. Murphy. Distribution of inspired air in the lungs. J Appl Physiol 7:645-659 (1955).

25. Mead, J. Contribution of compliance of airways to frequency-dependent behavior of lungs. J Appl Physiol 26:670-673 (1969).

FIGURES 1 - 9

for

Section XII (Part 1)

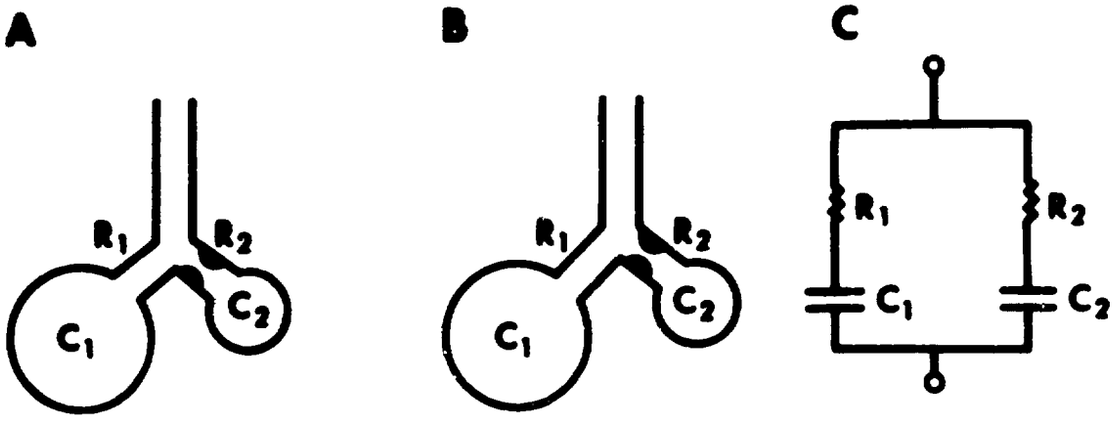

$n_1 = 0.7$	$n_2 = 0.3$	$n_1 = 0.7$	$n_2 = 0.3$
$R_1 = 0.71$	$R_2 = 11.7$	$R_1 = 0.71$	$R_2 = 11.7$
$C_1 = 0.03$	$C_2 = 0.06$	$C_1 = 0.14$	$C_2 = 0.06$
$T_1 = 0.02$	$T_2 = 0.70$	$T_1 = 0.10$	$T_2 = 0.70$

Figure 1. Example of even distribution of ventilation with uneven time constants.

(View A: $T_1 \neq T_2$, but at 60 breaths/min, distribution of ventilation is even. This is the case of altered compartmental elastic properties. View B: $T_1 \neq T_2$, and, since elastic properties are unchanged, distribution of ventilation is uneven at all breathing frequencies. View C: Otis' [ref. 1] two-compartment R-C model.)

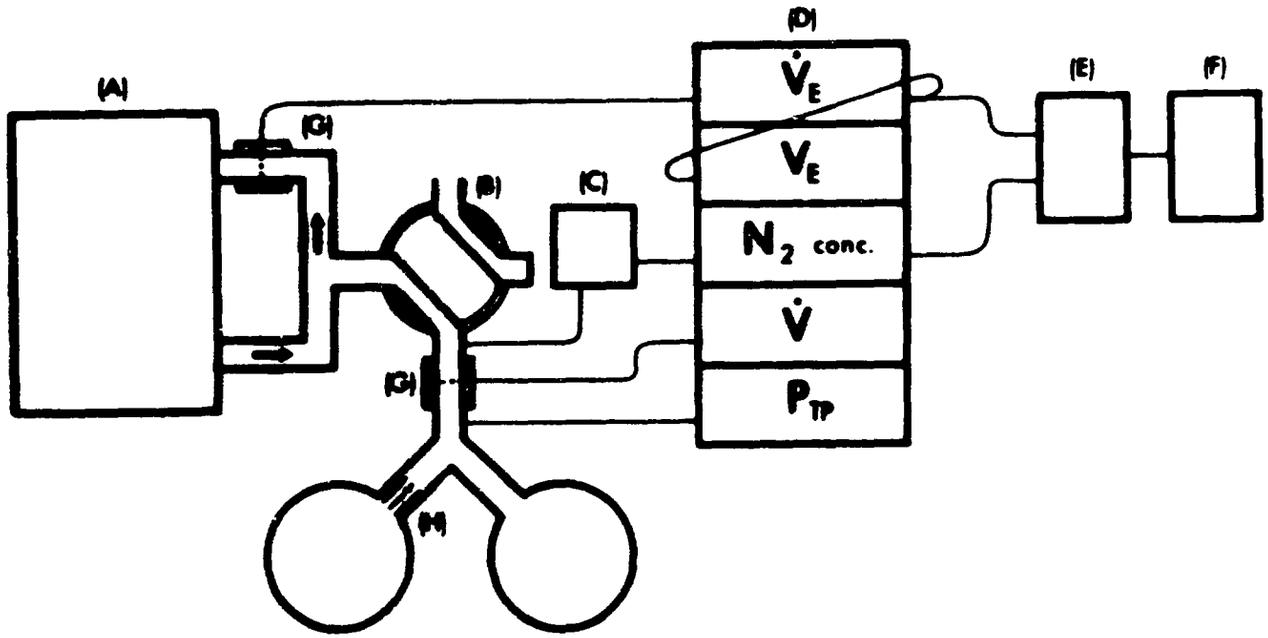

Figure 2. Two-compartment model for determination of dynamic compliance from N_2 washout curves. [Schematic diagram]

(A = respirator; B = 4-way valve; C = N_2 analyzer; D = recorder; E = A to D converter; F = computer; G = pneumotachograph; and H = graded resistance.)

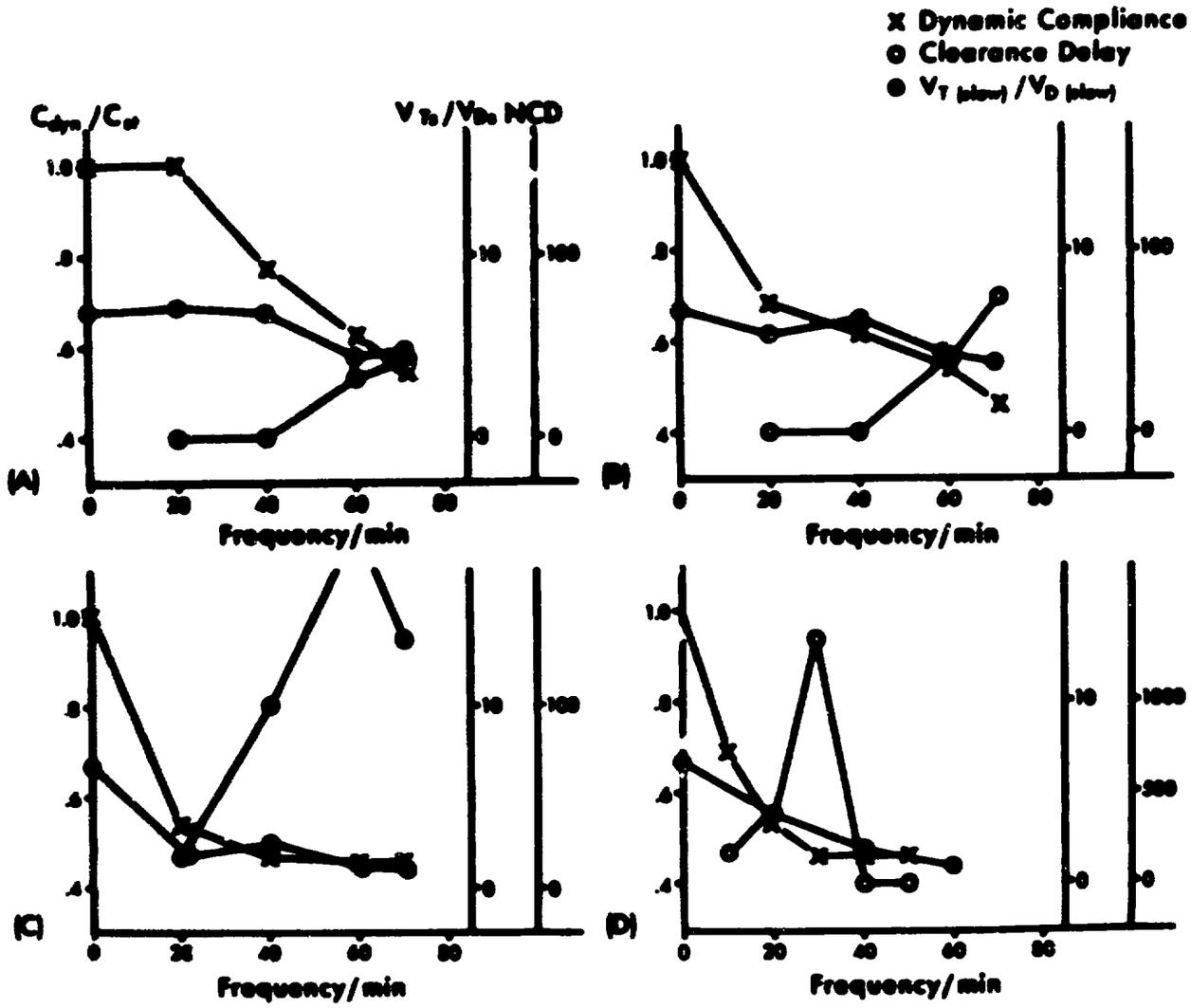

Figure 3. Experimental behavior of the lung model, showing frequency dependence of dynamic compliance (C_{dyn}/C_{st}), N_2 clearance delay (NCD), and the ratio of the tidal volume of the "slow" compartment to its dead space ($V_{T_S} : V_{D_S}$), for increasing unilateral obstructions (A, B, C, D). (Note the reduced scale of NCD for obstruction D.)

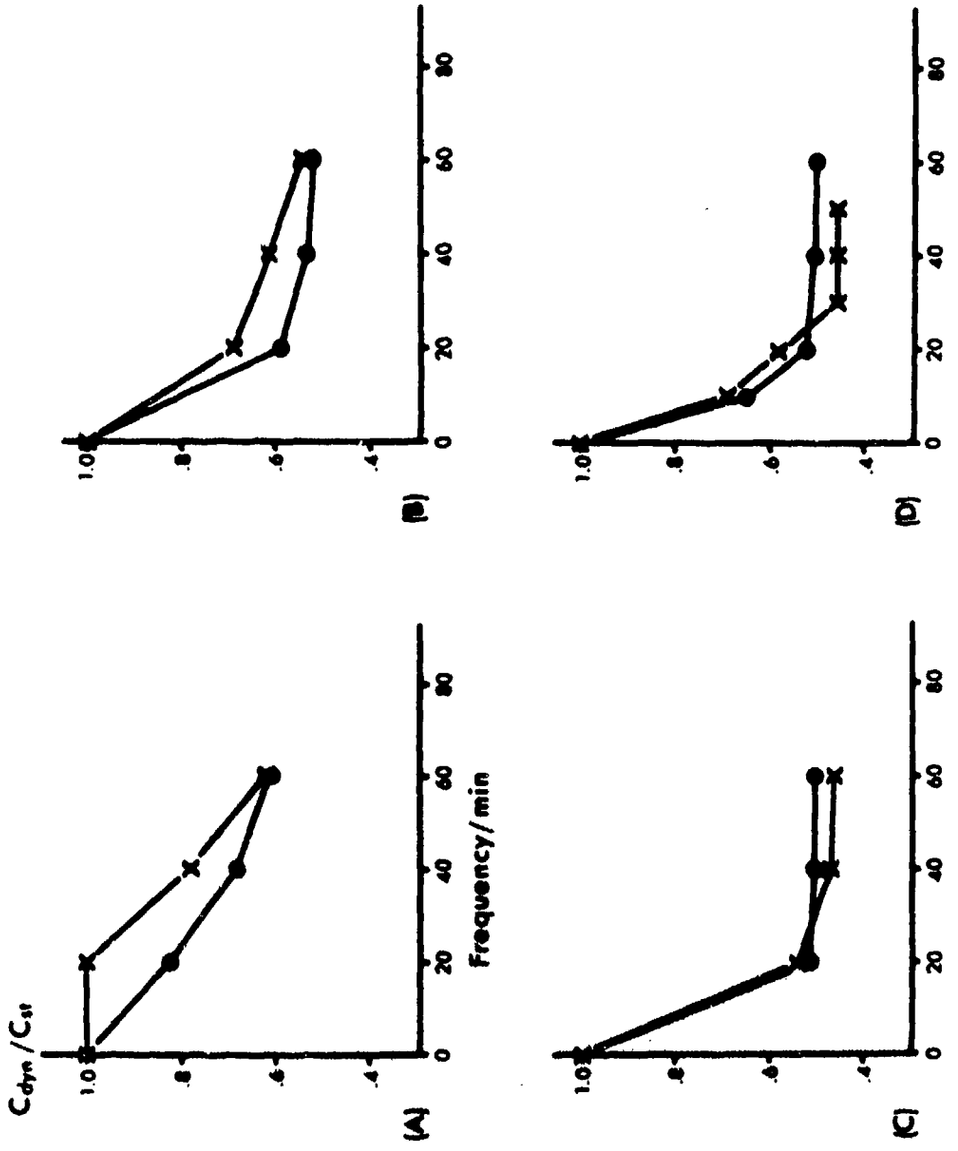

Figure 4. A comparison of actually measured dynamic compliance with the theoretical dynamic compliance predicted from Otis' two-compartment R-C (lung) model for increasing unilateral obstructions (A, B, C, D). [Symbols as in Fig. 3.]

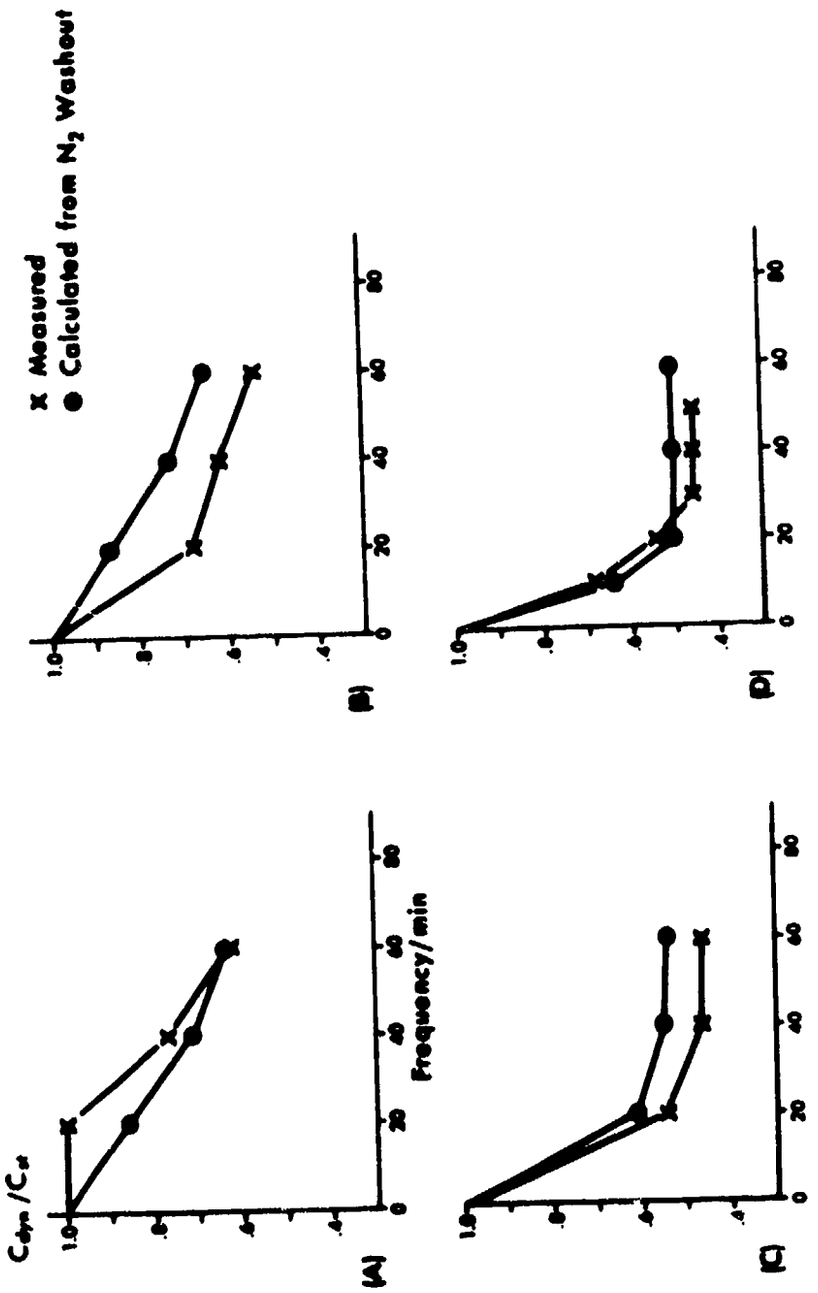

Figure 5. Lung model: A comparison of dynamic compliance calculated from the N_2 washout curves with actually measured dynamic compliance for various unilateral obstructions (A, B, C, D). [Symbols as in Fig. 3.]

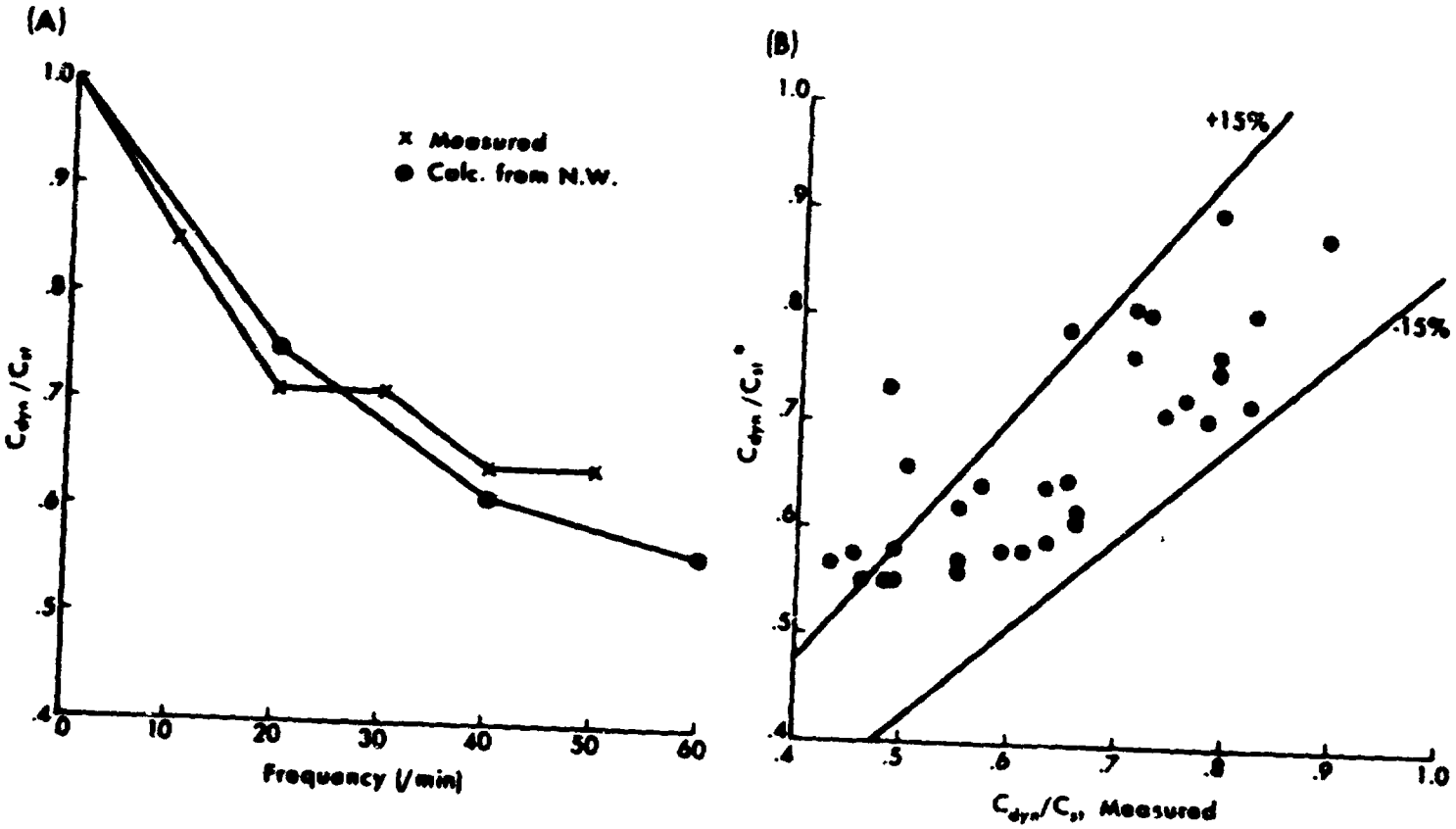

Figure 6. Comparison of calculated (from N_2 washout) and measured dynamic/static compliance (C_{dyn}/C_{st}) in dogs with bronchial obstructions.

View A: A representative case showing calculated and measured C_{dyn}/C_{st} as a function of respiratory frequency. View B: Identity comparison of calculated and measured C_{dyn}/C_{st} for all 10 dogs at respiratory frequencies of 20, 40, and 60/min.)

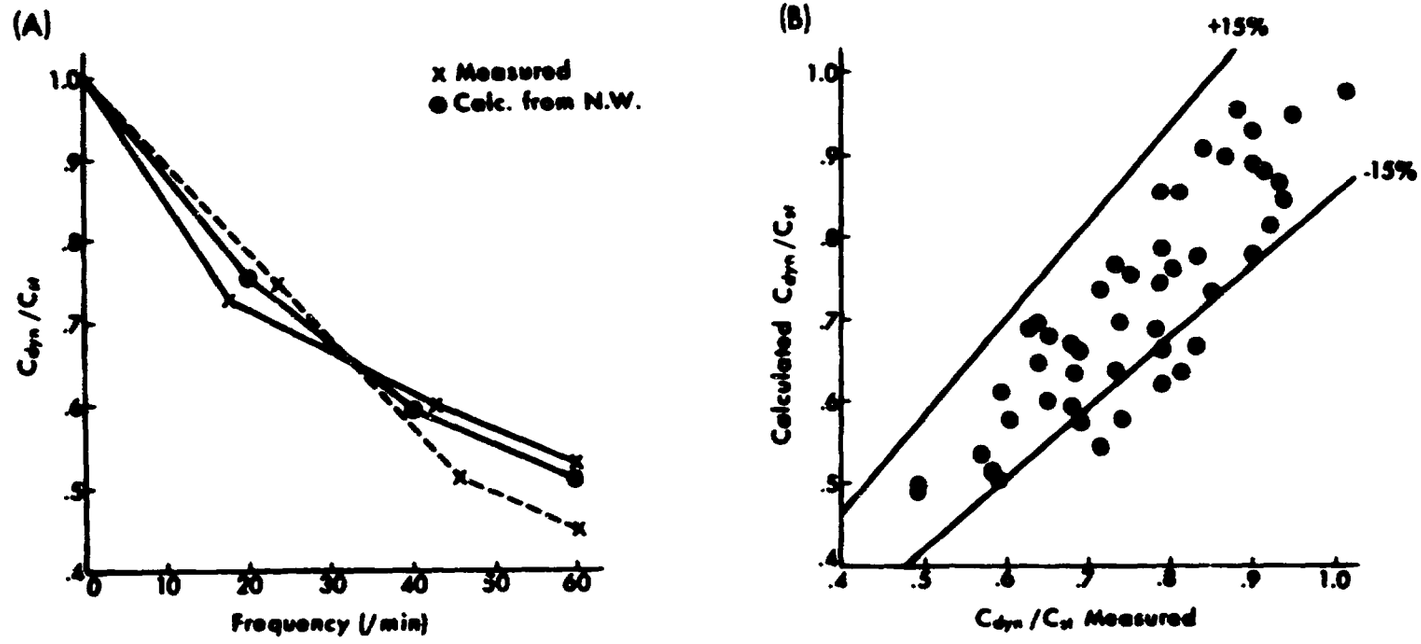

Figure 7. Comparison of calculated (from N_2 washout) and measured C_{dyn}/C_{st} in normal subjects after inhalation of carbachol (group A).

View A: A representative case showing calculated and measured C_{dyn}/C_{st} as a function of respiratory frequency. Since respiratory frequency could not be precisely controlled during measurement of C_{dyn}, an exponential curve was fitted to the measured points which were obtained in duplicate [solid and dotted lines] in order to allow comparison at any given respiratory rate. View B. Identity comparison of calculated and measured C_{dyn}/C_{st} for all 9 subjects at respiratory frequencies of 20, 40, and 60/min.)

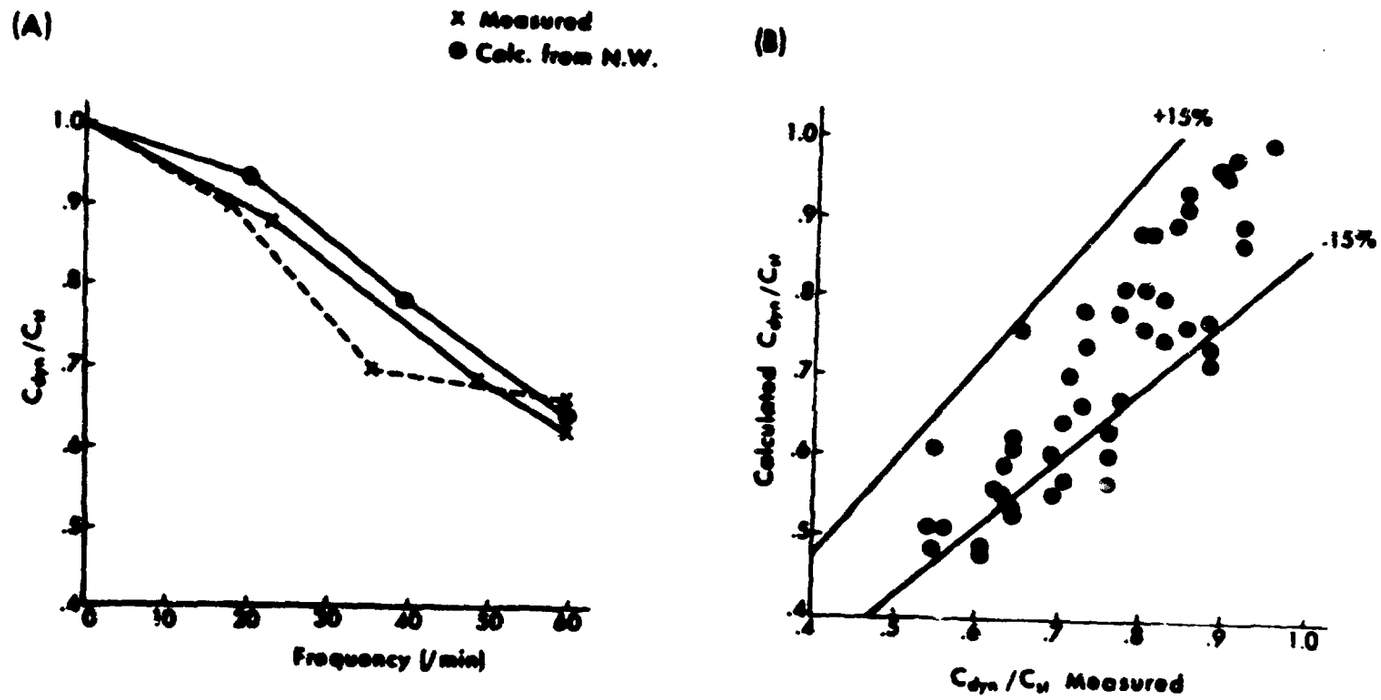

Figure 8. Comparison of calculated (from N_2 washout) and measured C_{dyn}/C_{st} in young smokers (group B).

View A: A representative case showing calculated and measured C_{dyn}/C_{st} as a function of respiratory frequency. [Procedure of comparison, as in Fig. 7.]
View B: Identity comparison of calculated and measured C_{dyn}/C_{st} for all 9 subjects at respiratory frequencies of 20, 40, and 60/min.)

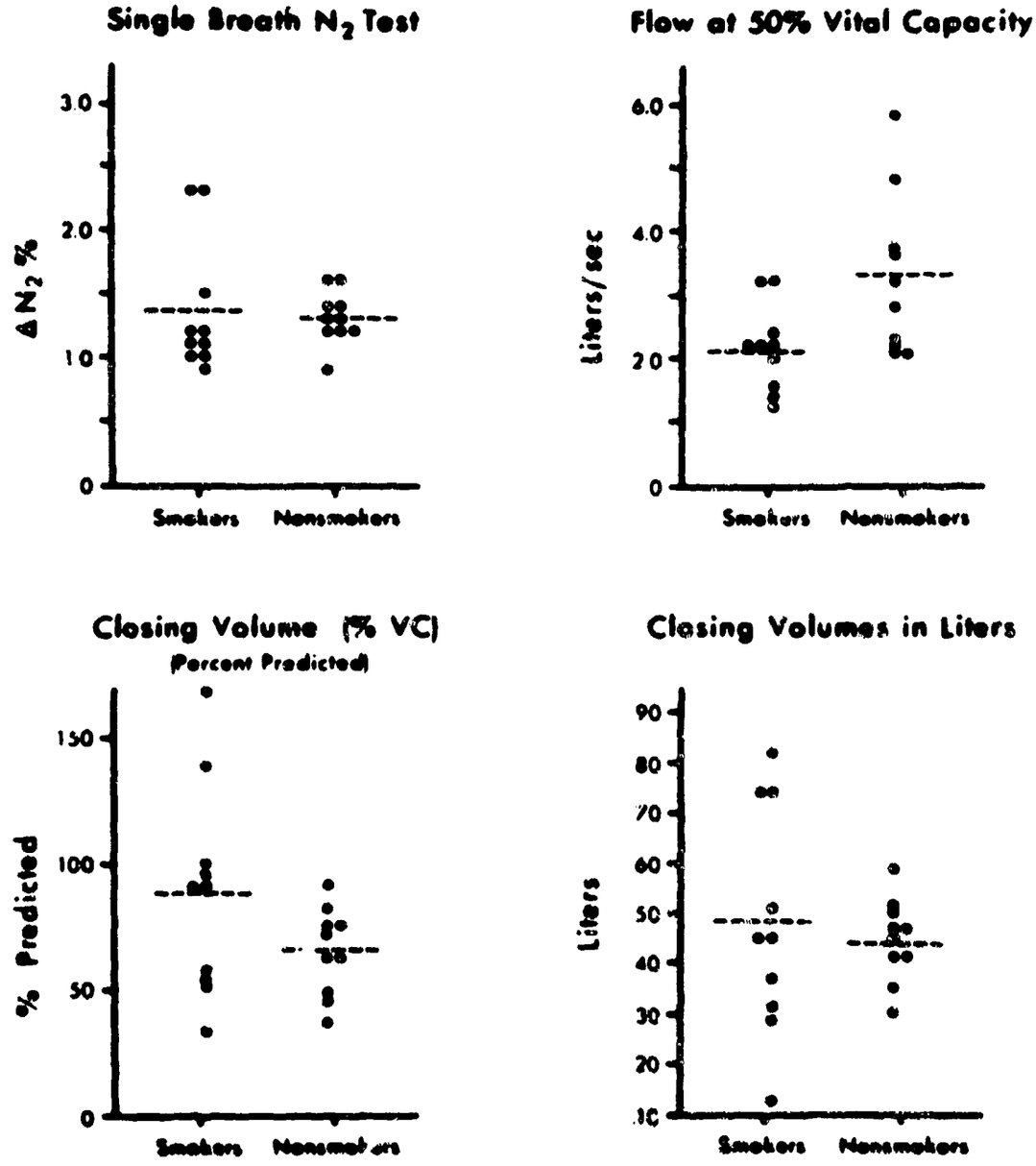

Figure 9. Comparison of commonly used screening test for early lung disease among 10 healthy young smokers and 10 healthy non-smokers (group C).

(The predicted normal values for closing volume are taken from McCarthy et al. [23].)

TABLES 1 - 3

for

Section XII (Part 1)

TABLE 1. RESULTS OF N_2 WASHOUT ANALYSIS IN NORMAL SUBJECTS AFTER CARBACHOL INHALATION (GROUP A) AND IN HEALTHY SMOKERS (GROUP B)

	GROUP A: NORMALS AFTER CARBACHOL							GROUP B: HEALTHY SMOKERS							
SUBJECT	FREQ	$\dot{V}_{A_1}$	$\dot{V}_{A_2}$	n_1	n_2	T_1	T_2	SUBJECT	FREQ	$\dot{V}_{A_1}$	$\dot{V}_{A_2}$	n_1	n_2	T_1	T_2
1	70.8	16.9	10.3	0.30	0.70	0.04	0.4	1	74.0	4.5	15.7	0.09	0.91	0.01	0.3
	55.5	30.5	4.3	0.62	0.38	0.02	0.8		--	--	--	--	--	--	--
2	73.0	12.9	5.3	0.44	0.56	0.001	0.5	2	--	--	--	--	--	--	--
	55.8	14.5	10.6	0.42	0.58	0.03	0.4		53.8	45.3	16.1	0.48	0.52	0.001	0.6
3	72.3	27.3	6.3	0.59	0.41	0.003	0.4	3	67.1	9.7	9.2	0.29	0.71	0.02	0.5
	55.3	10.8	19.8	0.25	0.75	0.1	0.2		52.1	10.5	7.6	0.35	0.65	0.02	0.4
4	73.5	18.4	8.8	0.49	0.51	0.02	0.3	4	70.8	7.0	6.5	0.34	0.66	0.02	0.4
	--	--	--	--	--	--	--		54.4	6.5	3.9	0.32	0.68	0.001	0.8
5	73.2	26.9	6.4	0.52	0.48	0.01	0.4	5	73.7	36.4	4.5	0.56	0.44	0.03	0.9
	55.8	21.9	2.7	0.64	0.36	0.02	0.3		56.4	25.2	7.1	0.46	0.54	0.02	0.8
6	73.3	21.9	9.7	0.44	0.56	0.004	0.4	6	73.5	6.6	12.8	.19	0.81	0.05	0.2
	--	--	--	--	--	--	--		55.8	6.2	14.2	0.24	0.76	0.1	0.6
7	71.7	16.0	21.5	0.24	0.76	0.06	0.2	7	71.0	15.8	16.0	0.17	0.83	0.03	0.4
	55.7	31.2	6.7	0.53	0.47	0.02	0.8		52.8	28.9	8.7	0.51	0.49	0.01	0.7
8	72.2	4.4	13.8	0.03	0.97	0.02	1.1	8	70.6	16.0	5.8	0.53	0.47	0.01	0.4
	55.6	7.0	21.2	0.11	0.89	0.03	0.4		56.5	19.6	2.2	0.74	0.26	0.01	0.6
9	73.9	19.4	5.2	0.45	0.55	0.02	0.7	9	71.1	59.9	15.2	0.52	0.48	0.01	0.4
	55.6	17.6	8.3	0.43	0.57	0.01	0.6		55.5	11.0	27.7	0.15	0.85	0.05	0.3

FREQ = Respiratory Frequency; $\dot{V}_{A_1}$ and $\dot{V}_{A_2}$ = Compartmental alveolar ventilations; n_1 and n_2 = fractional compartmental volumes;

T_1 and T_2 = Compartmental time constants calculated from N_2 washout results.

TABLE 2. ANTHROPOMETRIC DATA, SYMPTOMS, PULMONARY FUNCTION TESTS, AND NITROGEN CLEARANCE DELAY IN YOUNG SMOKERS (GROUP C)

SUBJECT NO.	AGE	SEX	HEIGHT (cm)	PKS/DAY YEAR	SPUTUM	DYSPNEA	Pulmonary Function Tests (%Predicted Normal, See Text) VC	FRC	RV	TLC	$FEV_{1.0}$	R_{AW}	D_LCO	NCD (%) (60)	NCD (%) (75)
1	28	M	185.0	5	NO	NO	93	73	76	68	104	146	82	33	36
2	36	M	172.6	40	NO	NO	107	80	76	98	89	125	102	37	12
3	23	M	175.5	10	YES	YES	96	84	68	92	102	182	94	31	37
4	23	M	177	3	NO	NO	97	82	64	89	93	141	85	0	8
5	28	F	162.5	7	NO	YES	107	82	80	99	86	120	89	28	8
6	28	M	168.5	1	NO	NO	102	91	105	96	93	183	88	0	10
7	26	M	187.0	3	YES	NO	97	78	67	88	92	154	106	26	20
8	42	M	167.5	8	NO	NO	102	105	123	108	91	176	107	51	93
9	21	M	175	7	NO	YES	90	90	101	93	84	226	116	20	18
10	18	M	180	5	NO	NO	87	76	69	83	85	223	100	0	22
MEANS:	27.3			8.9			97.8	84.1	82.9	93.4	91.9	167.6	96.9		
RANGE:	18-42			1-40			87-107	73-105	64-123	83-108	84-104	125-226	82-116		

VC = Vital Capacity; FRC = Functional Residual Capacity; RV = Residual Volume; TLC = Total Lung Capacity; $FEV_{1.0}$ = Forced Expiratory Volume in 1 sec; R_{AW} = Airway Resistance; D_LCO = Diffusing Capacity of the Lung for CO; and NCD = Nitrogen Clearance Delay in % at 60 and 75 breaths/min.

TABLE 3. ANTHROPOMETRIC DATA, SYMPTOMS, PULMONARY FUNCTION TESTS, AND NITROGEN CLEARANCE DELAY IN YOUNG NONSMOKERS (GROUP C)

SUBJECT NO.	AGE SEX	HEIGHT (cm)	PKS/DAY YEAR	SPUTUM	DYSPNEA	Pulmonary Function Tests (%Predicted Normal, See Text) VC	FRC	RV	TLC	$FEV_{1.0}$	R_{AW}	D_LCO	NCD (%) (60)	NCD (%) (75)
1	22 M	180.5	0	NO	NO	115	105	103	112	106	162	98	0	0
2	32 M	183	0	NO	NO	85	101	97	89	101	116	118	0	0
3	26 M	185.0	0	NO	NO	105	115	113	107	91	185	109	0	0
4	27 M	175	0	NO	NO	97	84	94	96	102	113	97	0	0
5	35 F	170	0	NO	NO	104	101	114	107	96	96	73	0	0
6	28 M	180	0	NO	NO	102	80	82	96	90	120	103	0	0
7	29 M	175	0	NO	NO	127	90	97	119	119	150	130	0	0
8	28 M	187.5	0	NO	NO	92	98	106	96	90	146	108	0	0
9	31 M	173.0	0	NO	NO	104	86	101	103	95	116	97	0	0
10	25 M	177	0	NO	NO	134	99	49	112	117	206	128	0	0
MEANS:	28.1					106.5	95.9	95.6	103.7	100.7	141.0	106.1		
RANGE:	22-35					85-134	80-115	49-114	89-119	90-119	96-206	73-130		

VC = Vital Capacity; FRC = Functional Residual Capacity; RV = Residual Volume; TLC = Total Lung Capacity; $FEV_{1.0}$ = Forced Expiratory Volume in 1 sec; R_{AW} = Airway Resistance; D_LCO = Diffusing Capacity of the Lung for CO; and NCD = Nitrogen Clearance Delay in % at 60 and 75 breaths/min.

-XII-
(Part 2)

RE: SAM-TR-75-25
Section XII (Part 2: A and B)

SUPPLEMENTARY INFORMATION on:

A. Determination of Average V_p/V_{T_2} and Its Effect On Calculated C_{dyn}/C_{st}.

B. Solutions to the Equations for the Time Constants of the Two-Compartment Lung Model.

In order for comprehensive information on this research to be readily accessible, microfiche have been made of the above-mentioned material. The microfiche are available through:

The Aeromedical Library
Documentation Section
Brooks AFB, Texas 78235

ABS test	3-dimensional design of co-variance
BE	base excess
BOX	body plethysmograph (an airtight chamber)
BSA	body surface area
BTPS	body temperature and pressure, saturated with water vapor
cm	centimeter(s)
CO	carbon monoxide
CPA	capillary pulse amplitude
cpm	cycles per minute
C_{AW}	compliance airways
C	centigrade
C_{dyn}/C_{st}	ratio of dynamic to static compliance
dB	decibel(s)
dc	direct current
DC	diffusing capacity
DCO_{RB}	pulmonary diffusing capacity using the carbon monoxide rebreathing technique
D_L	diffusing capacity of lung
D_M	membrane diffusing capacity
EDF	end-diastolic flow
EKG	electrocardiogram
FRC	Functional Residual Capacity
$F_{A_{CO}}$	fraction of alveolar air that is carbon monoxide (i.e., the concentration of CO in alveolar air)
F_{ACO_o}	same as $F_{A_{CO}}$, but at end expiratory point of lung ventilation where zero intrapleural pressure is recorded
Hg	mercury
hr	hour(s)

Hz	Hertz
H_2O	water
i.a.	intra-arterial
K	1,000 (in electronics)
kg	kilogram(s)
L	liter(s)
Laugh and Laughn	inhouse computer program developed by Mt. Sinai Hospital (consult p. 68)
LCI	lung clearance index
L/min	liters per min
LVET	left ventricular ejection time
mc	millicurie(s)
min	minute(s)
ml	milliliter(s)
mm	millimeter(s)
msec	millisecond(s)
NS	not significant
n_1 and n_2	fractional compartmental volumes
O_2	oxygen
P	probability values
Pendelluft	ventilation of one lobe of a lung from another lobe without first moving the air into the bronchus
PEP	pre-ejection phase
pH	units
PNS	phrenic nerve stimulation
PO	peak $\dot{Q}_C$
PPB	positive pressure breathing
PSF	peak systolic flow
psi	pounds per sq in
PVR	pulmonary vascular resistance
P_{O_2}	arterial oxygen tension

P_{CO_2}	carbon dioxide tension
$P_{\bar{C}O_2}$	pulmonary capillary oxygen tension
$P_{\overline{LA}}$	mean left atrial pressure
$P_{\overline{PA}}$	mean pulmonary arterial pressure
P_{TM}	transmural pulmonary arterial pressure
P_{TP}	transpulmonary pressure
$\dot{Q}_c$	pulmonary capillary blood flow
QRS complex	portion of waveform in EKG extending from points Q to S (includes maximum amplitude in an EKG trace)
QS_2	total electromechanical systole
$\dot{Q}_{PA}$	pulmonary blood flow
r	regression ratio
R-R	interval between R Waves (in EKG)
s.c.	subcutaneous
SD	standard deviation
$\pm$SD	mean
sec	second(s)
STPD	standard temperature and pressure, dry
SV	stroke volume
TGV	thoracic gas volume
TLC	total lung capacity
T_1 and T_2	compartmental time constants calculated from N_2 washout results
$T_{GV_{(L)}}$	thoracic gas volume (liters)
V	volt(s)
VDC	volt (direct current)
V_A	alveolar volume
$\dot{V}_{A_1}$ and $\dot{V}_{A_2}$	compartmental alveolar ventilation

V_C	pulmonary capillary blood volume
V_M	mouth flow
V_{PA}	pulmonary arterial blood volume
V_T	tidal volume
V_{TG}	thoracic gas volume
yr	year(s)

★U.S. GOVERNMENT PRINTING OFFICE: 1976- 671-613/36